CITY OF SAN DIEGO
Dry Weather Aerial Deposition Study

Final Report

Prepared For:

The City of San Diego
1970 B St., MS 27A
San Diego, CA 92102

September 4, 2007

WESTON SOLUTIONS

13.0 REFERENCES

Barbe, D.E., J.F. Cruise, and X. Mo. 1996. Modeling the Buildup and Washoff of Pollutants on Urban Watersheds. Water Resources Bulletin 32(3):511-519.

Brake Pad Partnership. 2005. Air Deposition Modeling of Copper from Brake Pad Wear Debris in Castro Valley Creek Watershed. Atmospheric and Environmental Research, Inc. September.

Brake Pad Partnership. 2006. BPP website. http://www.suscon.org/brakepad/ Accessed January 2007.

Butcher, Jonathan. 2003. Buildup, Washoff, and Event Mean Concentrations. Journal of the American Water Resources Association. p1521-1528.

Cal-trans. 2003. California Department of Transportation website: http://www.dot.ca.gov/.

Councell, T.B., Duckenfield, K.U., Landa, E.R., and E. Callender. 2004. Tire-Wear Particles as a Source of Zinc to the Environment. Environmental Science & Technology. Vol. 38, no. 15. pp. 4206-4214.

County of San Diego Air Pollution Control District. 2006. The Year's Air Quality. 2005 Annual Report.

EMFAC. 2002. Calculating Emission Inventories for Vehicles in California, User's Guide.

Environmental Protection Agency (EPA). 2007. EPA Website http://www.epa.gov/ednnrmrl/models/swmm/index.htm. Accessed January, 2007.

EPA. 1999. Compendium Method IO-3.3, Determination of Metals in Ambient Particulate Matter Using X-ray Fluorescence (XRF) Spectroscopy. *In* Compendium of Methods for the Determination of Inorganic Compounds in Ambient Air. EPA/625/R-96/010a.

Kennedy, P. 2003. Metals in Particulate Material on Road Surfaces. Written by Klingett Mitchell Ltd. Prepared for Ministry of Transport te Manatu Waka (New Zealand).

Moncrieff, I. and P. Kennedy. 2004. Road Transport Impacts on Aquatic Ecosystems. Issues and Context for Policy Development. Written by Fuels and Energy Management Group Ltd .and Klingett Mitchell Ltd. Prepared for Ministry of Transport te Manatu Waka (New Zealand).

Lin, J.-M., G.-C. Fang, T.M. Holsen, K.E. Noll. 1993. A comparison of dry deposition modeled from size distribution data and measured with a smooth surface for total particle mass, lead and calcium in Chicago. Atmos. Environ. 27, 1131-1138.

MEC Analytical Systems, Inc. 2002. 1999-2001 Chollas Creek Watershed Monitoring Final Report. Prepared for the City of San Diego and the Department of Pesticide Regulation.

National Atmospheric Deposition Program (NADP). 2001. Instruction Manual: NADP/NTN Site Selection and Installation. Prepared by: D.S. Bigelow, S.R. Dossett, and V.C. Bowersox. August 2001.

Paode, R.D., S.C. Sofuoglu, J. Sivadechathep, K.E. Noll, and T.M. Holsen. 1998. Dry Deposition Fluxes and Mass Size Distributions of Pb, Cu, and Zn Measured in Southern Lake Michigan during AEOLOS, Environ. Sci. Technol. 32:1629-1635.

Process Profiles. 2006. Copper Released from Brake Lining Wear in the San Francisco Bay Area. Prepared for the Brake Pad Partnership. January 2006.

Sabin, Lisa D., Jeong Hee Lim, Keith D. Stolzenbach, Kenneth C. Schiff. 2005. Contribution of Trace Metals from Atmospheric Deposition to Stormwater Runoff in a Small Impervious Urban Catchment. Water Research 39 (2005) 3929-3937. Available online August 2005.

SANDAG. 2006. San Diego Association of Governments website: http://www.sandag.org/. Accessed December 2006.

San Francisco Estuary Institute. 2005. Brake Pad Partnership Castro Valley Atmospheric Deposition Study. Submitted to the Brake Pad Partnership, May 2005.

SanGIS. 2003. City of San Diego Geographic Information Source website: http://www.sangis.org/. A Joint program of City of San Diego and County of San Diego.

Southern California Coastal Water Research Program (SCCWRP). 2007. Presentation by Ken Schiff to the San Diego Regional Water Quality Control Board. The Modeling and Monitoring for the Development of the TMDL for the Mouths of Chollas Creek, Switzer Creek, and Paleta Creek. 01/30/2007.

Stolzenbach, K.D., R. Lu, C. Xiong, S. Friedlander, R. Turco, K. Schiff, and L. Tiefenthaler. 2001. Measuring and Modeling of Atmospheric Deposition on Santa Monica Bay and the Santa Monica Bay Watershed. Final Report to Santa Monica Restoration Project. 41 pp.

Stolzenbach, Keith. 2006. Atmospheric Deposition in the Los Angeles Coastal Region, UCLA Institute for the Environment and the Southern California Coastal Water Research Project, Presentation to the Joint Air and Water Resources Control Board Meeting, February, 2006.

State Water Regional Control Board (SWRCB) and Joint Air Resources Control Board Meeting. 2006. Presentation entitled: Atmospheric Deposition in the Los Angeles Coastal Region. February 2006. Sacramento, CA.

United States Geological Service (USGS). 2006. USGS website: http://minerals.er.usgs.gov/minerals/pubs/commodity/zinc/. Accessed December 2006.

Weston Solutions, Inc. 2007. Proposition 13 PRISM Grant Agreement No. 04-17-559-0, San Diego Region Integrated Pest Management (IPM) Education and Outreach Project, Water and Sediment Quality Monitoring Data Mapping and Analysis for Chollas Creek Final Report. Prepared for the City of San Diego, January 2007.

Weston Solution, Inc. 2007. San Diego County Municipal Copermittees 2005-2006 Urban Runoff Monitoring. Volume 1- Final Report. Prepared for: County of San Diego. January.

Weston Solutions, Inc. 2006. Chollas Creek TMDL Source Loading, Best Management Practices, and Monitoring Strategy Assessment. Prepared for the City of San Diego. September, 2006.

12.0 CONCLUSIONS AND RECOMMENDATIONS

The purpose of this study was to assess the contribution of aerial deposition and its impact to concentrations of pollutants in storm water within the City of San Diego. Three separate but related studies were conducted from June through November 2006 to answer the study questions. The three studies included a pilot study, an area wide study, and a freeway transect study (Figure 12-1).

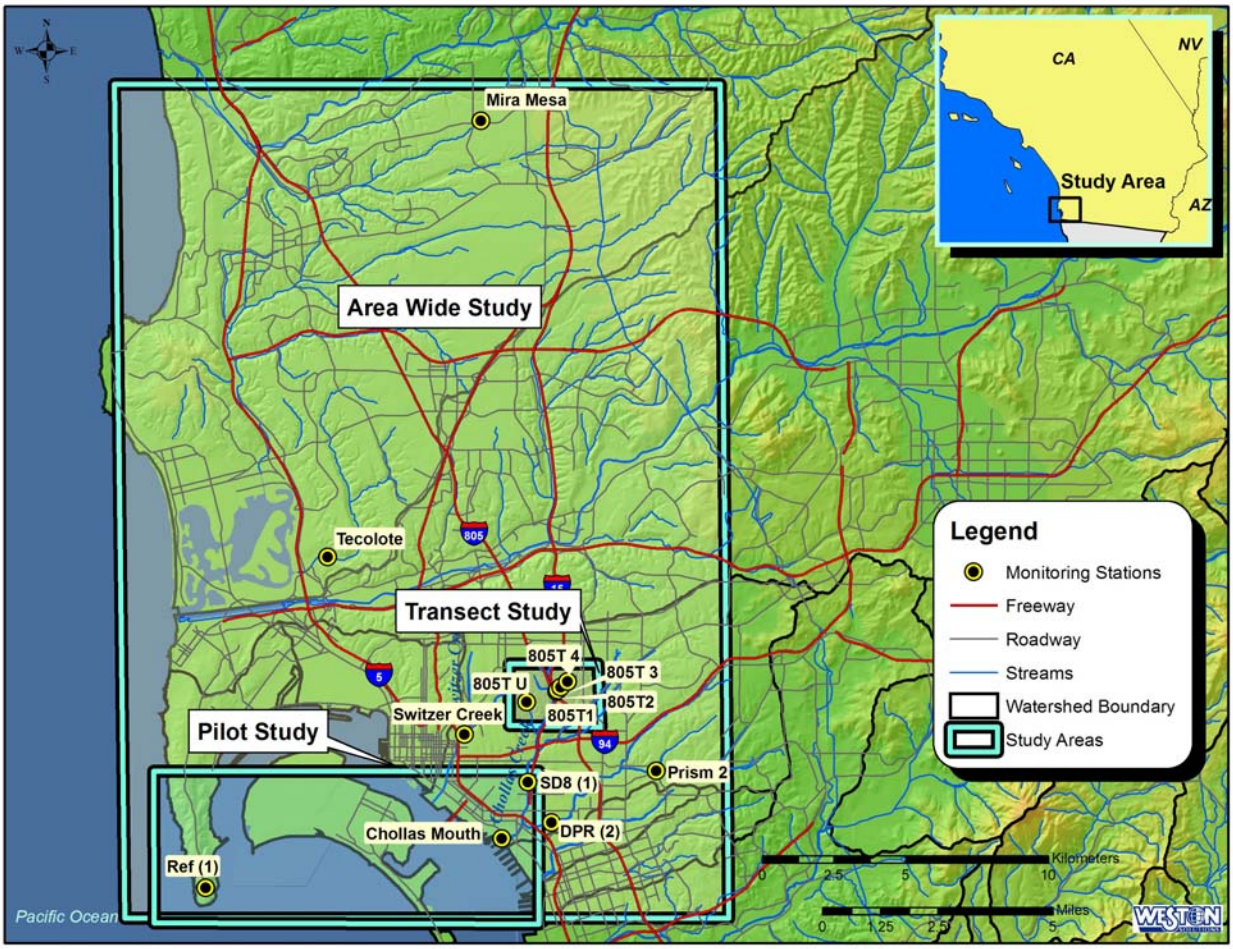

Figure 12-1. Sample location map.

12.1 Study Questions and Relationships

The study questions and conclusions are presented as follows:

1. *What are the aerial deposition contributions of metals (copper, lead, and zinc) and are they associated with different sources or land uses?*

The deposition rates or fluxes of total copper, lead, and zinc within the City of San Diego vary both spatially and temporally. This is to say that not all areas experience the same depositional

loading as others. The median aerial deposition flux of copper was highest in the North fork of Chollas Creek at Site SD8(1) (20.3 µg/m^2/day) and at the Mouth of Chollas Creek (17.5 µg/m^2/day). Copper was lowest at Site Ref(1) on Point Loma (1.8 µg/m^2/day). Lead was not frequently detected throughout the study but was highest at Site SD8(1) (median flux of 6.6 µg/m^2/day) and was never detected at site Prism2 (<4.8 µg/m^2/day). The median aerial deposition flux of zinc was highest at sites downwind or adjacent to freeways. Site 805T1, Switzer Creek, and SD8(1) had median zinc fluxes of 127, 97.8, and 90.9 µg/m^2/day respectively. In comparison, zinc was never detected during any of the ten weekly sample events conducted at Site Ref(1) on Point Loma (<1.9 µg/m^2/day).

Re-entrainment of dust from freeways and surface streets is most likely the largest contributor of aerial particulates throughout the City of San Diego. Air dispersion modeling showed that re-suspended roadway dust contributed significantly more particulates in estimates of aerial deposition flux, and local emission estimates showed that roadways had overall greater particulate emissions than industrial emissions. However, when metals emissions as a function of roadway dust were compared to industrial emission sources in a 4 km area near the Mouth of Chollas Creek, industrial emissions far outweighed the copper emissions from freeways and roadways combined. If industrial sources are continually emitting elevated concentrations of compounds that are not regulated by the Air Resources Control Board (e.g. copper and zinc), these sources may locally contribute a larger percentage of the copper and zinc deposition observed. Additionally, if these emissions have occurred over several decades, the re-entrained dust may contain significantly larger concentrations in areas near the original source.

Variations in sample fingerprints and wind directions did not allow for statistically determining one single land use as a predominating source throughout the study. The analysis did however suggest that transportation related sources do play a significant role in the distribution of the aerial deposition. One obvious relationship in the Chollas Creek area is the density and proximity of roadways and freeways that parallel the creek. Land use analysis using GIS and the traffic volume database showed that 41% of the freeways lie within 250 meters of Chollas Creek. In comparison, at the Tecolote Creek site, where aerial deposition of copper, lead, and zinc was not determined to be significant, only 10% of the freeway area in the watershed lies within 250 meters of Tecolote Creek. Although Tecolote Creek has water quality problems related to copper, lead, and zinc, aerial deposition was not considered to be related to freeway impacts in this watershed. In the Chollas Watershed, aerial emissions from industrial sources could not be ruled out as a contributing factor as illustrated by the limited emissions inventory data previously mentioned. The statistical analysis suggested that other trace elements measured on the deposition disks (strontium, bromine, manganese, chlorine, sulfur) might prove useful in resolving the roles of traffic and industrial emissions, if more data were available.

Review of the study results suggest that copper is likely a function of brake-wear debris and other transportation related particulates on a regional scale, which is consistent with current knowledge of vehicle emissions and deposition. However, other sources (e.g. aerial emissions from industrial, commercial, and construction) are likely additional contributing factors near the Chollas SD8(1) site and near the Mouth of Chollas Creek based on the emissions data reviewed and observations made. Zinc is likely associated with tire wear and as a function of proximity to roadways, though galvanized wear debris was also observed. Zinc associated with brake wear may also be a contributing factor. Lead, while less frequently detected, is likely a function of re-

suspended roadway dust, mobilization of soils during rain events, or other anthropogenic particulate sources (e.g. lead solder, paint chips, and other materials).

2. *What is the particle size distribution of metals in air particulates versus what particle size distribution is deposited?*

The only quantitative information on elemental mass distribution by particle sizes was for atmospheric particulates from the impactor analyses. Particle size distributions from the surrogate disks provided useful optical information. In general, the particle size distribution and elemental concentrations in air are different from the particle size distributions found on deposition disks. This is primarily a function of smaller particles generally having lower deposition velocities. Although higher concentrations of metals were generally found in the finer particle size range, these particles tend to disperse over larger distances. As a result, larger particle sizes > 2.5 µm account for higher flux rates than smaller particle sizes < 2.5 µm. In this study, while fine particles did settle out, their overall mass contribution was determined to be significantly lower than particles greater than 10 microns. Additionally, larger particles in the coarse silt to fine sand size range were the predominant size range (by cross-sectional surface area) found on deposition disks. This is consistent with other studies that have shown that coarse particles are typically responsible for the majority of the flux within urban settings (Holsen et al., 1998).

Results of the transect study showed that zinc concentrations decreased with distance from the freeway in both the deposition disks and impactor studies. Zinc oxide is used in the vulcanization process of rubber and studies have shown that zinc found in municipal MS4 systems are primarily derived from tire-wear particles (Councell et al., 2004). Tire wear particles were frequently observed in samples collected near roadways and generally decreased with distance from freeways. Particles from anthropogenic sources (e.g. mechanically worn metals, flux condensation spheres, rust, and paper) in addition to naturally occurring particles were also observed. In contrast to zinc, copper was not found to have a similar flux concentration gradient with respect to proximity to freeways.

Copper from brake wear debris is often found in the fine particle size fraction (1-5 µm) and will tend to disperse over greater distances. These particles will travel farther from the sources as shown by the air quality dispersion modeling and likely contribute a large percentage of the copper flux observed at other sites. This may be one explanation as to why copper was generally related to areas near urban roadway environments. However, copper was also found by electron microscopy in larger particles greater than 10 µm and in particles that appeared related to mechanically worn equipment (e.g., grinding and surface wear) and possibly other natural occurring sources (e.g., mineral grains). As previously mentioned, lead was not frequently detected in deposition samples. This may be a function of the generally finer fractions of lead contributing to a smaller percentage of the overall mass of the sample deposits.

3. *Where is pollutant loading from aerial deposition occurring within the City of San Diego?*

Aerially deposited copper and zinc is occurring at elevated rates near the mouth of Chollas Creek, the Switzer Creek site, within the proximity of the SD8(1) site, and more prevalently

between 0 and 250 meters downwind of freeways. Aerially deposited lead is occurring at elevated rates at the SD8(1) site but to a lesser degree. Once again, lead is typically associated with long-term accumulations due to the previous use of leaded gasoline. Lead was not determined to be a continually elevated constituent in air, yet may randomly occur due to mechanically worn anthropogenic sources such as paint chips from older homes, solder, and electronic parts.

While brake wear debris may play a contributing role in copper fluxes, it is evident that the proximity to significant industrial aerial emission sources may also play a role in elevating the concentrations of copper in specific areas. This is evident by the fact that the Switzer Creek and the 805 T1 sites are downwind (prevailing wind direction) from a major freeway. The SD8(1) and Chollas Mouth sites are on the upwind side of the freeways, are downwind of industrial sources, yet have the highest median copper fluxes. The transect study revealed that copper fluxes within 500 meters of freeways would be expected to have a median copper flux less than 10 $\mu g/m^2$/day. The SD8(1) site had a median flux of 20.3 $\mu g/m^2$/day and the Chollas Mouth Site had a median copper flux of 17.5 $\mu g/m^2$/day, double what would be expected from freeway sources in the surrounding area. This key finding supports the idea that aerial emissions from industrial or commercial sources in the Chollas Creek area are also contributing elevated levels of copper particulates. Although statistical differences did not single out one land use in particular, the overall observation of facilities in the proximity of Chollas Mouth is considered industrial in nature. Additionally, due west of the SD8(1) site, several industrial/commercial facilities (e.g., auto dismantling yards, recycling facilities, and painting facilities) located on Commercial Street may potentially contribute particulate aerial emissions to this area.

The industrial emissions reported to the Air Resources Control Board from the few large facilities near the mouth of Chollas Creek were shown to be significant in comparison to estimated emissions from roadways and freeways (proportioned from impactor results and dispersion modeling inputs) within 4 km of the mouth of Chollas Creek. On the basis of this approximation, industrial sources contributed 48.7% of the copper emissions in the 4 km area in comparison to 51.3% from roadways and freeways.

In comparison, tire wear, brake wear, exhaust, and re-entrained dust extrapolated from the impactors and air dispersion modeling emissions accounted for 84% of the total zinc, while industrial emissions accounted for 17% percent of the total zinc. The association of zinc with proximity to roadways is also supported by the elevated zinc concentrations observed at the 805 T1 and Switzer Creek sites. Regardless, if 17% of the emissions of zinc are from industrial areas, the relative load contribution from industrial sources will proportionally increase as one approaches an emission source.

4. *What is the contribution of aerial deposition to water quality concentrations observed in Chollas Creek?*

The contribution of aerial deposition to water quality in the Chollas Creek Watershed was evaluated using the EPA Storm Water Management Model (SWMM). The SWMM model has a buildup and washoff function that allows for the estimation of water quality concentrations as a function of aerial deposition flux. The flux measurements obtained from this study were used for the model inputs to calculate the buildup rate and the predicted run off concentrations in the

north fork of Chollas Creek. Results showed that aerial deposition potentially accounts for the majority of the copper and zinc load from the north fork of Chollas Creek in comparison to the average loads observed from 13 years of data. Lead accounted for less than half of the observed load suggesting that lead is more likely related to the mobilization of soils during rain events or other industrial sources. While the modeling performed is an estimate and both aerial deposition data and storm water concentration is highly variable in nature, the predicted runoff concentrations fall within the ranges of observed results over time. The results are also consistent with a separate study conducted in Los Angeles that attributed 57%-100% of the runoff concentrations to aerial deposition (Sabin et al., 2005).

Additional information related to the modeling is the estimate of the number of days of deposition it takes to reach the estimated mean water quality concentrations observed historically. The estimate is important in determining the frequency of street sweeping needed to reduce the impacts due to aerial deposition. This estimate should be used with respect to the variable nature of deposition and wash off. Regardless, the results suggest that results for zinc reaches the dissolved metals water quality objective (WQO) in an estimated 9 days, copper reaches the WQO in roughly 7 days, and lead reached the WQO in 20 days. This suggests that street sweeping would need to occur on a weekly basis to be effective at reducing copper, lead, and zinc concentrations found in water quality.

12.1.1 Study Data Gaps

Although the data assessed presents evidence of the processes and sources of aerial deposition, there were several questions identified with need for further study:

Question 1. What is the average deposition rate over the course of entire year?

This question arises since the study was conducted over a five month period to evaluate the dry weather loading to surfaces prior to the first rainfall of the season. Understanding the annual deposition variability will provide a more robust data set to use for assessing the buildup and wash off process in a watershed.

Question 2. How soluble are the metals that deposit on surrogate surfaces?

This question arises since the study assessed only the total metal fraction. Although this study presents data related to metals concentrations and is directly applicable to the TMDLs the City faces, the direct link to dissolved metals concentrations from aerial deposition is not fully understood. There are very few studies that have evaluated the solubility of metals in aerially deposited particles. Information from the Brake Pad Partnership suggests that copper from brake wear is highly soluble. However, we do not understand the solubility of particles from other sources and those specific to the Chollas Creek Watershed.

Question 3. What is the relationship between buildup and wash off from different surfaces in a watershed?

The processes of buildup and subsequent wash off are not well understood and some general assumptions are made for modeling purposes. Factors such as surface roughness,

accretion/cohesion, gradient, and surface area are highly variable and may vary from one location to another. Additionally, rainfall intensity and storm totals also vary over the course of a storm season may result in wash off of material that was deposited from previous years deposition. As such, modeling of these processes is relatively new and requires further refinement.

12.2 Final Conclusions

The Chollas Creek Dissolved Metals TMDL states that *"MS4 discharges are point source discharges because they are released from channelized, discrete conveyance pipe systems and outfalls. Background loads and loads from air deposition are negligible compared to the loads delivered from the MS4s..."*

This study demonstrates that aerially deposited particulates are not negligible and can account for the majority of the concentration of copper and zinc, and to a lesser degree lead in storm water runoff found in Chollas Creek. These particulates originate from a variety of sources including, but not limited to transportation related emissions, industrial facility emissions, resuspended soil, and physical wear and weathering of consumer products.

Results suggest that aerial loading of metals to watersheds is likely driven by localized deposition of larger particles near transportation and industrial sources. The relative contribution of "background" deposition of finer particles from other regions of Southern California is not considered to be an issue within the City of San Diego. Aerially deposited copper, lead, and zinc do not appear to be occurring at elevated levels on a regional airshed scale which is considerably larger than a watershed area. The sources appear to originate from the activities related to urban processes (traffic volume, construction, industry, and historical contaminants in soil) within localized areas. Concentrations of copper, lead and zinc vary within different areas of the City of San Diego, within different watersheds, and within different sub watershed areas as previously discussed.

Freeways and surface streets are not the only contributors of copper and zinc particulates. Small un-permitted facilities may also contribute particulates that result in elevated fluxes, yet there are no regulatory programs that restrict facilities from emitting coarse particulates greater than 10 microns in aerodynamic diameter. Particulates finer than 10 microns aerodynamic diameter, or PM_{10}, are regulated on both the State and Federal levels. Air quality programs in California address some sources of toxic air pollution. However, there are two major components paramount to the deposition of metals which subsequently result in watershed impacts that are not captured in the air toxics program. The first issue is the disconnect between contaminants of concern across the different media and environmental regulations. Copper and zinc are not considered toxic air compounds of concern but are of concern in water quality. The second is the nature of these emissions, often from a large number of small unregulated businesses originating from activities such as soldering, welding, painting, brazing and scrap metal operations to name a few. The need to understand where industrial sources may be contributing to degradation of water quality is important. Water quality regulators may need to consider the daily practices of industrial activities and how their emissions may impact sub-watershed and watershed areas. Performing inventories of facility activities and establishing their proximity to receiving waters is an important factor.

Air quality and water quality are of significant importance to the public. However, the regulatory differences and pollutants of concern create a regulatory gap that allows some pollutant sources to slip through. The RWQCB regulates point source runoff and relies on the municipalities to perform industrial inspections. Storm water regulations focus on reducing pollution runoff from sites and not particulate emissions. An example is that a large industrial facility could release a significant amount of particulate matter that pollutes its own property and any property downwind of the source. The industrial facility is only required to control the runoff from its property, which they likely do as a result of the focus on controlling storm water runoff. However, a commercial facility with no industrial activities would have no reason to suspect it has a problem since it is not required to monitor for the same pollutants. Based on the buildup of these pollutants over time as a result of the industrial activities, and possibly the proximity to freeways, the facility in this example may be targeted as violating the Chollas Creek TMDL waste load allocation even though it may not be related to the source of the pollution.

As previously mentioned, the emissions may not be of concern to the San Diego Air Pollution Control District if the emissions are related to copper, zinc, or particulate matter greater than 10 microns. Copper and zinc emissions are not considered toxic air compounds (to human health via the inhalation pathway) by the Air Resources Control Board and are not regulated. However, copper is toxic to aquatic organisms and is one of the primary water quality concerns in the Chollas Creek Watershed. Water quality regulatory agencies promote controlling sources as the first step in reducing the impacts to water quality. Some of these facilities have NPDES permits regulating the runoff from their sites but not the air emissions. The importance of this gap in regulatory control is significant because it does not prevent these facilities from emitting copper containing particulates that may settle out on areas directly adjacent to the facility, and are not required to be monitored or controlled offsite by the responsible parties. These particulates will then accumulate and become the responsibility of the owner of the MS4 system (in this case the City of San Diego and other jurisdictions in the Chollas Creek Watershed). Based on this finding, the implementation of treatment BMPs to control copper and zinc may not be successful at reducing the impact of copper loading near the Mouth of Chollas Creek which the Chollas Creek Metals TMDL is intended to protect.

12.3 Recommendations

Based on the findings of this report, the City of San Diego is constrained by complying with water quality regulations with no regulatory means to control several of the sources of the pollutants. It is apparent that the 10-year compliance schedule for the Chollas Creek Dissolved Metals TMDL implementation plan is unrealistic without controlling the aerial deposition sources, too.

Nearly every water quality professional, educator or regulatory agency will state that "Controlling storm water pollution is best addressed by controlling the pollution source." Involvement with the Brake Pad Partnership may help in influencing manufacturers and regulatory agencies to require product formulation changes to eliminate copper from brake pads. In addition, pursuing legislative routes to address the inconsistencies between air quality and water quality regulations may also prove useful at inducing positive long-term changes in

environmental policy. In a final report to the Santa Monica Bay Restoration Project (Stolzenbach et al., 2001), researchers stated the following implications for management options; *"Reductions of non-point source inputs may require a coupling between air quality and water quality regulatory actions and policies. For metals, the most important sources of emission to the atmosphere appear to be non-permitted area sources, which may be relatively difficult to regulate."* Five years later, this study has arrived at similar conclusions. It is evident that copper and zinc emissions from industrial, commercial, construction, and other sources will only be reduced via regulatory means. While awareness of this issue is observed, little to no regulatory change has occurred to reduce these emissions containing large particles, copper, or zinc.

This is not to say there are not actions the City can implement. The City may be able to reduce the amount of particulate matter available to runoff into water bodies from roadways and impervious surfaces using a variety of BMPs. Examples of BMPs that may reduce particulate matter (and metals) from entering the storm drain systems were discussed in depth in the Chollas Creek Source Loading, Best Management Practices, and Monitoring Strategy Assessment Report (Weston, 2006). These BMPs included focused street sweeping, low impact design to reduce the volume of water and flow rates. However, the effectiveness of these BMPs must be measured to ensure a positive beneficial reduction of the target pollutants, with consideration of the operations and maintenance.

BMPs focused on removing particle sizes greater than 10 microns in size may have the greatest success in reducing the concentrations of zinc found in roadway dust and subsequently urban runoff. Additional benefits may be gained by removing smaller particles, but with diminishing returns on a cost per benefit relationship as the particle size decreases below 5 microns. Large particles containing lead and copper may also be reduced by implementing these BMPs. However, copper associated with brake-pad wear is less likely to be removed effectively without using treatment train BMPs as mentioned in the Chollas Creek Source Loading, Best Management Practices, and Monitoring Strategy Assessment Report (Weston, 2006).

These key findings lead to the following recommended management actions with regard to storm water management and meeting load reductions under current and future TMDLs in the City of San Diego watersheds.

It is recommended that:

- tiered best management practice (BMP) presented in the Chollas Creek Source Loading, Best Management Practices, and Monitoring Strategy Assessment Report (Weston, 2006) be implemented with the first tier emphasizing source controls, pollution reduction measures, and source identification studies. Source control measures are recommended to be the current focus over storm water treatment BMPs at this phase to reduce loads;
- The City participate in product substitution efforts through involvement with the Brake Pad Partnership to reduce the load of metals to storm water and receiving waters;
- Inspections and monitoring of metal-related industries (both water quality and air quality monitoring) be increased based on the recommendations in the Chollas Creek Source Loading, Best Management Practices, and Monitoring Strategy Assessment Report, and this report, to identify higher loading facilities and ensure compliance with applicable storm water and air pollution control regulations;

- The Regional Water Quality Control Board partner with the Air Resources Control Board and the Environmental Protection Agency to further define the source contributions from industrial emissions to water quality and determine if additional measures are needed in cases where facilities are meeting current water quality regulations;
- The Chollas Creek Dissolved Metals TMDL re-evaluate the contribution of aerial deposition.

The following recommendations are presented as options that may be useful in reducing the impacts from aerial deposition:

- Perform "windshield surveys" and collect inventories of facilities within areas that show elevated fluxes. With the inventories that are obtained, the San Diego Air Pollution Control District can then implement programs to reduce industrial particulate emissions, engage business owners to maintain clean facilities, and possibly implement low cost BMPs within areas exhibiting elevated fluxes.
- Based on the lead results, source identification studies (e.g., soils investigations or facility inspections) may prove useful in determining sources of lead in the Chollas Creek Area.
- Enhance the industrial facilities inspection program by coordinating with educational programs that provide informational material about air pollutants within areas exhibiting elevated depositional fluxes.
- The City can also implement focused street sweeping programs in subwatershed areas that show elevated fluxes that may be a result of resuspended dust from surface streets. This focused street sweeping should be done with consideration of the buildup rate of pollutants of concern prior to rainfall.
- The water quality modeling efforts conducted under this study could also be expanded to predict the effectiveness of the BMPs recommended prior to implementation in specific subwatersheds.
- Air dispersion modeling could also be expanded to estimate the flux contributions from industrial sources and roadways.
- Analysis of roadway dust may also prove useful in determining the fingerprints of surface dust from source areas available for re-suspension.
- Strategic collection of deposition sample sets over a year-long period in high-flux areas would facilitate more conclusive identification of sources influencing deposition using only chemical analysis. Such a data set would also provide valuable information on flux variability over time for water quality modeling, as well as a means for gauging trends in deposition as BMPs and other beneficial practices are implemented.

Education and outreach to area residents and business may also be effective at inducing positive changes throughout the City. This outreach would be targeted at reducing the amount of aerial particulates that may be emitted. Recommended practices that may reduce particulate emissions and provide additional environmental benefits are provided as follows:

- Raising awareness of the issues in the Chollas Creek Watershed
- Using broom sweeping or raking as opposed to leaf blowers
- Using electric lawn mowers

- Promoting bike-to-work, carpooling or mass transit use
- Keeping your car in good working condition, keeping tires inflated, and changing tires when needed
- Ask for copper free brake pads during replacement (though these may not be available, it can't hurt to ask and get the ball rolling)
- Support the smog check program
- Preventing the sanding of boat hulls in the open air in the vicinity of Shelter Island
- Shifting from copper based antifouling paint
- Painting using rollers and brushes as opposed to high pressure sprayers
- Painting in a controlled environment
- Using wet sanding techniques or using HEPA filtered vacuum sanders
- Promote wet sawing of concrete/tile/stone as opposed to dry cutting
- Encouraging businesses to reduce their emissions to the atmosphere
- Encouraging businesses to increase general facilities housekeeping

The challenge the City faces is there are currently no regulatory mechanisms to control many of these emissions and wear processes. Brake pads will continue to contain copper until the manufacturers are required to, or agree to, change their product formulations. Tires, fan belts, and other rubber products will continue to contain roughly 1% zinc as a function of the vulcanization process of rubber. Galvanized metals will continue to weather and erode. Residual lead concentrations in soil will continue to decline, but will continue to erode, resuspend, redeposit, and be found in urban runoff for some time. In the case of lead, it has taken well over 20 years to see a reduction in the background soils concentrations as a result of the elimination of leaded gasoline. Similar to lead, this process would also be replicated if copper was eliminated from brake pads. Emissions of non-regulated airborne particulates (e.g., those greater than 10 microns, and also particulates containing copper and zinc) will continue until air quality regulatory agencies acknowledge the impacts to water quality and the public welfare. Given these findings, source control measures that include bridging regulatory gaps are recommended to be the current focus over storm water treatment BMPs at this phase in meeting the Chollas Creek TMDL requirements.

11.0 BUILDUP/WASH OFF MODELING

One primary reason for performing the aerial deposition study is to determine the relationship between the particles that settle out on surfaces and subsequently wash off during storm water events. Depending on rainfall amount and intensity, aerially deposited particles will primarily be washed off impervious surfaces such as roadways, sidewalks, parking lots, plants, and rooftops. A recent atmospheric deposition study conducted in Los Angeles concluded that aerially deposited trace metals accounted for 57 – 100% of the total trace metal load in storm water run off (Sabin et al., 2005). Chollas Creek typically only flows during rainfall events, or during releases of imported water from irrigation, car washing, or other activities during dry weather. Over the past 68 years, Chollas Creek has been modified, diverted, or channelized in several locations primarily for flood control purposes as was discussed in the Chollas Creek Source Loading, Best Management Practices, and Monitoring Strategy Assessment Report (Weston, 2006). The impervious nature of the Chollas Creek Watershed made it a good candidate for estimating wash off concentrations from aerial deposition.

The purpose of this section is to determine how the predicted wash off concentrations from modeling compare to the measured water quality concentrations observed in the North fork of Chollas Creek.

11.1 Examples of Storm Water Runoff

This sub-section is presented for illustrative purposes only. Storm water samples were collected under a separate monitoring program during a rainfall event on 12/10/06. The samples were collected from four of the study areas within the City of San Diego. The samples were collected as part of water quality permit monitoring requirements and are shown in Figure 11-1 to illustrate the visual appearance of the samples. The four samples from left to right are Los Peñasquitos Creek, Tecolote Creek, the North fork of Chollas Creek [site SD8(1)], and the South fork of Chollas Creek [site DPR(2)].

Figure 11-1. Picture of storm water samples collected on 12/10/06 from four study areas as part of permit monitoring requirements.

Of the four samples shown in Figure 11-1, the air deposition results have shown some of the highest net deposition rates and highest metals flux rates occur near the SD8(1) site. Within this group, Tecolote Creek had a relatively high net deposition rate but relatively few metals detections. Site DPR(2) had lower net flux yet had higher metals fluxes, and lastly, the Mira Mesa site which drains to Los Peñasquitos Creek had lower net flux but variable metals fluxes.

11.2 Model Selection

The EPA Storm Water Management Model (SWMM) was chosen to model the impact of air deposition on water quality in the Chollas Creek Watershed. The EPA SWMM is a dynamic rainfall-runoff simulation model used for single event or long-term (continuous) simulation of runoff quantity and quality from primarily urban areas. The runoff component of SWMM operates on a collection of subcatchment areas that receive precipitation and generate runoff and pollutant loads. The routing portion of SWMM transports this runoff through a system of pipes, channels, storage/treatment devices, pumps, and regulators. SWMM tracks the quantity and quality of runoff generated within each subcatchment, and the flow rate, flow depth, and quality of water in each pipe and channel during a simulation period comprised of multiple time steps (EPA, 2007). Pollutant land surface buildup and wash off mechanisms are built into SWMM.

11.3 Methods

11.3.1 Setup

Setting up the SWMM model required obtaining land use and topography information for the Chollas watershed. ESRI's ArcGIS9.2 geographic information system software was used to gather and analyze watershed information.

A high resolution 3-meter radar-based digital elevation model (DEM) called IfSAR was obtained from NOAA. Interferometric Synthetic Aperture Radar (IfSAR) is an aircraft-mounted sensor designed to measure surface elevation, which is used to produce topographic imagery. The MS4 system for the City of San Diego was then "burned" into the DEM so depressions were created where storm drains were present. The DEM was then processed in ArcGIS to remove artificial "sinks" or depressions that would interrupt water flow and cause problems in catchment delineation and modeling later on.

Using the ArcHydro extension for ArcGIS, slope and natural flow pathways were calculated from the DEM. This information was then used to create 14 subwatersheds in the Chollas Creek Watershed (Figure 11-2). These subwatersheds, along with flow pathways, form the basic objects used in the SWMM model. Basic information of the subcatchments and flow conduits such as average slope, area, and lengths were calculated using ArcGIS. Land use data (SANDAG, 2006) was then brought into ArcGIS to calculate estimates of the subcatchments' imperviousness.

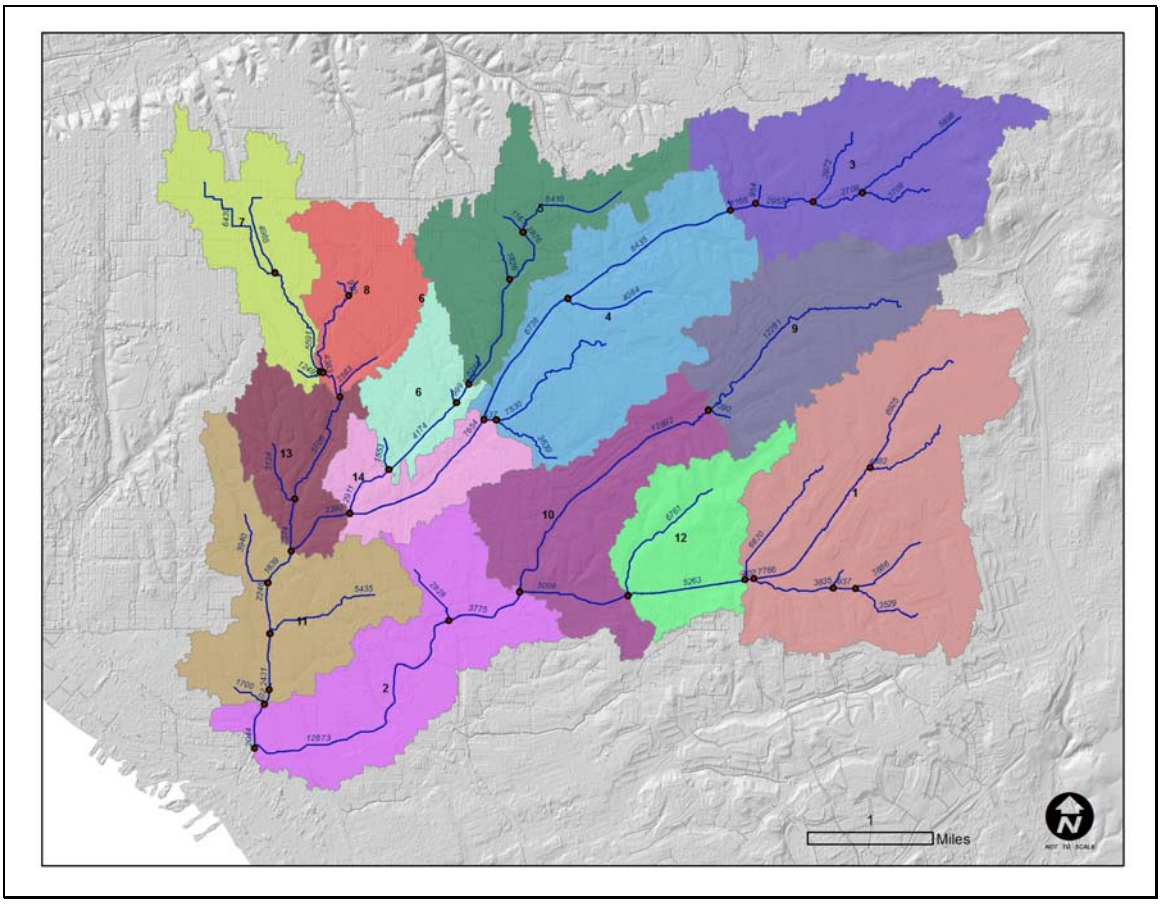

Figure 11-2. Chollas Creek SubWatersheds

11.3.2 Hydrologic Calibration

Once the estimates of the subcatchments hydrologic parameters were calculated from the GIS, the parameters were then calibrated to measured data. The October 14, 2006 hydrograph storm event was used for calibration (Figure 11-3). The Genetic Algorithm Based Calibration Tool in PCSWMM was used to calibrate the hydrologic data. This algorithm created several different scenarios with different parameter values of imperviousness, storage, roughness, and overland flow width. Different scenarios are paired together to create "offspring" scenarios using some parameter values from each "parent" scenario. This process is then repeated with child scenarios, with the least error surviving. In this way, a properly calibrated scenario with adjusted parameter values "evolves."

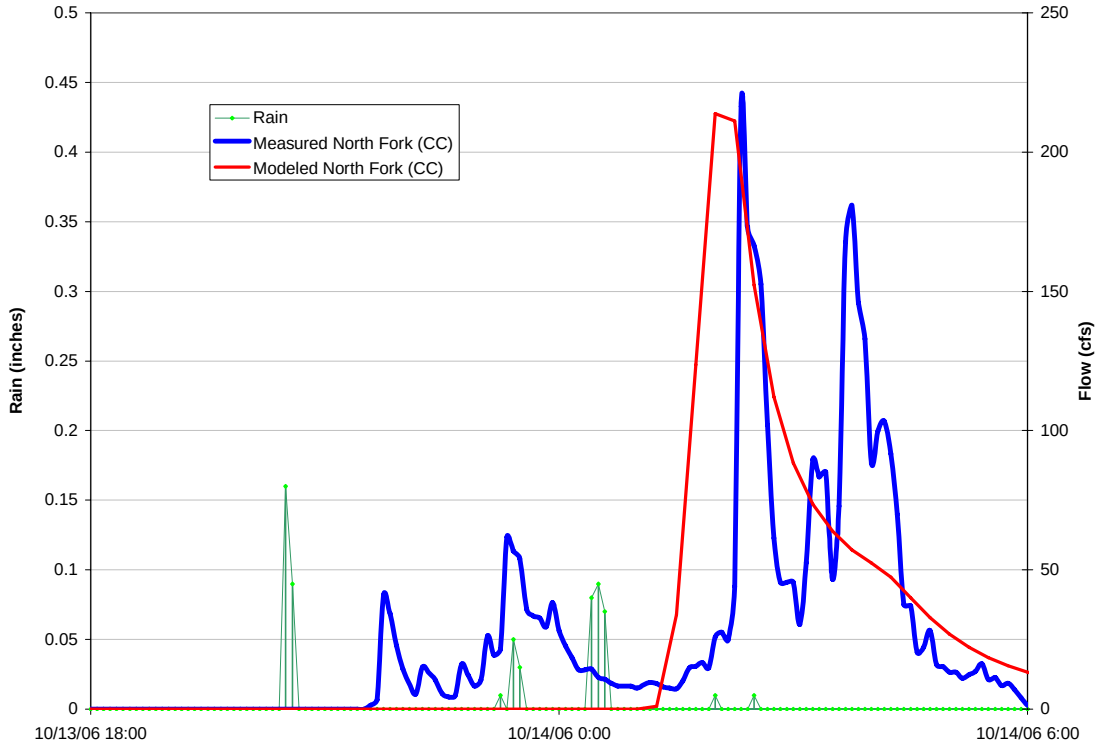

Figure 11-3. October 14, 2006 Storm Event Hydrograph.

11.3.3 Pollutant Buildup and Wash Off Calibration

Figure 11-4 illustrates the buildup and wash off process that was modeled in SWMM. The chart is based on storm water quality measurements and estimates of copper buildup and wash off in the north fork of the Chollas Creek Watershed for a year starting in February 2006. The majority of the buildup can be seen occurring during the dry summer months. The drop in pollutant load shown in the figure occurs during the wash off resulting from a storm event. A reduction in pollutant load would also result from activities such as street sweeping. It is common to model the buildup and wash off processes with the functions described below. The coefficients are calibrated with actual water quality data. The calibrated data is then checked against additional measured data that was not used in the calibration for verification of the results.

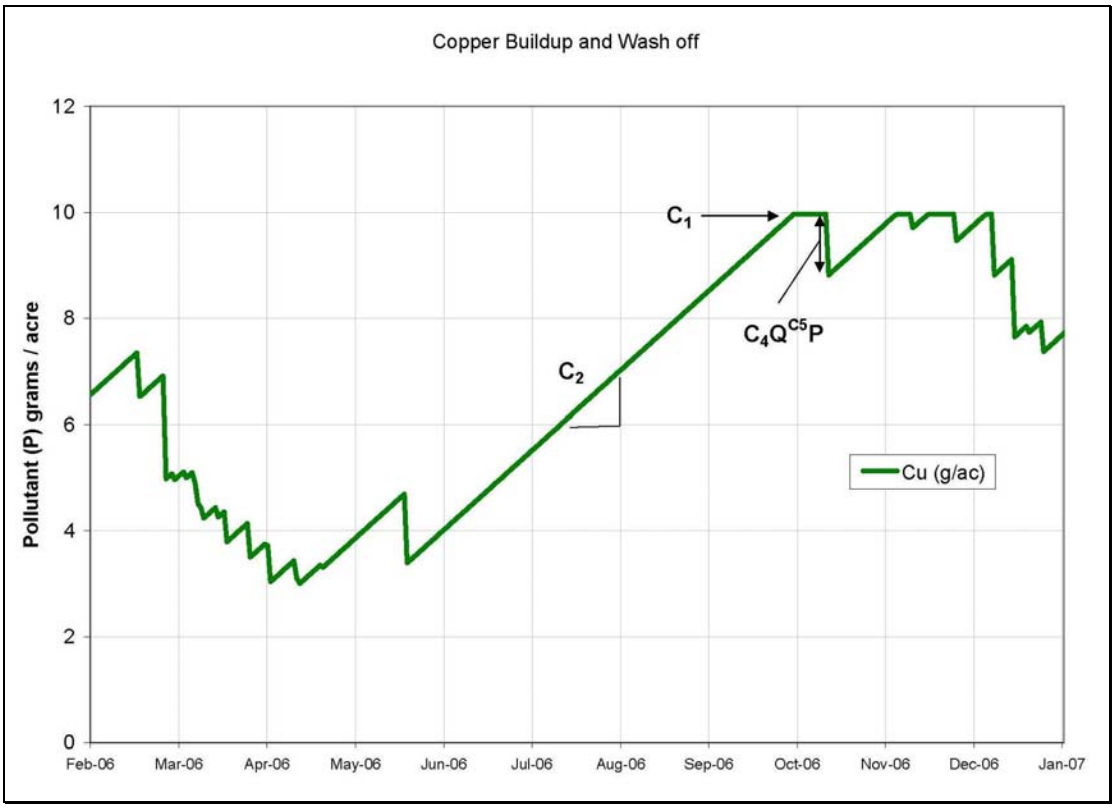

Figure 11-4. Pollutant Buildup and Wash Off Process.

A power function was used to model the buildup process.

$$P = \text{Min}(C_1 , C_2 T^{C3})$$

where C_1 = maximum buildup possible per acre
C_2 = buildup rate constant, and
C_3 = time exponent.

In the above equation, the buildup rate constant (C_2) is estimated for each subwatershed from the air deposition results discussed earlier. The mean daily air deposition flux rates found in this study are plotted in Figure 11-5. These rates were interpolated across the Chollas Creek Watershed to calculate buildup rate estimates for each subwatershed and are shown in Table 11-1. The maximum buildup is assumed to be approximately ten times the buildup rate. Because the air deposition rate is assumed to be linear based on the results observed in this study, C_3 is set to one.

The measured lead buildup flux rate was frequently below the variable detection limit of around 3-10 micrograms per square meter per day. Therefore, the flux rate in these cases was conservatively assumed to be equal to the detection limit. The actual lead buildup would be somewhat lower.

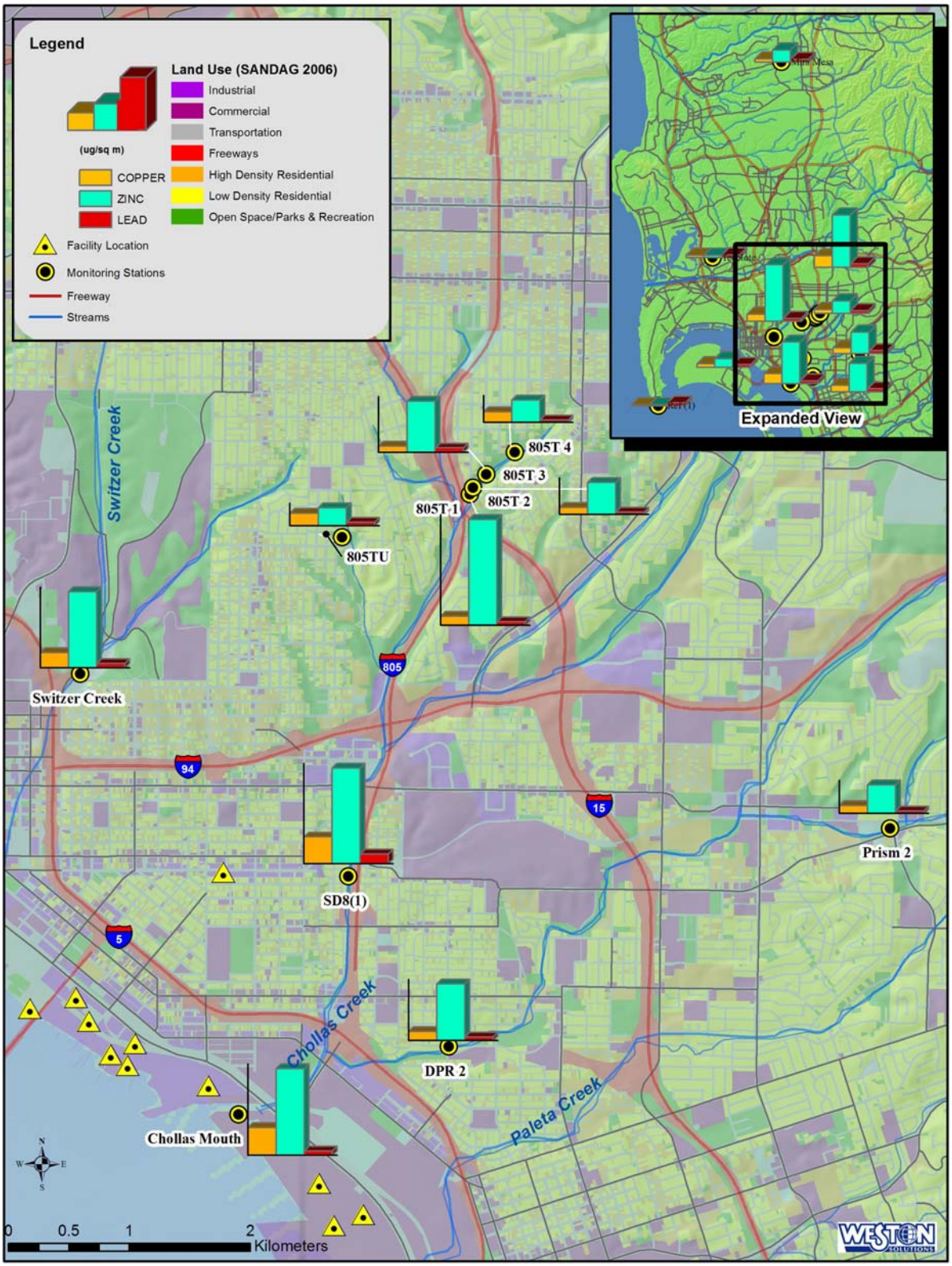

Figure 11-5. Mean Measured Air Deposition Rates.

Table 11-1. Buildup Rates by SubWatershed (kg/ac*d).

Catchment	Copper	Lead	Zinc
1	0.049	0.017	0.211
2	0.057	0.02	0.267
3	0.049	0.017	0.223
4	0.049	0.017	0.219
5	0.045	0.016	0.219
6	0.04	0.015	0.219
7	0.045	0.017	0.223
8	0.04	0.015	0.211
9	0.053	0.017	0.215
10	0.045	0.015	0.186
11	0.085	0.029	0.324
12	0.04	0.014	0.17
13	0.053	0.018	0.211
14	0.049	0.017	0.243

Pollutant wash off was modeled using an exponential function.

$$W = C_4 Q^{C5} P$$

Where C_4 = wash off coefficient,
C_5 = wash off exponent,
Q = Runoff rate per unit area
P = pollutant buildup

The wash off load is assumed to be proportional to the runoff rate raised to some power and then multiplied by the pollutant buildup. The wash off coefficient was assumed to be 0.9 based on a typical storm in an urban watershed (Butcher, 2003). The wash off of pollutants has been found to be nearly linear in relation to flow (Barbe, 1996). Therefore, the wash off exponent was assumed to be one. At this time, there is not sufficient data to calibrate these parameters. Pollutographs, which are based on discrete water quality measurements taken at several times during a storm, are needed to do an adequate wash off calibration. This data should be available, however, in the near future at the conclusion of a Chollas Creek Study currently being conducted by the Southern California Coastal Water Research Project.

A calibrated SWMM model can give predictions of storm water flow and pollutant concentrations over time. Figure 11-6 shows the hydrograph and pollutograph results of a model run for the north fork of Chollas Creek. Because the wash off parameters could not yet be adequately calibrated without additional data, modeled pollutant variability during a storm is not discussed. However, total wash off estimates based on 13 years of event mean concentrations are discussed below.

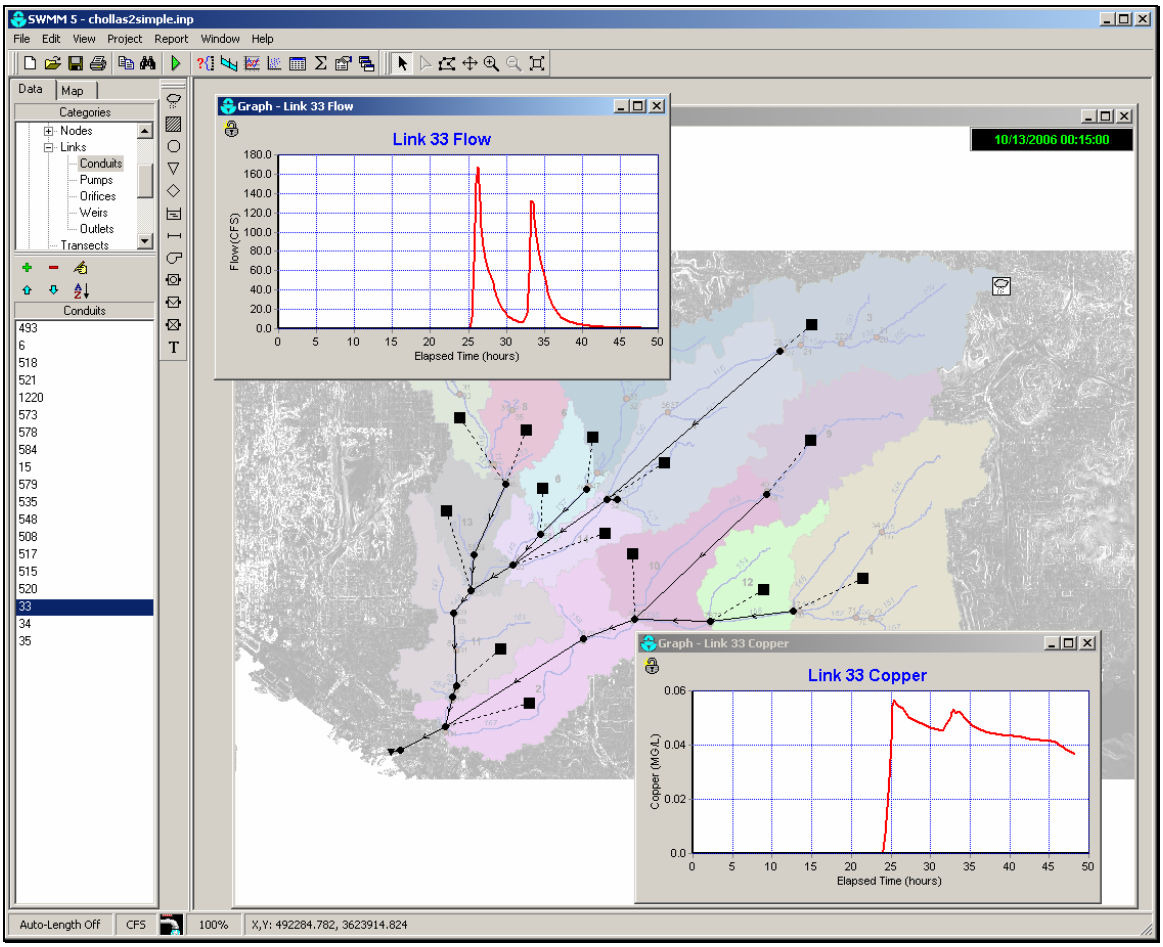

Figure 11-6. Chollas Creek SWMM model.

11.4 Buildup and Wash Off Load Estimates

Figure 11-7 shows estimates of the typical metal loads that are built up and washed off in a typical year within the Chollas Creek Watershed. The range bars in Figure 11-7 indicate the ranges between the 25th percent and 75th percentiles of the load estimates and give an indication of the variability found at each site. Because the buildup load is based on spatially interpolated aerial deposition rates found in this year's study, the temporal variability may be greater. The wash off rate was estimated based on storm water mass loading station data from both the 2005/2006 storm season and historical information on storm water pollutant concentrations in Chollas Creek from 1993 to 2006.

According to the buildup and wash off load estimates, the copper load that is built up in the Chollas Creek Watershed is *greater than* the wash off load estimate. Therefore, during a typical year, it appears that copper from aerial deposition could account for most, if not all of the washed off load.

In contrast, the lead load that is built up in the watershed is *less than* the typical lead load that is washed off. Therefore, is appears that the lead pollutant load in storm water may be coming

from some sources other than aerial deposition. Soil may also be a source of lead pollution within the Chollas Creek Watershed. Over time, area soils may have accumulated and sequestered lead from leaded gasoline use and decay of lead-based paints. The lead is likely being released gradually over time during storm events.

The zinc load that is built up is generally more than is estimated to wash off in a typical year. However, the wash off load for zinc is highly variable. During the 2005/2006 storm season, more zinc load is estimated to have washed off than was built up during the previous year, therefore it appears that zinc from aerial deposition could account for most, if not all, of the washed off load.

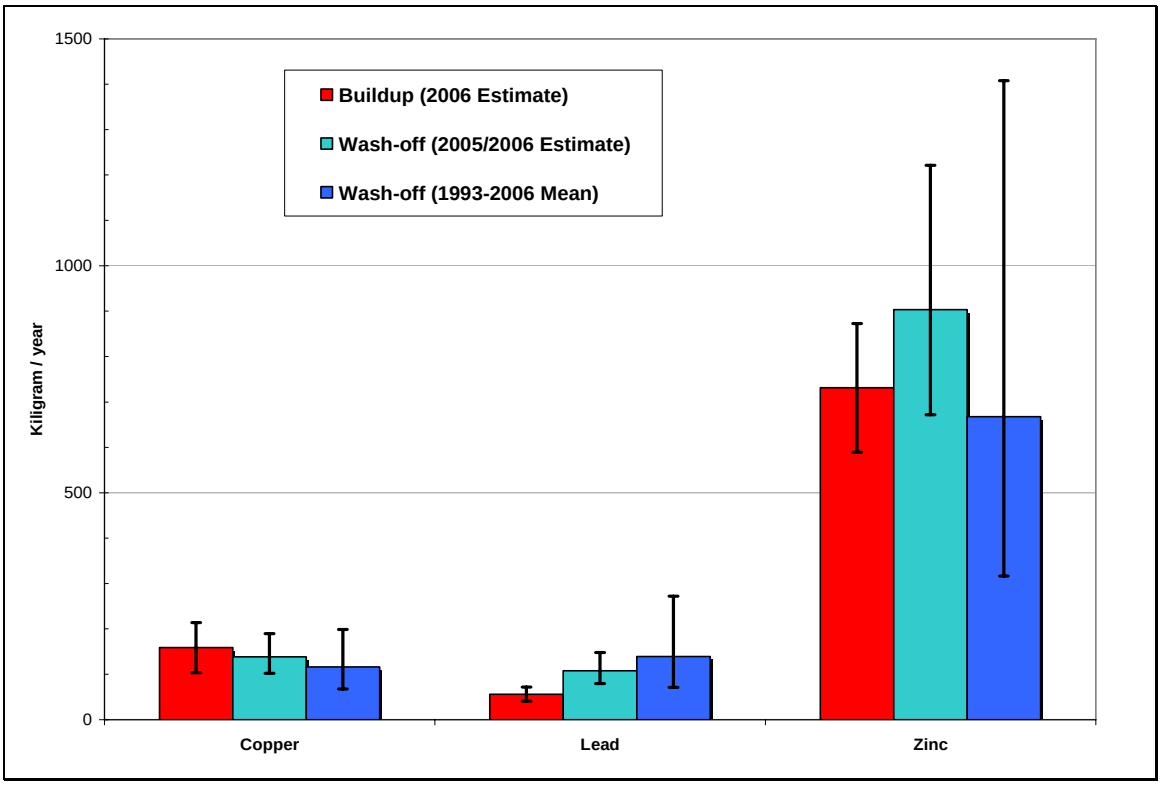

Figure 11-7. Chollas Creek Watershed Buildup and Wash Off Load Estimates

Another way to compare the buildup and wash off estimates is to calculate wash off concentrations and the estimated buildup contributions to these concentrations. Figure 11-8 shows recent and historical event mean pollutant concentrations. The red bar shows the concentration amount that could be accounted for by the recently measured air deposition rates. The copper and zinc concentrations could be accounted for by the air deposition rates. The lead air deposition can only account for a fraction of the wash off concentrations.

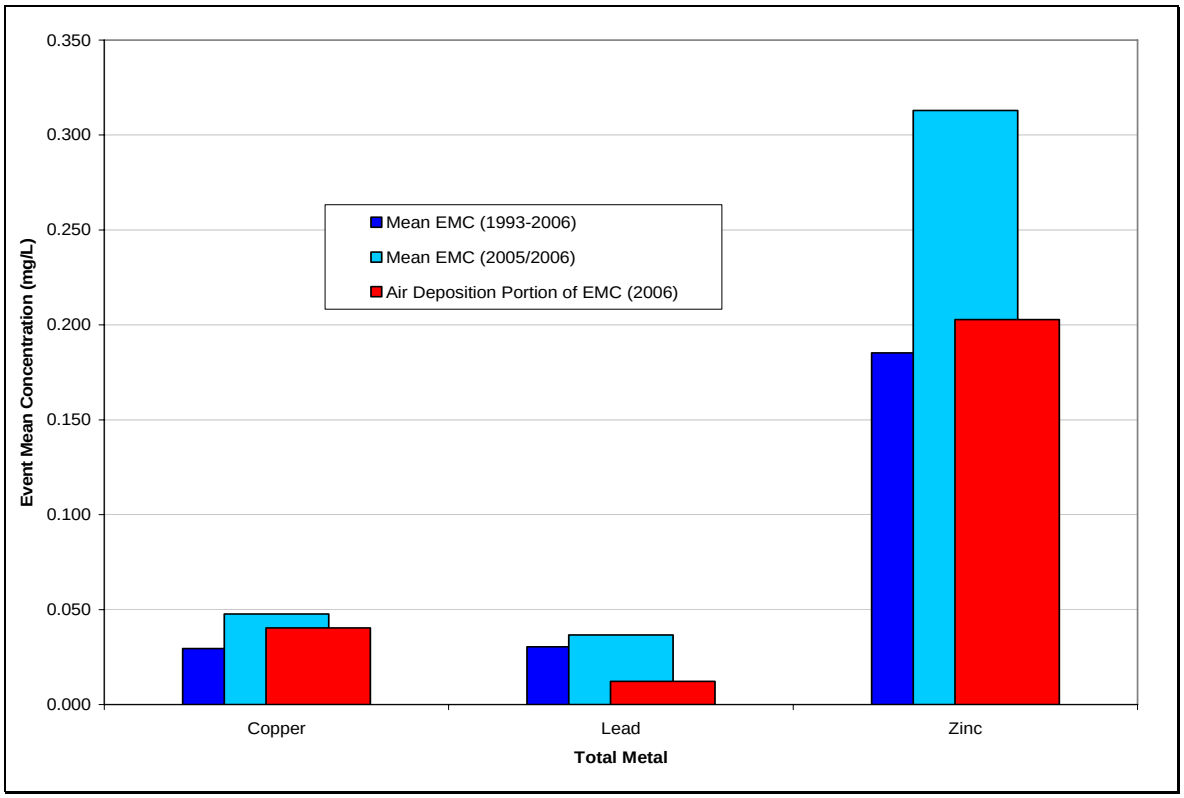

Figure 11-8. Chollas Creek Watershed Buildup and Wash Off Load Estimates

Given the buildup and wash off assumptions and estimates above, an estimate of the resulting storm water metal concentration can be computed. This estimate assumes 90 percent of the built up pollutants will be washed of in a 0.2 inch rainstorm. This simplified comparison of the resulting metals concentrations from buildup and wash off estimates are compared to historic event mean concentrations in Figure 11-9. The amount of copper and zinc that is built up and washed off from aerial deposition after approximately one week is comparable to the historic event mean concentrations measured at the SD8(1) monitoring location. It takes approximately 20 days for aerial lead deposits to buildup sufficient lead to supply the concentrations typically measured in runoff during storm events.

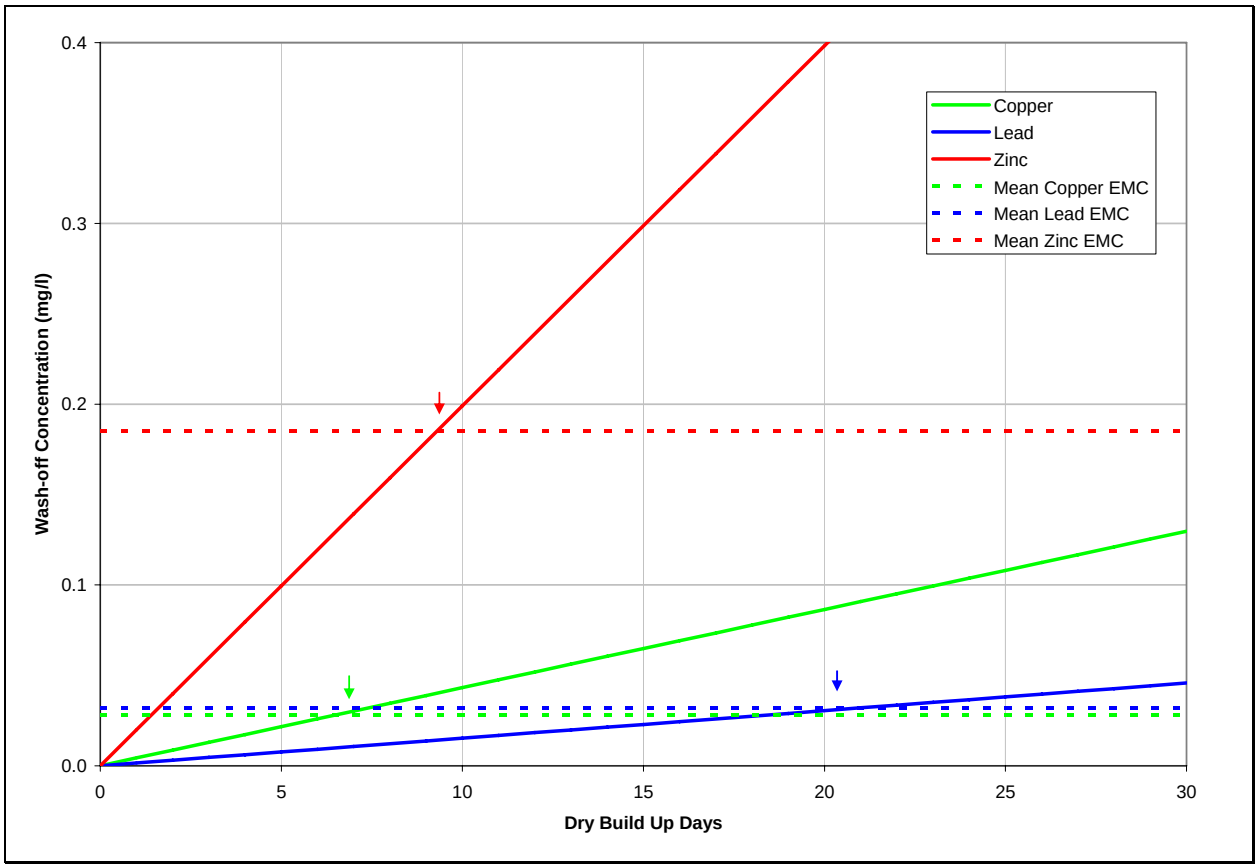

Figure 11-9. Chollas Creek Watershed Pollutant Buildup/Wash off Compared to Mean Event Mean Concentrations.

11.5 Buildup/Wash Off Modeling Summary

Particulates and associated metals can buildup across large portions of land within a watershed through aerial deposition. As storm events occur, these particulates are washed off and end up in local creeks.

Predicted metal event mean concentrations (EMC) values fell within the range of historic metals concentrations when using the SWMM model to calculate the buildup and wash off process in the Chollas Creek Watershed. It appears that aerial deposition accounts for the majority of the total copper and zinc, and less than half of the lead measured in storm water. This indicates that other sources are likely contributing to quantities of lead, possibly from erosion of soil with elevated lead that does not typically get suspended in the air.

There appears to be a strong link between the aerial deposition flux and the measured water quality concentrations in Chollas Creek. It is apparent that controlling the sources of air deposition may improve water quality. However, the processes of buildup and subsequent wash off are not well understood. Factors such as surface roughness, accretion/cohesion, gradient, and surface area are highly variable and may vary from one area to another. Additional modeling work is recommended in the future in order to accurately simulate a variety of storm events and to verify buildup and wash off parameters.

10.0 INDUSTRIAL EMISSIONS INVENTORIES

During the course of this study, it was evident that higher metal deposition rates were occurring in the lower subwatershed areas of Chollas Creek. Investigation of emission data revealed that several facilities in the San Diego Region report emission data to the Air Resources Control Board.

The Air Toxics "Hot Spots" Information and Assessment Act (AB 2588, 1987, Connelly) was enacted in September 1987. The act requires stationary sources to report the types and quantities of certain substances their facilities routinely release into the air. This information is readily available for the San Diego Region on the California Air Resources Board (ARB) Community Health Air Pollution Information System (CHAPIS) website (http://www.arb.ca.gov/ch/chapis1/chapis1.htm). Additional emissions inventories were also obtained from the San Diego Air Pollution Control District's website (http://www.sdapcd.org/toxics/Project1/SourceEmissions.html). Emissions inventories of industrial sources from four generalized areas were evaluated. The four generalized areas were Chollas Creek, Point Loma, Tecolote, and Mira Mesa. Emission sources within each of the four areas are summarized below in Table 10-1. It should be noted, however, that facilities which were not required to report their annual emissions were not included as part of the data set used to generate the tables and figures presented in this section.

Table 10-1. Industrialized emission sources within four study areas in the San Diego Region.

Area	Facility	Address
Chollas Creek	Applied Energy - Naval Station	USN Nav Sta 32nd St., San Diego, Ca 92135
	CP Kelco	2025 Harbor Dr E., San Diego, Ca 92113
	National Steel & Shipbuilding	28th St & Harbor Dr., San Diego, Ca 92113
	Southwest Marine Inc.	Foot Of Sampson St., San Diego, Ca 92113
	USN 32nd St. Naval Station	Naval Station, San Diego, Ca 92136
	Cabrillo Power II LLC Naval St	Vista St & Ward Rd Navsta Gt., San Diego, Ca 92136
	Cabrillo Power II LLC Division	3200 Harbor Dr Division Gt., San Diego, Ca 92113
	Staite R E Engineering	2140 Tidelands Ave., National City, Ca 91950
	Continental Maritime	1995 Bay Front St., San Diego, Ca 92113
	Millbrook Baking Co - San Diego	1955 Julian Ave., San Diego, Ca 92113
	North Star Propeller, Inc.	2285 Newton Ave., San Diego, Ca 92113
	Isp Alginates Inc	2145 Belt St E, San Diego, Ca 92113
Point Loma	S. D. City Pt. Loma Waste Water	1902 Gatchell Rd., San Diego, Ca 92106
Tecolote	Univ. of San Diego	5998 Alcala Park, San Diego, Ca 92110
	Sea World Inc.	500 Sea World Dr., San Diego, Ca 92109
Mira Mesa	Hanson Aggregates - Carroll Ca	9255 Camino Santa Fe, San Diego, Ca 92121
	Cabrillo Power II LLC Miramar	6897 Consolidated Way Miramar G, San Diego, Ca 92121

A summation by area of the emissions inventories from the sources listed in Table 10-1 are provided in Table 10-2 in order to compare the amount of the total particulate matter, particulate

matter less then 10 µm, particulate matter less than 2.5 µm, and selected metals such as copper, lead, and zinc between the areas. Because these emission figures are based solely upon the relatively few industrial facilities that were required to provide detailed emission reports, they may significantly underestimate actual aerial emissions in these areas. Emissions inventories are presented graphically in Figure 10-1.

Table 10-2. Reported yearly emissions from San Diego area sources

Area	PM/TSP	PM_{10}	$PM_{2.5}$	Chromium	Copper	Lead	Manganese	Nickel	Zinc
	Tons/Yr	Tons/Yr	Tons/Yr	Lbs/Yr	Lbs/Yr	Lbs/Yr	Lbs/Yr	Lbs/Yr	Lbs/Yr
Chollas Crk	65.1	65.0	57.9	87.3	4214.4	25.4	365.4	109.8	926.6
Pt. Loma	11.3	11.3	11.2	0	0	0	0	0	0
Tecolote	1.5	1.5	1.5	0	0	0	0	0	0
Mira Mesa	245.1	102.1	75.5	15.2	17	19.1	97.8	11.8	58.5

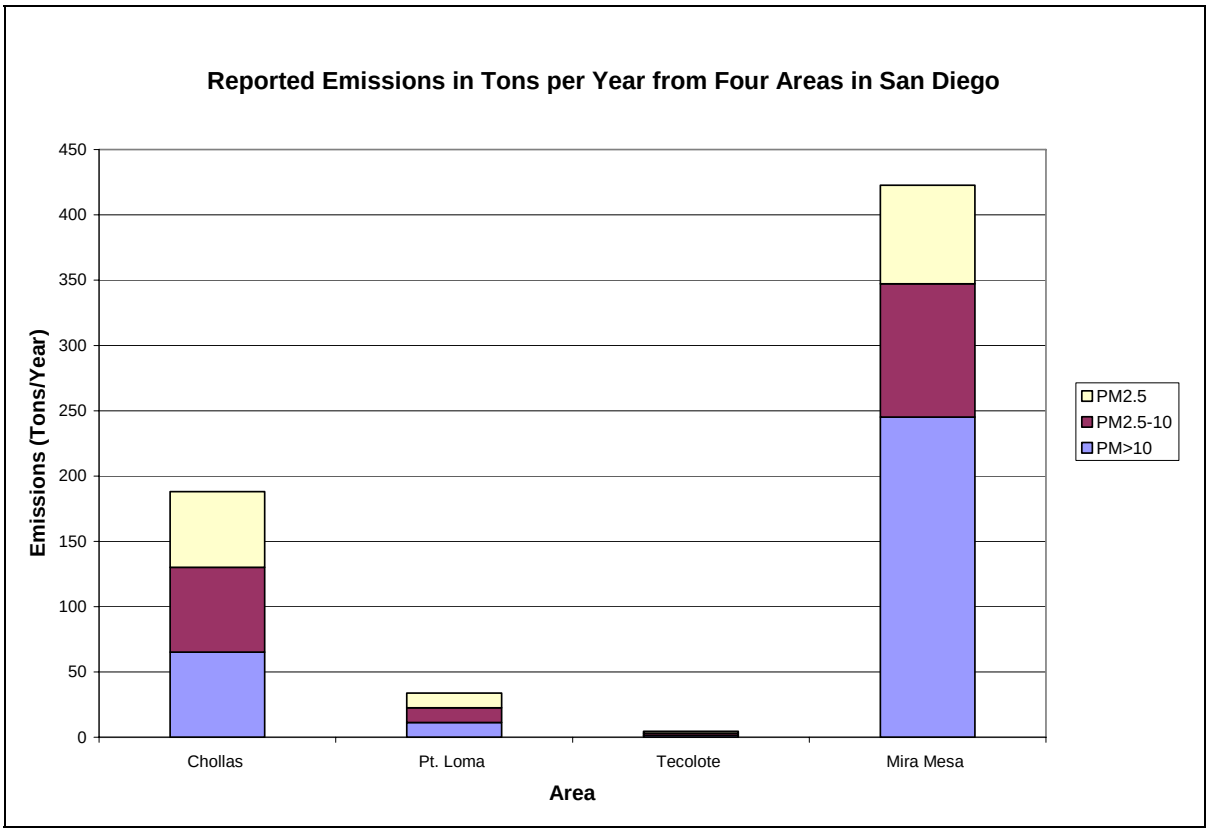

Figure 10-1. Yearly emission inventory of particulates from facilities residing within the four study areas in San Diego.

Yearly emissions data from those sources listed in Table 10-1 indicate that among the four study areas, Mira Mesa had the greatest amount of total emissions (245.1 tons/year). Of the total emissions within Mira Mesa, 75.5 tons of particulate matter was 2.5 µm or less in size, while 26.6 tons of particulate matter was in the $PM_{2.5\text{-}10}$ size class (between 2.5 µm and 10 µm in size).

Chollas Creek facilities reported releasing 65.1 annual tons of total suspended particulate matter (TSP), comprised of 57.9 tons in the $PM_{2.5}$ size class (less than 2.5 µm in size), and 7.1 tons that were in the $PM_{2.5-10}$ size class. Aerial emissions in the Point Loma area, which had only one facility reporting emissions data, were significantly lower than both the Mira Mesa and Chollas Creek areas. Point Loma emissions were reported to be 11.3 tons per year of TSP, 99 percent of which were particulates in the $PM_{2.5}$ size class. Within the Tecolote area, TSP was reported to be 1.5 tons per year, of which 100 percent was less than 2.5 µm in size. It should be noted that because some facilities may have only reported emissions in the $PM_{2.5}$ range and/or in the PM_{10} range, particulates greater than 2.5 µm and 10 µm in size may be underrepresented. However, sources emitting exclusively or primarily $PM_{2.5}$ may be indicative of fuel combustion sources such as boilers. Therefore, facilities with only combustion sources would be expected to have a majority of particulate emissions as $PM_{2.5}$.

As discussed above, the available emission inventories reviewed in this study revealed that the Mira Mesa area had the largest industrial emissions of total particulate material, followed by Chollas Creek, Point Loma, and Tecolote. While the total particulate emissions from the facilities in the study areas were high at Mira Mesa (245 tons/year) and Chollas (65 tons/year), they are considerably lower than the overall total particulate emissions from all sources combined county-wide. The SDAPCD reports that an estimated 15,300 tons of toxic air contaminants are emitted annually in San Diego County (note that large particulate matter (>10 µm) in general is not considered a toxic air contaminant). Of all airborne contaminants, automotive sources emit 70 percent, consumer products and architectural sources are responsible for emitting approximately 17 percent, the 200 large industrial facilities and 1,600 smaller businesses emit roughly 10 percent, and 3 percent are from wildfires (SDAPCD, 2006).

Metals emissions

Metals emissions from the four study areas in San Diego are presented in tabular form in Table 10-2, and graphically in Figure 10-2. Point Loma and Tecolote facilities did not report emissions of any metals in data spanning the years 1997 through 2004. Although emissions data from multiple years was examined, only the most recent data for a given facility was used to calculate emissions totals for this report. The Chollas Creek area had by far the highest reported metals emissions of any of the four study areas. Total metals emissions in the Chollas Creek area were 5,730 pounds per year. Of this total, copper represented 73.5 percent of the metals emissions, or 4,214.4 pounds per year. Zinc emissions (926.6 lbs./yr) were the second leading metal released by Chollas area facilities, followed by manganese (356.4 lbs./yr), nickel (109.8 lbs./year) chromium (87.3 lbs./yr), and lead (25.4 lbs./yr). Mira Mesa had relatively low metals emissions when compared against the Chollas Creek area. Total metals emissions at Mira Mesa equaled 219.4 pounds per year. Of this amount, 45 percent was comprised of manganese, 26 percent was comprised of zinc, 9 percent was comprised of lead, and the remaining 20 percent was comprised of nearly equal amounts of copper, chromium, and nickel.

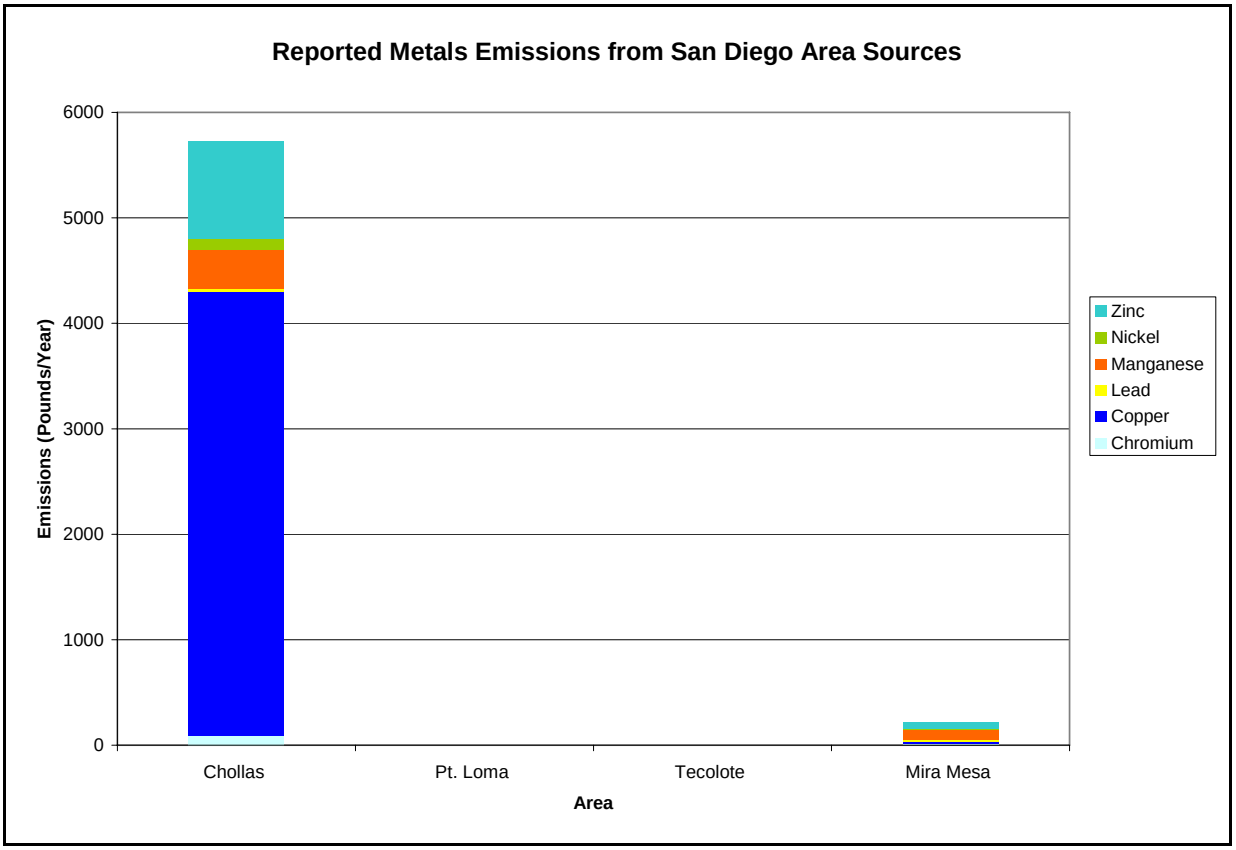

Figure 10-2. Metals emissions in pounds per year reported by area facilities within San Diego

Comparison of Facility Emissions to Roadway Emissions

In an effort to quantify and compare roadway and industrial emissions in the area surrounding Chollas Creek, total industrial emissions, reported by facilities located within a 4km radius of the Chollas Creek Mouth, were summed and compared against estimated emissions from roadways in the same 4km area. Roadway emissions factors in grams per vehicle mile by source type and particle size ranges were determined based upon EPA (AP-42 Paved Roadways) and ARB (EMFAC, 2002) specified methodologies detailed in Section 9 and Appendix D of this report. Roadway emissions were broken down into four categories: brake wear, tire wear, exhaust, and re-entrained dust. Emissions calculations assumed 15.82 miles of freeway (used by a total of 170,000 vehicles per day) and 25 miles of commercial roads (used by 55,000 vehicles per day) within the 4km study of the mouth of Chollas Creek (Figure 10-3 and Figure 10-4). Industrial emissions were based upon emissions data reported to the San Diego Region of the California Air Resources Board by the ten facilities within the 4km study area.

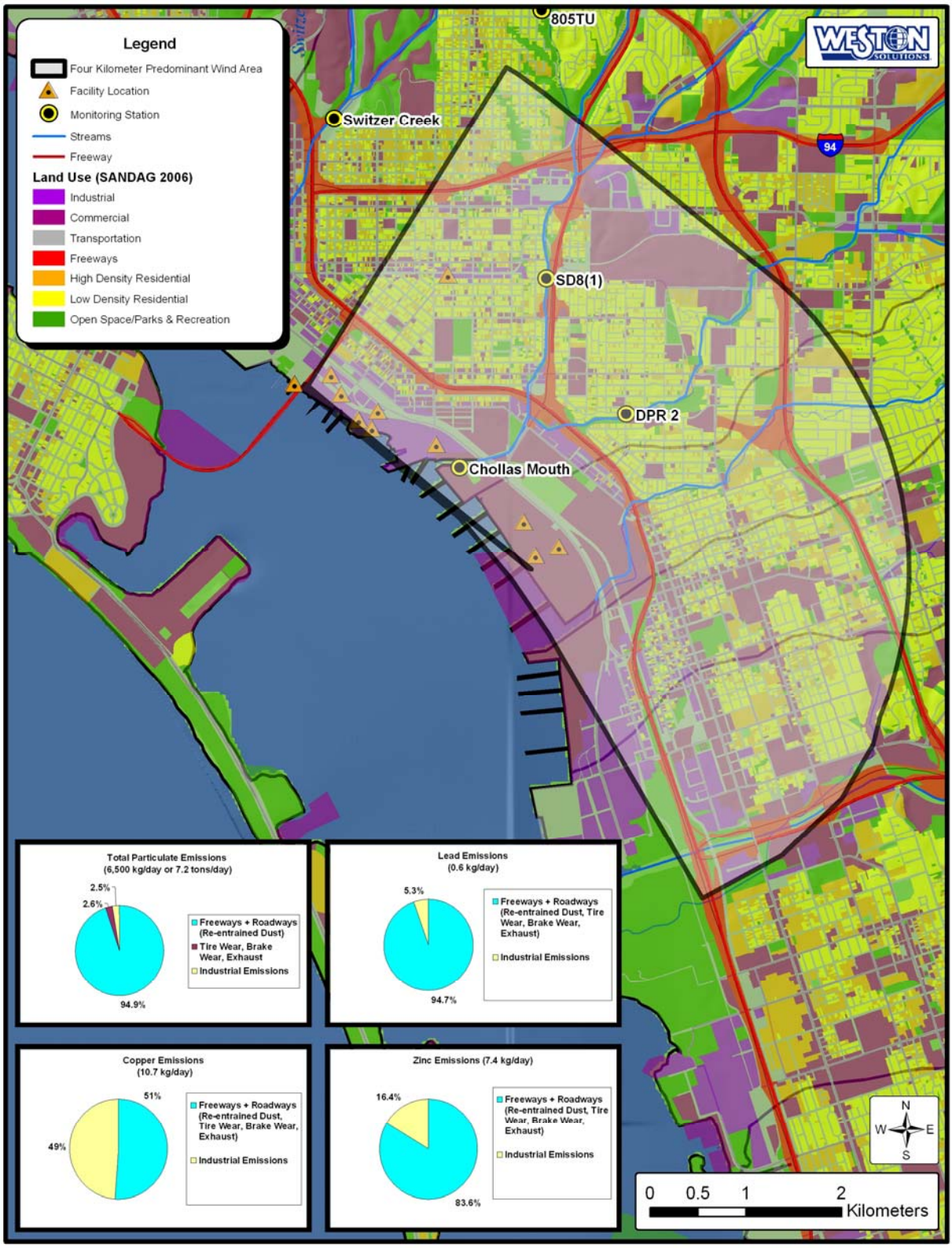

Figure 10-3. 4 km Area for Comparison of Roadway and Industrial Emissions.

A comparison of industrial and roadway emissions (measured in grams per day) within 4km of Chollas Creek are provided in Figure 10-4.

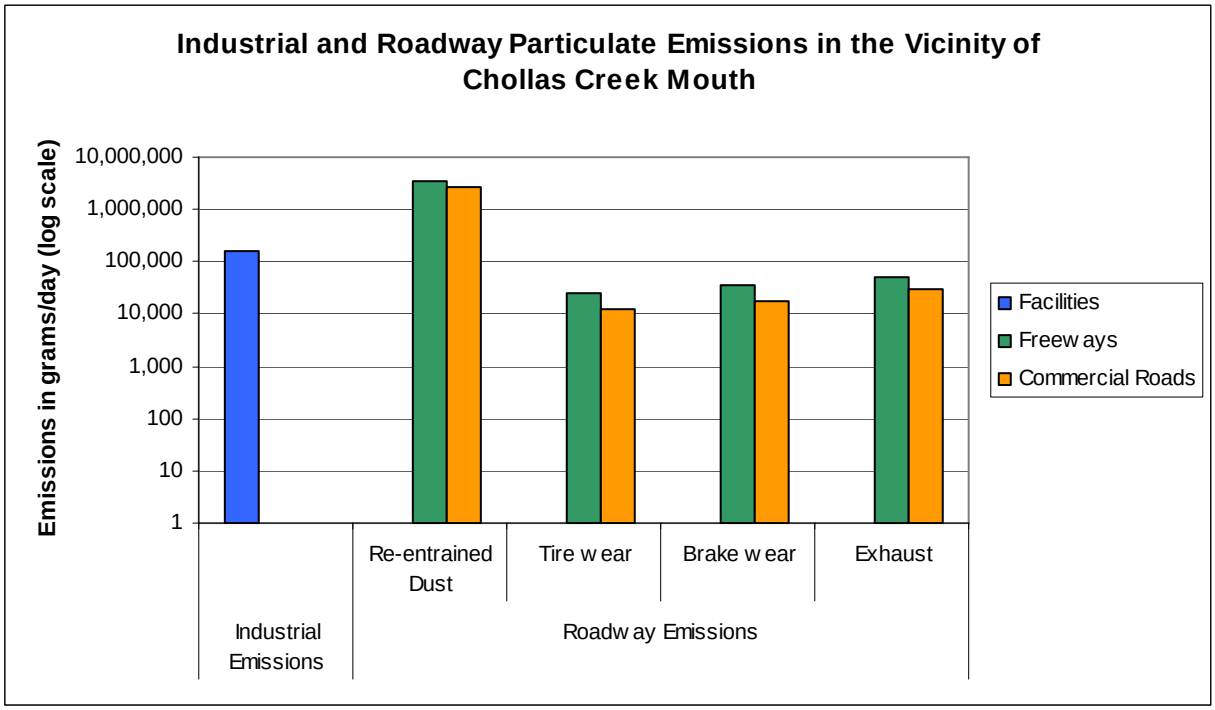

Figure 10-4. Industrial and roadway particulate emissions within 4km of the mouth of Chollas Creek.

As shown in Figure 10-4, roadway dust that is swept into the air by passing vehicles constitutes the vast majority of inventoried industrial and estimated roadway total emissions within the area surrounding the mouth of Chollas Creek. Re-entrained dust resulting from vehicular travel on the area's 15.82 miles of freeway accounted for 55.8 percent of total roadway emissions while dust from commercial road travel comprised 41.5 percent of all roadway emissions. Emissions resulting from tire wear, brake wear, and vehicle exhaust amounted to only 2.6 percent of total roadway-generated particulates. By comparison, industrial emissions from the ten facilities within 4km of the mouth of Chollas Creek resulted in 161,800 grams per day of airborne particulates, or 2.5 percent of the total reported emissions within the study area.

Metals emissions of copper, lead, and zinc within 4km of the mouth of Chollas Creek were quantified using industrial emissions data, as reported by facilities to the ARB, and calculated roadway emissions using EPA and ARB-approved methodologies along with the previously assumed representative daily traffic counts. Copper emissions from brake pads were developed by using emissions factors from a study conducted for the Brake Pad Partnership (Process Profiles, 2006). Lead and zinc emissions were estimated using the average elemental concentrations (µg/g) measured in the SD8(1) site deposition disks. A depiction of the industrial and roadway emissions in the Chollas Creek study area is provided in Figure 10-3 and Figure 10-5. Although industrial facilities accounted for less than three percent of total emissions

within the Chollas Creek area, 48.7 percent of copper emissions originated from industrial sources. Roadway emissions of copper, presumably from copper brake wear, accounted for 5,513 g/day, or 51.3 percent of total copper emissions. Both industrial and roadway emissions of lead were low in comparison to copper and zinc emissions. Industrial lead emissions within the study area averaged 31.6 grams per day, or 5.3 percent of total lead emissions while freeways and commercial roadways were responsible for contributing 560.2 grams (94.7 percent) of lead per day to the study area. Overall zinc concentrations were heavily influenced by roadway emissions. Tire wear, brake wear, exhaust, and re-entrained dust accounted for 84.4 percent of the total zinc, while industrial zinc emissions accounted for 16.6 percent of all zinc within 4km of the mouth of Chollas Creek.

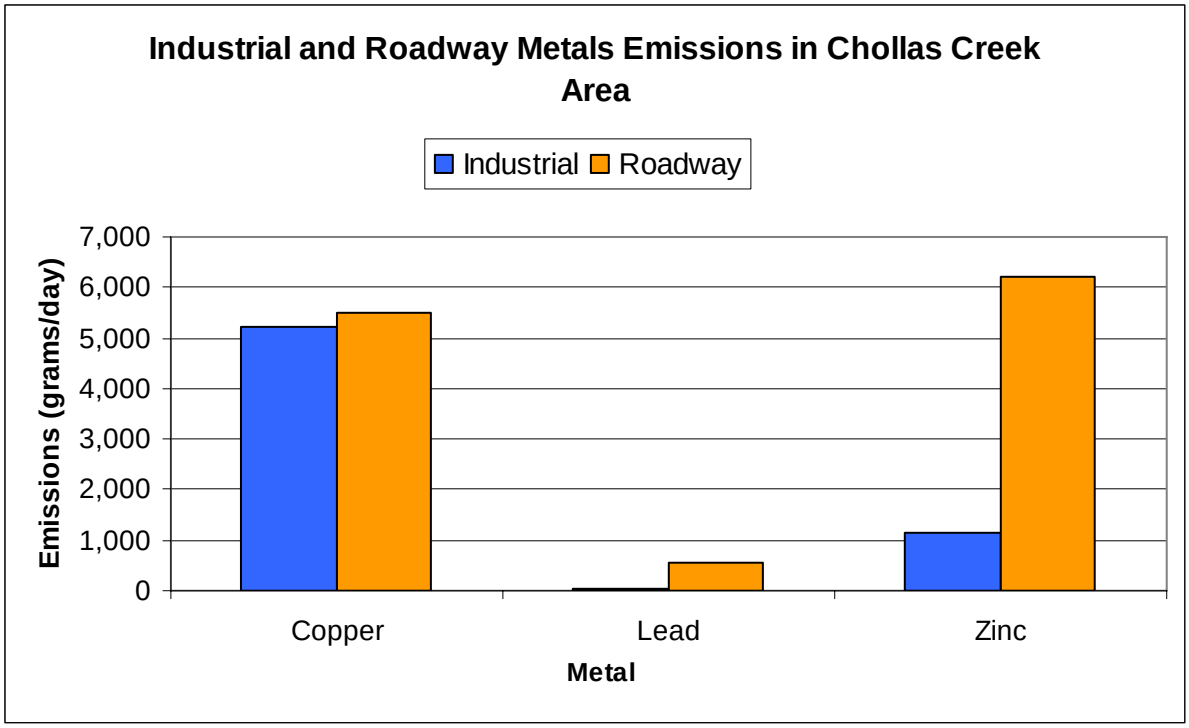

Figure 10-5. Industrial and roadway metals emissions within 4km of the mouth of Chollas Creek.

Based on these emissions data, it is clear that both industrial and roadway-generated particulates can significantly impact metal concentrations in the Chollas Creek area, and likely impact water quality within this region. However, it is important to realize that in other areas, overall metal contributions from roadways and industries will largely remain area-specific. Variables such as the total amount of roadways within a given area, the respective amount of traffic on those roadways, wind direction, wind velocity, and the types and locations of industrial facilities within the area will combine to determine the impact of aerial deposition upon a specific watershed.

Wind impacts

The information provided from the industrial emissions inventories and the understanding of the prevailing wind directions and modeling estimates can allow for an estimation of the aerial

deposition flux contribution from industrial sources alone. The prevailing wind direction in San Diego, based on historical wind data from 1985-1995 at Lindbergh Field, is shown in Figure 10-6. The prevailing wind blows to the east/southeast 28% of the time and to the west 16% of the time. It should be noted that wind directions vary based on topography and location and are presented merely to provide a general wind distribution. Localized conditions likely influence the distribution of wind (e.g., buildings, traffic flow, and land topography) at specific site locations.

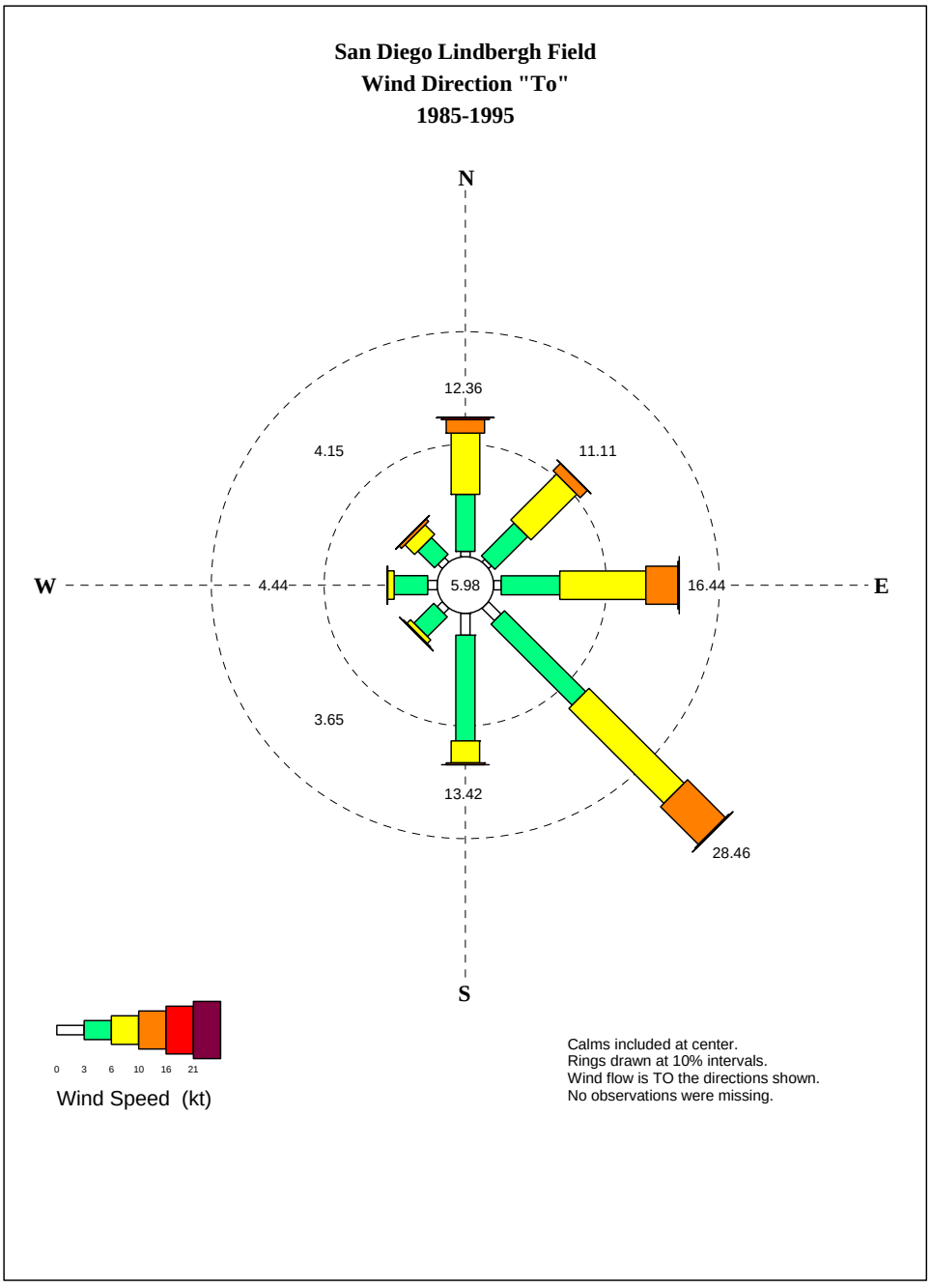

Figure 10-6. Historical Daily Wind Distributions at San Diego Lindbergh Field from 1985-1995

In summary, the industrial emissions from sources throughout the San Diego Region may contribute significantly to particulate levels on a localized basis. While these facilities may not be considered point sources in terms of a NPDES permitted discharge, they may be considered point sources in terms of their emissions of particulate matter. Emissions from even small operations can result in elevated depositional fluxes within an estimated 2 km circumference of the particulate emitting facility. Mobile emissions from predominantly automobile use and area-wide emissions from industrial sources likely dominate the total particulate matter emissions on a regional basis. The SDAPCD reports that an estimated 15,300 tons of toxic air contaminants are emitted annually in San Diego County. Of these toxic emissions, 70 percent are emitted by automotive sources, 17 percent are emitted by consumer products and architectural sources, 10 percent are released from an estimated 200 large industrial facilities and 1,600 smaller businesses, and three percent are the result of wildfires (SDAPCD, 2006). It should be noted that these published estimates of toxic emissions do not explicitly consider total particulate matter greater than 10 µm in size, nor do they consider compounds such as copper or zinc, which are not generally relevant to human health risks via the inhalation pathway. Although area-wide emissions may be the predominant factor in overall depositional flux, as the distance from a major industrial emission source decreases, a single facility's emissions may exceed the area-wide emissions and dominate the mass depositional flux in that area, such as the case with Chollas Creek. Over time, these deposits will accumulate and disperse during dry conditions and eventually wash away as urban runoff during rain events. In the case of Chollas Creek, the aerial emissions of copper from the area near the mouth of Chollas Creek will likely return in the form of particulate laden storm water.

9.0 AIR QUALITY MODELING

Air quality modeling is being used for two purposes in the deposition study:

1) to understand the area of influence of deposition from different roadway types for several vehicle-related emissions sources, and
2) to assist in the estimation of deposition across entire drainage basins.

Understanding the downwind extent of areas affected by deposition of particles from brake wear, tire wear, and resuspended road dust will help define regions where wash off of these particles is most likely, and where BMPs may be most effective.

The modeling results can also be used to estimate zones of deposition influence for roadways. The widths of these influence zones can be used with GIS data on roadways to indirectly extrapolate measured deposition fluxes to wider geographic areas.

Air dispersion modeling can also be used to directly estimate deposition on a drainage basin scale, provided an appropriate source inventory exists. Developing such an inventory and performing regional modeling is beyond the scope of this study. However, the cascade impactor data from this study could provide a useful surrogate for actual source particle size distributions in future dispersion modeling of roadway and background sources in the study area.

Several of the deposition field measurement sites can be described as being representative of locations influenced by three types of roadways:

- Freeways, represented by the I-805 transect sites;
- High-Traffic Local Roads, represented by the Mira Mesa and Prism 2 sites; and
- Low-Traffic Local Roads, represented by the Tecolote and DPR 2 sites.

These three roadway types were modeled using Industrial Source Complex Short Term Version 3 (ISCST3) to examine the dropout patterns of particles emitted by the roadways. Short (approximately 200 meter or 1/8 mile) segments of each roadway source category were simulated. The road segments were modeled with a wind perpendicular to the road, and the road was located on the upwind edge of a receptor grid that extended far enough downwind and crosswind to capture the majority of the mass deposited by the road segment. Traffic volumes and emissions profiles characteristic of each roadway type were developed using engineering guidance from USEPA and ARB, and were used to obtain particulate matter emission rates for the model.

The following subsections describe the specific procedures used in the modeling analysis. Section 10.1 describes the model selected. Section 10.2 describes the emissions calculations. Section 10.3 describes the model runs and discusses the results. Section 10.4 provides a summary of the modeling analysis.

9.1 Model Selection

The ISCST3 model (version 02035) was used for the modeling evaluation. ISCST3 is a widely used U.S. Environmental Protection Agency (EPA) dispersion model that is useful for both generic and source-specific assessments. ISCST3 uses a steady-state Gaussian calculation of concentration, and a resistance-based deposition algorithm. The model also includes a depletion feature to simulate material dropout from particulate plumes. ISCST3 was chosen for its ability to simultaneously estimate multiple particle sizes and its relatively sophisticated deposition algorithms.

The ISCST3 model represents a roadway as a series of square volume sources. The spacing of the volume sources is dependent on the width, since the length of each source is equal to its width. For this study, the width and spacing of the volume sources was taken as the width of the traveled way of each road type. Based on the road width, a number of sources was used that would represent a segment approximately 200 meters in length (about 1/8 mile). Because only whole multiples of the road widths are used, the actual segment length varied slightly depending on the ratio of the width to the desired 200 m length.

The dispersion of each volume source is defined by an initial vertical dimension and an initial horizontal dimension. The initial horizontal dimensions were based on default ISCST3 guidance, dividing the source separation by a factor of 2.15. This factor is used to simulate a downwind concentration profile for a line source. The initial vertical dimensions were based on the algorithm used in the CALINE3 traffic model, which is related to the wind speed and width of the roadway. This factor is based on empirical data and is designed to account for the enhanced dispersion over and immediately downwind of the roadway.

9.2 Emissions Development

Several of the deposition field measurement sites can be described as being representative of locations influenced by three types of roadways:

- Freeways (I-805 transect sites),
- High-Traffic Local Roads (Mira Mesa and Prism 2 sites), and
- Low-Traffic Local Roads (Tecolote and DPR 2 sites).

These three roadway types were modeled using ISCST3 to examine the dropout patterns of particles emitted by the roadways. Short (approximately 200 meter or 1/8 mile) segments of each roadway source category were simulated. Traffic volumes and emissions profiles characteristic of each roadway type were developed using engineering guidance from USEPA and ARB.

The emissions data were developed by both emissions type and particle size range, since particle size is a significant factor in calculating deposition velocity. Emission rates by source type and particle size ranges were determined consistent with EPA (AP-42 Paved Roadways) and ARB (EMFAC, 2002) specified methodologies. The details of the breakdown of emission rates are contained in Appendix D.

Emission rates were derived for four types of sources and four particle size ranges. The four source types were:

- Re-entrained roadway dust,
- Brake wear,
- Tire wear, and
- Exhaust.

The four particle size ranges were:

- 15 to 30 microns (PM_{15-30}),
- 10 to 15 microns (PM_{10-15}),
- 2.5 to 10 microns ($PM_{2.5-10}$), and
- less than 2.5 microns ($PM_{2.5}$).

An important limitation of the modeling analysis is that the particle sizes modeled are limited to ranges less than 30 microns aerodynamic diameter. It is possible that there are larger size particles of re-entrained road dust that are not accounted for in the modeling analysis. This would result in the model potentially underestimating deposition amounts very near the source.

Table 9-1 summarizes the total emissions for each type of roadway modeled. The grams per day emissions in Table 9-1 are extrapolated from the grams per mile emission rates developed in Appendix D, using the length of the modeled roadway segment and the traffic volume shown in the table. For the model, the daily emissions were scaled to an hourly rate by dividing by 24.

Table 9-1. Modeled Roadway Emission Rates from Various Sources

Roadway Type	Modeled Emissions (g/day)				Modeled Length (mi)	Daily Vehicles
	Exhaust	Tire Wear	Brake Wear	Re-entrained Dust		
Freeway	401.4	190.1	274.6	27,929.4	0.124	170,000
Commercial	114.8	49.2	71.1	10,487.8	0.099	55,000
Residential	1.9	0.6	0.9	571.5	0.099	700

The primary source of roadway emissions is the dust re-entrained into the air from the road. As shown in Table 9-1, road dust comprises from 97% to 99% of the total emissions based on the engineering calculations. The emission calculations assume that the source of this material is silt deposited on the road. The silt loadings used in the calculations (see Appendix D) ranged from 0.02 g/m^2 for the freeway to 0.32 g/m^2 for the residential road. This fine material in most cases will be primarily comprised of elements commonly found in the Earth's crust, and will not generally contain significant amounts of metals such as zinc, copper, or lead.

The particle size distributions based on mass fractions for each roadway type are summarized in Table 9-2. For summary purposes only, the tire wear, brake wear, and exhaust categories of emissions have been combined into an aggregate category referred to as "vehicular emissions". This category represents the particulate emissions derived from the vehicles themselves.

Table 9-2. Modeled Roadway Emissions Based Upon Particulate Size

Size Range	Portion of Total Mass Emitted in Size Fraction (%)					
	Re-entrained Dust			Vehicular Sources		
	Freeway	Commercial	Residential	Freeway	Commercial	Residential
PM_{15-30}	78.7%	78.1%	76.8%	0.0%	0.0%	2.0%
PM_{10-15}	4.6%	4.5%	4.5%	0.0%	0.0%	0.0%
$PM_{2.5-10}$	13.7%	13.9%	14.4%	40.9%	39.0%	33.5%
$PM_{2.5}$	3.0%	3.5%	4.4%	59.1%	61.0%	64.5%

As indicated in Table 9-2, the vehicular emissions are almost exclusively in the size fractions less than 10 microns in aerodynamic size and with the majority in the $PM_{2.5}$ range. In contrast, road dust particles are predominantly larger than 15 microns aerodynamic size, with a secondary peak in the $PM_{2.5-10}$ range. This bimodal distribution is consistent with the size distribution of dust generated from general erosion of crustal material. For all types of emissions, the engineering calculations yielded almost identical size distributions across roadway types.

9.3 Model Results and Discussion

Using the emissions information described in Section 9.2, the ISCST3 model was run to simulate a single hour. The road segments were modeled with a wind perpendicular to the road, and the road was located on the upwind edge of a receptor grid that extended far enough downwind and crosswind to capture the majority of the mass deposited by the road segment.

The meteorological conditions modeled were neutral (Pasquill Class D) stability and 3 m/s (7 mph) wind speed. Neutral is the most common category of atmospheric stability. The climatological mean wind speed for the San Diego Lindbergh Field National Weather Service (NWS) station is 7.5 mph (based on hourly data from 1985-1995). These conditions were chosen to represent a condition typical to the San Diego area. Other combinations of wind speed and stability will produce greater or lesser amounts of deposition. For the academic purpose of examining general particle dropout patterns, a snapshot in time at a single combination is sufficient.

The model domain extended 4 km downwind and ±1 km crosswind of the segment. This domain size was designed to provide coverage sufficient to encompass the majority of the plume emitted by the line source. Receptors were distributed on a Cartesian grid spaced at 20 meter intervals, for a total of 20,301 receptors.

The ISCST3 model only performs calculations at designated points in space, so a large number of points were chosen to obtain better spatial resolution. The model produces outputs of point deposition fluxes as mass per area. The square area represented by each receptor (400 m^2) was used to calculate a total mass deposited from the model outputs. A post-processing program was developed to generate summaries of mass deposited over the domain by each emission category (exhaust, brake wear, tire wear, and re-entrained road dust).

9.3.1 Model Mass Balance

The principal result of the modeling is that only a small proportion of the mass emitted by the roadway sources is deposited within the model domain. Table 9-3 summarizes the total amounts of material deposited over the entire model domain by source type as a percent of the mass emitted. For example, 3.2% of the total brake wear mass emitted from the freeway segment was deposited in the model domain. Road dust and brake wear particles had approximately 10% and 2.5% of emitted mass deposited, respectively. Less than 1% of exhaust and tire wear emissions were deposited. Overall, deposition to the 8 km^2 model domain accounts for roughly 10% of the total mass emitted regardless of roadway type. Percentages by emission type are also nearly constant across roadway types.

Table 9-3. Fraction of Mass Deposited

Roadway Type	Modeled Deposition to 4 km Downwind (% of mass emitted)				
	Exhaust	Tire Wear	Brake Wear	Re-entrained Dust	Total
Freeway	0.1%	0.8%	3.2%	9.6%	9.4%
Commercial	0.1%	0.3%	2.2%	11.7%	11.5%
Residential	0.1%	0.3%	2.2%	11.8%	11.7%

The differences in the percentages deposited are explained by the differing nature of the particles. Road dust is modeled with a much higher fraction of large particles (roughly 75% PM_{10-30}), which have greater deposition velocities. Although the three vehicular emissions sources have similar distributions mainly in the fine fractions (roughly 60% $PM_{2.5}$), brake wear particles have a higher density. The particle densities modeled vary, based on the origins of the material:

Exhaust = 0.70 g/cc (diesel particulate / organic soot),
Tires = 1.20 g/cc (rubber),
Brakes = 3.00 g/cc (metallic particles), and
Dust = 2.65 g/cc (soil).

The higher particle density for the metallic brake wear particulate would explain its greater deposition relative to the other vehicular fine particles. The brake wear particle density used was from an air dispersion modeling study sponsored by the Brake Pad Partnership (BPP) for the San Francisco Bay region (Brake Pad Partnership, 2005).

The mass balance results have the important implication that the majority of particle mass emitted by road-related sources is transported considerable distances downwind. Although more greatly diluted and more gradually depositing, these emissions will contribute to background air concentrations and deposition fluxes in regions several kilometers downwind of their sources. This result highlights the concept that deposition is a regional-scale issue, rather than simply an issue in the immediate vicinity of sources.

9.3.2 Particle Dropout Rates

The modeling results were also examined to understand the downwind range where most of the mass would be deposited. This would define a "zone of influence" of the roadway, and suggest a buffer radius where BMPs might be most effective. The modeled deposition amounts at each downwind distance of the receptor grid were summed (i.e., for 20 m downwind by 2 km crosswind strips), and the distances at which 50%, 75%, 90%, and 95% of the total deposited mass were determined. Table 9-4 summarizes the results by roadway type, and for both re-entrained dust and other vehicular emissions.

Table 9-4. Modeled Extents of Accumulated Deposition

Distance to % Mass Deposited Over 4 km Downwind				
Roadway Type	**50%**	**75%**	**90%**	**95%**
From Re-entrained Dust (m)				
Freeway	180	640	1,780	2,620
Commercial	140	600	1,800	2,680
Residential	140	600	1,800	2,660
From Vehicular Emissions (m)				
Freeway	260	960	2,220	2,980
Commercial	280	1,120	2,460	3,140
Residential	260	1,060	2,360	3,060

The re-entrained road dust portion of Table 9-4 also represents the total mass deposited from the roadways, since the absolute magnitude of the vehicular emissions deposition is negligible compared to the re-entrained dust. On that basis, the results indicate that 50% of the total deposition has occurred within roughly 200 m, and 75% by roughly 600 m, regardless of roadway type. Due to the exponential decrease in deposition with distance from the source, the 90% level is reached significantly farther out at 2,000 m. Only 10% of the total mass deposited within the modeled domain is found in the farther downwind half of the domain.

The vehicular emissions, made up of finer particles as previously noted, travel somewhat farther downwind than the re-entrained dust particles. However, half of these particles still deposit relatively close to the roadways (within roughly 300 m), and 75% of the total in the modeled domain has been deposited by roughly 1,000 m.

The results in Table 9-4 suggest a practical zone of influence buffer of 200 m as representative of the most significant deposition impacts for any roadway or emissions type. This distance encompasses over 50% of the modeled total mass deposited in the near field (as defined by the 4 km downwind modeling domain). Many streets in residential areas are within 200 m of one another, as are many streets in business and industrial districts. The proximity of these streets would result in potentially overlapping deposition impacts from multiple roads in the intervening areas.

9.3.3 Regional Modeling Implications

The modeled deposition results were also examined to gain insight on the relative importance of freeways versus surface roads for evaluating basin-wide deposition. Simply on the basis of the relative emissions of the freeway versus the surface road sources modeled, it would be expected that freeways would dominate deposition to the Chollas basin. However, there are significantly more miles of surface roads than freeways within the Chollas basin. Therefore, it is possible that the lower-volume surface roads could have similar overall deposition contributions on a regional scale.

Figure 9-1 presents profiles of total deposition flux as mass per area with distance from each roadway type. The units are micrograms per square meter ($\mu g/m^2$), and are plotted versus a logarithmic vertical scale (i.e., one division equals a factor of 10). The deposition amounts are along the centerline of the plume (midpoint of the road segment) for the single hour modeled. Hourly deposition amounts over longer periods would vary with differences in traffic volume, wind speed, wind direction, and atmospheric stability.

The curves in Figure 9-1 indicate that the modeled deposition fluxes for the residential roadway are roughly 30 times (1.5 orders of magnitude) lower than freeway or commercial roadways. If the total length of non-freeway roads in the Chollas basin were 10 times the total length of the freeways, deposition amounts over the entire basin would be within the same order of magnitude.

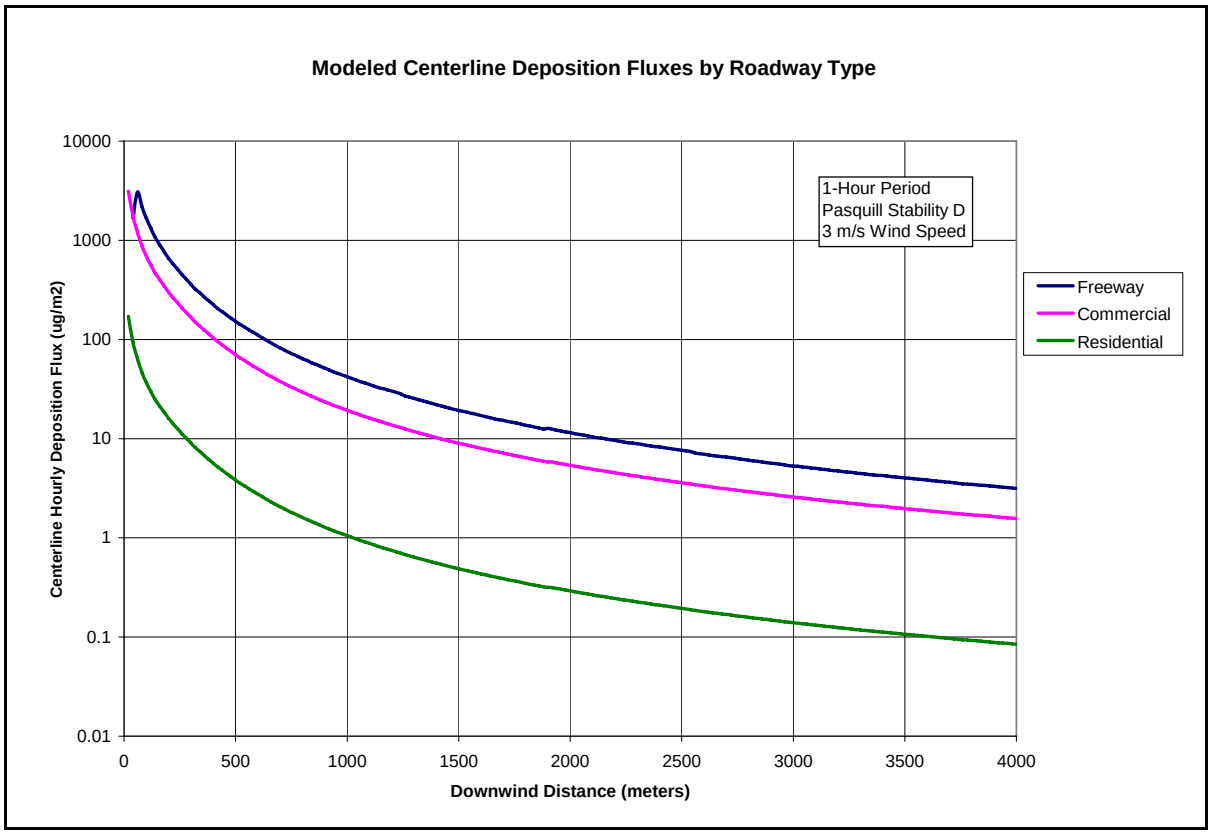

Figure 9-1. Modeled Deposition Fluxes by Roadway Type.

The curves also provide perspective on the importance of viewing aerial deposition on a regional scale. For example, the model indicates that 0.1 µg/m^2/hr is a relatively low aerial deposition rate for dust emissions four km downwind of the roadway emission source. A material that deposits at that rate would impart 16.8 grams of material across one km^2 in a week. Diluting this material into the full volume of a 0.10" rainfall event (2.54 million liters over the same 1 km^2 area) would generate a 6.6 µg/L concentration. This exercise illustrates how a small rate of deposition can result in potentially significant runoff concentrations of material over time as well as over a large geographic area. Extrapolating the 0.1 µg/m^2/hr deposition rate to the entire Chollas basin (87 km^2) would translate to accumulating 1.46 kg/week of material over the basin.

9.4 Air Quality Modeling Summary

Roadways are known to be significant sources of particulate emissions. These particulates will also contribute to deposition. Air quality modeling was used in this study:

- to understand the area of influence of roadway-related deposition from different roadway types, and
- to understand the contributions of roadway-related deposition on a regional level.

Understanding the area of influence of roadways is useful in defining regions where washoff of aerially deposited particulates is most likely and where BMPs may be most effective. The modeled areas of influence can be used in conjunction with land use and measured deposition data to extrapolate the potential contributions of traffic-related deposition on a regional scale.

Air dispersion modeling can also be used to directly estimate deposition on a regional scale using emissions and meteorological data. Such a regional modeling exercise was beyond the scope of this study. However, the cascade impactor data from this study could be used as a basis for input data for such modeling in the future.

The dispersion modeling examined the dropout patterns of particles emitted by three types of roadways:

- Freeways,
- High-Traffic Local Roads, and
- Low-Traffic Local Roads.

Particle-size segregated emissions profiles were developed for each type of roadway, using available traffic volumes and emission calculations guidance from USEPA (AP-42 Paved Roadways) and CARB (EMFAC, 2002). Emissions profiles were categorized as re-entrained road dust or direct vehicular emissions (exhaust, tire wear, and brake wear). Short (approximately 200 meter or 1/8 mile) segments of each roadway source category were simulated using the USEPA ISCST3 air dispersion model. Deposition rates were simulated for a single hour using a receptor grid extending two km crosswind and four km downwind of the road segments. Modeling results were examined to assess: mass balance (how much mass emitted was deposited), the area of influence of the roadways, and the relative fluxes from the three roadway types.

The mass balance assessment showed that only a small proportion of the mass emitted by the roadway sources is deposited within the model domain. Overall, deposition to the eight km^2 model domain accounts for roughly 10% of the total mass emitted regardless of roadway type. This result indicates that roadway emissions will also contribute to background aerial deposition fluxes in broader regions extending several kilometers downwind of the local vicinity of their sources.

The area of influence analysis indicated that 50% and 75% of the total deposition to the model domain occurs within roughly 200 m and 600 m of the roadway, respectively. These distances are consistent across the three roadway types. Based on these results, a zone of influence of 200 meters is suggested as representative of the majority of near-field deposition impacts from roadway emissions, regardless of the type of roadway.

The flux comparison indicated that freeway and commercial roadways have similar magnitudes of deposition flux (within a factor of 2), while residential roadways produce deposition fluxes that are roughly 30 times lower than freeway fluxes. When gauging the importance of residential roads versus freeways on a regional scale, quantity of emissions alone tends to indicate that freeways would be dominant in determining deposition. However, there are significantly more miles of residential and commercial roadways in urbanized drainage basins such as the Chollas basin. The relative flux results suggest that higher total lengths of the lower-emissions roadways could equalize the relative deposition contributions of those roads on a regional scale.

8.0 QUALITY CONTROL

To ensure that the data used in this study was robust and without bias, quality control techniques were employed by both the field sampling staff and the associated laboratories. This section describes the quality control techniques and results.

8.1 Chain of Custody (COC) Procedures

Samples were considered to be in custody if they are (1) in the custodian's possession or view, (2) retained in a secured place (under lock) with restricted access, or (3) placed in a container and secured with an official seal such that the sample could not be reached without breaking the seal. The principal documents used to identify samples and to document possession were COC records, field logbooks and field tracking forms. COC procedures were used for all samples throughout the collection, transport and analytical process.

COC procedures were initiated during sample collection. A COC record was provided with each sample or group of samples. Each person who had custody of the samples signed the form and ensured the samples were not left unattended unless properly secured. Documentation of sample handling and custody included the following information:

- Sample identifier
- Sample collection date and time
- Any special notations on sample characteristics or analysis
- Initials of the person collecting the sample
- Date the sample was sent to the analytical laboratory
- Shipping company and waybill information.

Completed COC forms were placed in a plastic envelope and kept inside the container containing the samples. Once delivered to the analytical laboratory, the COC form was signed by the person receiving the samples. The condition of the samples was noted and recorded by the receiver. COC records were included in the final laboratory reports prepared by the analytical laboratories and are considered an integral part of the laboratory report.

8.2 Method Blanks

Method blanks were used to evaluate the sample handling process and to ensure that positive bias was not introduced during the sampling events. Method blanks were used at a rate of once per monitoring event for each week of surrogate disk sampling. Method blanks were used once for every 10 sampling events for the Tisch impactor sampling. Method blank results are provided with the Data Analysis Tables in Appendix A. Method blank results for copper and lead on the surrogate disks were less than three times the uncertainty (non-detect) for all sample events. Method blank results for zinc on the surrogate disks were less than three times the uncertainty (non-detect) for 12 of 13 sample events. Zinc was detected in the surrogate disk method blank for the 10/6/06 sample event. The mass of zinc on the blank would equate to a flux of 5 $\mu g/m^2$/day over a 3-day exposure period, which is not significant relative to fluxes detected in the actual samples.

8.3 Accuracy

Accuracy was measured for each analytical batch of surrogate disk samples by analyzing a NIST Standard Reference Material (SRM 1832 and SRM 1833). Results of the SRM samples for copper, lead and zinc were +/- 10% of the certified value for every analytical batch.

8.4 Replicate Analysis

Replicate analyses were performed in duplicate or triplicate during each week of sampling to evaluate the variability within each sample site. The replicates were performed a minimum of once at each sampling location over the course of the study. While the replicates are not used to reject data, they are used for evaluation of the site and sample variability only. Sample variability is measured based on the coefficient of variation (CV) between sample replicates. Variation was grouped as low, medium, or highly variable based on the following criteria:

- Low variability was defined as CV < 40%
- Medium variability was defined as CV between 40% - 100%
- Highly variable data was defined as CV > 100%.

The coefficient of variation for each set of replicates at sites in the area wide study were determined and are presented in Table 8-1, Table 8-2, and Table 8-3. The coefficient of variation varied between sample sites, sample dates, and element measured. Sample replicates were performed for 10 sample events at the mouth of Chollas Creek, 5 sample events for Site SD8(1), and once for the remaining area wide sites.

Coefficients of variation for copper and lead at the Chollas Mouth Site (Table 8-1) ranged from low to highly variable, with a mean variation of 58.7% and 32.8% respectively. The coefficient of variation for zinc ranged from low to medium with a mean variation of 36.5%.

Table 8-1. Coefficient of Variation for the Chollas Mouth Site Replicate Analyses.

Element	# of Replicates	Chollas Mouth		
		Min	Max	Mean
Copper	10	11.3%	127%	58.7%
Lead	10	0.0%	123%	32.8%
Zinc	10	12.7%	74.8%	36.5%

Coefficients of variation for copper at the SD8(1) site (Table 8-2) ranged from low to highly variable, with a mean variation of 50.4%. The coefficient of variation for lead ranged from low to medium with a mean variation of 42.2%. The coefficient of variation for zinc was always low with a mean variation of 10.3%.

Table 8-2. Coefficient of Variation for Site SD8(1) Replicate Analyses.

Element	# of Replicates	SD8(1)		
		Min	Max	Mean
Copper	5	16.3%	123%	50.4%
Lead	5	11.1%	95.8%	42.2%
Zinc	5	3.70%	21.0%	10.3%

The coefficient of variation for the remaining area wide sites are presented in Table 8-3. The coefficient of variation for copper was highest at the Switzer Creek site (110%) and lowest at the Tecolote site (15.4%). Lead variability was highest at the DPR(2) site and lowest at the Tecolote site (7.1%). The coefficient of variation of zinc was primarily low at the remaining area wide sites with the highest variation considered medium at the Prism2 site (46.5%).

Table 8-3. Coefficient of Variation for Area Wide Site Replicate Analyses.

Element	Switzer Creek	DPR(2)	Mira Mesa	Prism2	Ref (1)	Tecolote
	7/21/2006	8/25/2006	8/11/2006	9/1/2006	6/30/2006	8/18/2006
Copper	110%	22.4%	20.9%	37.3%	39.4%	15.4%
Lead	86.7%	111%	30.6%	68.3%	18.6%	7.1%
Zinc	29.7%	34.9%	22.0%	46.5%	23.8%	30.6%

Coefficient of variation results for the transect study at the I-805 freeway are presented in Table 8-4. Sample variability was higher for copper than for lead or zinc. Coefficients of variation for copper ranged from 14.8% to 104%. Sample variability for lead and zinc are considered low and were always less than 25%.

Table 8-4. Coefficient of Variation for the I-805 Transect Site Replicate Analyses.

Element	8/25/2006	8/25/2006	8/25/2006	8/25/2006	10/13/2006	10/13/2006
	805T1	805T2	805T3	805T-Up	805T1	805T4
Copper	19.4%	104%	52.4%	103%	14.8%	17.6%
Lead	8.8%	8.8%	8.8%	8.8%	0.0%	0.0%
Zinc	10.2%	14.7%	17.0%	13.3%	20.7%	13.5%

It is apparent that the variability of copper is considerably higher than that of lead and zinc. As previously shown in the results section, lead was not frequently detected and was generally low in comparison to other elements detected. Non-detect values were reported at the detection level. Thus, in instances where all measurements were at or below the detection limit, the coefficient of variation was 0. Zinc variability was also low and tended to be lower at sites near freeways in comparison to sites farther from freeways.

8.5 Sample Inspection Process

All samples were inspected for acceptable quality prior to submittal to the analytical laboratory. Samples that had obvious tears, abrasion, damage, bird droppings, or other factor causing suspect sample integrity were rejected from lab submittal (Figure 8-1). Sample inspection information was documented on the field sample forms.

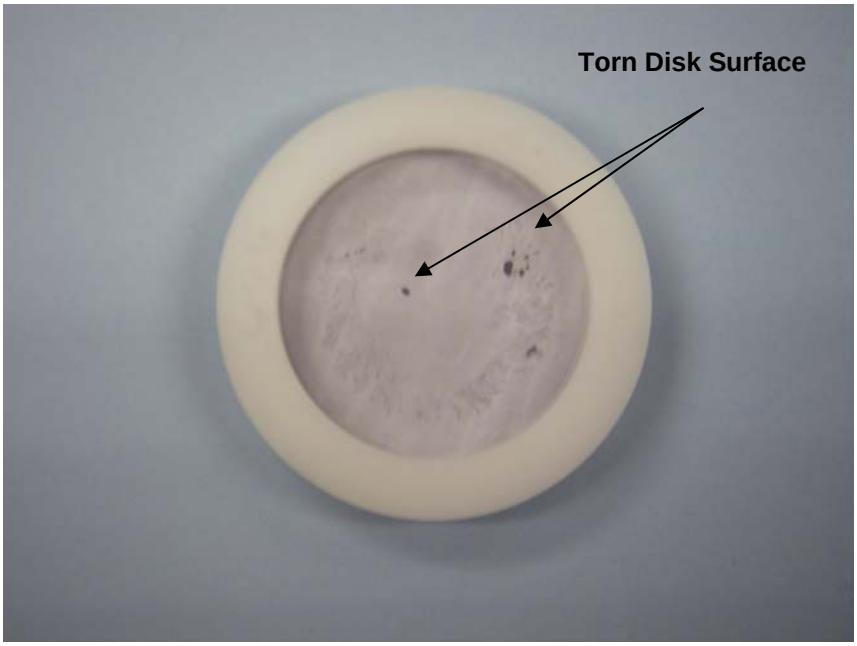

Figure 8-1. Example of surrogate sample disk rejected from sample submittal to laboratory.

A total of 169 sample disks and 13 method blank disks were deployed during the study. A total of 13 sample disks were rejected due to sample integrity issues. The primary reason for sample rejection was due to wildlife tampering with the disks. In several cases, disks were found on the ground in the surrounding area indicating birds likely removed the disks from the surrogate plate. In other instances, bird feces were also found in the disks. All method blank disks were submitted for analysis.

7.0 DATA ANALYSIS RESULTS

With the amount of data collected for this project, an analysis of how all the parts of the project fit together is important to answer the original questions of the study. The purpose of this section is to analyze all data collected for the project: regional sites, transect sites, land use, particle size distribution, impactor data, and wind direction, and use this information to help answer the study questions. The results of these data have been presented previously in the document. A multivariate analysis of these data will enable us to look at all of the data together and answer some of the original questions of the study. These questions included:

1. What are the aerial contributions of pollutants and are they associated with different sources or land uses?
2. What particle size and load of pollutants are deposited on roadways and impervious areas and washed off?
3. Where is pollutant loading from aerial deposition occurring within the City of San Diego?

This section will specifically address how pollutants may be associated with different sources or land uses, and where pollutant fluxes are highest for copper, lead, and zinc. This section is divided into an analysis of specific elemental spatial patterns, and how they may relate to traffic volume. This is followed by a multivariate analysis of the chemical "fingerprints" for each site.

7.1 Copper, Lead, Zinc, and Net Flux Analysis

7.1.1 Methods

To provide a comparison of regional copper, lead, zinc, and net flux results, all data from all sites were plotted in box-whisker plots (Figure 7-1 through Figure 7-4). In this manner, the median, 25^{th}, and 75^{th} percentiles of the data can be readily observed. The boxes are bounded on the top and bottom by the 25^{th} and 75th percentiles of the data set, and the line inside is at the median (50^{th} percentile). The whiskers extend out to the maximum and minimum values. Distributions that have significantly overlapping boxes are considered to be statistically similar to one another on a cursory basis.

Traffic volume relationships to copper, lead, zinc, and net flux were analyzed using a multiple regression technique. Average daily traffic volumes nearest each site were taken as reported by CALTRANS (2003). Because these values are constants for a given roadway, it would be pointless to compare the constants to the differing flux results from each sampling event. Therefore, the traffic volumes from each site were weighted by the percent of time that the wind was from the freeway direction during each sampling event. These variables were specific to each sampling event, and the newly generated variables (traffic volume * % wind direction) were named TV%W. If there was more than one freeway within 500 meters, then there was more than one predictor variable.

7.1.2 Results

Copper was detected in a majority of flux samples at nearly every site during the course of the study, with the exception of Ref(1). Copper fluxes at SD8(1) and Chollas Mouth were highest, with Switzer Creek following closely (Figure 7-1). The variance, or range of values, at SD8(1) was greater than Chollas Mouth, but the median values of the data were very close at 20.3 and 17.5 µg/m^2/day respectively (Table 7-1). Site SD8(1) had one extreme event of 206 µg/m^2/day. Ref(1) had detectable levels of copper during only two sampling events. Tecolote copper fluxes were also very low, with more detectable amounts of copper, but still much lower than all other sites.

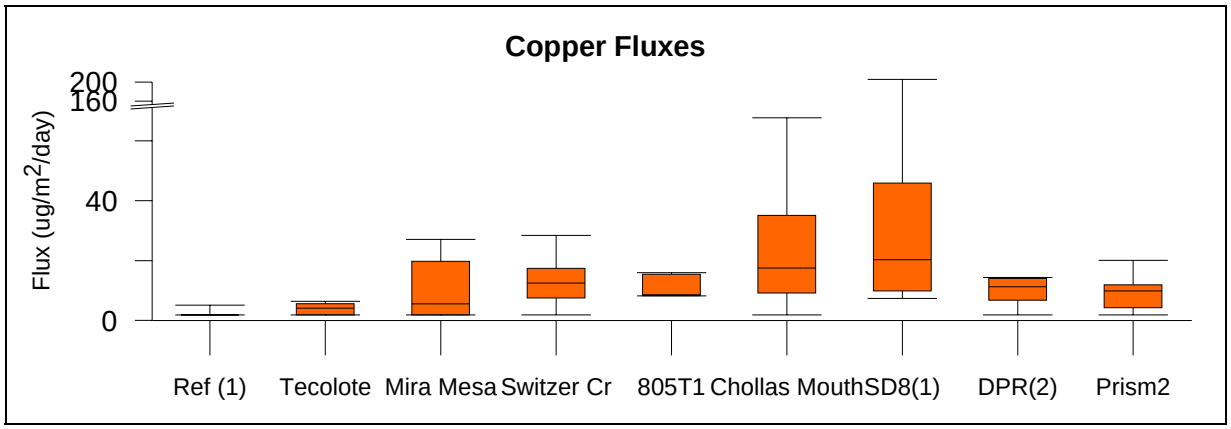

Figure 7-1. Box-whisker plot of copper fluxes at all regional sites over the study period

Lead flux results at all regional sites indicate that lead was not commonly found during this study, except at site SD8(1), which had the most detections of lead, as well as the highest median and maximum values (Figure 7-2).

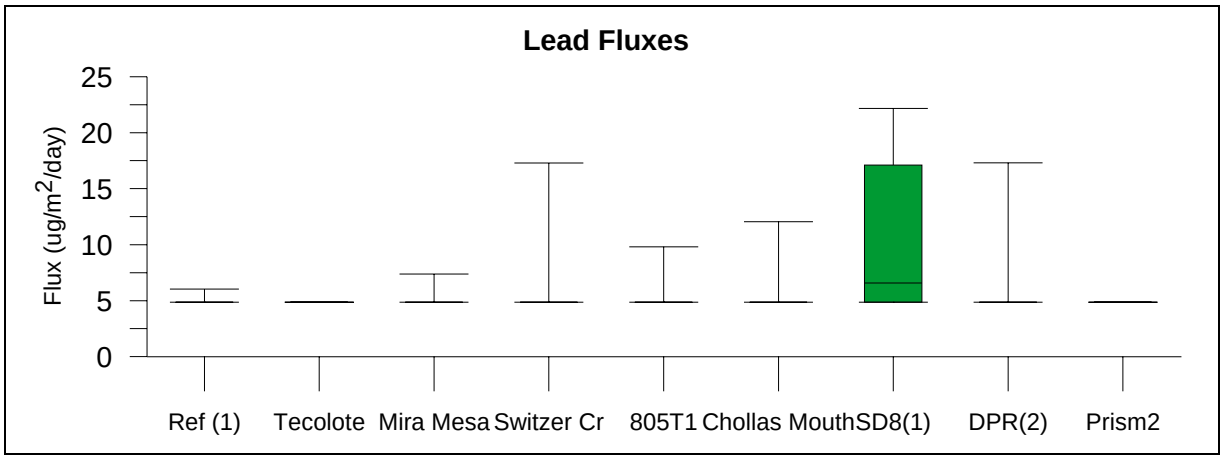

Figure 7-2. Box-whisker plot of lead fluxes at all regional sites over the study period

Zinc flux results were more variable over the study area than copper flux results, with the highest median flux found at site 805T1, a transect site, and the second at Switzer Creek. SD8(1) was next, followed closely by Chollas Mouth (Figure 7-3). These three sites are also the most closely located to a major freeway. Mira Mesa had one flux result that was much higher than all other flux results, but the median value at the site was still low in comparison to other sites.

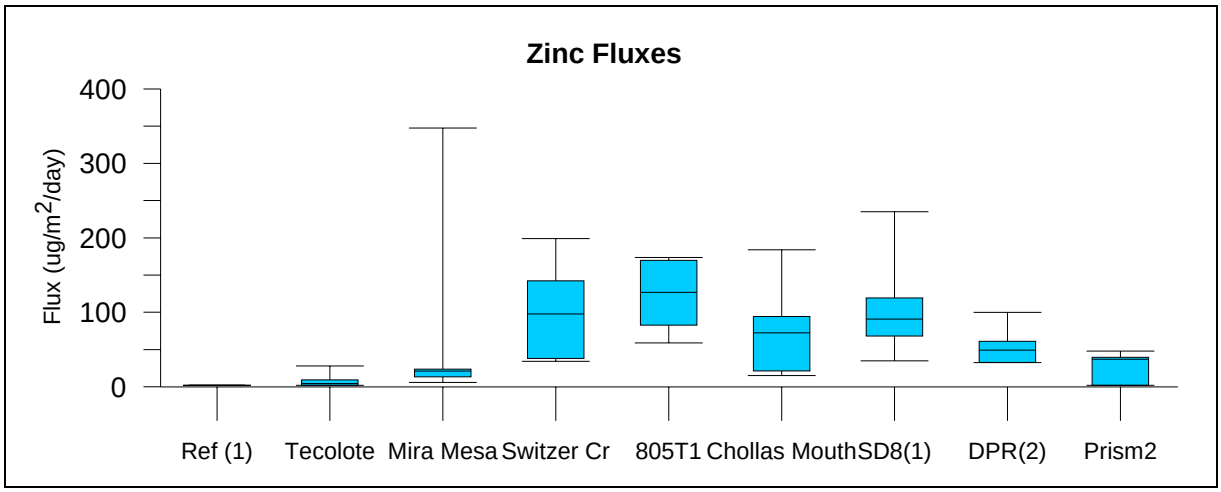

Figure 7-3. Box-whisker plot of zinc fluxes at all regional sites over the study period

Net flux results were somewhat similar, when compared spatially, to zinc flux results (Figure 7-4). Note that the mass units of net flux in this section are micrograms (rather than milligrams as in Section 6). However, Tecolote had the fourth highest net flux, instead of Chollas Mouth. Again, the sites with the highest net flux rates were also most closely located to major freeways.

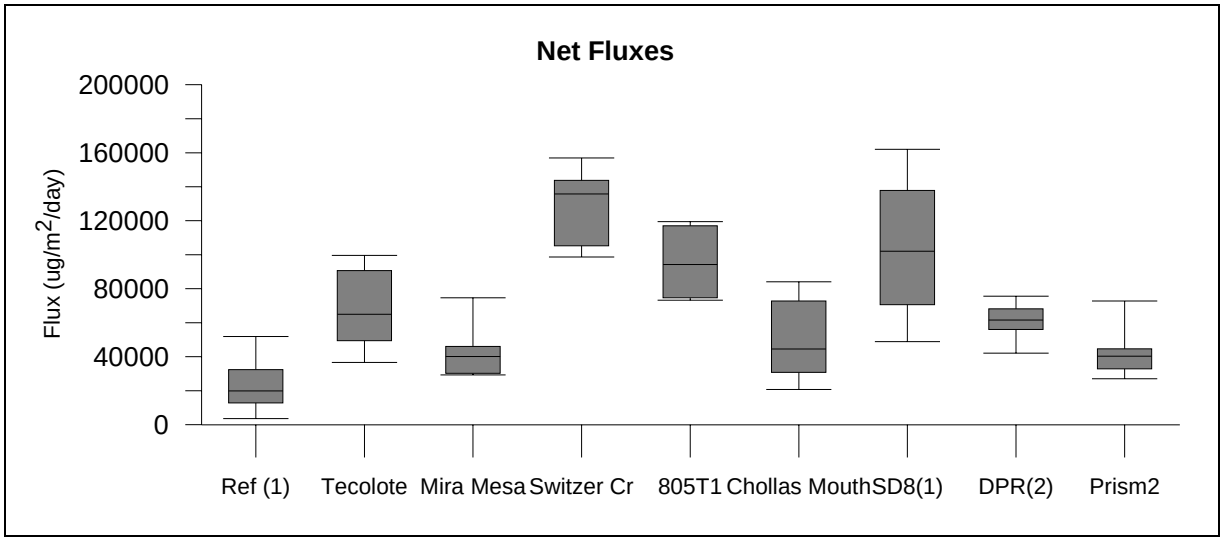

Figure 7-4. Box-whisker plot of net fluxes for at all regional sites over the study period

Summary statistics are presented in Table 7-1, below. These results are the numerical values of the median, 25th percentile, 75th percentile, minimum, and maximum values presented in the box-whisker plots, above.

Table 7-1. Summary statistics of Copper, Lead, Zinc, and Net Fluxes

	Ref (1)	Tecolote	Mira Mesa	Switzer Creek	805T1	Chollas Mouth	SD8(1)	DPR(2)	Prism2
	Copper µg/m^2/day								
Median	1.8	4.1	5.5	12.5	8.6	17.5	20.3	11.3	9.9
25th Percentile	1.8	2.7	3.2	7.5	8.3	9.7	10.8	7.3	5.2
75th Percentile	1.8	5.2	11.1	15.0	12.9	30.9	32.1	13.0	10.6
Maximum	5.1	6.4	27.0	28.4	16.0	67.7	205.9	14.4	20.1
Minimum	1.8	1.8	1.8	1.8	8.2	1.8	7.3	1.8	1.8
	Lead µg/m^2/day								
Median	4.9	4.9	4.9	4.9	4.9	4.9	6.6	4.9	4.9
25th Percentile	4.9	4.9	4.9	4.9	4.9	4.9	4.9	4.9	4.9
75th Percentile	4.9	4.9	4.9	4.9	4.9	4.9	15.9	4.9	4.9
Maximum	6.0	4.9	7.4	17.3	9.8	12.0	22.2	17.3	4.9
Minimum	4.9	4.9	4.9	4.9	4.9	4.9	4.9	4.9	4.9
	Zinc µg/m^2/day								
Median	1.8	4.2	21.1	97.8	126.7	72.4	90.9	49.3	37.0
25th Percentile	1.8	1.8	14.7	41.4	90.0	25.0	72.7	38.5	26.2
75th Percentile	1.8	9.1	23.4	122.1	158.0	92.6	116.4	59.8	38.5
Maximum	1.8	28.0	347.3	199.1	173.7	183.9	235.0	99.9	47.8
Minimum	1.8	1.8	5.7	34.1	58.8	15.1	34.8	32.5	1.8
	Net µg/m^2/day								
Median	19,900	64,700	40,100	135,700	94,300	44,500	102,100	61,500	40,400
25th Percentile	14,200	57,200	34,800	110,000	81,400	32,400	77,700	56,300	35,800
75th Percentile	27,800	77,700	43,400	142,000	112,000	69,600	132,000	67,200	44,500
Maximum	51,900	99,600	74,700	157,000	119,000	84,100	162,000	75,600	72,800
Minimum	3,670	36,600	29,300	99,000	73,300	20,700	48,900	42,100	27,000

7.1.3 Transect Results

An analysis of transect flux results was completed in the same manner as the regional site analysis. The results of all copper, lead, zinc, and net flux results were graphed using box-whisker plots (Figure 7-5 through Figure 7-8, below). A statistical summary of the results is presented in Table 7-2.

Copper flux results were unexpectedly consistent, with medians for all five sites within 2.3 µg/m^2/day of each other (Figure 7-5). However, the flux pattern did follow the expected spatial pattern, highest at 805T1, and dropping off toward site 805T4. The surprising aspect of the results is that the 25th-75th percentiles overlapped for all results, indicating no real difference between the medians at the five sites.

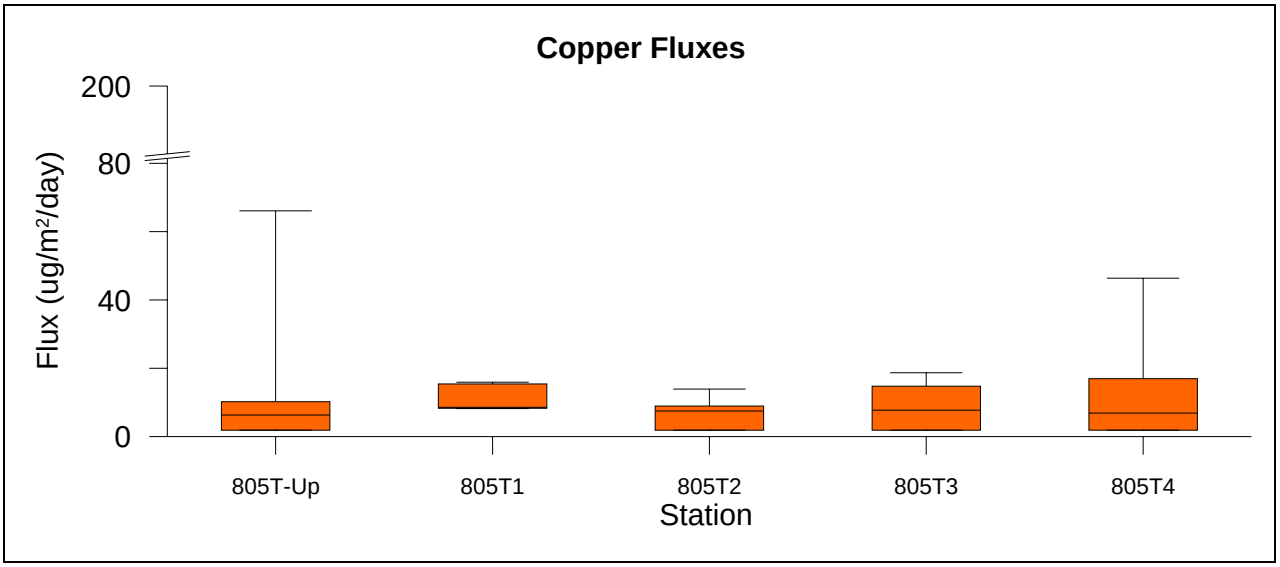

Figure 7-5. Copper flux results for all transect sites

Lead results were also generally low, with most results of non-detect at the upwind site (805T-Up), 805T1, 805T3, and 805T4. However, the maximum value for lead flux occurred at site 805T2 (Figure 7-6).

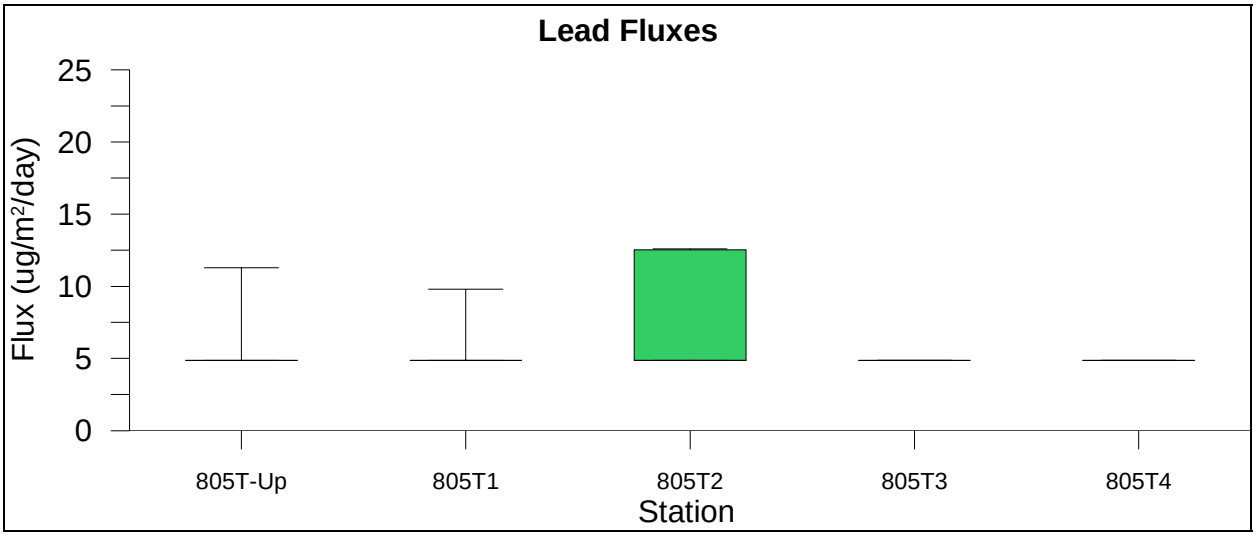

Figure 7-6. Lead flux results for all transect sites

Zinc flux results did follow the expected pattern, with the highest median value (15.2 µg/m^2/day) at site 805T1, and dropping off toward the end of the transect (805T4). The upwind site results were also lower than sites 805T1-805T4 (Figure 7-7).

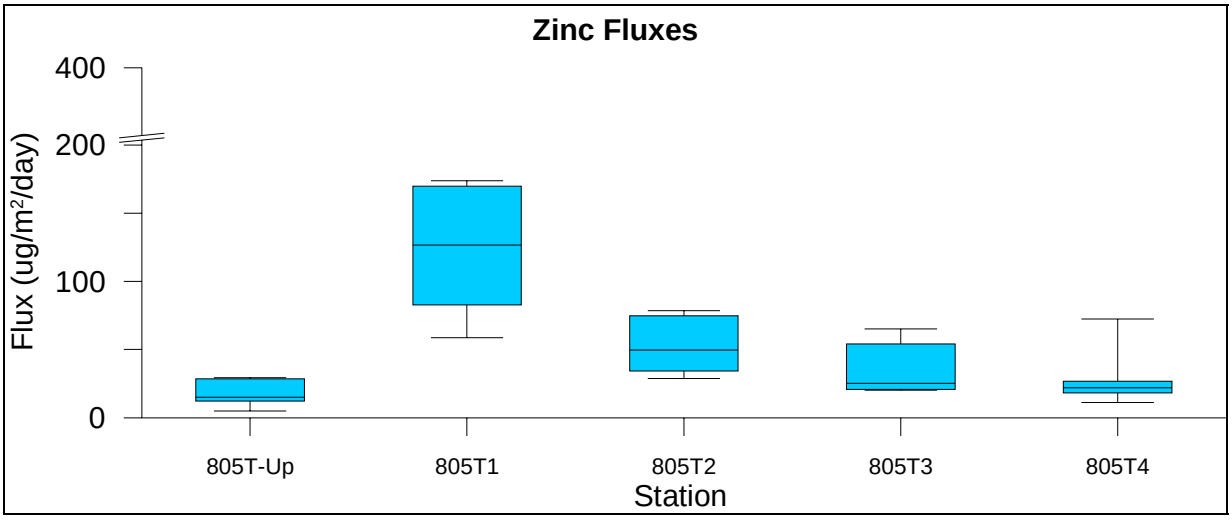

Figure 7-7. Zinc flux results for all transect sites

Net flux median results followed the same pattern as zinc, however the range of flux results at site 805T4 is unexpectedly high, considering its distance from the freeway. The 75th percentile result (63,300 µg/m^2/day) was higher than the median value at site 805T2 (Figure 7-8).

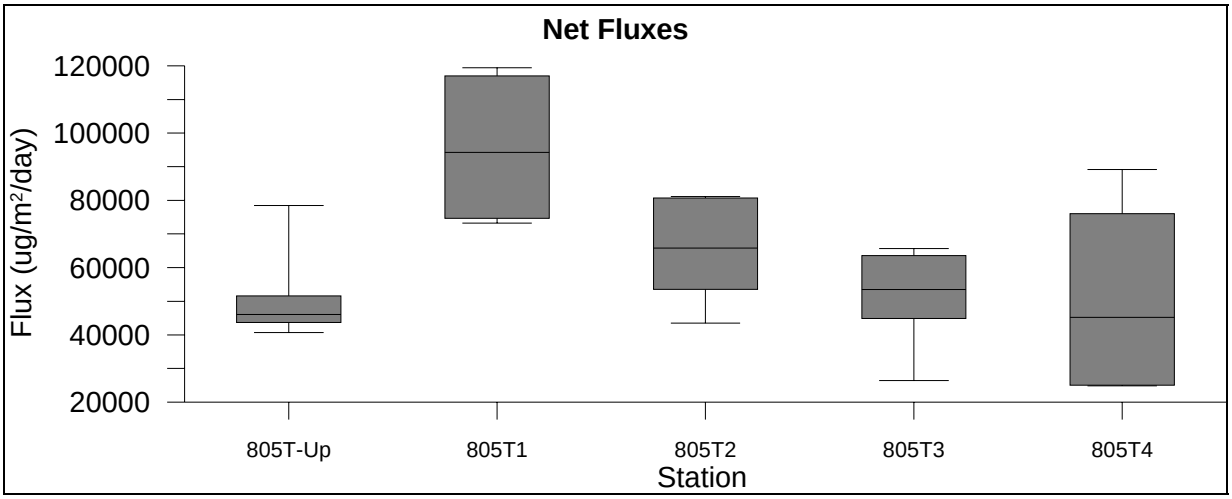

Figure 7-8. Net flux results for all transect sites

Table 7-2. Transect summary statistics for Copper, Lead, Zinc, and Net Flux

	805T-Up	805T1	805T2	805T3	805T4
	Copper µg/m^2/day				
Median	6.3	8.6	7.5	7.7	6.9
25th Percentile	2.6	8.3	3.2	1.8	3.6
75th Percentile	9.6	12.9	8.7	12.3	14.5
Maximum	66.1	16.0	13.9	18.7	46.3
Minimum	1.8	8.2	1.8	1.8	1.8
	Lead µg/m^2/day				
Median	4.9	4.9	4.9	4.9	4.9
25th Percentile	4.9	4.9	4.9	4.9	4.9
75th Percentile	4.9	4.9	6.8	4.9	4.9
Maximum	11.3	9.8	12.6	4.9	4.9
Minimum	4.9	4.9	4.9	4.9	4.9
	Zinc µg/m^2/day				
Median	15.2	126.7	49.7	25.2	21.8
25th Percentile	12.9	90.0	41.1	22.3	19.3
75th Percentile	25.2	158.0	60.3	40.5	25.3
Maximum	29.6	173.7	78.6	65.1	72.4
Minimum	5.1	58.8	28.8	20.3	11.3
	Net µg/m^2/day				
Median	46,100	94,300	65,800	53,400	45,200
25th Percentile	43,700	81,400	54,800	48,700	26,600
75th Percentile	50,700	112,000	78,100	59,000	63,300
Maximum	78,500	119,000	81,100	65,700	89,200
Minimum	40,700	73,300	43,500	26,400	24,900

7.1.4 Traffic Volume Weighted Regression Analysis

An analysis of traffic volume related to copper, lead, zinc, and net flux results at each site was carried out. Traffic volumes were weighted by the percentage of time wind was from the direction of the freeway (Table 7-3), based on the one of eight wind direction sectors producing the best downwind alignment at each site. A linear regression was calculated to compare the wind direction with weighted traffic volumes to fluxes of the elements of interest. Results indicate that there was a weak linear relationship between copper flux and wind direction with weighted traffic volume at Switzer Creek. Switzer Creek zinc flux results were also weakly correlated to wind direction weighted traffic volume, as well as at Mira Mesa. Site SD8(1) had net flux results weakly correlated with traffic volume. These results indicate that, although there are several significant relationships, none are strong enough to make flux predictions at the indicated site based on traffic volume and wind direction.

The fact that some sites did not show correlation where it would be expected (such as 805T1) could be due to local wind patterns. Since regional meteorological stations were used to represent wind directions at all the sites, microscale wind patterns at individual sites (such as channeling by artificial canyons) might confound the correlation analysis.

Table 7-3. Regression Analysis of Fluxes to Traffic Volume Weighted by Wind Direction

Site	Copper Flux		Lead Flux		Zinc Flux		Net Flux	
	R^2	p-value	R^2	p-value	R^2	p-value	R^2	p-value
805T1	0.01	0.80	0.01	0.84	0.01	0.78	0.02	0.76
Chollas Mouth	0.04	0.56	*	*	0.04	0.57	0.02	0.71
Switzer Creek	0.63	0.02	*	*	0.54	0.04	0.19	0.29
DPR(2)	0.32	0.14	*	*	0.06	0.56	0.30	0.16
Mira Mesa	0.09	0.78	*	*	0.70	0.05	0.39	0.29
PRISM2	0.21	0.26	*	*	0.00	0.88	0.25	0.21
Ref (1)	*	*	*	*	*	*	0.15	0.24
SD8(1)	0.15	0.49	0.41	0.09	0.23	0.30	0.51	0.04
Tecolote	0.41	0.26	*	*	0.34	0.35	0.08	0.80

- High number of non-detects precludes regression analysis
- Highlighting indicates values that are statistically significant

7.2 Particle Size Analysis

Relationships of particle size to deposition were examined using two sources of data: the impactor sampling, and the PSD by microscopy of the surrogate disks. Impactor sampling provided information on atmospheric distribution of target metals by particle size range. The microscopy-based PSD from the surrogate disks provided information on the particle sizes contributing to the observed net fluxes.

The primary focus of the cascade impactors was to assess what size particles each of the target metals are associated with in the atmosphere. Particle size is a key determinant of deposition velocity. Other factors being equal, a metal associated with large particles would have greater aerial deposition fluxes than a metal associated with fine particles.

In terms of atmospheric particle sizes, the first stage of the impactors (>7.2 µm) represent large particles. The second and third stages (1.5 to 7.2 µm) represent "medium" particles. The remaining two stages (<1.5 µm) represent "fine" particles. The percentages of each metal on each stage of the impactor samples were determined and plotted on ternary diagrams.

Ternary diagrams are a tool used to compare mixtures. They are often seen in a geological context to compare sediments based on percentages of silt, sand, and clay. In the context of this section, they are used to compare the large, medium, and fine particle distribution of each of the metals. Figure 7-9 shows ternary plots for copper (Cu), iron (Fe), zinc (Zn), and lead (Pb). Each site is represented by a letter as in the table below:

ID	Site		
A	80T1	G	Switzer Creek
B	80T2	H	DPR(2)
C	80T3	I	Mira Mesa
D	80T4	J	PRISM2
E	80T-Up	K	Ref(1)
F	Chollas Mouth	L	SD8(1)
		M	Tecolote

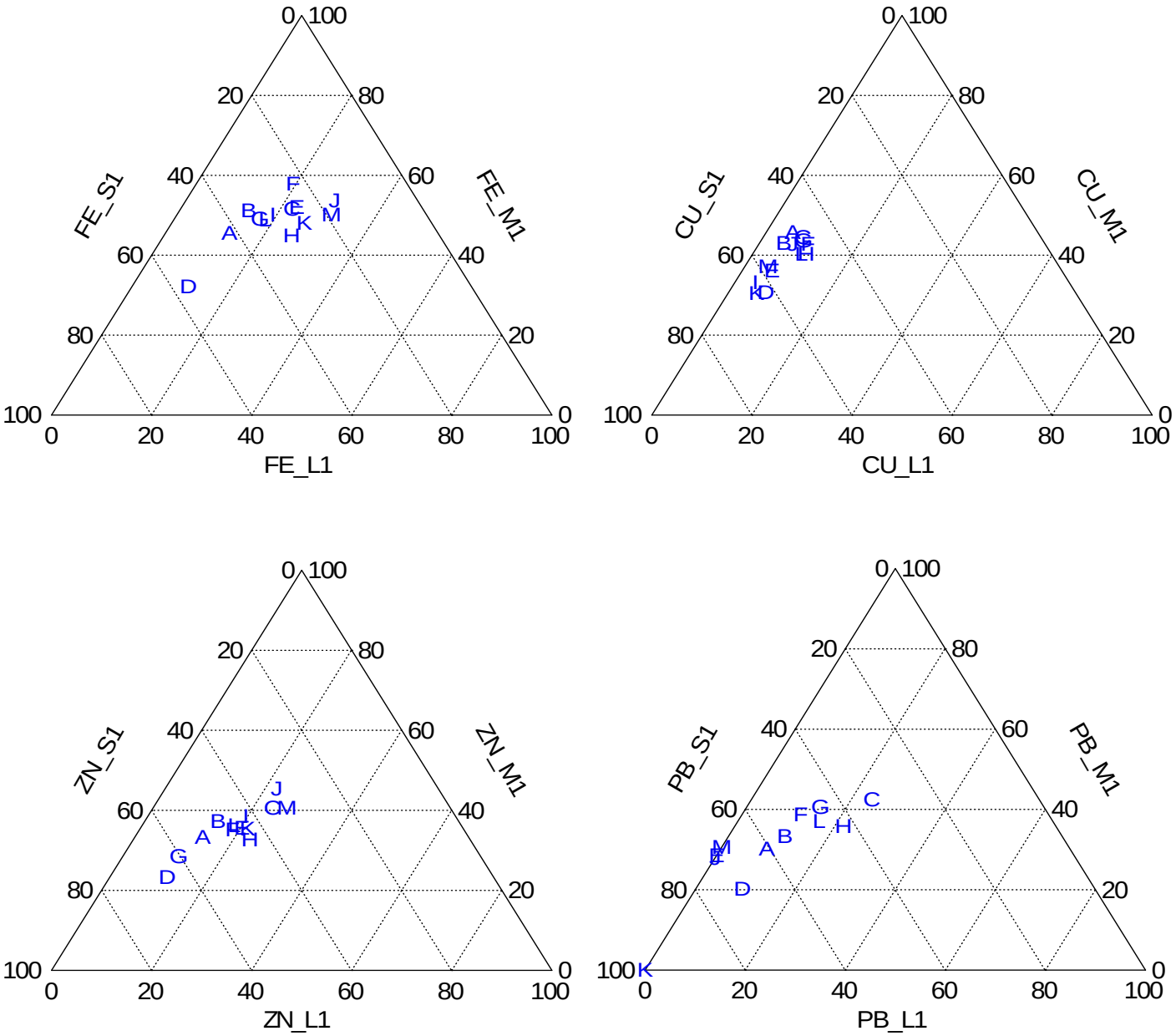

Figure 7-9. Comparison of Particle Size Distributions by Metal from Cascade Impactor Samples - Atmospheric Aerosols Size Ranges

The ternary plot is based on three variables that sum to 100%. This makes it possible to plot a 3-dimensional point in 2 dimensions, because the point position is fixed by any two of the percentages (the 3rd is 100% minus the other two). On the ternary plots in this section, the base axis of the triangle represents the large particle fraction. The grid lines for the base axis slope up and to the right. The right axis of the triangle represents the medium particles fraction, and its grid lines are horizontal. The left axis represents the fine particles, and has grid lines that slope down and to the right. As an example, see the location of the "D" (805T4) sample on the Figure 7-9 iron plot. Its size breakdown is approximately 10% on large particles, 30% on medium particles, and 60% on fine particles.

Figure 7-9 shows that the four metals follow relatively independent size distributions. There is some variability in distributions between sites, but all of the sites tend to cluster in certain regions of the plots. Iron tends to be found 20% on large particles, 50% on medium particles, and 30% on fine particles. Copper was found only about 5% on large, 40% on medium, and 55% on fine particles. Zinc was found roughly 15% on large, 35% on medium, and 50% on fine particles. Lead was found roughly 10% on large, 35% on medium, and 55% on fine particles. The lead and zinc distributions are somewhat similar overall, but lead was distinct from zinc in that no lead was detected in the large and/or medium size fractions at some sites.

Figure 7-10 shows the range of variability of the total mass distribution by size range. Fine particles tend to dominate, with about 50% of the total particulate mass. Large particles only contribute around 15% of net mass, and the remaining 35% is medium particles. However, atmospheric size distributions by mass do not indicate higher depositional flux. Deposition is governed primarily by deposition velocity. Most of the particles will be dispersed over a larger distance.

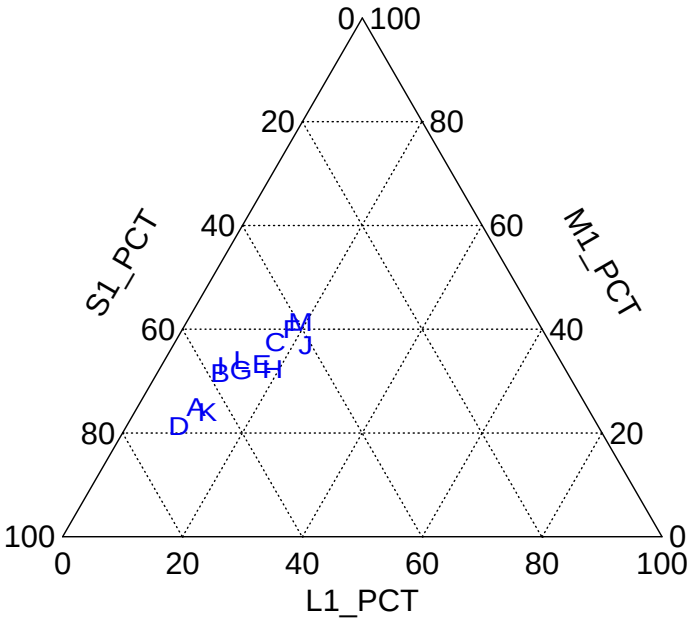

Figure 7-10. Comparison of Particle Size Distributions for Total Mass from Cascade Impactor Samples - Atmospheric Aerosols Size Ranges

7.2.1 Particle Size Summary

The impactor results indicate that iron is associated more with larger particles in the atmosphere, which is consistent with its mostly crustal-derived nature. Copper is seldom found on larger particles in the impactor sample results which would be consistent with the Brake Pad Partnership studies (BPP website, 2006) that suggest copper attributable to brake wear is found in the 1-5 µm size fraction. For all of the impactor metals except iron, about 50% of the mass was associated with the fine particle fraction. This fraction would be expected to have the lowest atmospheric deposition flux. Lead was found in low atmospheric concentrations, close to the detection limits of the high-volume air sampling method employed. This fact, combined with the association of lead with slowly-depositing finer particles, explains the infrequent detection of lead in the passive deposition samples. Additionally, the impactor results also suggest that the concentrations found as a result of regional particulate dispersion (e.g. fine particulates) provide less influence in comparison to localized sources.

The photomicroscopy PSDs (presented in Sections 6.2 and 6.3) provided quantitative data based on the particles that were deposited on the surrogate disks. The PSD results showed a surprising variability in the mix of particles larger and smaller than 15 µm (areas for particles > 15 µm ranged from 35% to 90%), indicating that deposition is a highly variable phenomenon.

The particle size distributions found on the deposition disks generally had a larger percentage of particles in the greater than 15 µm size range. The primary size range of particles deposited on deposition disks would generally be considered silts and very fine sands. While clay size fractions were present in nearly every sample, the influence on the overall mass flux would likely be considered minimal. This finding is consistent with other studies that have shown that larger particle sizes are likely the driving factor on net depositional flux. In a study conducted in the Los Angeles area, (Stolzenbach et al., 2001) researchers concluded that large particles (>10 µm) accounted for the majority of the deposition and that most deposition occurs relatively close to the emission sources. Another study conducted in the Chicago area (Paode et al., 1998) also concluded that 90 % of the flux measured was attributable to particles greater than 2.5 µm, even though the majority of the anthropogenic metals were found in the fine fraction. This information suggests that BMPs that remove particles greater than 2.5 µm may be more effective at reducing metals concentrations overall, than those targeting only the dissolved or fine fraction metals on a mass basis.

7.3 Multivariate Analysis

7.3.1 Multivariate Methods

A multivariate analysis of regional, transect, land use, and wind direction data was completed to address the main questions of the project. The XRF analyses produced data for 38 elements on each disk (Section 4.3.1). Results of all analyses are presented in Appendix A. The deposition flux data for the subset of elements detected greater than 50% of the time at all sites was used to examine relationships among the sampling sites. These relationships may provide insights into possible links to pollutant sources or land uses.

The multivariate analysis of flux results for this project consisted of a four-phased approach. The first step was to develop and standardize the dataset used for all further analysis. All data were examined for frequency of detection, because non-detects were an issue with several elements, and only those with a frequency of detection greater than 50% (in the pooled set of all samples from all sites) were included in further analysis. The exception to this was lead (Pb), which was an element of interest in the study and therefore included in the analysis. This reduction resulted in the retention of 15 elements for multivariate analysis (Al, Br, Ca, Cl, Cu, Fe, K, Mn, Ni, S, Si, Sr, Ti, Zn, Pb). Nickel was included in the dataset although it seems to have had some issues with detection on method blanks. This metal was not a driving force related to land use, and was therefore retained in the dataset. The other components of the dataset included percent wind direction (eight sectors) for each sample, and land use (eight categories) associated with each sample site.

The second step in the analysis was to examine the data based on two-way cluster analyses. The purpose of this analysis was to portion the sample sites into land use groups, as well as to examine patterns of wind and chemical flux results. Using a two-way analysis allows the user to determine what variables are driving the clusters. The variables most like each other will group together in a cluster. A hierarchical clustering algorithm was used, whereby each sample starts as its own group, and is clustered with the sample most like itself. This is repeated until all data are included in one cluster. The Bray-Curtis distance metric was used as the measure of cluster similarity.

Phase three included a Principal Components Analysis (PCA), which is a data reduction technique. This analysis was selected because the number of variables (at minimum, 15) was prohibitive of interpretation. It is difficult to recognize patterns of information in a forest of 15 or more variables analyzed together, so this technique was used to help reduce the complexity of the dataset. The advantage of utilizing this technique is that patterns in the data can be recognized, such as which samples from what sites are similar to each other, and the components can also be used in further analysis as a proxy of the 15 variable dataset. The components can also be used to estimate "fingerprints" of chemical flux that may potentially be related to land use. A PCA was run for each land use group (pooling results for all sites within the land use groups), and the results used to examine relationships between sample sites, and also for inclusion in phase four of the analysis.

The fourth phase of the analysis was a canonical correlation analysis of the PCA components from phase three, by the percent wind direction data collected for each sample date. The purpose of the analysis was to relate the reduced dataset to predominant wind directions. This will enable examining possible links to land uses.

7.3.2 Two-Way Cluster Results

The land use summary used for the cluster analysis is shown in Table 7-4.

Table 7-4. Percent Land Uses Within 1 Kilometer Radius by Site

SITE	Low Density Residential	High Density Residential	Industrial	Freeways	Transportation	Commercial	Open Space	Water
805T 1	42.9	7.3	0.0	17.3	18.2	1.3	13.1	0.0
805T 2	42.1	7.6	0.0	17.3	18.6	1.5	12.9	0.0
805T 3	38.8	8.7	0.0	16.8	19.7	2.2	13.8	0.0
805T 4	33.3	10.9	0.1	15.1	21.4	3.8	15.4	0.0
805TU	43.6	8.9	0.0	5.8	21.6	2.7	17.4	0.0
Chollas Mouth	1.4	4.7	29.4	4.3	12.9	6.8	4.2	36.2
Switzer Creek	4.2	9.8	0.1	13.2	25.0	26.5	21.3	0.0
DPR 2	32.0	6.9	6.8	9.4	23.3	11.5	10.0	0.0
Mira Mesa	35.5	17.8	0.0	0.0	21.6	20.5	4.5	0.0
Prism 2	49.4	7.6	2.2	0.0	20.4	6.5	13.9	0.0
Ref (1)	0.0	0.0	3.1	0.0	0.6	8.6	27.2	60.6
SD8(1)	29.8	8.5	3.7	7.9	25.7	9.4	15.0	0.0
Tecolote	36.1	5.2	1.1	0.4	20.7	16.5	19.9	0.0

The two-way cluster analysis by land use for all regional sites (Figure 7-11) indicates four major land use groups:

Land Use Group 1 – Includes the Ref(1) site and is dominated by water and open space/parks.

Land Use Group 2 – Includes Chollas Mouth and is dominated by water and industrial land uses.

Land Use Group 3 – Includes Switzer Creek, DPR(2) and SD8(1), and is dominated by freeways, with a mix of transportation, residential, and commercial.

Land Use Group 4 – Includes Mira Mesa, Prism2, and Tecolote, and is dominated by low and high density residential, as well as some commercial.

The transect sites were assumed to represent similar land use for all five sites, and so were not included in the two-way cluster analysis, but are labeled Land Use Group 5 for all future analysis.

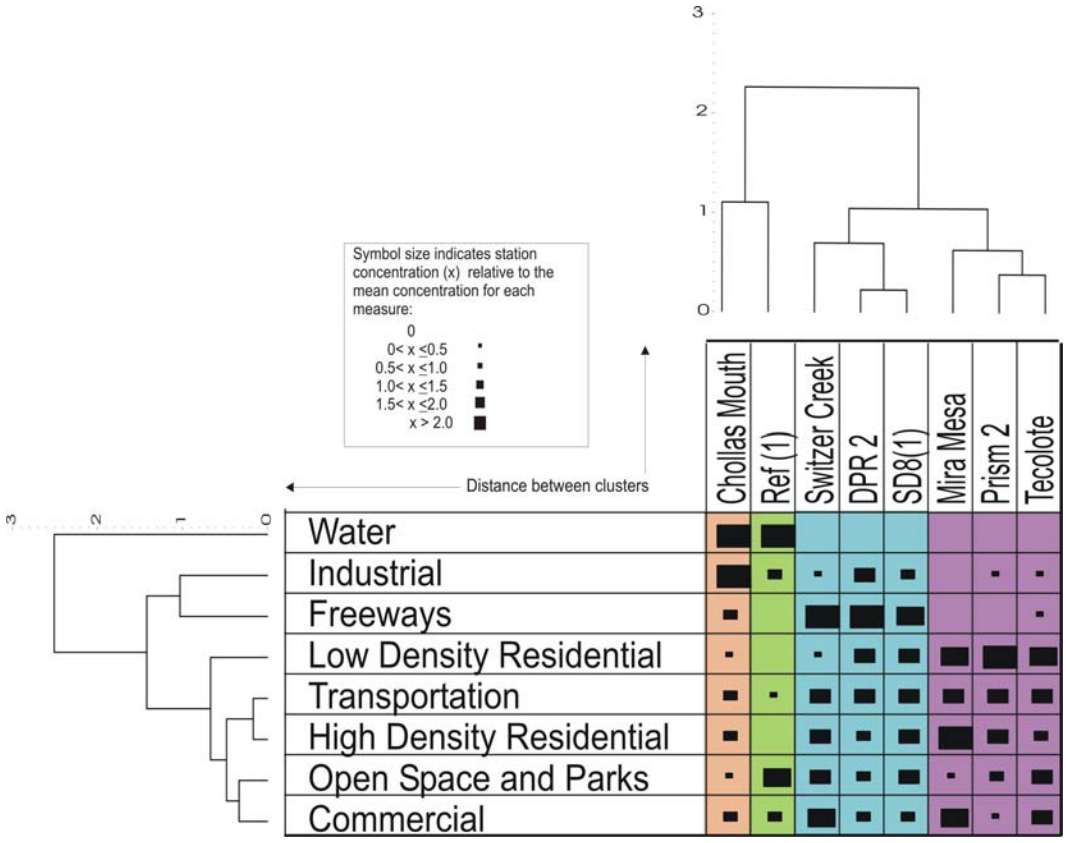

Figure 7-11. Two-way cluster analysis of sample site land use

The percent wind direction at each site for each sample was analyzed and presented in Figure 7-12. The data fell in two distinct clusters, represented by yellow and blue in the figure. Cluster one (in yellow) was dominated by winds from the north, northeast, northwest, and west, while cluster two (in blue) was dominated by winds from the south, southwest, southeast, and east. Individual days, if they were tightly clustered, are indicated by gradations of color.

The wind direction data for all of the sites except for Mira Mesa was taken from the same station, AQMD's Downtown monitoring station (Mira Mesa data was taken from AQMD's Del Mar station). Therefore it is not surprising that samples collected over roughly the same time periods tend to cluster together.

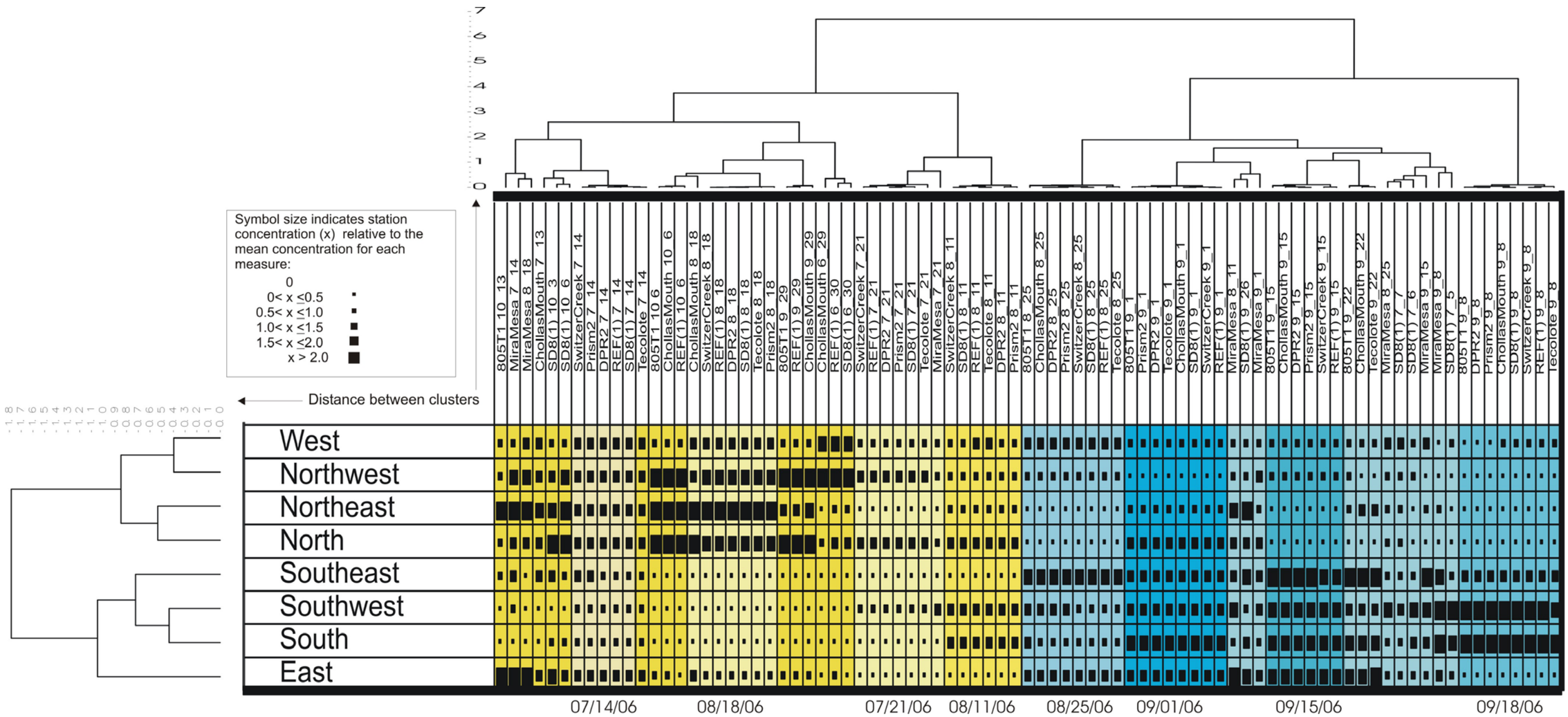

Figure 7-12. Two-way cluster analysis of percent wind direction for each sample site and date

The chemical flux data from all regional sites, including 805T1, are included in Figure 7-13. There are three major groups, indicated by blue, green, and purple. Only three sites clustered tightly together over the entire sampling period; Ref(1), SD8(1), and Chollas Mouth. However, not all samples from these sites are included in their individual clusters. Other sites were much more variable, especially Mira Mesa, DPR(2), and Switzer Creek. Flux results from these sites can be found throughout the dendrogram. Nearly all of the Tecolote results were included in the green cluster, with sample dates 8/25 and 9/1 included with the reference site. There is a weak pattern of sample results not included in the majority of their site's cluster. Many of the outliers, or samples that do not fit from a sample site, for SD8(1), Chollas Mouth, and Ref(1) were from September or late August. Wind direction may have some role in these differences. The cluster analysis based on wind direction indicated that many of the periods in late August and September were characterized by winds more from the south-southeast (specifically, from the four octants clockwise from east through southwest).

Figure 7-13 illustrates the highly variable nature of the data. Although there are some general patterns to the elemental fluxes, it illustrates the fact that most sample sites did not have consistent chemical fingerprints associated with them. There are, however, three groups of potential fingerprint metals that appear to follow patterns across the three primary clusters: bromium, strontium, and manganese (Br/Sr/Mn); zinc and copper (Zn/Cu), and the crustal elements (Ti, Si, K, Fe, Ca, Al). The blue cluster is characterized by high fluxes of the crustal elements and Cu/Zn. The green cluster has high fluxes of Br/Sr/Mn, contrasted with low Cu/Zn fluxes. The purple cluster has generally low fluxes of all three groups.

On a land use basis, the three metals clusters appear to be highly associated with land use groups. A summary of sample counts by cluster and land use groups is presented in Table 7-5. The blue cluster contains 31 samples, 17 of which are from Land Use 3 (Switzer Creek, DPR(2) and SD8(1)). The green cluster contains 35 samples, 17 belonging to Land Use 4 (includes Mira Mesa, Prism2, and Tecolote). The purple cluster contains 15 samples, 10 of which are from Land Use 1 (Ref(1)). Land Use Group 2 (Chollas Mouth) has 8 of its 10 samples in the blue cluster. Land Use 5 (represented solely by 805T1 here) has 5 of its 8 samples in the green cluster.

Table 7-5. Sample Distribution by Land Use and Metals Cluster

Cluster	Land Use Group				
	1	2	3	4	5
Blue	0	8	17	3	3
Green	1	1	11	17	5
Purple	10	1	0	4	0

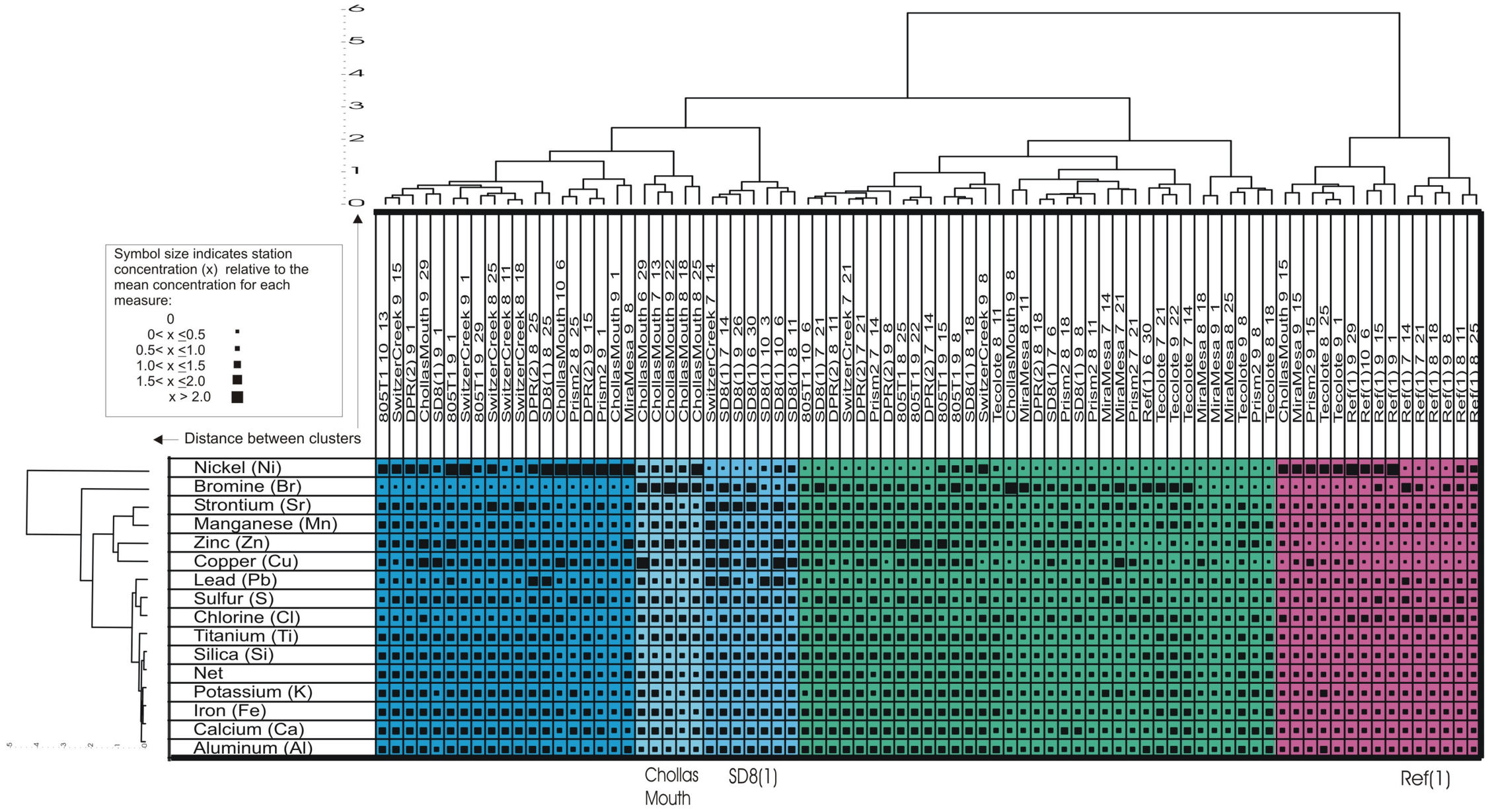

Figure 7-13. Two-way cluster analysis of chemical flux for each sample site and date

This breakdown suggests some possible land use relationships to fluxes. The purple group is characterized by generally low fluxes of all metals, indicating a more background nature. This is consistent with the majority of its samples belonging to the Ref(1) site. The other samples in that cluster may reflect days when few sources were impacting deposition at other sites. The mix of samples in the green cluster may be indicative of a mixed signature from freeway/transportation and residential areas, which is the main differentiator between Land Use Groups 3 and 4. The prevalence of Chollas Mouth samples in the blue cluster suggests industrial source influences.

The transect sites at 805 were analyzed separately from the regional sites, and the chemical flux two-way cluster analysis is presented in Figure 7-14. These samples clustered into two major groups, indicated by green and orange. The green cluster was dominated in general by copper, and the seven samples in the lighter-shaded cluster had more influence from zinc and strontium. The orange cluster was overall dominated by manganese, with the lighter-shaded 11 samples more strongly influenced by bromine. The sites do not cluster by site or date. The reason for the clustering pattern is not clear, although it may be related to wind direction or other site-specific characteristics not considered here.

It is interesting to note that copper, bromine, strontium, and manganese also appeared to play significant roles in the clustering of the area-wide samples (which included the 805T1 and 805T-Up sites). This suggests that these elements may be part of a signature group, possibly related to traffic.

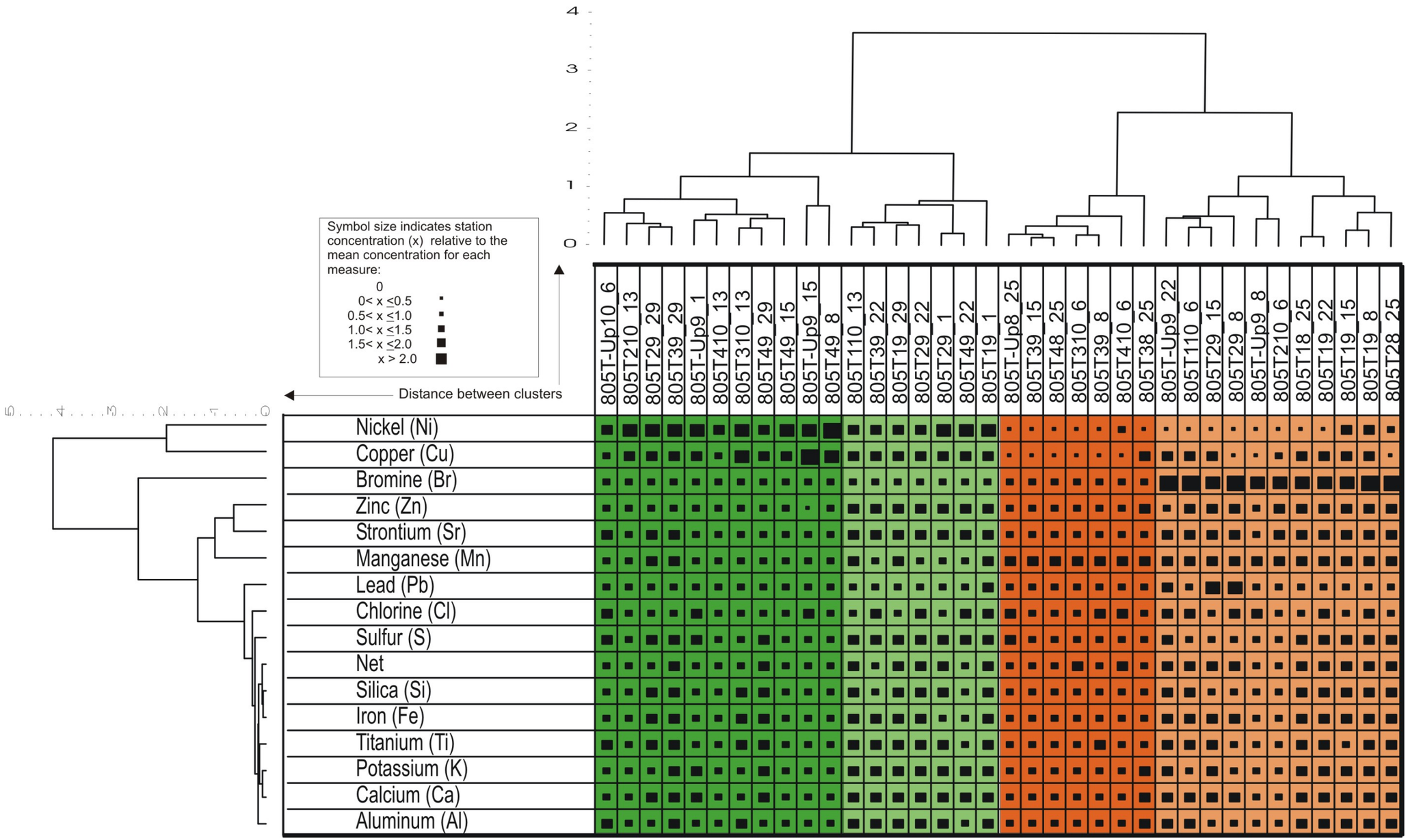

Figure 7-14. Two-way cluster analysis of chemical flux for all transect samples

7.3.3 Principal Components Analysis Results

As discussed above, a principal components analysis was completed for each land use group. The PCA replaces the original 15 flux variables with a statistically equivalent set of new variables that are combinations of the originals. The new variables are the components, and represent combinations of the original variables that share similar patterns of variation. In PCA, the components are ordered by the amount of variation in the original variables they represent. The 1st component represents the greatest amount, followed by the 2nd, 3rd, etc. Typically, PCA on a set of variables this size typically produces a few components that will represent the majority of the variation in the original variables. In addition, the components have the useful statistical properties that they are on a standard normal scale (mean of zero, standard deviation of one), and are not correlated to one another.

Original variables (here the metals) strongly correlated on a component are said to be 'loaded' on the component. Usually a component will only have positive loadings associated with it. Positively loaded metals are strongly positively correlated in the original data, and high fluxes will create higher values of the factor score.

Table 7-6 presents a summary of the first three principal components for each land use group, and the percent of the original variation explained by the three components. For all five land uses, the first three components represent from 50.2% to 68.4% of the variation found in the original 15 variables. These results indicate that for all land use groups except for Group 3 (Switzer Creek, DPR(2) SD8(1)), roughly 30% of the variability in the original data are explained by the 3 or 4 metals loaded on the first component. For Group 3, 51.4% of the variability is represented by the 8 metals loaded on the 1st component.

Table 7-6. Principal Components Summary by Land Use Groups

Land Use	Component Number						Total
	1		2		3		
Group	Elements	% Var	Elements	% Var	Elements	% Var	% Var
1	Cu Fe Si Ti	35.9	Cl S	20.0	Ni	12.5	68.4
2	Cu Fe Zn	28.2	Cl	23.1	Mn	16.3	67.6
3	Al Ca Fe K Mn Si Sr Ti	51.4	Ni	9.6	Cu	7.6	68.6
4	Al Fe K Si	31.0	Ni	11.6	Cl	9.1	51.7
5	Ca K S Ti	34.4	Cu	8.2	Zn	7.6	50.2

The elements on the 1st components for all of the land uses load one or more of the metals common in the Earth's crust: aluminum (Al), calcium (Ca), iron (Fe), potassium (K), silicon (Si), and titanium (Ti). This indicates that significant portions of the deposition fluxes at all sites are derived from eroded rock and soils. The 2nd and 3rd components represent from about 10-20% each of the variability in each land use, and load one or more of copper (Cu), zinc (Zn), chlorine (Cl), sulfur (S), nickel (Ni), and manganese (Mn). These trace metals may be indicative of other sources of particulates, including traffic and industry. The metals fall on different components in different land use groups due to the specific flux patterns at each site.

The loadings in Table 7-6 show some interesting features. Mainly, trace metals copper, manganese, and strontium appear as significant elements. Sometimes these metals appear together with the more common crustal elements. All three of these metals also featured in the cluster analyses for the area-wide and transect samples. Strontium and manganese appear in the cluster analyses and are associated with Land Use Group 3, which is primarily freeway and other roadway land use. This indicates that the 1st components represent a combined influence of crustal and other sources. The presence of chlorine and sulfur together on the 2nd components at Chollas Mouth and Ref(1) is also interesting. Even though the sample sizes for these two groups are small and the results therefore not relatively strong, this pairing is suggestive of natural maritime influences. These are the two most coastal locations, and chloride and sulfate are components of sea spray.

The components from the PCAs were used to visualize the samples within each land use group. The samples were plotted based on the new component variables, or scores. Graphs were generated using either the first and second factors, or the first and third factors. Factor 1 is always on the x-axis, while factors 2 and 3 are on the y-axis. The dominant elements for each component are represented on the axis by elemental abbreviation.

Figure 7-15 presents the samples from the Ref(1) site (Land Use Group 1). The samples are labeled by date, and color coded according to the prevailing winds. As an example of reading the plots, the samples collected on 6/30/06 and 9/29/06 have high values of both Cu/Si/Ti flux and Cl flux. The majority of the other samples are in the top left of the plot, indicating low Cu/Fe/Si/Ti fluxes occurring together with high Cl fluxes. There is one outlier in the analysis, 9/1/06. This sample has very low Cl flux, with moderate Cu/Fe/Si/Ti flux.

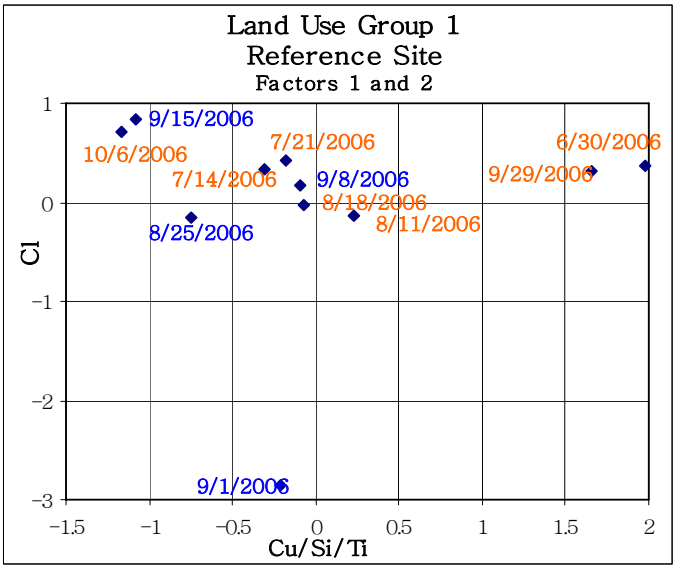

Figure 7-15. Land use 1, Ref(1), PCA results for factors 1 and 2

As a baseline estimate of how wind might affect the results, the samples collected on days when the winds were from the west/northwest/northeast/north are coded in orange, and samples collected when the predominant wind direction was from the southeast/southwest/south/east are coded in blue. This is consistent with the warm and cool color coding in Figure 7-12, the two-way cluster analysis of wind direction. There is no clear pattern of how wind might affect these results, except that all samples collected when the wind was from the southeast/southwest/south/east fall on the left site of the plot. This means that these samples had lower levels of copper, iron, silicate, and titanium.

Results from the Chollas Mouth PCA are somewhat more revealing when compared to Ref(1). All samples collected when the winds were predominantly from the west/northwest/northeast/ north cluster (Figure 7-12) generally contained higher levels of copper, iron, and zinc, but not necessarily chlorine and sulfur (Figure 7-16).

Figure 7-16 and Figure 7-17 show results for Land Use Group 2, which is the Chollas Mouth site. Figure 7-16 shows the 2nd component (chlorine/sulfur), and Figure 7-17 shows the 3rd component (manganese). Wind results are color coded as in Figure 7-15. Again, the sample on 9/1/2006 in Figure 7-16 is an outlier, as at Ref(1) (Figure 7-15). In Figure 7-16 and Figure 7-17, nearly all of the west/northwest/northeast/north wind sample dates are on the right side of the plot, showing higher flux of copper, iron, and zinc. Sample 8/18/2006 is near the middle of Factor 1, indicating more average influence of the copper/iron/zinc component. A slight difference between Figure 7-16 and Figure 7-17 is for the samples on 9/8/2006 and 9/15/2006. Both samples have relatively high chlorine/sulfur fluxes (Figure 7-16), but relatively low manganese fluxes (Figure 7-17). This suggests a different mix of source influences on those dates.

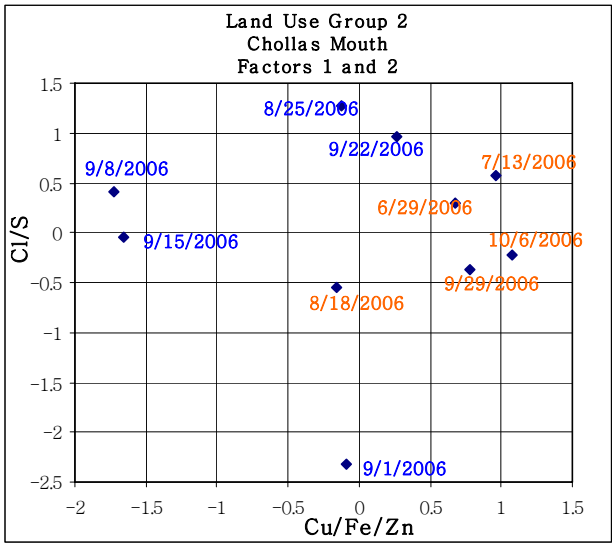

Figure 7-16. Land use 2; Chollas Mouth, PCA results for factors 1 and 2

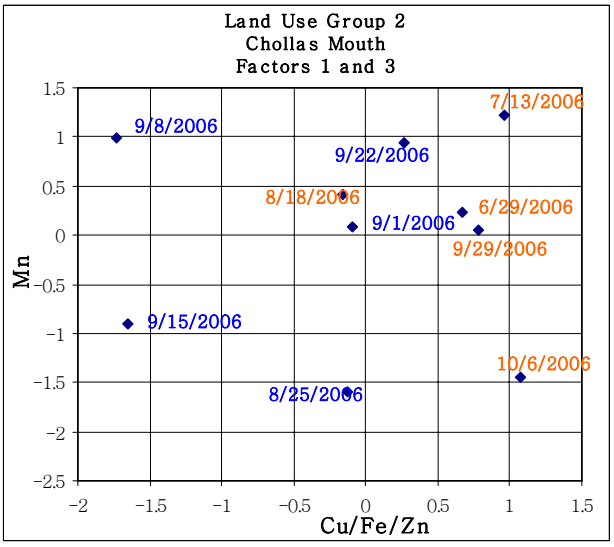

Figure 7-17. Land use 2; Chollas Mouth, PCA results for factors 1 and 3

Figure 7-18 graphs samples from Land Use Group 3, which includes SD8(1), Switzer Creek, and DPR(2). These three sites had potentially different source mixes due to the relative proximity of freeways, despite the overall similarity of the land use distributions within 1000 m of the sites. However, as shown in Figure 7-18, there are no distinctive patterns in the first two components that would suggest different source impacts. The only noticeable pattern is that Switzer Creek samples tend to fall on the right side of the plot along the crustal elements component axis. This may be due to greater influence from resuspended dust particles.

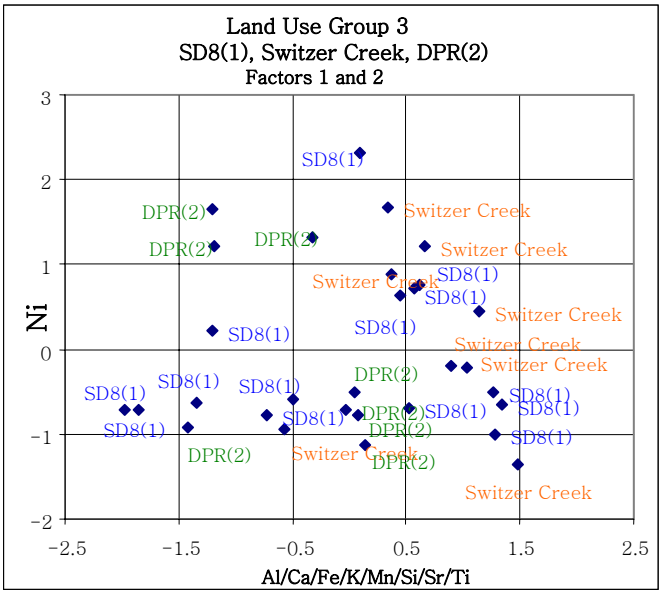

Figure 7-18. Land use 3; SD8(1), Switzer Creek, DPR(2), PCA results for factors 1 and 2

Using Factor 3 for the Land use 3 plot (Figure 7-19) shows an interesting relationship to copper. Nine of the SD8(1) samples show some degree of relatively elevated copper flux results, while the other sample sites and events have the lower copper fluxes. This parallels the observed results presented in Figure 7-1, that show SD8(1) has the highest fluxes of copper. Switzer Creek and DPR(2) have lower fluxes of copper than does SD8(1). In general, since the component values are surrogates for the original variables, the fact that the sites can not be readily distinguished in this scatterplot supports their grouping in the land use cluster analysis. They share similar chemical signatures (three components), but these signatures occur in different mixes among the sites and sample periods.

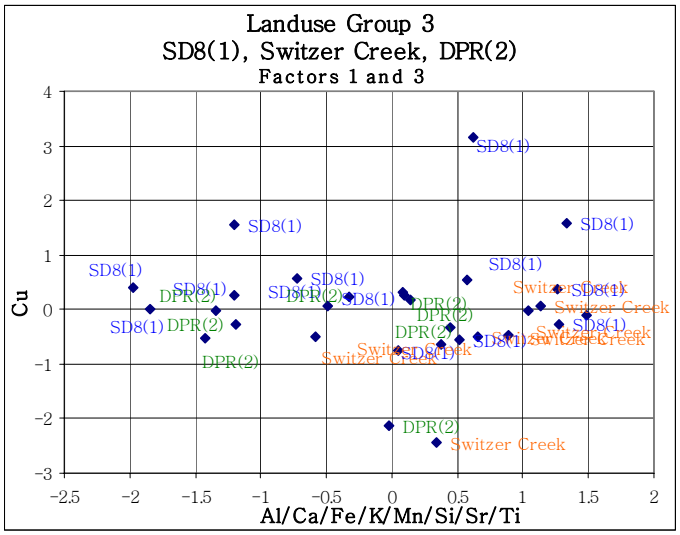

Figure 7-19. Land use 3; SD8(1), Switzer Creek, DPR(2), PCA results for factors 1 and 3

Analysis of the 1st and 2nd components for Land Use Group 4 (Figure 7-20) shows that samples from Mira Mesa and Prism2 are not easily distinguishable, but Tecolote samples have a slightly different pattern of chemical flux. Tecolote results tend to be higher in crustal elements than either Prism2 or Mira Mesa. Again, the results are supportive of these sites being grouped together in the land use cluster analysis.

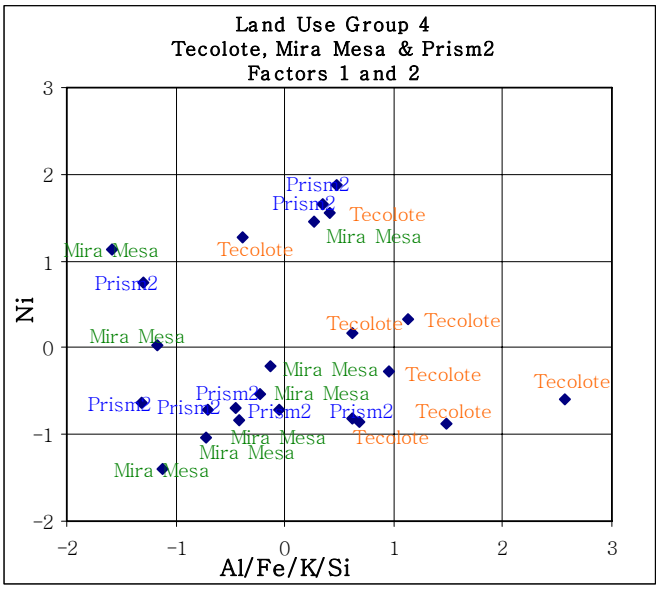

Figure 7-20. Land use 4; Tecolote, Mira Mesa, Prism2, PCA results for factors 1 and 2

Figure 7-21 charts the main components from the Transect sites (Land Use Group 5). The graph indicates that most of the results are clustered together in a general region, with two outliers from 805T4 and 805T-Up. The 805T-Up sample was collected on 9/15/2006, and has a crustal component score that is fairly typical, but is significantly elevated in copper flux. The 805T4 sample was collected on 9/8/2006, and has a very low crustal flux but a significantly elevated copper flux.

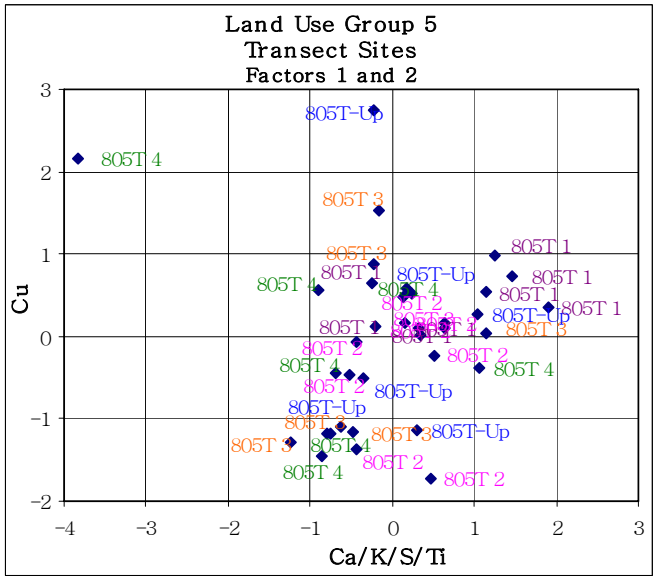

Figure 7-21. Land use 5; Transect sites 805T-up-805T4, PCA results for factors 1 and 2

7.3.4 Canonical Correlation Analysis Results

This analysis was used to correlate the percent of time the wind was from each of the eight direction sectors with the components of each individual PCA analysis. The importance of the analysis was to asses how chemical flux patterns (or fingerprints) may be related to wind direction. Relationships to a wind direction can help in source location and identification.

For Land Use Group 1, Ref (1), the small sample size dictates caution when interpreting the results. However, winds from the south were found to be correlated (0.78) with PCA factor 1 (Cu/Fe/Si/Ti), and winds from the north were found to be correlated (0.68) to factor 3 (Ni).

For Land Use Group 2, Chollas Mouth, the small sample size again dictates caution when interpreting the results. Winds from the northeast were negatively correlated (-0.72) to the 1st component (Cu/Fe/Zn). This result is indeterminate, since negative wind direction correlations are very difficult to interpret. Southwest winds are positively correlated (0.64) with PCA factor 2 (Cl/S), and southerly wind is correlated (0.67) with PCA factor 3 (Mn).

There were no positive wind direction correlations found for the major principal components of Land Use Groups 3, 4, or 5.

7.4 Data Analysis Summary

Exploratory data analysis of copper, lead, zinc, and net flux revealed that elevated copper fluxes are likely attributable to both transportation related activities and industrial/commercial activities. The median copper flux results at the I-805 transect site were relatively similar, with all sites downwind of the freeway having median values less than 10 µg/m^2/day. This is likely consistent with the finer particle sizes found in brake-wear debris. Finer particles will generally travel farther distances. However, the median copper fluxes were still considerably higher than the fluxes observed at the Ref(1) and Tecolote Creek sites. This also suggests that transportation related emissions may be related to copper flux at this location. Additionally, with no industrial sources near by, the copper fluxes within 500 meters of freeways in other locations would be expected to have a median flux less than 10 µg/m^2/day (based on the results of copper flux near freeways). This finding supports the idea that industrial or commercial sources in the Chollas Creek area are also contributing elevated levels of copper particulates. The SD8(1) site had a median flux of 20.3 µg/m^2/day and the Chollas Mouth Site had a median copper flux of 17.5 µg/m^2/day, double what would be expected from freeway sources in the surrounding area. Although statistical differences did not single out one land use in particular, the overall observation of facilities in the proximity of Chollas Mouth is considered industrial in nature. Additionally, due west of the SD8(1) site, several industrial/commercial facilities (e.g., auto dismantling yards, recycling facilities, and painting facilities) located on Commercial Street may potentially contribute particulate emissions to this area.

The impactor size distributions indicated that roughly 50% of the overall atmospheric particulate mass, as well as the atmospheric masses of copper, lead, and zinc, are found in the fine particle fraction less than 1.5 µm in aerodynamic diameter (higher percentages of fines were noted for copper and lead). However, the photomicroscopy size analysis indicated that large particles greater than 15 µm in size dominate the deposition mass.

Low concentrations of lead (generally just above method detection limits) were detected in the high-volume air samples for the impactor analysis. Lead was also found mainly in the finest particle fractions. Being both present at very low levels in the atmosphere and on the slowest-depositing particles makes it logical that lead was seldom detected on the surrogate disks. However, the fact that lead was detected in a majority of samples at the SD8(1) site indicates that the surrogate disk method is capable of detecting more significant fluxes of lead.

The cluster analysis revealed that there are distinctive differences between land use patterns within a 1 kilometer radius of each site. The Ref(1) and Chollas Mouth sites were unique in their proportions of water and industrial land uses. The Switzer Creek, DPR(2) and SD8(1) sites are dominated by freeways and other roadways. The Mira Mesa, Prism2, and Tecolote sites are dominated by a mix of residential and freeways/roadways.

Cluster analysis by the individual metal fluxes indicated grouping patterns that were distinct by land use type, but indistinct by elements. Of the trace elements, copper, manganese, bromine, strontium, and zinc appeared to be involved in differentiating the clusters. The analysis did not produce any readily obvious source fingerprints. However, the high degree of association between the chemically-derived clusters and the land use clusters strongly suggests that there are chemical signatures that may be relatable to specific land uses.

Principal component analysis by land use groups indicated that crustal elements are responsible for roughly 30-50% of variability in fluxes in all the groups, indicating re-suspended dust as a significant region-wide influence. Comparisons of the specific crustal factor scores indicated that the Switzer Creek and Tecolote sites showed more influence of re-suspended dust than the other sites in their respective land use groups. The trace metals copper, zinc, strontium, and manganese also accounted for significant proportions of the variations, indicating industrial and/or traffic source influences. Copper, manganese, and strontium combined with crustal components in some land use groups, indicate mixed source-type influences. Also, the PCA indicated a chlorine/sulfur component suggestive of sea spray influence at the two most coastal sites (Ref(1) and Chollas Mouth).

Canonical correlation of wind direction frequencies to the principal components only revealed significant positive relationships at Ref(1) and Chollas Mouth (Land Use Groups 1 and 2, respectively). At Ref(1), south and north winds were associated with the crustal/copper (1^{st}) and nickel (3^{rd}) components, respectively. At Chollas Mouth, south winds were associated with the manganese component, and southwest winds were associated with the chlorine/sulfur component. This latter wind correlation supports the interpretation of the chlorine/sulfur component as being maritime in nature.

The highly variable nature of the data, added to the multiple-day sampling events and associated significant variability of wind direction, makes finding relationships in a dataset of this size more difficult. As a rule, multivariate analysis is apt to be more effective if there are least as many samples as there are variables in each subset being considered. This was not the case in this study, particularly for the two sites with singular land use profiles, which only had about half as many observations as variables. The relatively weak indications of source fingerprints and land use relationships that were able to be seen, however, suggest that collecting a larger data set may yield more definitive results.

6.0 RESULTS

The following sections present the results of the pilot study, the area wide study, and impactor analyses performed during the course of this study.

6.1 Pilot Study Results and Discussion

A pilot study was performed as an initial sampling event to determine the optimal number of days required for adequate loading on the sample disks and for comparison to the Apiezon grease method used by SCCWRP at the mouth of Chollas Creek. Sampling for the pilot study occurred at sites SD8(1), the mouth of Chollas Creek, and the Reference Site at Point Loma. Samplers were deployed for durations of two days at the mouth of Chollas Creek, three days at the SD8(1) site, and four days at the reference site. Samples collocated with SCCWRP occurred only at the mouth of Chollas Creek. Results are available for all sampling events in Appendix A.

6.1.1 Pilot Study Flux Results

Results of the pilot study conducted at the mouth of Chollas Creek for copper, lead, and zinc are presented below in Table 6-1.

Table 6-1. Results of the pilot study conducted at the mouth of Chollas Creek. Samples were exposed from 6/27/06 through 6/29/06.

	Mass Flux (µg/m2/day)							RPD of Average Results
	Apiezon Grease Method	Apiezon Grease Method	Surrogate Disk Method	Surrogate Disk Method	Surrogate Disk Method	Apiezon Grease Method	Surrogate Disk Method	
Analyte	Rep1	Rep2	Rep1	Rep2	Rep3	Average	Average	%
Copper	**52.8**	**64.9**	**67.4**	**96.4**	**56.7**	58.8	73.5	22.2
Zinc	**105**	**124**	**63.0**	**214**	**140**	115	139	19.1
Lead	**5.7**	**8.7**	**12.0**	<5.0	<2.5	7.2	6.5	10.0

The average depositional fluxes measured at the mouth of Chollas Creek using the Apiezon grease method for copper, zinc, and lead were 58.8, 115, and 7.2 µg/m^2/day respectively. The average depositional fluxes measured at the mouth of Chollas Creek using the surrogate disk method for copper, zinc, and lead were 73.5, 139, and 6.5 µg/m^2/day respectively. Target analytes were detected in all samples with the exception of lead in the surrogate disk method replicates 2 and 3. Analytes that were detected but were less than 3 times the method detection limit were presented as the detection limit for XRF analyses. The relative percent difference between the two methods for copper, zinc, and lead (including the < values) were 22.2%, 19.1%, and 10.0% respectively. The average fluxes of copper, zinc, and lead are graphically presented in Figure 6-1 for visual comparison of the two methods.

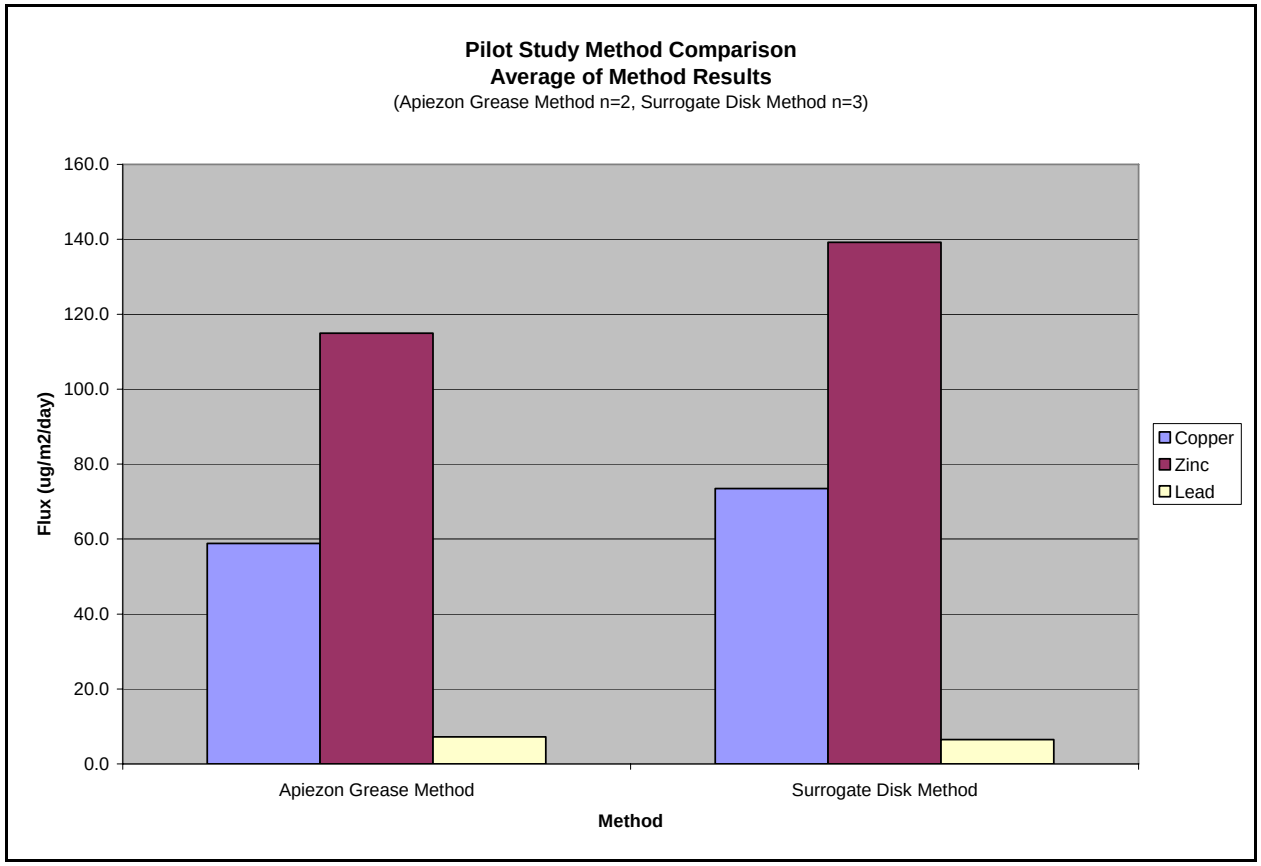

Figure 6-1. Comparison of the average deposition flux of copper, zinc, and lead from two different air deposition sampling and analysis techniques. Apiezon grease and ICP-MS at left and surrogate disk and XRF at right.

Samples were also deployed in triplicate at the reference site on Point Loma and at the SD8(1) location for comparison of the different sites and differences in replicates. Only the surrogate disk method was used at the reference site and the SD8(1) site. A method blank was also used and was opened and exposed to the ambient surroundings during sample transfers at Weston's facility.

Samples were exposed for a duration of four days (06/26/06 through 06/30/06) at the reference site on Point Loma. Results for the Point Loma reference site are presented below in Table 6-2.

Table 6-2. Results of the pilot study reference site (Point Loma). Samples were exposed from 06/26/06 through 06/30/06.

Surrogate Disk Method	Mass Flux (µg/m^2-day)			
	Rep1	Rep2	Rep3	Average
Copper	**5.4**	**6.6**	<3.3	5.1
Zinc	**8.7**	**13.1**	<2.7	8.2
Lead	<2.1	<4.2	<4.2	<3.5

The average depositional fluxes measured at the reference site for copper, zinc, and lead were 5.1, 8.2, and < 3.5 µg/m^2/day respectively. Lead was not detected above the uncertainty value at the reference site. Copper and zinc were not detected above the uncertainty value at the reference site in replicate #3 which shows these analytes are near the limit of detection even with four days of exposure.

Samples were exposed for a duration of three days (06/27/06 through 06/30/06) at the SD8(1) site. Results for the SD8(1) site are presented below in Table 6-3.

Table 6-3. Results of the pilot study SD8(1) site. Samples were exposed from 06/27/06 through 06/30/06.

Surrogate Disk Method	Mass Flux (µg/m^2/day)			
	Rep1	Rep2	Rep3	Average
Copper	**35.1**	**27.7**	**101**	54.6
Zinc	**146**	**112**	**120**	126
Lead	**12.1**	<9.4	<7.0	9.5

The average depositional fluxes measured at the reference site for copper, zinc, and lead were 54.6, 126, and 9.5 (including the < values) µg/m^2/day respectively. Lead was not detected above the uncertainty value in replicates 2 and 3.

Method blank results are presented below in Table 6-4. Samples were exposed for a brief duration representing sample preparation, transfer, and handling. The equivalent sample result fluxes are based on three days of exposure. No copper, zinc, or lead was detected in the method blanks during the sample events from 06/26/06 through 06/30/06.

Table 6-4. Results of the pilot study method blank. Samples were exposed during sample transfer and handling (fluxes based on 3 days of exposure).

Surrogate Disk Method	Mass Flux (µg/m^2/day)
Copper	<1.6
Zinc	<2.0
Lead	<6.2

The depositional fluxes for all samples collected during the pilot study are presented graphically in Figure 6-2. Based on a comparison of the results, it is evident that higher depositional fluxes of copper and zinc occurred at the mouth of Chollas Creek and the SD8(1) site in comparison to the reference site at Point Loma. While lead was detected in only one of the three replicates at both the mouth of Chollas Creek and the SD8(1) site, lead was not detected at the reference site or method blank. This does present the challenge that aerially deposited lead concentrations may be at or near the detection limit of the surrogate disk method, but indicated that lead should be distinguishable where fluxes are greater in magnitude.

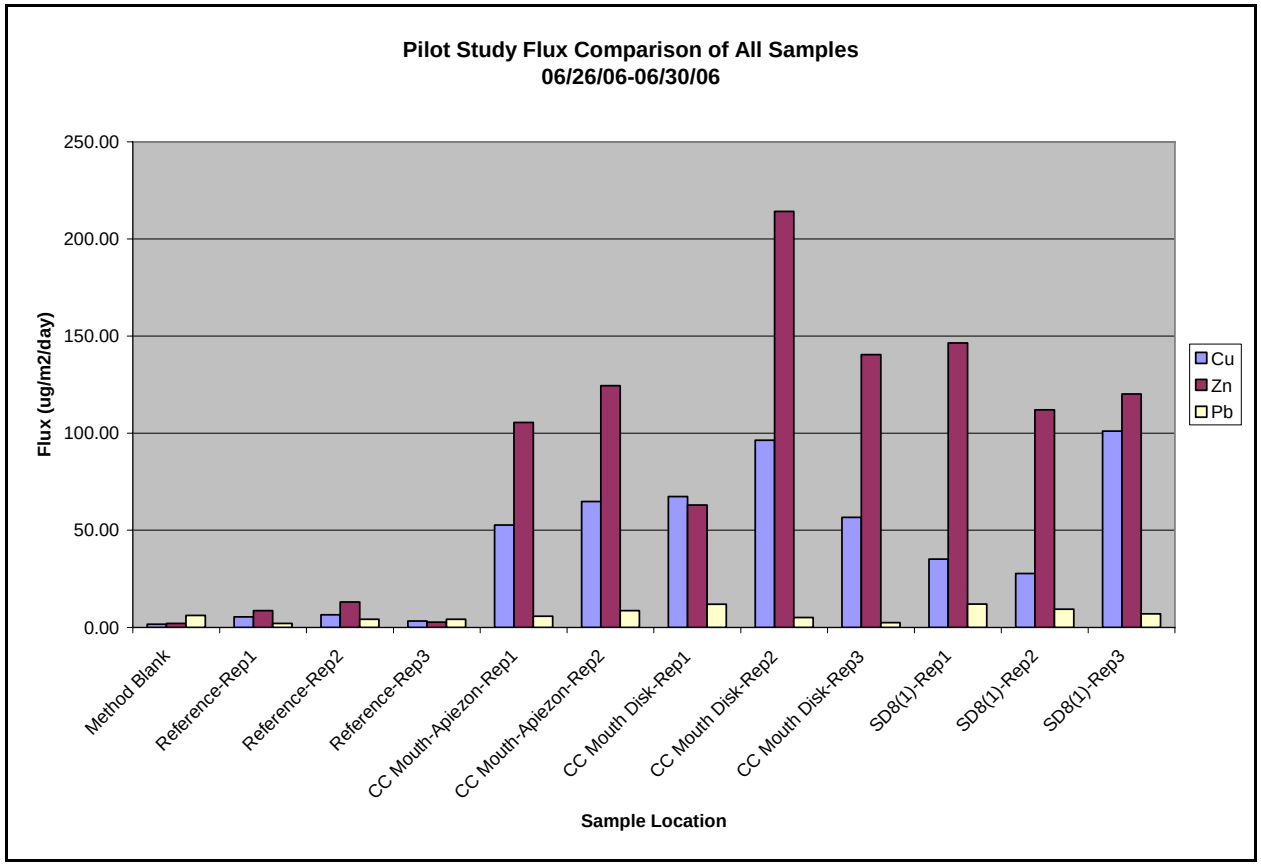

Figure 6-2. Comparison of all results from the pilot study conducted from 06/26/06 through 06/30/06.

A second study was performed at the SD8(1) site during the week of July 3, 2006. A total of 3 sample cassettes were deployed for durations of 2-days, 3-days, and 4-days respectively to determine the variation in deposition over the deployment duration. Sample results are presented below in Table 6-5.

Table 6-5. Results of the pilot study SD8(1) site. Samples were exposed for 2, 3, and 4, days respectively.

Surrogate Disk Method	Mass Flux (µg/m^2/day)		
	2 Days	3 Days	4 Days
Copper	**5.4**	**9.7**	**15.8**
Zinc	<1.8	**34.6**	**61.2**
Lead	<9.5	<3.1	**7.9**

An evaluation of the results in Table 6-5 showed that four days of exposure resulted in detections of copper, zinc, and lead. However, the variability in the lead detections from all sample results from the pilot study shows that even with four days of exposure, lead concentrations may not be detected.

It was determined that the analytical sensitivity of the surrogate disk method was acceptable for use in the area wide and transect studies based on the comparison of all the results from the Apiezon grease and surrogate disk methods at the mouth of Chollas Creek, the reference site at Point Loma, site SD8(1), and the method blank. Though the sample results using the surrogate disk method did result in values being below the analytical uncertainty of the XRF method, the ultra-low detection limit was still sufficient for comparing where elevated depositional fluxes are occurring.

6.1.2 Advanced Particle Analysis

Advanced particle analysis of the deposition disks collected from Chollas Mouth during the pilot study was performed. This study includes performing annotated photomicrography, particle size distribution, and scanning electron microscopy-energy dispersive x-ray diffraction.

Chollas Mouth

Green flux condensation spheres and metallo-oxides were particles of interest observed at 100x magnification on the Chollas Mouth Site sample presented in Figure 6-3.

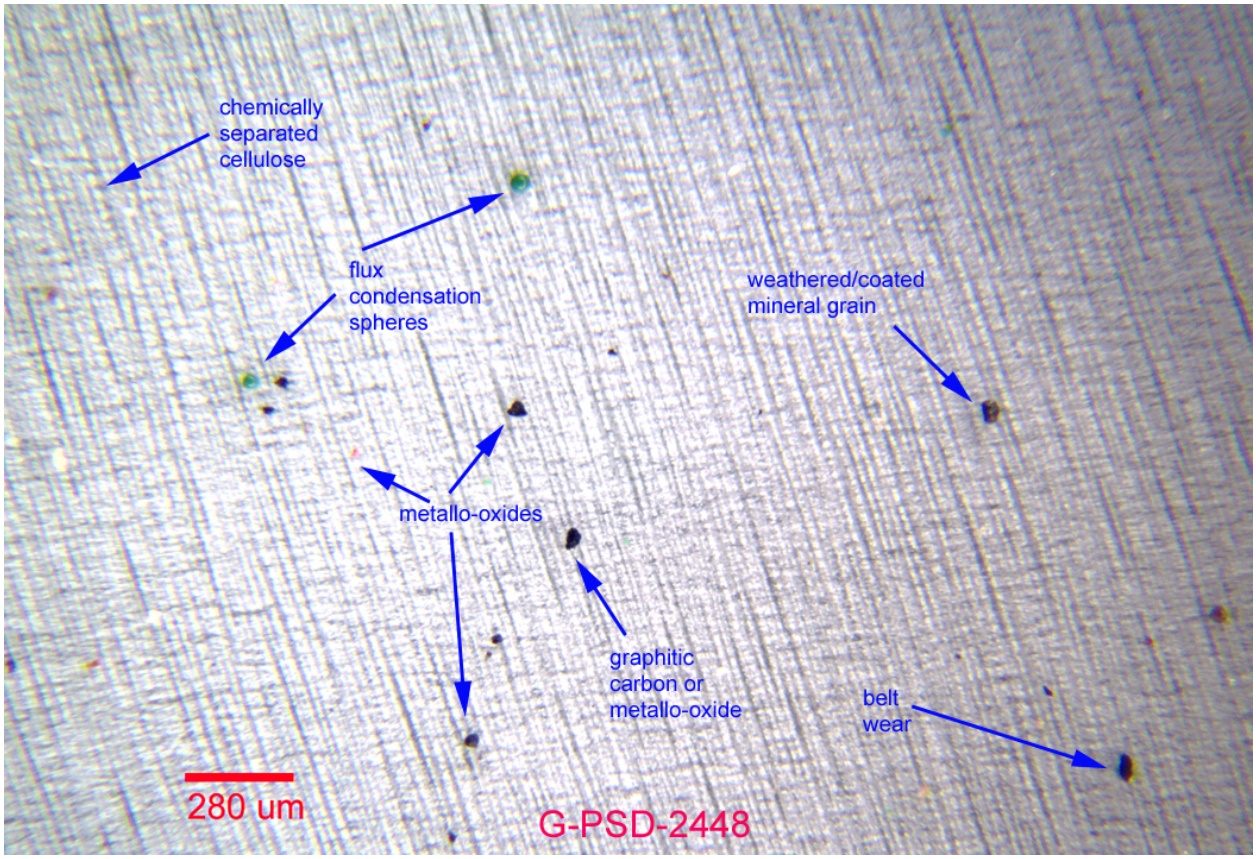

Figure 6-3. Photomicrograph of surrogate deposition disk collected at the mouth of Chollas Creek on June 29, 2006.

Particle size distribution indicate that the majority of observed disk area was obscured by particles generally between 15-100 µm in size though finer particles were observed (Table 6-6).

Table 6-6. Particle Distribution from Chollas Mouth Sample Above

Size Range (µm)	Relative Percent Area
	6/29/2006
0.8-2	1.1
2-5	1.7
5-15	3.4
15-25	8.2
25-50	44.1
50-100	41.6
100-1000	0.0
% >15 um	**93.8**
% <15 um	**6.2**

Further analysis using SEM-EDX was performed on selected individual particles. Copper was detected in several particles ranging from 2-5 µm in size. Copper was not detected in the green flux condensation spheres present in the sample (Figure 6-4).

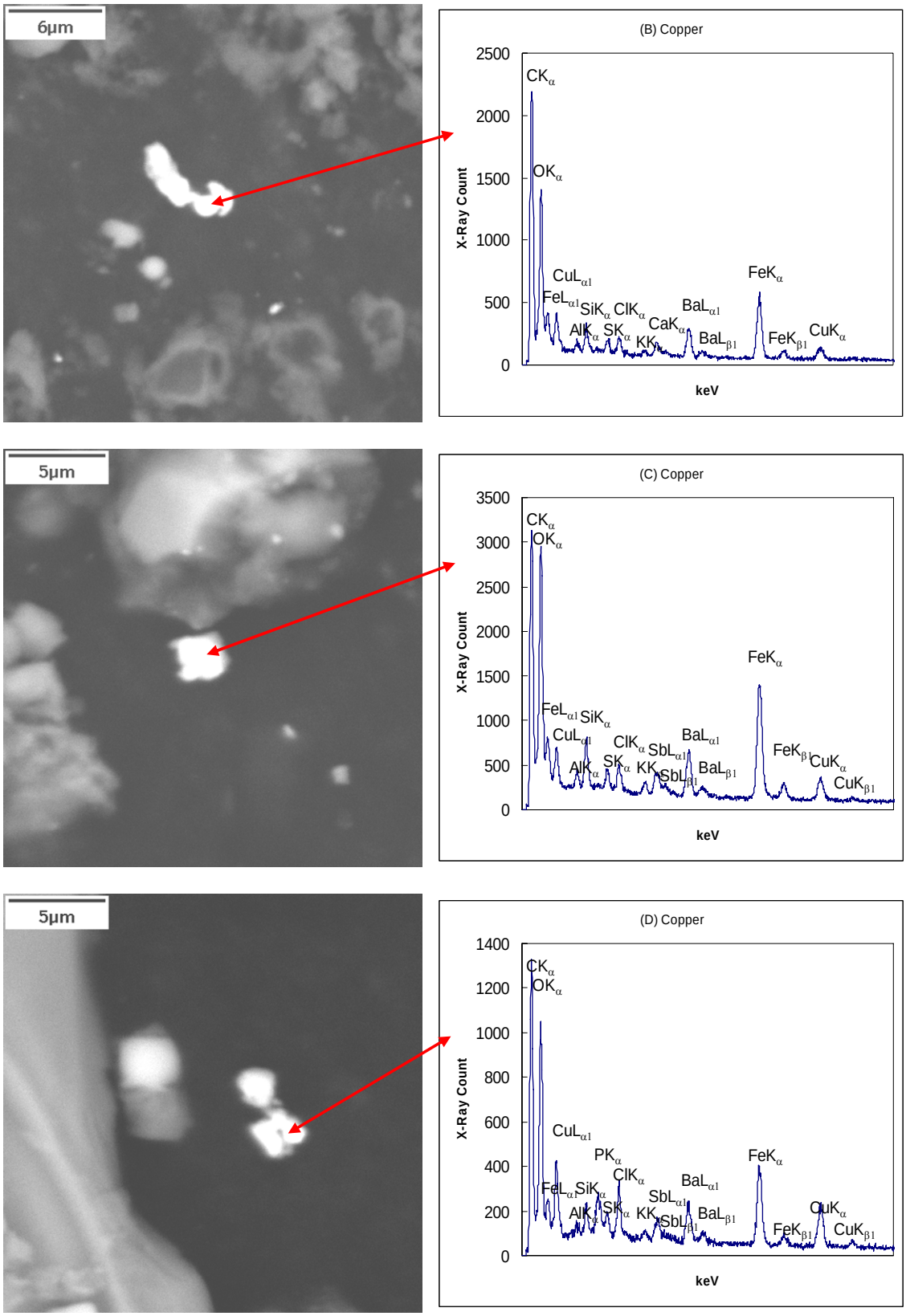

Figure 6-4. SEM back scattering images and EDX spectra of particles from the Chollas Mouth Site Sample Collected on 6/29/06

The figure below shows one of the green spherical particles. The EDX profiles from three different points on the sphere show that the particle's makeup is somewhat heterogeneous. However, the consistent presence of barium and sulfur peaks led to an interpretation as an organic suspension with finely granulated barium sulfate. This type of particle and compound are consistent with overspray of paint or other surface coatings. The sphere's 'luster' is a result of charging from electron bombardment.

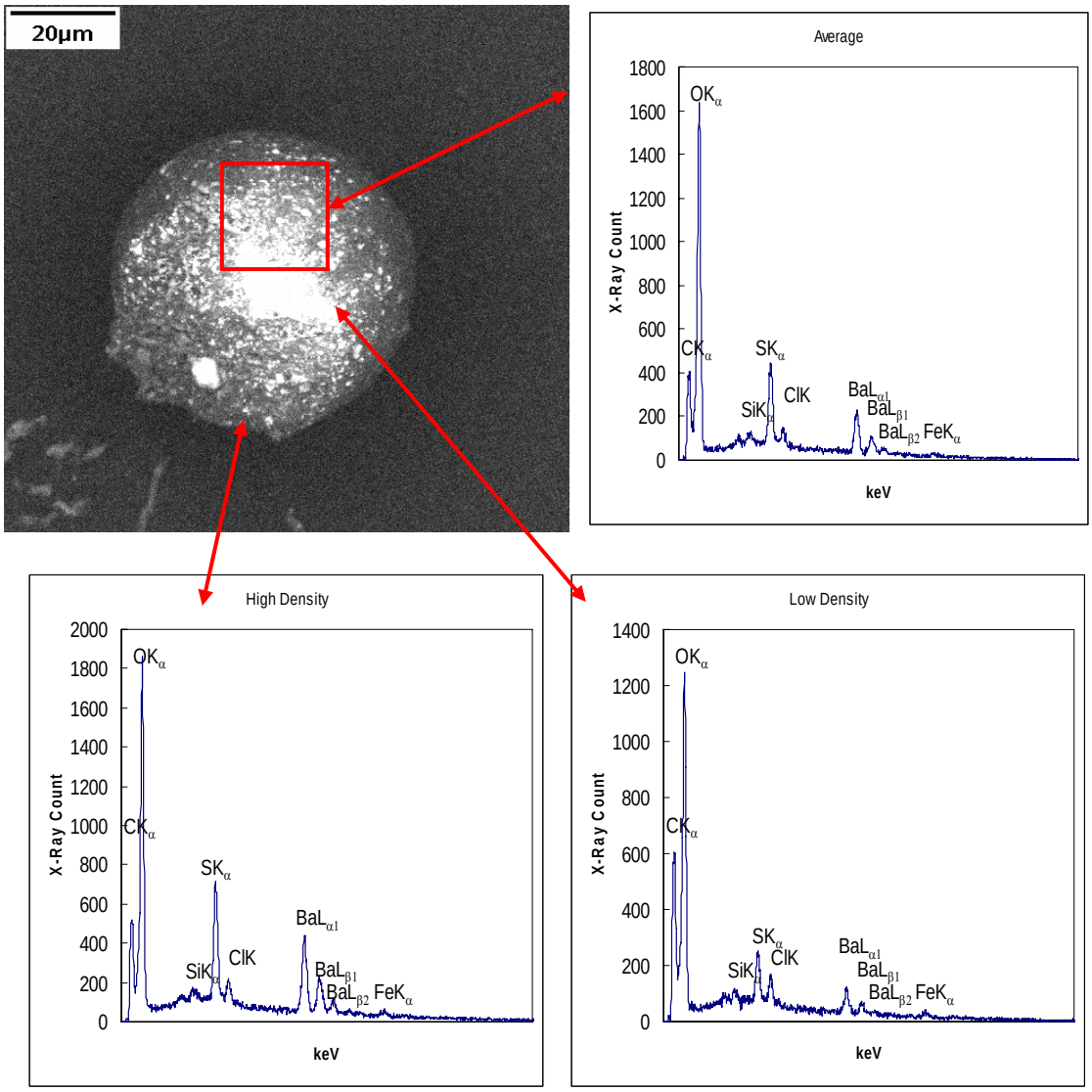

Figure 6-5. SEM back scattering images and EDX spectra of green flux condensation spheres from the Chollas Mouth Site Sample Collected on 6/29/06

Summary of Chollas Mouth particle analysis

It should also be noted that a solvent-like smell was detected during the deployment of the sample disks on this date. The analysis confirms the presence of paint-like particulates and may be coincident with the higher copper flux recorded on this date. Additionally, barium fluxes were highest on this sample date at this location than during any of the remaining sample dates or sites throughout the duration of this study.

Annotated photomicrography was also performed for samples collected from Site SD8(1) and Ref(1) and are presented in Figure 6-6 and Figure 6-7.

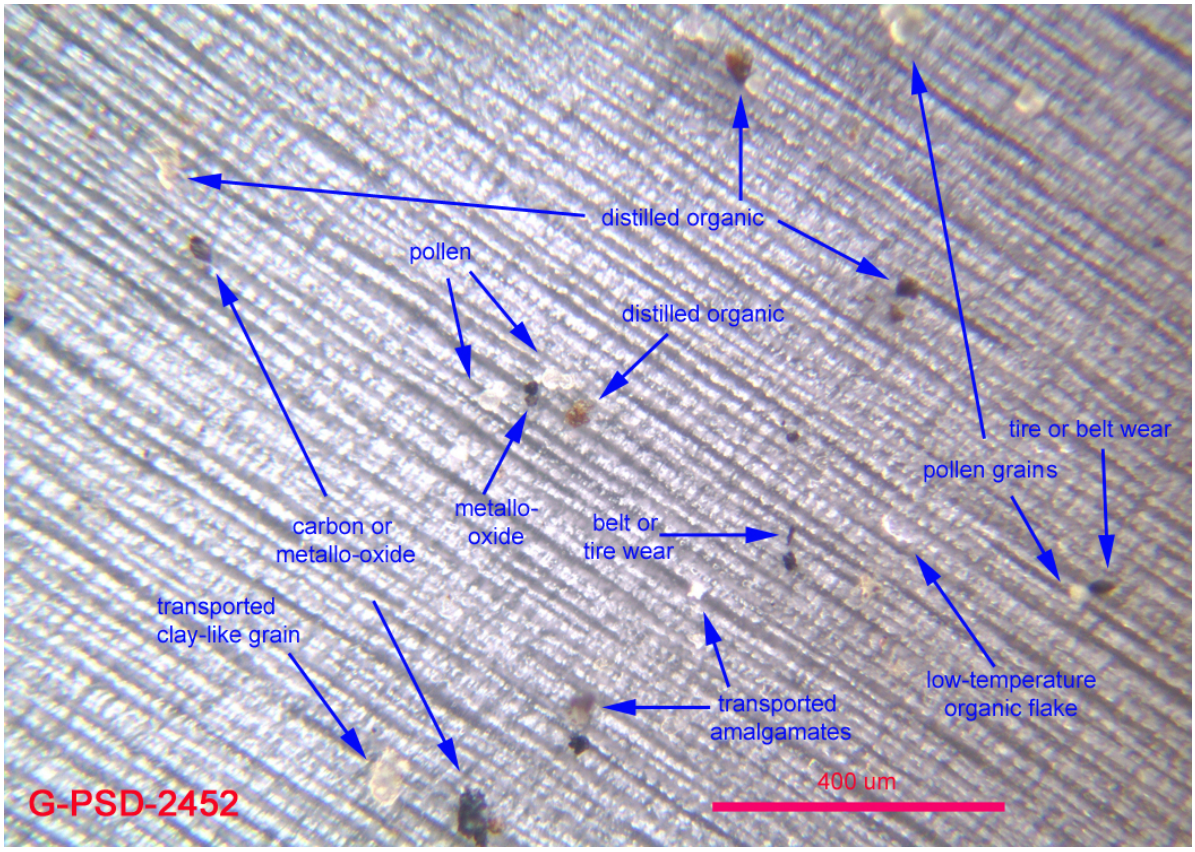

Figure 6-6. Photomicrograph of surrogate deposition disk collected at site SD8(1) on June 30, 2006.

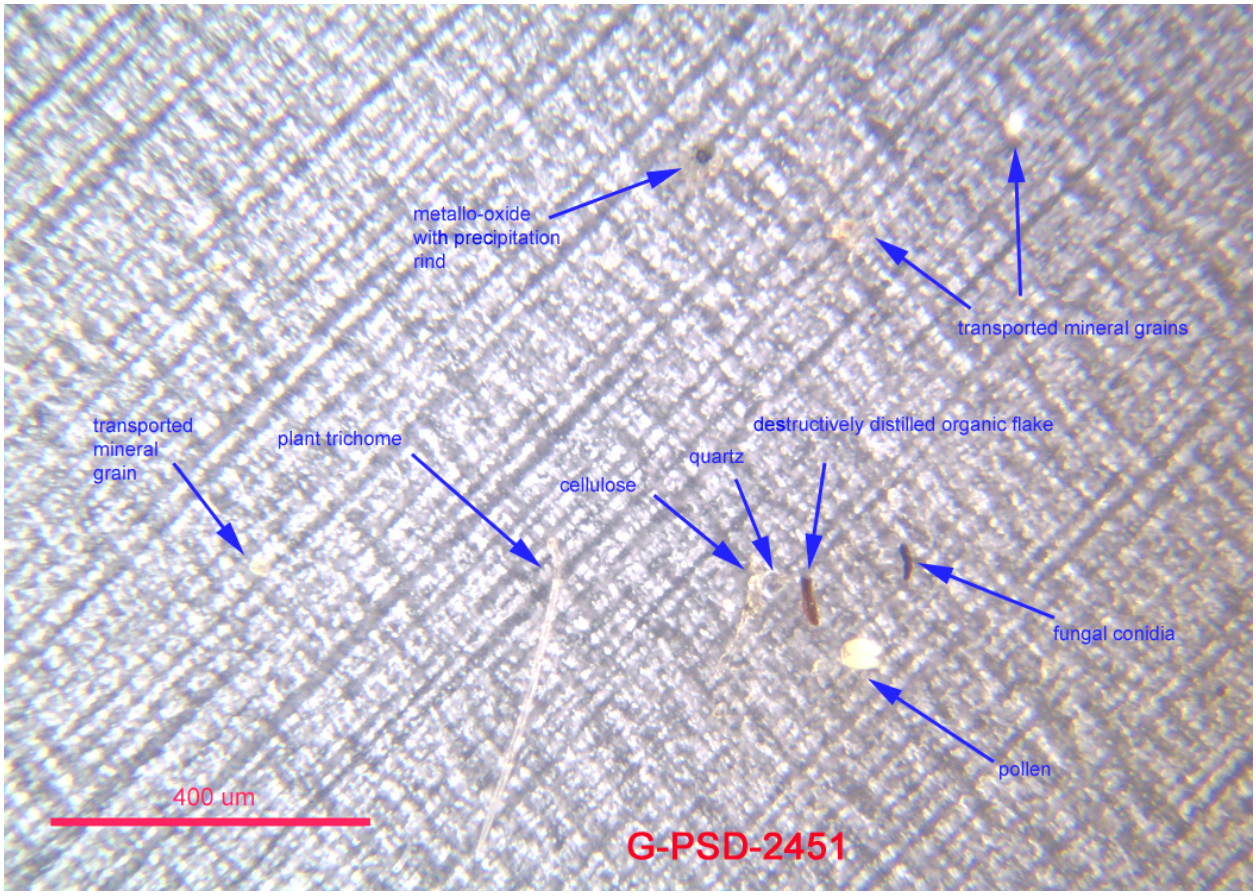

Figure 6-7. Photomicrograph of surrogate deposition disk collected at the reference site on Point Loma on June 30, 2006.

6.1.3 Pilot Sampling Conclusions

The surrogate disk method approach was determined to be sufficient to differentiate between the sample areas of interest. Advanced analyses performed on the surrogate disks indicate that transportation and industrial related particulates were evident in the Chollas Mouth and SD8(1) samples. In comparison, the Ref(1) site sample was primarily associated with naturally occurring crustal material and other plant like particulates. Non-uniform deposition and higher depositional fluxes are coincident with the larger particle sizes and differing types of particulates found in the urban areas near roadways and industrial sources verses the rural areas farther from major roadways. Based on the findings of the pilot study, it was evident that sample variability between sites and dates was to be expected.

6.2 Area Wide Results

Results for the Area Wide study are presented in this section. Results are presented by site, beginning with the Reference site [Ref(1)] and then arranged in geographical order from north to south. Results are presented for each site by the following analyses:

- XRF Results
- Photomicroscopy results
- Particle size distribution on deposition disks
- SEM-EDX particle analysis on the surrogate deposition disks
- Impactor sampling results (elemental concentrations by particle size in air)

Within each site, discussion of results for the XRF analysis occurs in groups; total net flux for total particulate matter, and depositional fluxes for copper, lead, and zinc. Analytes that were not detected or were detected at concentrations less than three times the detection limit (DL) for XRF analysis are presented as Below Detection Limit (BDL) and are shown in tables as a "<" value for the analyte-specific instrument detection limit. Site-specific depositional flux average values are calculated using a value equal to one-half the DL for results that were BDL.

The particle size distributions from the individual surrogate sample disks were determined by microscopy for a subset of the area wide study samples. These distributions are based on counts of the two-dimensional footprints of particles in the field of view. The microscopy particle size distribution uses seven ranges starting at a lower bound of 0.8 µm, with upper bounds of: 2, 5, 15, 25, 50, 100, and 1000 µm. To put the particle size ranges in perspective, the National Resources Conservation Service (NRCS) classifies particles by the following size ranges (in microns):

- Clay, total: <2.0
- Silt, fine: 2.0 - 20
- Silt, coarse: 20 - 50
- Very fine sand: 50 - 100
- Fine sand: 100 - 250
- Medium sand: 250 - 500
- Coarse sand: 500 - 1000

6.2.1 Site Ref(1)

6.2.1.1 XRF Results

Surrogate deposition disks were deployed at site Ref(1) for a total of eleven week-long events. The deposition disks were exposed for a duration of three days during each event. Analytical results from the surrogate deposition disks at the Ref(1) site are presented in Table 6-7.

Table 6-7. Depositional flux results at site Ref(1).

Date	Net	Copper	Lead	Zinc
	(mg/m^2/day)	(µg/m2/day)		
6/30/06	46.4	5.1	<4.9	<1.9
7/14/06	32.3	<1.7	6.0	<1.9
7/21/06	18.6	<1.7	<4.9	<1.9
8/11/06	19.9	<1.7	<4.9	<1.9
8/18/06	12.9	<1.7	<4.9	<1.9
8/25/06	12.1	<1.7	<4.9	<1.9
9/1/06	1.8	<1.7	<4.9	<1.9
9/8/06	23.2	<1.7	<4.9	<1.9
9/15/06	15.5	<1.7	<4.9	<1.9
9/29/06	51.9	4.5	<4.9	<1.9
10/6/06	23.1	<1.7	<4.9	<1.9

The net flux for total particulate matter ranged from 1.8 to 51.9 mg/m^2/day and averaged 23.4 mg/m^2/day for the series of deployment events. The highest net flux occurred during the week of 9/29/06.

The depositional flux for copper ranged from BDL to 5.1 µg/m^2/day and averaged 1.6 µg/m^2/day during the deployment event series (Figure 6-8). Copper was BDL for nine of the deployment week events. The highest depositional flux, 5.1 µg/m^2/day, was detected during the week of 6/30/06.

Lead was typically not detected at the Ref(1) site except for a single deployment event occurring during the week of 7/14/06 when the depositional flux measured 6.0 µg/m^2/day (Figure 6-8).

Zinc was not detected at the Ref(1) site during any of the deployment events (Figure 6-8).

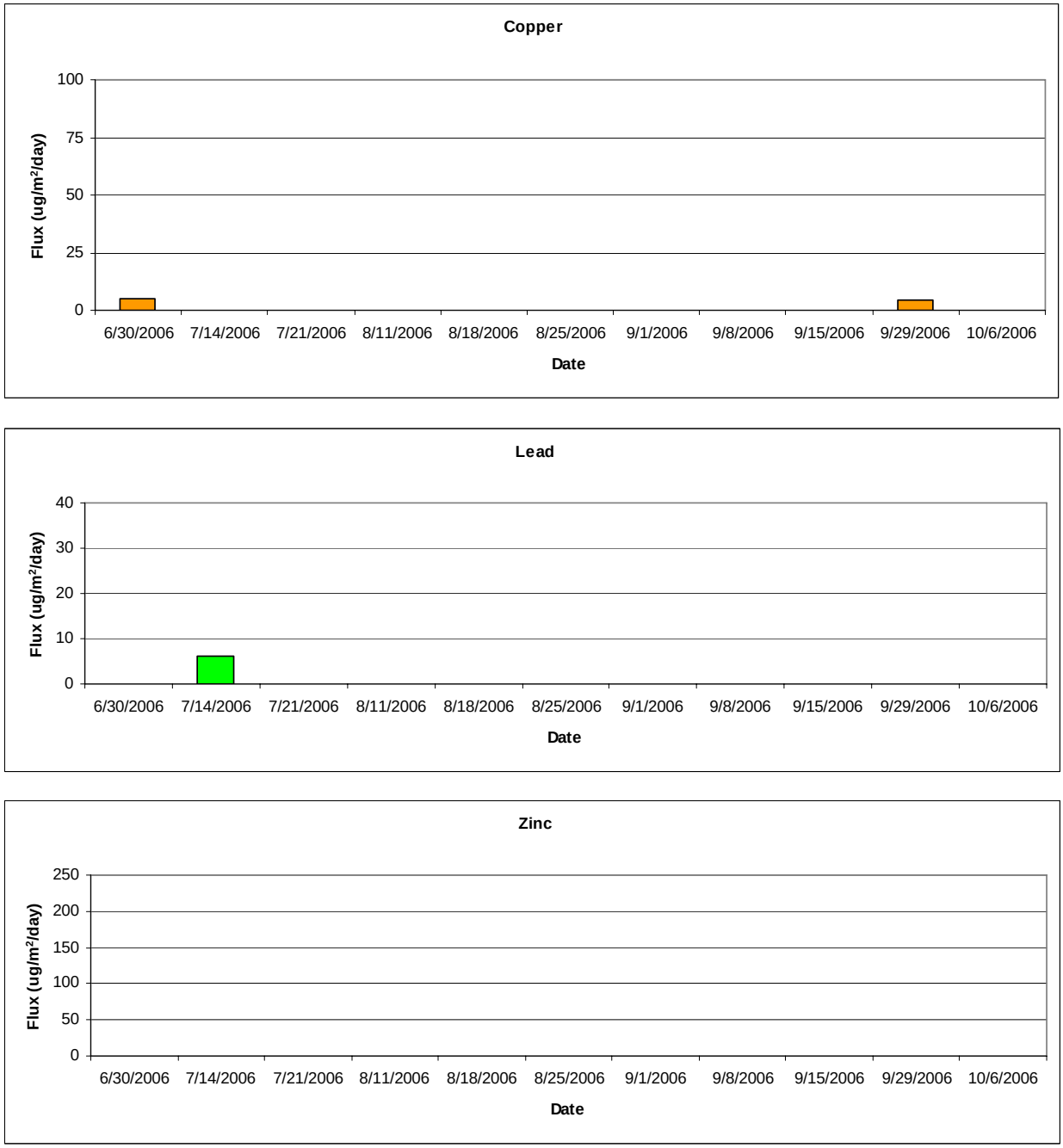

Figure 6-8. Copper, Lead, and Zinc Flux at Site Ref(1).

6.2.1.2 Photomicroscopy Results

A representative result for the photomicroscopy analysis performed on surrogate disks deployed at site Ref(1) is presented in Figure 6-9. The sample date for the surrogate disk represented in Figure 6-9 is 9/1/06.

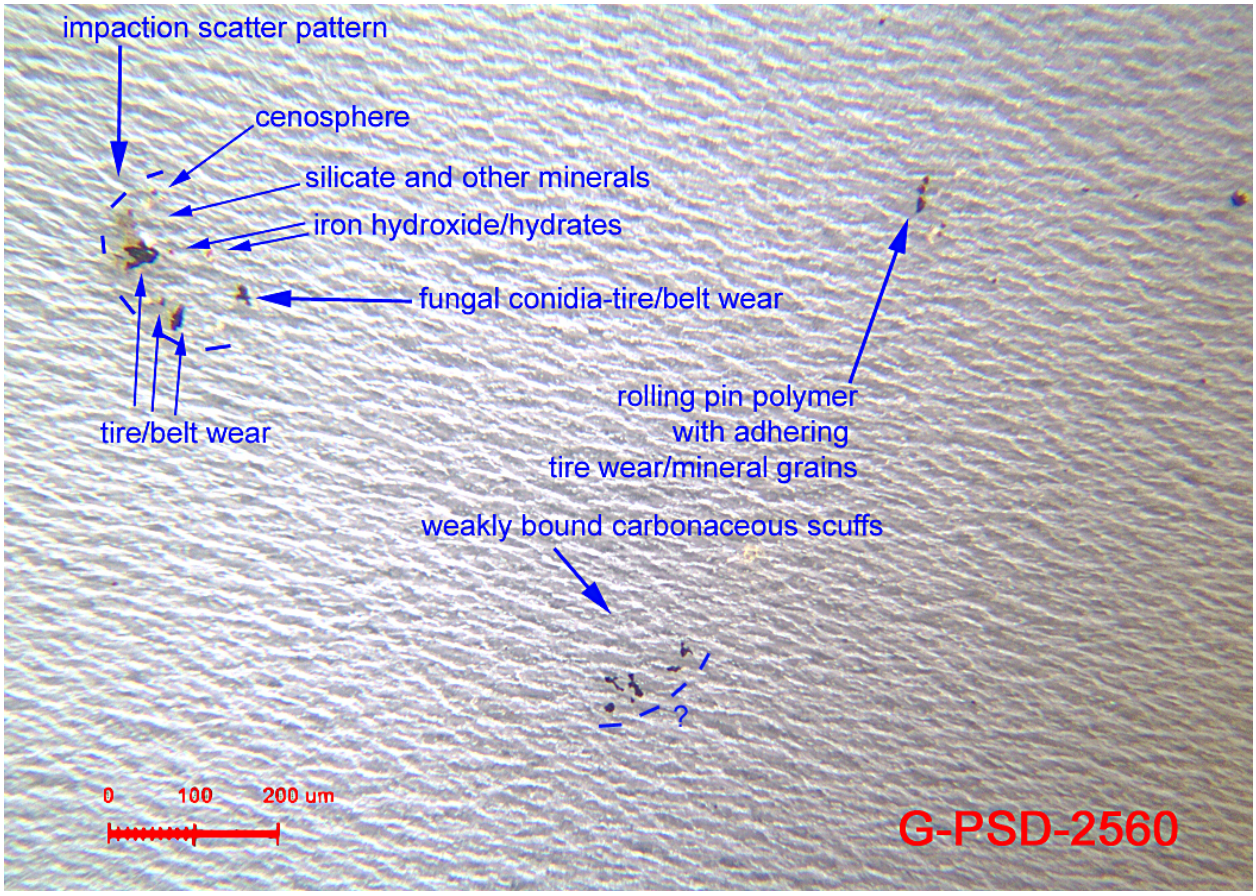

Figure 6-9. Photomicroscopy analysis for site Ref(1) on 9/1/06.

Frequently identified particles in photomicroscopy analysis at this site included silicate, weakly bound carbonaceous scuffs, and fungal conidia-tire/belt wear as well as calcium carbonate/dolomite, resin overspray, and chemically separated cellulose. All photomicroscopy results for samples collected at site Ref(1) are presented in Appendix B.

6.2.1.3 Particle Size Distribution

Particle size distributions from surrogate disk samples collected at the reference site on Point Loma were determined for four sample dates. Particulate size distributions for these four dates are shown in Table 6-8. The size distribution of particles varied for each of the four samples analyzed. With the exception of the sample collected on 7/14/06, the relative percent area was generally higher in the fractions less than 15 µm in size. One large particle > 100 µm was observed in the sample view field which dominated the percent area overall for the 7/14/06 sample. Aerially deposited particle sizes at Site Ref(1) would be classified as primarily fine silt and coarse silts with few sand size particles.

Table 6-8. Particle Size Distribution at Site Ref(1).

Size Range (µm)	Relative Percent Area			
	6/30/2006	7/14/2006	7/21/2006	8/11/2006
0.8-2	9.4	0.8	13.3	20.5
2-5	14.4	1.1	24.4	20.6
5-15	31.0	10.2	26.5	24.3
15-25	20.1	10.3	8.5	3.7
25-50	25.0	17.9	27.4	0.0
50-100	0.0	0.0	0.0	30.8
100-1000	0.0	59.7	0.0	0.0
% >15 um	**45.1**	**87.9**	**35.8**	**34.6**
% <15 um	**54.9**	**12.1**	**64.2**	**65.4**

6.2.1.4 SEM-EDX Results

SEM/EDX analysis results of particles from the sample collected at Site Ref(1) on 9/1/06 are presented in Figure 6-10. Copper was identified as flux condensation spheres in the 1-2 µm size range. Lead particles were also detected as particles associated with sliding contact in the 1-2 µm size range. Zinc particles were not detected using SEM/EDX. In comparison, the sample results from the XRF analyses were below the analytical detection limit for copper, lead, and zinc. Based on the small particle sizes containing copper and lead in this sample, it is likely the elemental mass of these particles are not present in significant quantities to be of environmental significance.

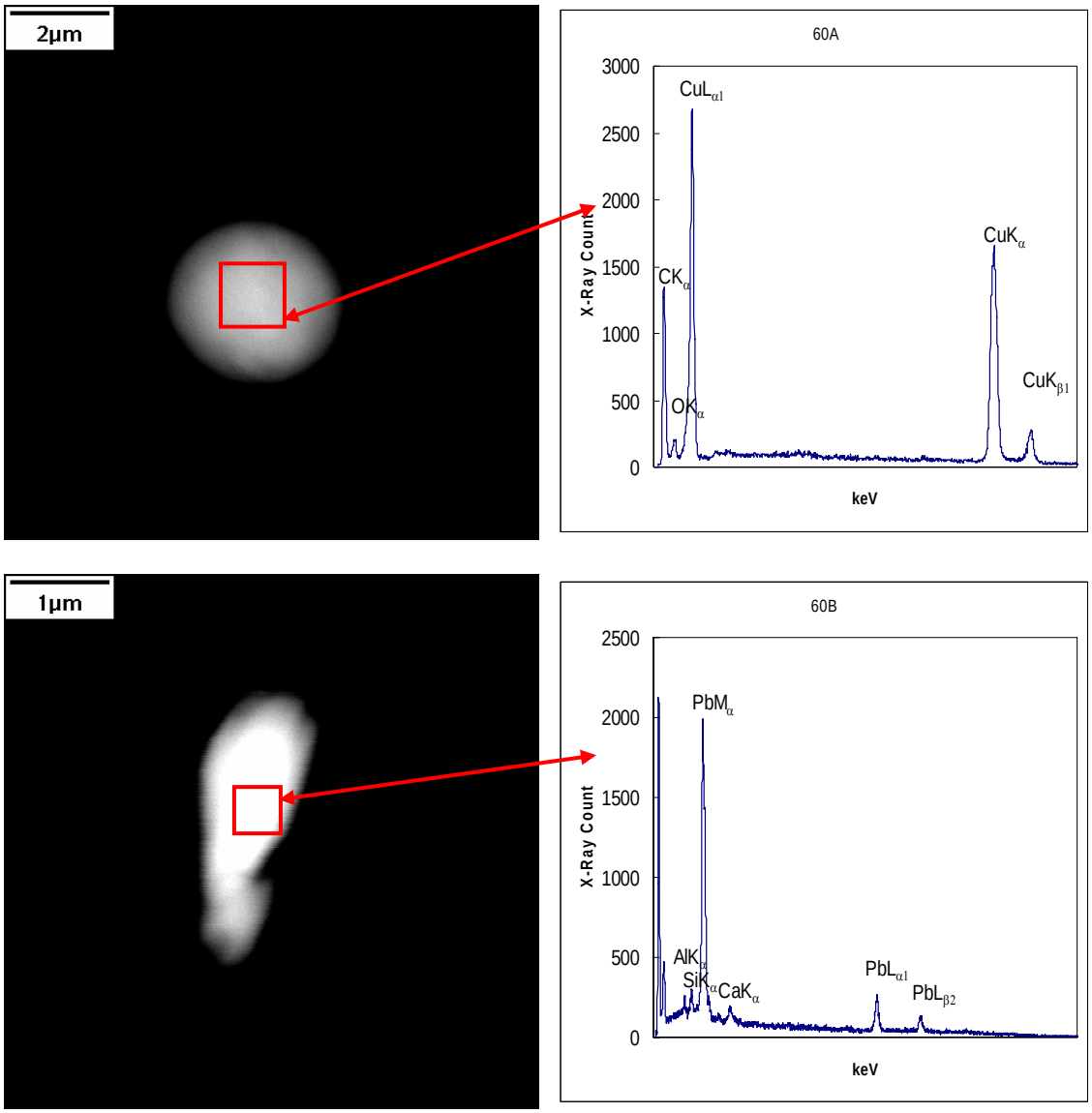

Figure 6-10. SEM/EDX analysis results of particles from the Ref(1) site sample collected on 9/1/06. Copper here was represented as flux condensation spheres. Lead was represented by particles showing a history of sliding contact.

6.2.1.5 Impactor Sampling Results

Air concentrations of site Ref(1) particulates, characterized by size and by analyte, are shown in Table 6-9. The impactor sample was collected over a 12-hour period on 8/17/06. Across most size ranges, iron concentrations were highest, followed by copper and zinc concentrations. Lead particulates were not detected in four of the five size classes and total zinc and chromium concentrations across all size classes were below 12 ng/m^3. In general, measured particulate concentrations were low, and the analyzed metals concentrations comprising only 0.82 percent of the 32.2 µg/m^3 total particulate concentration across all size classes.

Table 6-9. Distribution of the concentrations of total particulates and five metals according to particle size in ambient air collected at Ref(1).

Particle Size	Total Particulate	Chromium	Iron	Copper	Zinc	Lead
(µm)	(µg/m^3)	(ng/m^3)				
< 0.95	19.1	2.12	27.0	26.5	3.76	2.67
0.95 - 1.5	1.47	0.677	17.3	19.0	1.36	<0.82
1.5 - 3.0	2.08	1.09	23.5	7.90	1.26	<0.82
3.0 - 7.2	5.64	0.727	60.2	13.9	2.95	<0.82
> 7.2	3.92	0.726	46.2	4.03	2.55	<0.82
Total	32.2	5.34	174	71.3	11.9	4.31*

* One half the detection limit was used for values less than the MDL to calculate total lead.

Atmospheric size distributions for site Ref(1) are presented in Figure 6-11. Overall, the greatest percentage of mass for each analyte, with the exception of iron, was less than 0.95 µm in size. Greater than 30 percent of all copper, chromium, and zinc, and greater than 50 percent of total mass particulates, as well as 100 percent of all lead particulates were found within the less than 0.95 µm size class. The 0.95 – 1.5 µm size class contained 26.6 percent of the total copper particulates and contained less than 10 percent of the iron, zinc, lead, and total mass particulates. Twenty percent of all chromium particulates were between 1.5 and 3.0 µm in size while all other analytes had less than 15 percent of their respective total mass in the 1.5 – 3.0 µm size class. Among the coarse particulate sizes, particulates in the 3.0 – 7.2 µm size range contained greater than 20 percent of the zinc, 19.4 percent of the copper, and 17.5 percent of the total mass particulates as well as over 30 percent of the iron particulates, while particulates greater than 7.2 µm in size contained greater than 20 percent of the iron and zinc particulates and just slightly more than 10 percent of the chromium and total mass particulates. Similar to other locations, the mass of copper particulates was lowest in the greater than 7.2 µm size class.

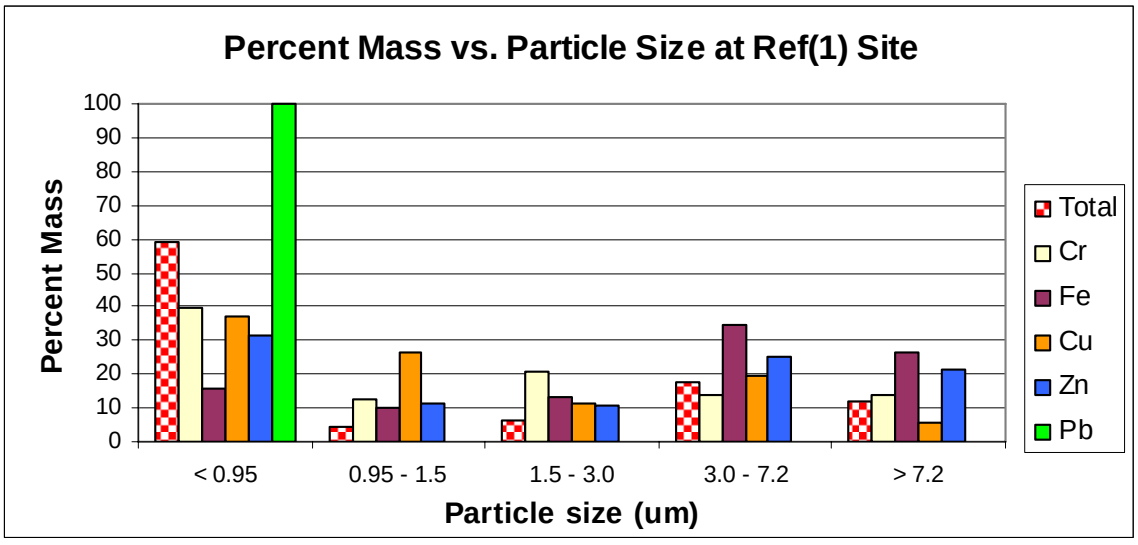

Figure 6-11. Percent mass versus particle size in air samples collected at Ref(1).

6.2.2 Site Mira Mesa

6.2.2.1 XRF Results

Surrogate deposition disks were deployed at Mira Mesa for a total of eight week-long events. The deposition disks were exposed for a duration of three days during each event. Analytical results from the primary surrogate deposition disks at the Mira Mesa site are presented in Table 6-10. Replicate disk analyses are provided in Appendix A.

Table 6-10. Depositional flux results at site Mira Mesa.

Date	Net	Copper	Lead	Zinc
	(mg/m^2/day)	(µg/m2/day)		
7/14/06	42.5	3.7	7.4	15.2
7/21/06	46.1	27.0	<4.9	13.3
8/11/06	30.3	<1.7	<4.9	22.4
8/18/06	36.3	19.7	<4.9	19.7
8/25/06	40.8	<1.7	<4.9	23.6
9/1/06	29.3	5.3	<4.9	23.3
9/8/06	74.7	8.2	<4.9	347
9/15/06	39.5	5.7	<4.9	5.7

The net depositional flux for total particulate matter ranged from 29.3 to 74.7 mg/m^2/day and averaged 42.4 mg/m^2/day for the series of deployment events. The lowest net flux occurred during the week of 9/1/06 and the highest net flux occurred during the week of 9/8/06.

The depositional flux for copper ranged from BDL to 27.0 µg/m^2/day and averaged 8.9 µg/m^2/day during the deployment event series. Copper was BDL on the weeks of 8/11/06 and 8/25/06. The highest depositional flux, 27.0 µg/m^2/day, was detected during the week of 7/21/06.

Lead was typically not detected at the Mira Mesa site except for a single deployment event occurring during the week of 7/14/06 when the depositional flux measured 7.4 µg/m^2/day (Figure 6-12).

The depositional flux for zinc ranged from 5.7 to 347 µg/m^2/day and averaged 58.8 µg/m^2/day during the deployment event series. However, the highest zinc average depositional flux that occurred during the week of 9/8/06 was greater than ten times the average depositional flux measured for all seven other events. The average depositional flux without this outlying value was 17.6 µg/m^2/day. This high zinc flux was coincident with the highest net flux (74.7 µg/m^2/day), which was also unusually high. The lowest depositional flux occurred during the week of 9/1/06 (Figure 6-12).

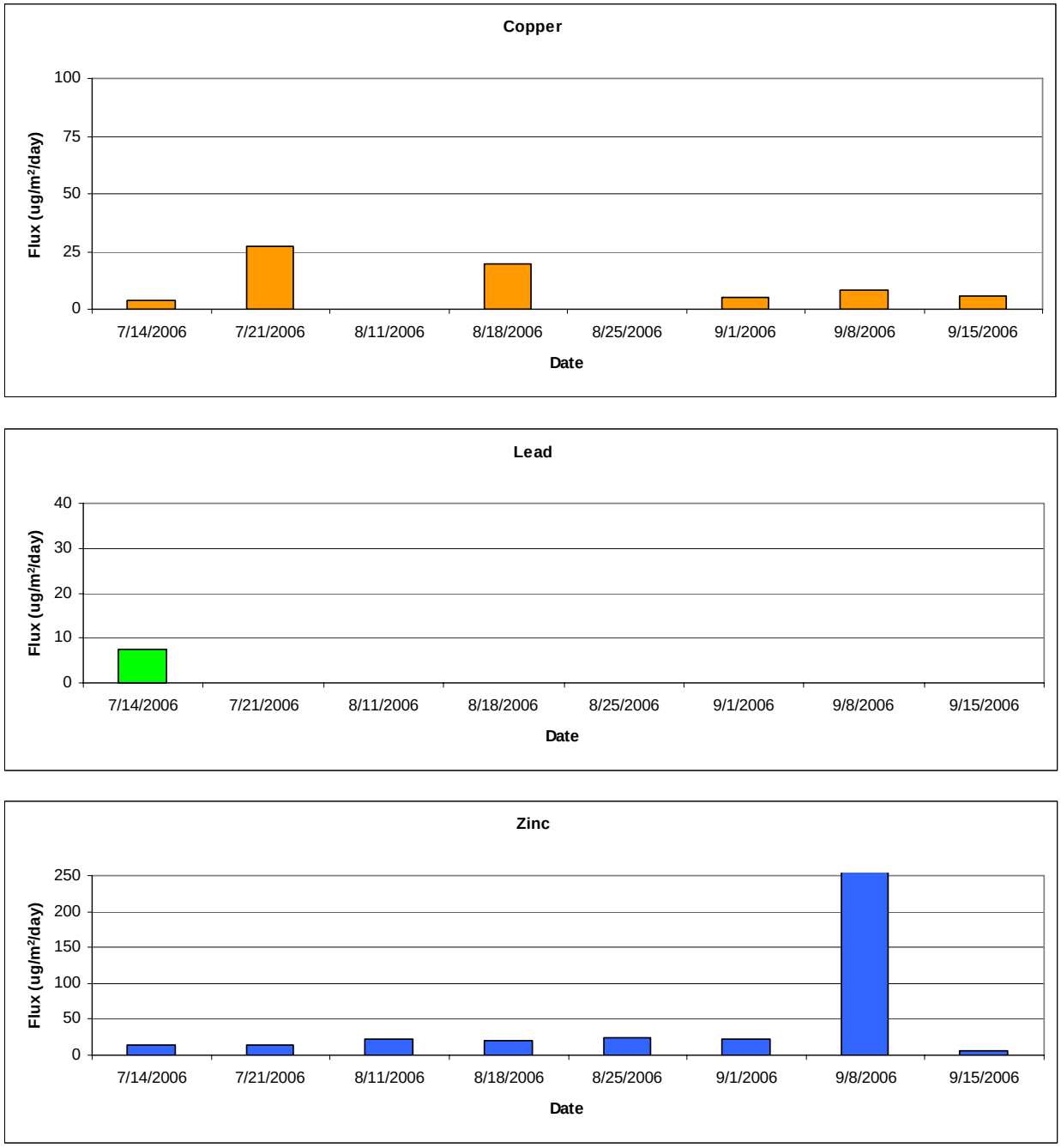

Figure 6-12. Copper, Lead, and Zinc Flux at Site Mira Mesa.

6.2.2.2 Photomicroscopy Results

Representative results for the photomicroscopy analysis performed on surrogate disks deployed at site Mira Mesa are presented in Figure 6-13 and Figure 6-14. The sample date for the surrogate disk represented in Figure 6-14 is 8/18/06 and the sample date for the surrogate disk in Figure 6-14 is 9/8/06.

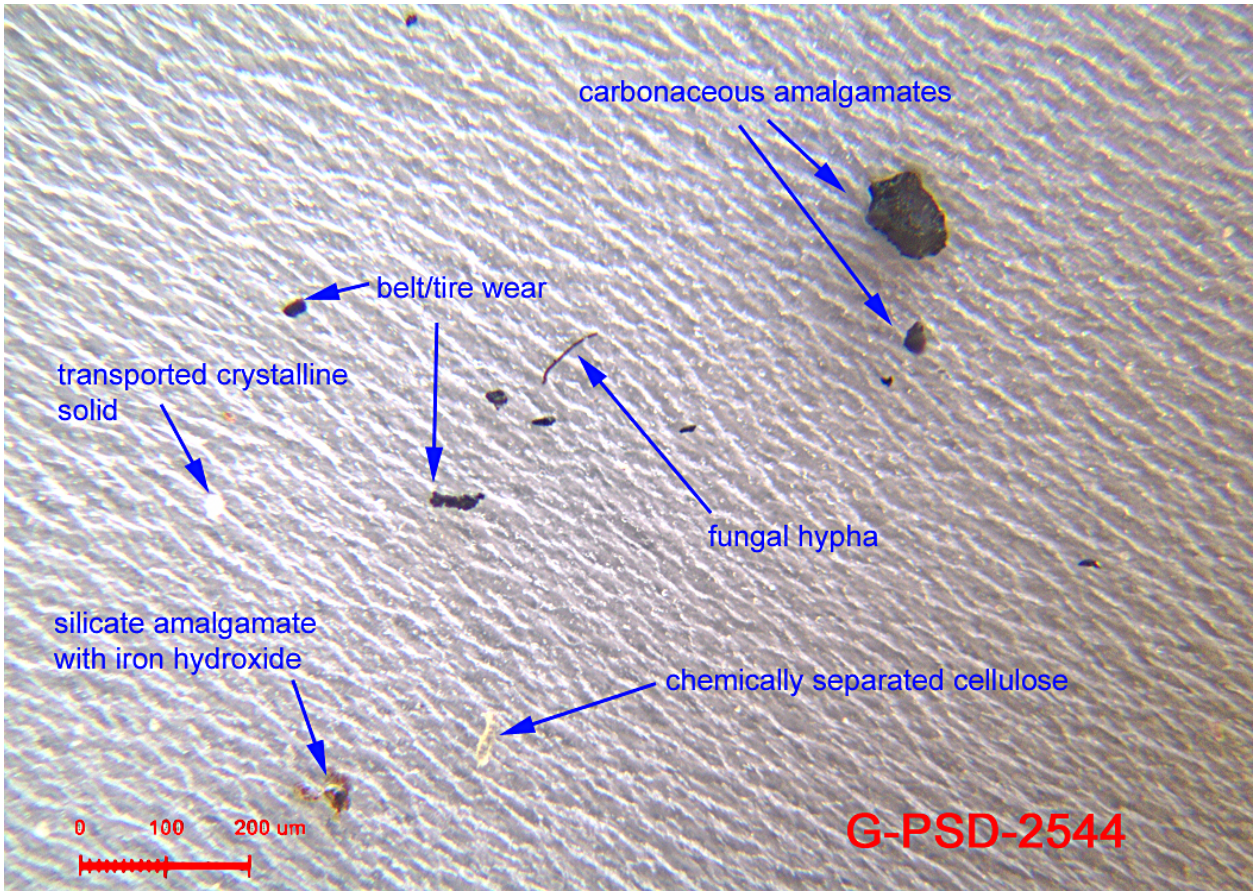

Figure 6-13. Photomicroscopy analysis for site Mira Mesa on 8/18/06.

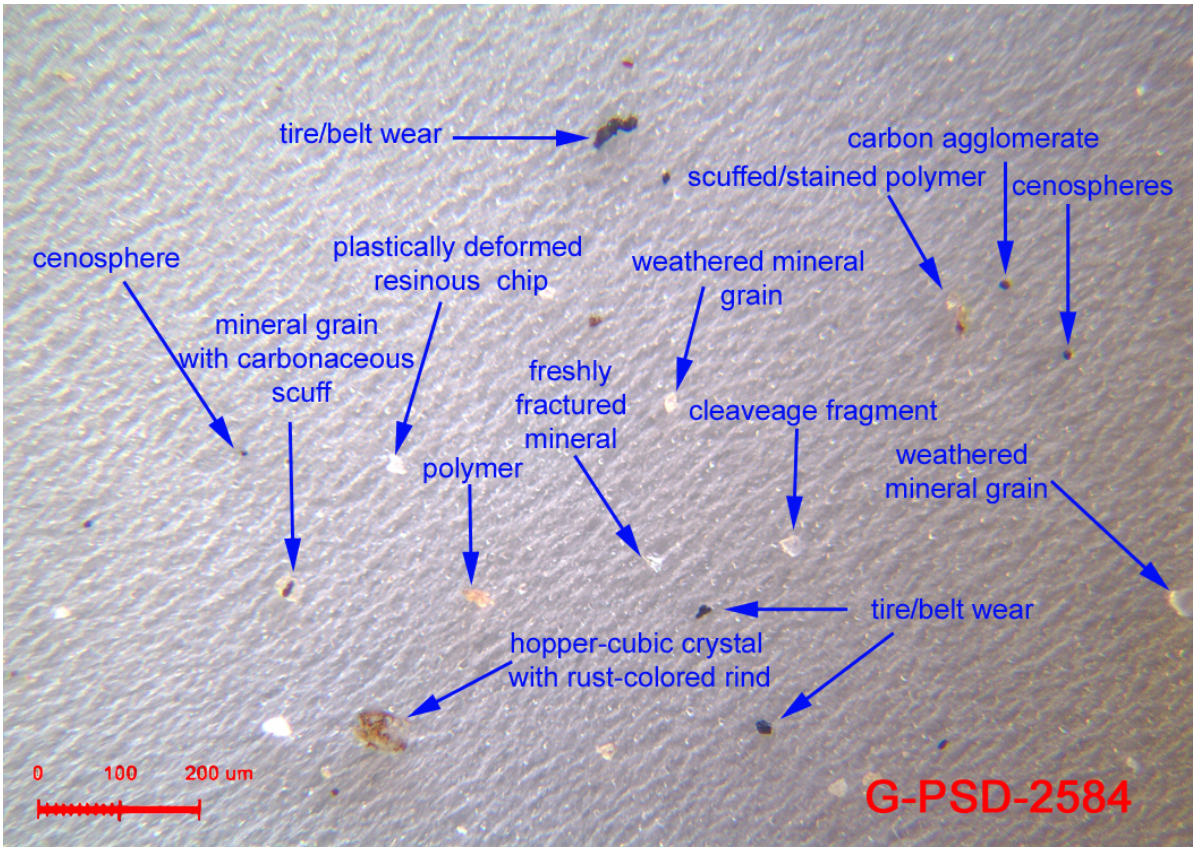

Figure 6-14. Photomicroscopy analysis for site Mira Mesa on 9/8/06.

Frequently identified particles in photomicroscopy analysis at this site included tire/belt wear, cenospheres, and weathered mineral grains as well as scuffed soft polymer, carbonaceous amalgamate, and resin flakes. All photomicroscopy results for samples collected at site Mira Mesa are presented in Appendix B.

6.2.2.3 Particle Size Distribution

Particle size distributions from surrogate disk samples collected from the Mira Mesa site were determined for three sample dates, and are summarized in Table 6-11. The relative percent area from samples collected was highest in the 50-100 µm size range for the 7/14/06 and 7/21/06 sample dates, and was highest in the 2-5 µm size range during the 8/11/06 sample event. The 7/14/06 sample date had a higher percentage of particles in the > 15 µm size range (66%), whereas the remaining two sample events were evenly distributed between the two size ranges. Aerially deposited particle sizes at Site Mira Mesa would be classified as primarily fine silt and coarse silts with clay and very fine sand size particles.

Table 6-11. Particle Size Distribution at Site Mira Mesa.

Size Range (µm)	Relative Percent Area		
	7/14/2006	7/21/2006	8/11/2006
0.8-2	6.1	12.4	10.5
2-5	9.7	21.6	23.8
5-15	17.7	18.1	16.1
15-25	22.0	7.5	14.3
25-50	19.3	11.7	14.4
50-100	25.3	28.7	20.8
100-1000	0.0	0.0	0.0
% >15 um	**66.6**	**48.0**	**49.5**
% <15 um	**33.4**	**52.0**	**50.5**

6.2.2.4 SEM-EDX Results

SEM/EDX analysis results of particles from the sample collected at Site Mira Mesa on 8/18/06 are presented in Figure 6-15. Zinc was identified as mechanical, wear-like particles associated with iron from galvanized metal in the 10 µm size range. Copper was not detected using SEM/EDX. The sample results from the XRF analyses showed a flux rate of 19.7 µg/m^2/day for both copper and zinc. Lead was not detected in this sample using either XRF or SEM/EDX analyses.

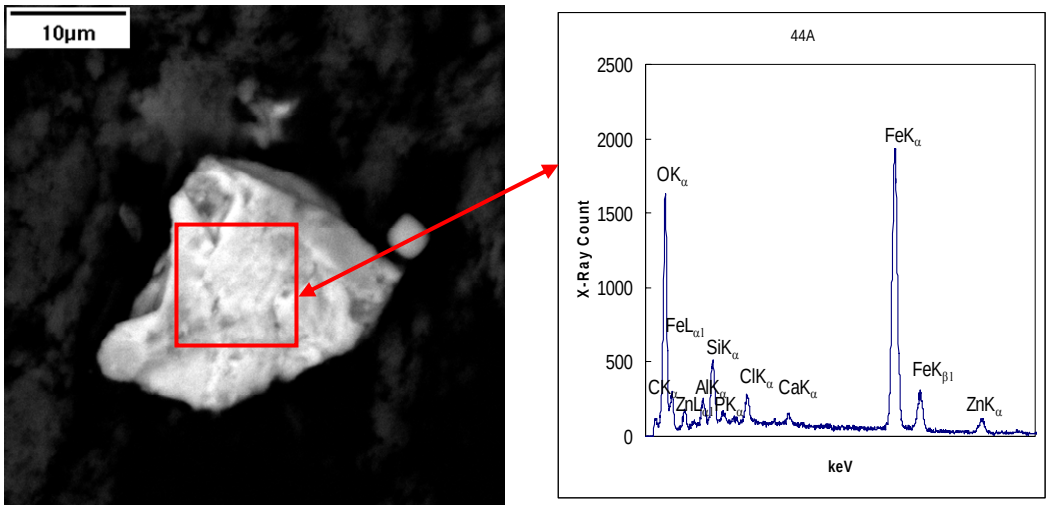

Figure 6-15. SEM/EDX analysis results of particles from the Mira Mesa site sample collected on 8/16/06.

An additional sample was also submitted for SEM/EDX analysis from a sample collected at Site Mira Mesa on 9/8/06 (Figure 6-16). This sample was submitted due to a higher than expected flux rate for zinc in this sample (347 µg/m^2/day). Lead particles were identified in the 2-5 µm size range. Lead was associated with tin as solder. Zinc was also identified associated with lead and iron but without the tin. The zinc particle was also in the 5 µm size range. Copper was not detected using SEM/EDX. The sample results from the XRF analyses showed a flux rate of 8.2 µg/m^2/day for copper and 347 µg/m^2/day zinc. Lead was not detected in this sample using XRF analyses.

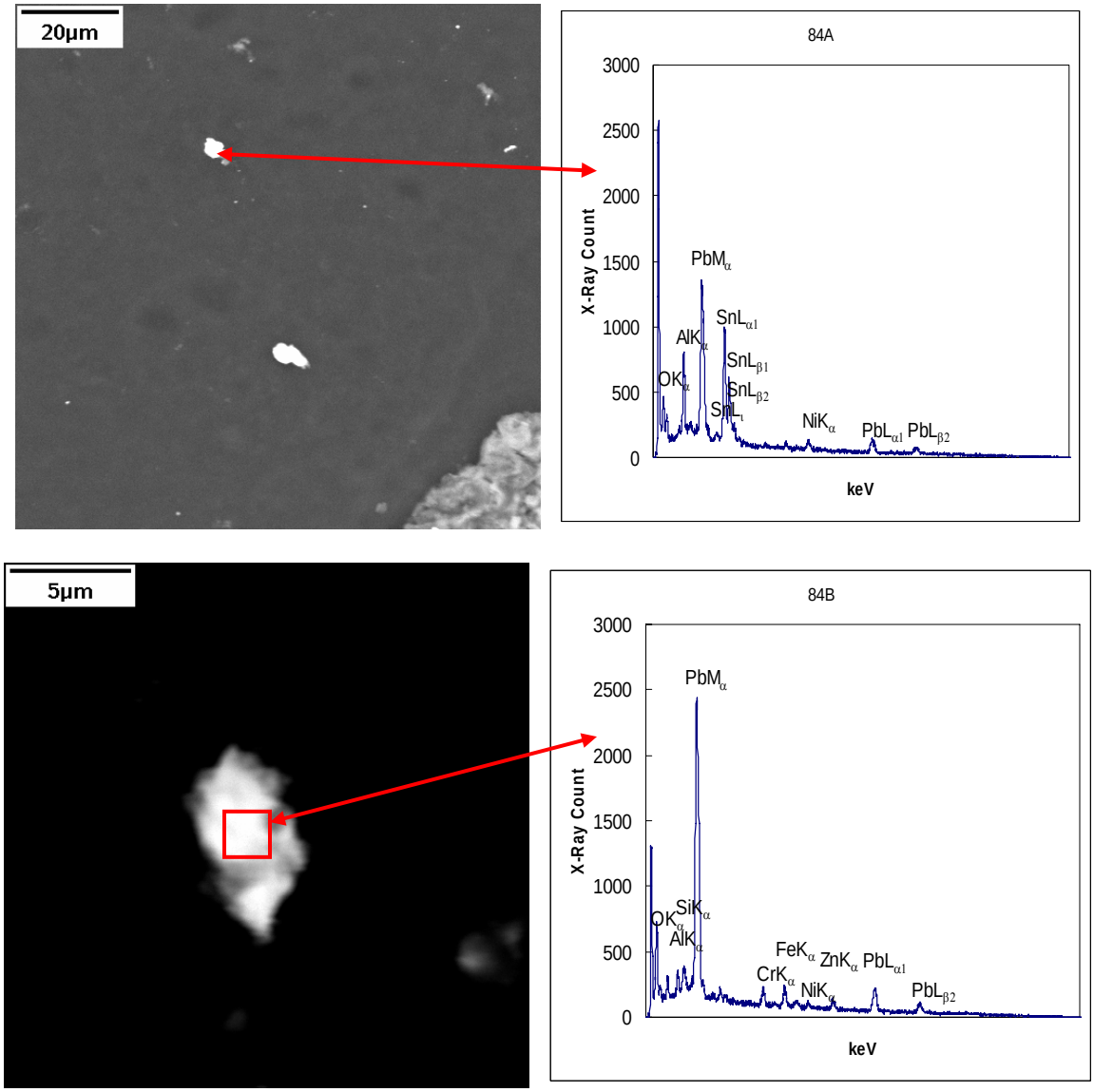

Figure 6-16. SEM/EDX analysis results of particles from the Mira Mesa site sample collected on 9/8/06.

6.2.2.5 Impactor Sampling Results

Air concentrations of Mira Mesa particulates, characterized by size and by analyte, are shown in Table 6-12. The impactor sample was collected over a 12-hour period on 8/10/06. Across all size classes, iron concentrations were significantly higher than copper, chromium, zinc and lead concentrations. Copper and zinc were the second and third most prevalent metals in Mira Mesa air samples, respectively, across all size classes with the exception of the less than 0.95 µm size class. No lead was detected in the particulates collected from any of the five size classes. In total, the analyzed metals concentrations constituted 1.53 percent of the 58.1 µg/m^3 total particulate concentration.

Table 6-12. Distribution of the concentrations of total particulates and five metals according to particle size in ambient air collected at Mira Mesa.

Particle Size	Total Particulates	Chromium	Iron	Copper	Zinc	Lead
(µm)	($\mu g/m^3$)	(ng/m^3)				
<0.95	28.8	2.34	151	30.9	11.7	<0.82
0.95-1.5	4.41	0.824	83.2	21.3	3.27	<0.82
1.5 - 3.0	6.37	0.904	121	13.5	4.61	<0.82
3.0 - 7.2	12.8	1.19	262	14.2	9.20	<0.82
> 7.2	5.76	0.906	146	3.40	7.02	<1.49
Total	58.1	6.16	763	83.3	35.8	2.39*

* One half the detection limit was used for values less than the MDL to calculate total lead.

Atmospheric size distributions for Mira Mesa are presented in Figure 6-17. Overall, the greatest percentage of particle mass for each analyte, with the exception of iron, was contained within the less than 0.95 µm size class. Greater than 30 percent of all chromium, copper, and zinc particulates and nearly 50 percent of total particulates were less than 0.95 µm in size. In contrast, the 0.95 - 1.5 µm size class contained the lowest percentages of iron, zinc, chromium and total particulates of any size class. Twenty-five percent of detected copper particles, however, fell into this size range. Relatively uniform percentages of copper, zinc, lead, iron, and total mass (between 11 and 16 percent) particulates were between 1.5 µm and 3.0 µm in size. In the coarse particle size classes, the 3.0 - 7.2 µm size class contained greater than 20 percent of zinc and total mass, and more than 30 percent of the total iron while , the > 7.2 µm size class contained greater than 20 percent of the iron, zinc, chromium and total mass particulates, but only 4.0 percent of copper particulates.

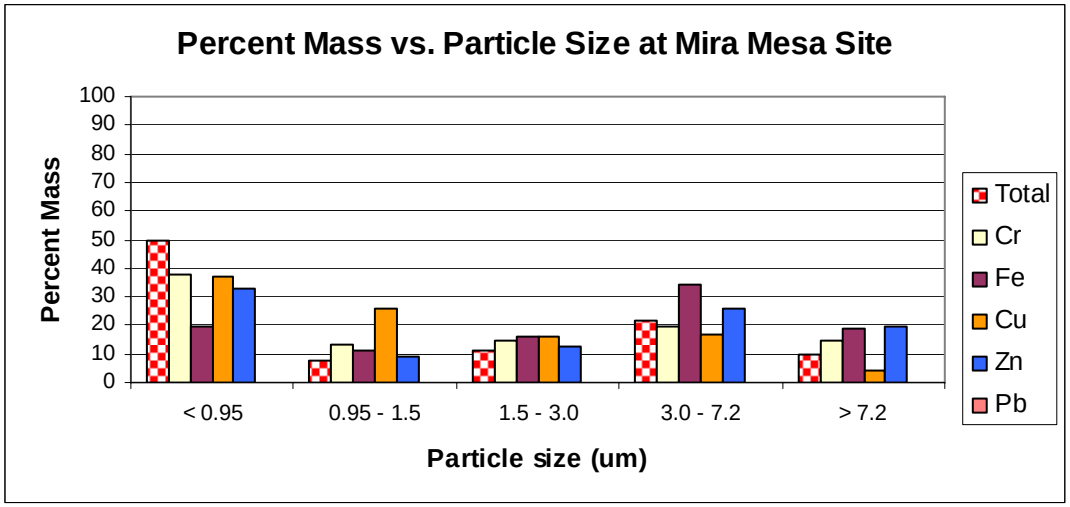

Figure 6-17. Percent mass versus particle size in air samples collected at Mira Mesa.

6.2.3 Site Tecolote

6.2.3.1 XRF Results

Surrogate deposition disks were deployed at Tecolote for a total of eight week-long events. The deposition disks were exposed for a duration of three days during each event. Analytical results from the primary surrogate deposition disks at the Tecolote site are presented in Table 6-13. Replicate disk analyses are provided in Appendix A.

Table 6-13. Copper, Lead, and Zinc Flux at Site Tecolote.

Date	Net	Copper	Lead	Zinc
	($mg/m^2/day$)	(µg/m2/day)		
7/14/06	99.6	6.4	<4.9	<1.9
7/21/06	59.9	2.9	<4.9	<1.9
8/11/06	62.9	5.0	<4.9	9.2
8/18/06	73.3	<1.7	<4.9	6.7
8/25/06	49.4	4.0	<4.9	<1.9
9/1/06	36.6	4.1	<4.9	<1.9
9/8/06	67.0	5.6	<4.9	28.0
9/22/06	90.7	<1.7	<4.9	9.0

The net depositional flux for total particulate matter ranged from 36.6 to 99.6 $mg/m^2/day$ and averaged 67.4 $mg/m^2/day$ for the series of deployment events. The lowest net depositional flux occurred during the week of 9/1/06 and the highest net flux occurred during the week of 7/14/06.

The depositional flux for copper ranged from BDL to 6.4 $\mu g/m^2/day$ and averaged 3.7 $\mu g/m^2/day$ during the deployment event series. Copper was BDL on the weeks of 8/18/06 and 9/22/06. The highest depositional flux, 6.4 $\mu g/m^2/day$, was detected during the week of 7/14/06.

Lead was not detected at the Tecolote site during any of the deployment events (Figure 6-18).

The depositional flux for zinc ranged from BDL to 28.0 $\mu g/m^2/day$ and averaged 7.1 $\mu g/m^2/day$ during the deployment event series. Zinc was BDL on the weeks of 7/14/06, 7/21/06, 8/25/06, and 9/1/06. The highest depositional flux for zinc occurred during the early part of September during the 9/8/06 deployment event (Figure 6-18).

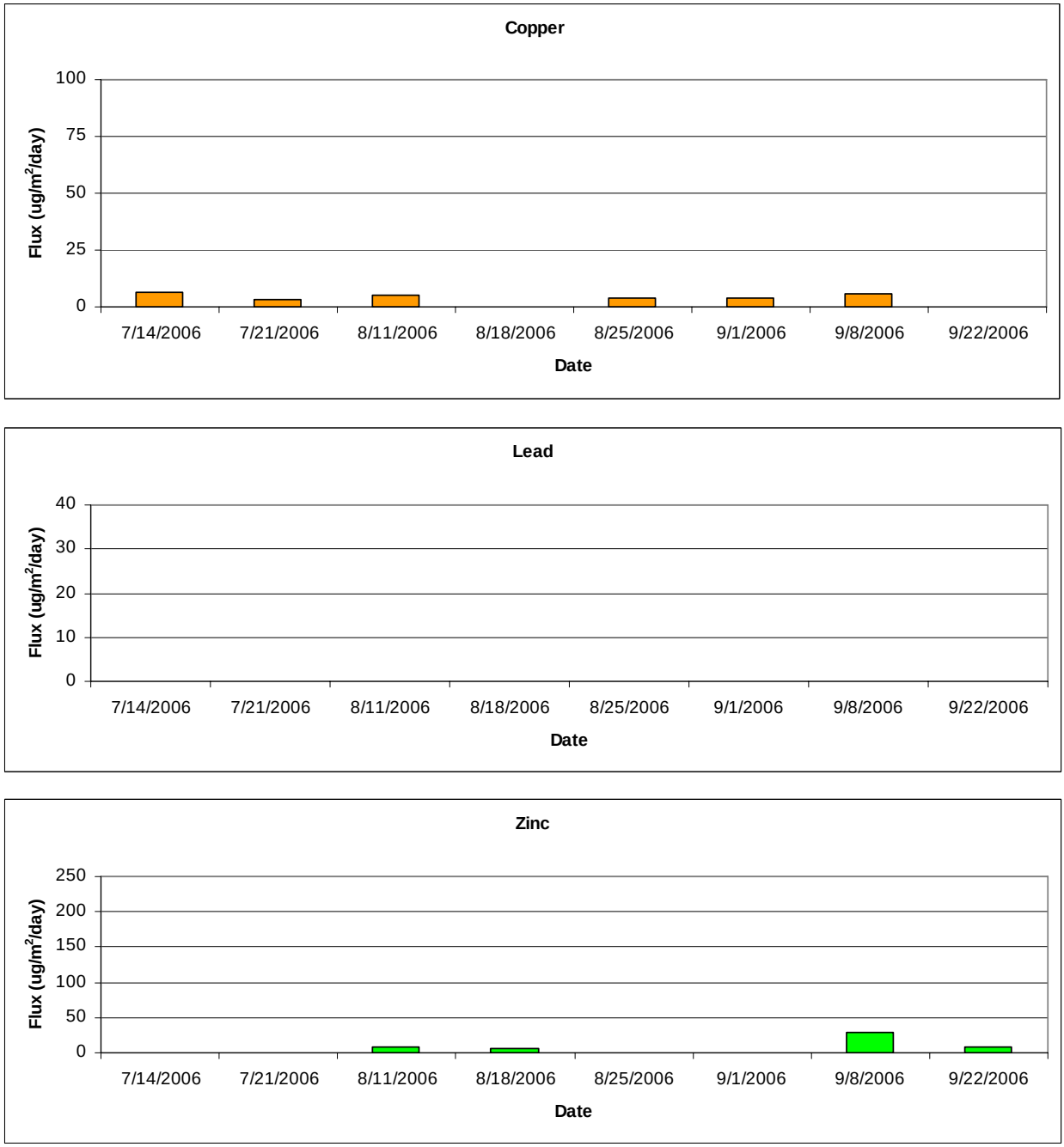

Figure 6-18. Copper, Lead, and Zinc Flux at Site Tecolote.

6.2.3.2 Photomicroscopy Results

A representative result for the photomicroscopy analysis performed on surrogate disks deployed at site Tecolote is presented in Figure 6-19. The sample date for the surrogate disk represented in Figure 6-19 is 8/11/06.

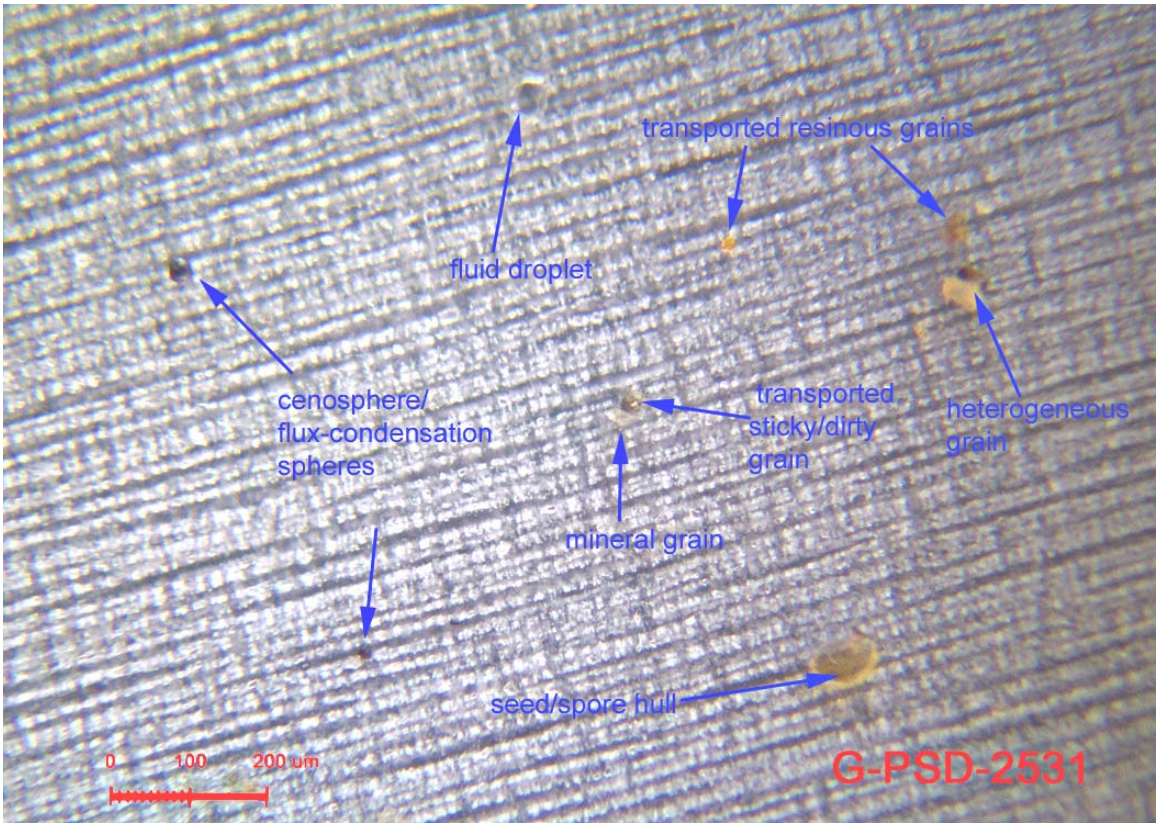

Figure 6-19. Photomicroscopy analysis for site Tecolote on 8/11/06.

Frequently identified particles in photomicroscopy analysis at Tecolote included transported resinous grains, cenospheres, and seed/spore hulls as well as cellulose from cardboard, tire/belt wear, and quartz with resinous rind. All photomicroscopy results for samples collected at site Tecolote are presented in Appendix B.

6.2.3.3 Particle Size Distribution

Particle size distributions from surrogate disk samples collected from site Tecolote were determined for three sample dates, and are summarized in Table 6-14. The relative percent area was highest in the 100-1000 µm size range for the 7/14/06 and 8/11/06 sample dates and was highest in the 25-50 µm size range during the 7/21/06 sample event. All three sample dates at site Tecolote had a higher percentage of particles in the > 15 µm size range. Aerially deposited particle sizes at Site Tecolote would be classified as primarily fine and coarse silts with sand and clay size particles.

Table 6-14. Particle Size Distribution at Site Tecolote.

Size Range (um)	Relative Percent Area		
	7/14/2006	7/21/2006	8/11/2006
0.8-2	4.7	9.3	2.7
2-5	11.6	16.5	4.8
5-15	20.4	20.8	7.9
15-25	11.2	16.1	2.2
25-50	16.3	27.9	30.0
50-100	13.4	9.5	22.1
100-1000	22.4	0.0	30.3
% >15 um	**63.3**	**53.5**	**84.6**
% <15 um	**36.7**	**46.5**	**15.4**

6.2.3.4 SEM-EDX Results

SEM/EDX analysis results of particles from the Tecolote Site sample collected on 8/11/06 are presented in Figure 6-20. Aluminum and tin were identified with copper in mechanically derived grains generally in the 5-10 µm size range. Lead and zinc were not detected in the particles analyzed using SEM/EDX. The sample results from the XRF analyses for copper showed a flux rate of 5.0 µg/m^2/day and a zinc flux of 9.2 µg/m^2/day.

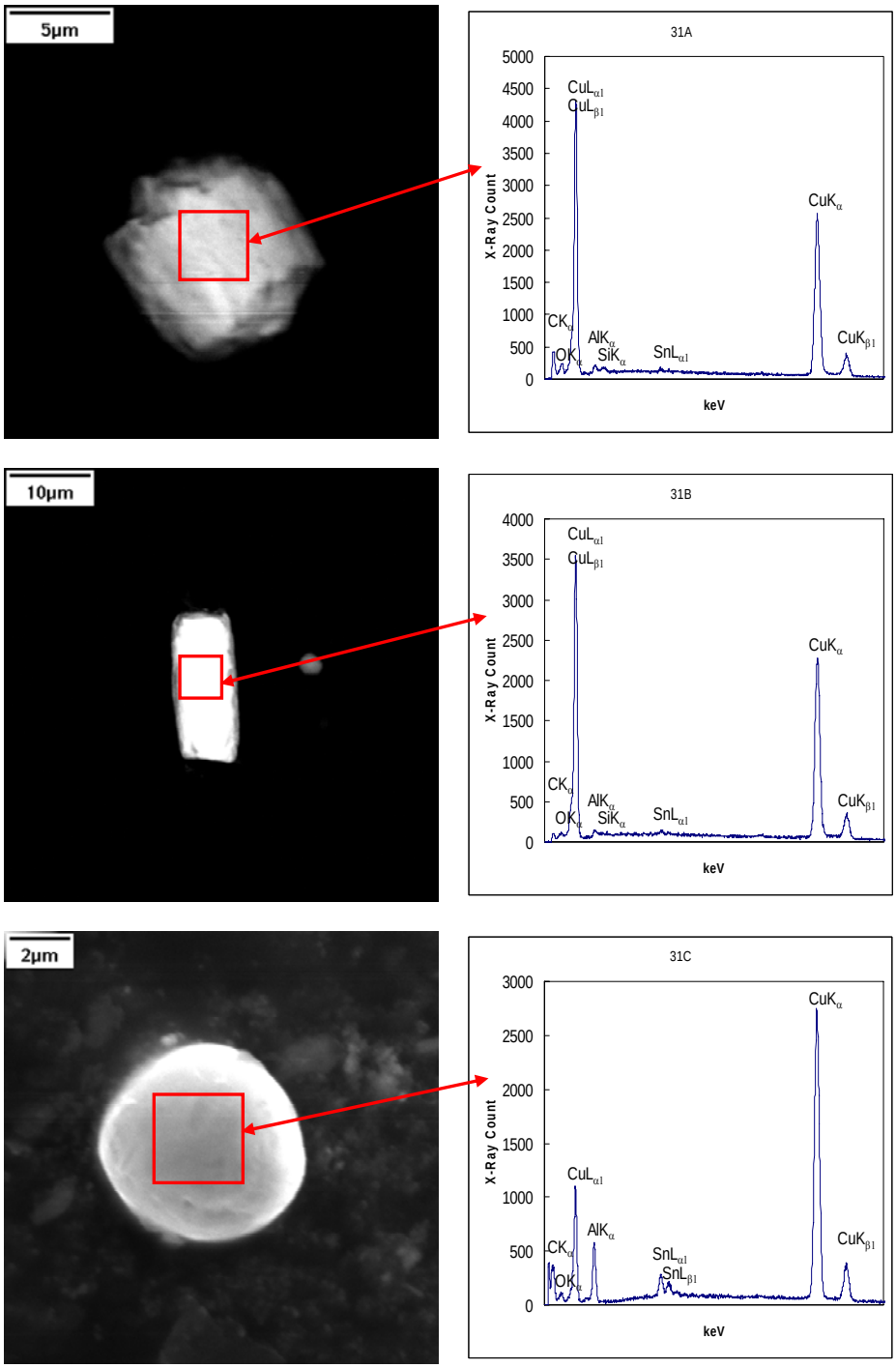

Figure 6-20. SEM/EDX analysis results of particles from the Tecolote Site sample collected on 8/11/06

6.2.3.5 Impactor Sampling Results

Air concentrations of Tecolote particulates, characterized by size and by analyte, are shown in Table 6-15. The impactor sample was collected over a 12-hour period on 8/25/06. Across all size classes, iron concentrations were significantly higher than copper, chromium, zinc and lead concentrations. Copper and zinc were the second and third most prevalent metals in Tecolote air samples, respectively, across all size classes with the exception of the greater than 7.2 µm size. No lead was detected in particulates ranging in size from 0.95 µm to 3.0 µm or from particulates greater than 7.2 µm in size. In total, the analyzed metals concentrations constituted 1.47 percent of the 53.5 µg/m^3 total particulate concentration.

Table 6-15. Distribution of the concentrations of total particulates and five metals according to particle size in ambient air collected at Tecolote.

Particle Size	Total Particulates	Chromium	Iron	Copper	Zinc	Lead
(µm)	(µg/m^3)	(ng/m^3)				
< 0.95	17.4	2.12	94.9	19.4	2.73	1.94
0.95 - 1.5	3.80	0.700	40.0	14.3	0.853	<0.82
1.5 - 3.0	6.25	0.744	88.7	10.2	1.25	<0.82
3.0 - 7.2	15.8	1.00	267	11.4	3.22	0.854
> 7.2	10.2	0.983	219	2.66	2.94	<0.82
Total	53.5	5.55	710	58.0	11.0	4.02*

* One half the detection limit was used for values less than the MDL to calculate total lead.

Atmospheric size distributions for Tecolote are presented in Figure 6-21. Overall, the greatest percentage of particle mass for each analyte, with the exception of iron, was contained within the less than 0.95 µm size class. Greater than 30 percent of all chromium, copper, and total mass particulates and 70 percent of lead particulates were less than 0.95 µm in size. In contrast, the 0.95 – 1.5 µm size class contained the lowest percentages of iron (5.6%), zinc (7.8%), chromium (12.6%), lead (0%) and total particulates (7.1%) of any size class. Twenty-five percent of detected copper particles, however, were in the 0.95 – 1.5 µm size range. Relatively uniform percentages (between 11 and 18 percent) of copper, zinc, lead, iron and total mass particulates were between 1.5 µm and 3.0 µm in size. The 3.0 – 7.2 µm size class contained approximately 30 percent or greater of all iron, zinc, lead, and total mass, and nearly 20 percent of all copper and chromium mass. Similarly, the greater than 7.2 µm size class contained greater than 30 percent of the iron mass, greater than 20 percent of the zinc mass, and slightly less than 20 percent of the chromium mass and total mass. Only 4.6 percent of copper and none of the lead mass were contained in particulates greater than 7.2 µm in size.

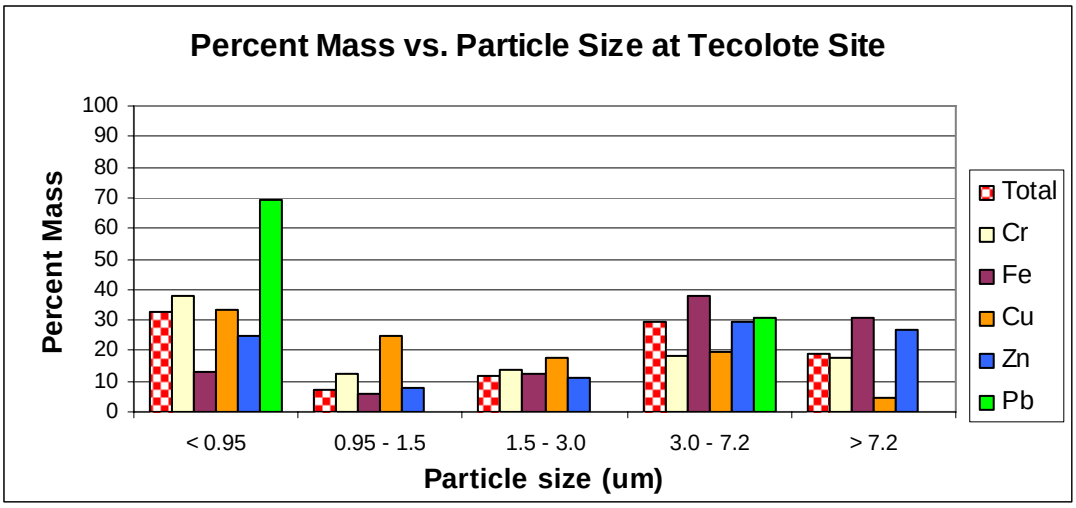

Figure 6-21. Percent mass versus particle size in air samples collected at Tecolote

6.2.4 Site 805T-Up

6.2.4.1 XRF Results

Surrogate deposition disks were deployed at 850T-Up for a total of eight week-long events. The deposition disks were exposed for a duration of three days during each event. During two of the deployment events, disks were damaged or contaminated by bird droppings in the field which resulted in those disks being withheld from laboratory analysis. Analytical results from the primary surrogate deposition disks at the 805T-Up site are presented in Table 6-16. Replicate disk analyses are provided in Appendix A.

Table 6-16. Copper, Lead, and Zinc Flux at Site 805T-Up.

Date	Net	Copper	Lead	Zinc
	(mg/m^2/day)	(µg/m^2/day)		
8/25/06	40.7	<1.7	<4.9	28.5
9/1/06	48.3	10.2	<4.9	15.2
9/8/06	44.0	<1.7	<4.9	15.3
9/15/06	43.6	66.1	<4.9	5.1
9/22/06	78.5	7.8	11.3	29.6
10/6/06	51.6	4.9	<4.9	12.1

The net depositional flux for total particulate matter ranged from 40.7 to 78.5 mg/m^2/day and averaged 44.1 mg/m^2/day for the series of deployment events. The lowest depositional flux was observed during the week of 8/25/06 while the highest net depositional flux occurred during the week of 9/22/06.

The depositional flux for copper ranged from BDL to 66.1 µg/m^2/day and averaged 15.1 µg/m^2/day during the deployment event series. The depositional flux for copper was BDL during the weeks of 8/25/06 and 9/8/06 while the highest depositional flux, 66.1 µg/m^2/day, was detected during the week of 9/15/06.

Lead was typically not detected at the 805T-Up site except for a single deployment event occurring during the week of 9/22/06 when the depositional flux measured 11.3 µg/m^2/day (Figure 6-22).

The depositional flux for zinc ranged from 5.1 to 29.6 µg/m^2/day and averaged 17.6 µg/m^2/day during the deployment event series. The lowest zinc depositional flux occurred during the week of 9/15/06 while the highest zinc flux occurred during the week of 9/22/06.

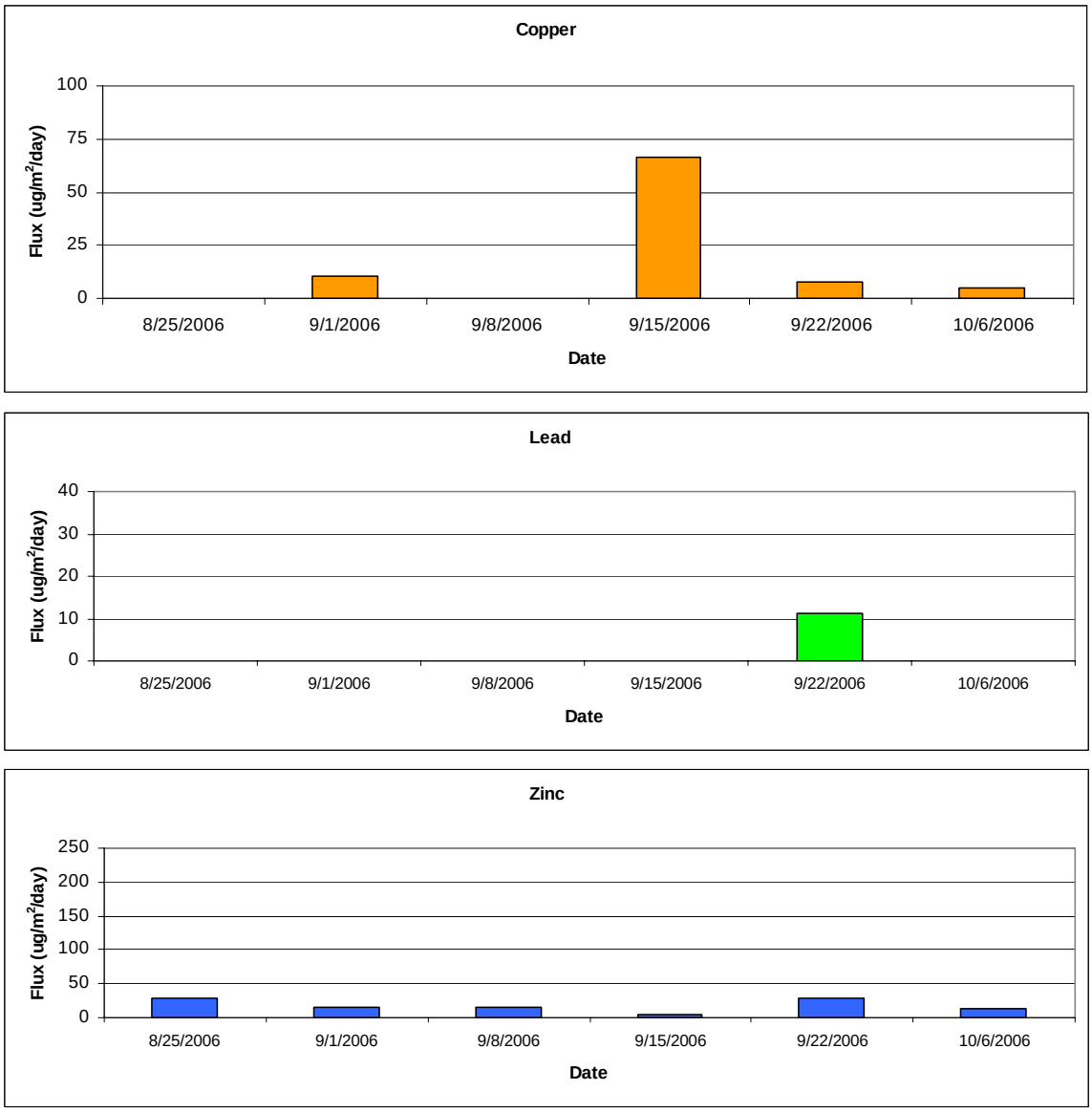

Figure 6-22. Copper, Lead, and Zinc Flux at Site 805T-Up.

6.2.4.2 Photomicroscopy Results

A representative result for the photomicroscopy analysis performed on surrogate disks deployed at site 805T-Up is presented in Figure 6-23 and Figure 6-24. The sample date for the surrogate disk represented in Figure 6-23 is 9/15/06 and the surrogate disk represented in Figure 6-24 is 9/22/06.

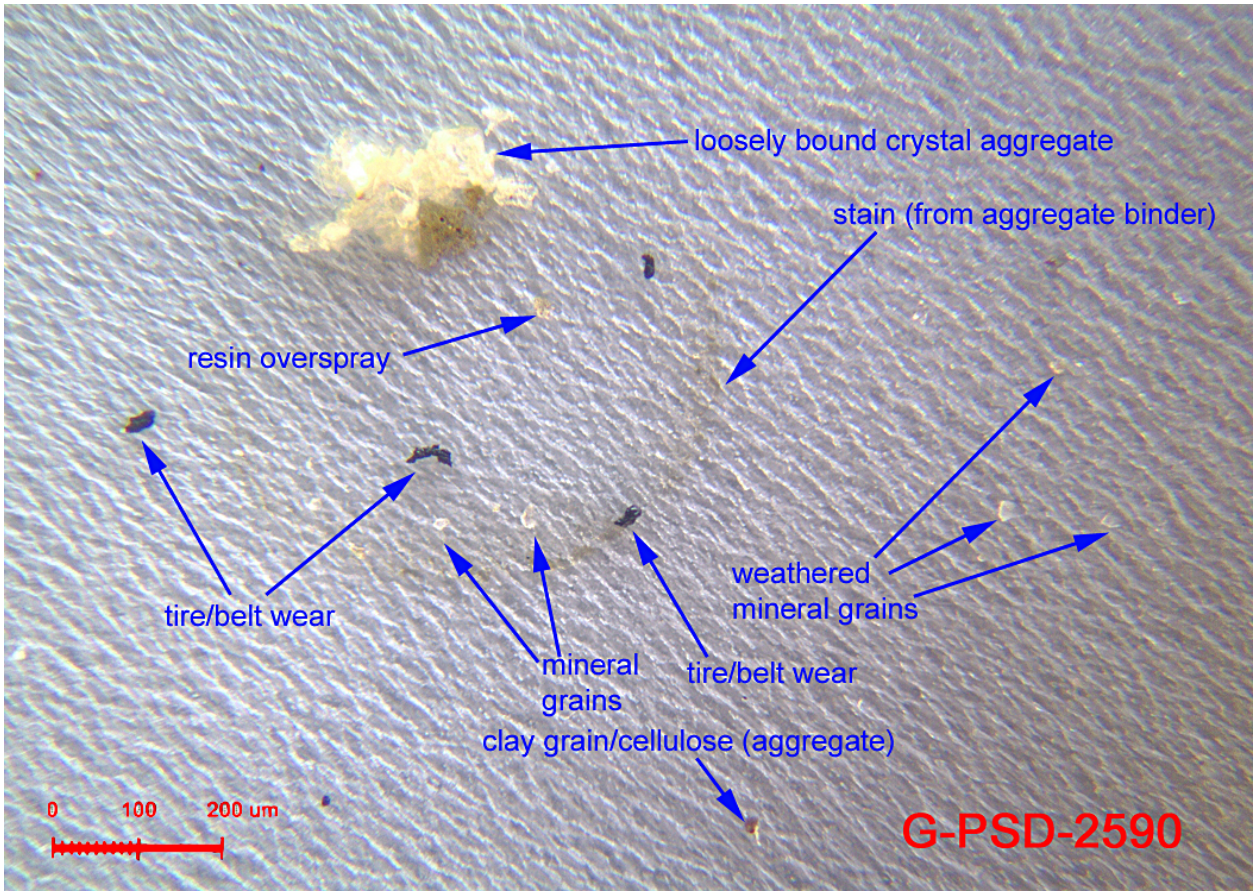

Figure 6-23. Photomicroscopy analysis for site 805T-Up on 9/15/06.

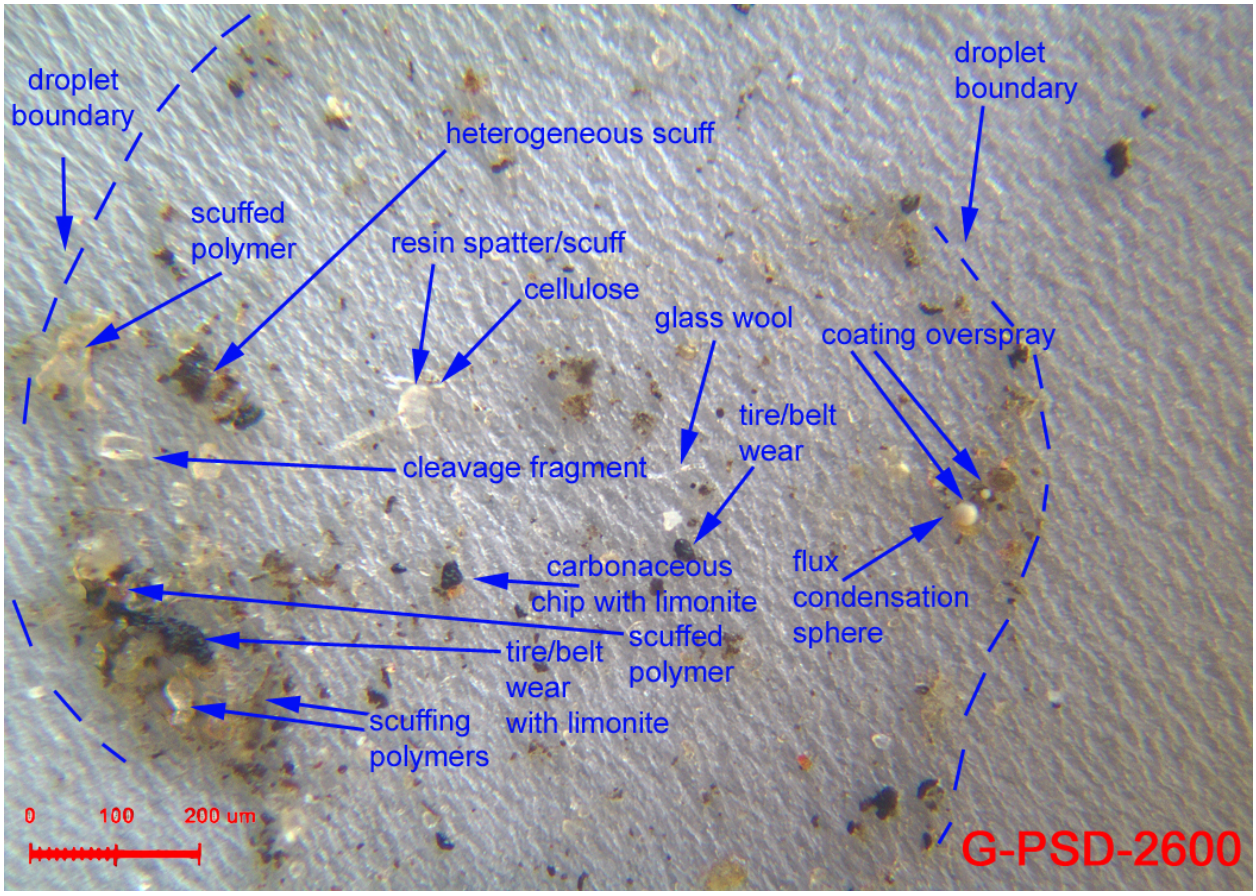

Figure 6-24. Photomicroscopy analysis for site 805T-Up on 9/22/06

Frequently identified particles in photomicroscopy analysis at 805T-Up included mineral grains, tire/belt wear, and clay grain/cellulose (aggregate) as well as flux condensation sphere, scuffed polymer, and pollen. All photomicroscopy results for samples collected at site 805T-Up are presented in Appendix B.

6.2.4.3 Particle Size Distribution

Particle size distributions were not analyzed on samples from this site.

6.2.4.4 SEM-EDX Results

SEM/EDX analysis results of particles from the sample collected at Site 805TU on 9/15/06 are presented in Figure 6-25 and Figure 6-26. Copper particles were detected as steel scuffing fatigue particles in the 10 – 40 µm size range (Figure 6-25). Particles in Figure 6-25 are observed in the 10 – 20 µm size range as elemental copper associated with iron. These particles also showed chemical wear as opposed to mechanical wear. Lead and zinc particles were not identified using SME/EDX. In comparison, the sample results from the XRF analyses showed a flux rate of 66.1 µg/m^2/day for copper and 5.1 µg/m^2/day for zinc. Lead was not detected in this sample using XRF analysis.

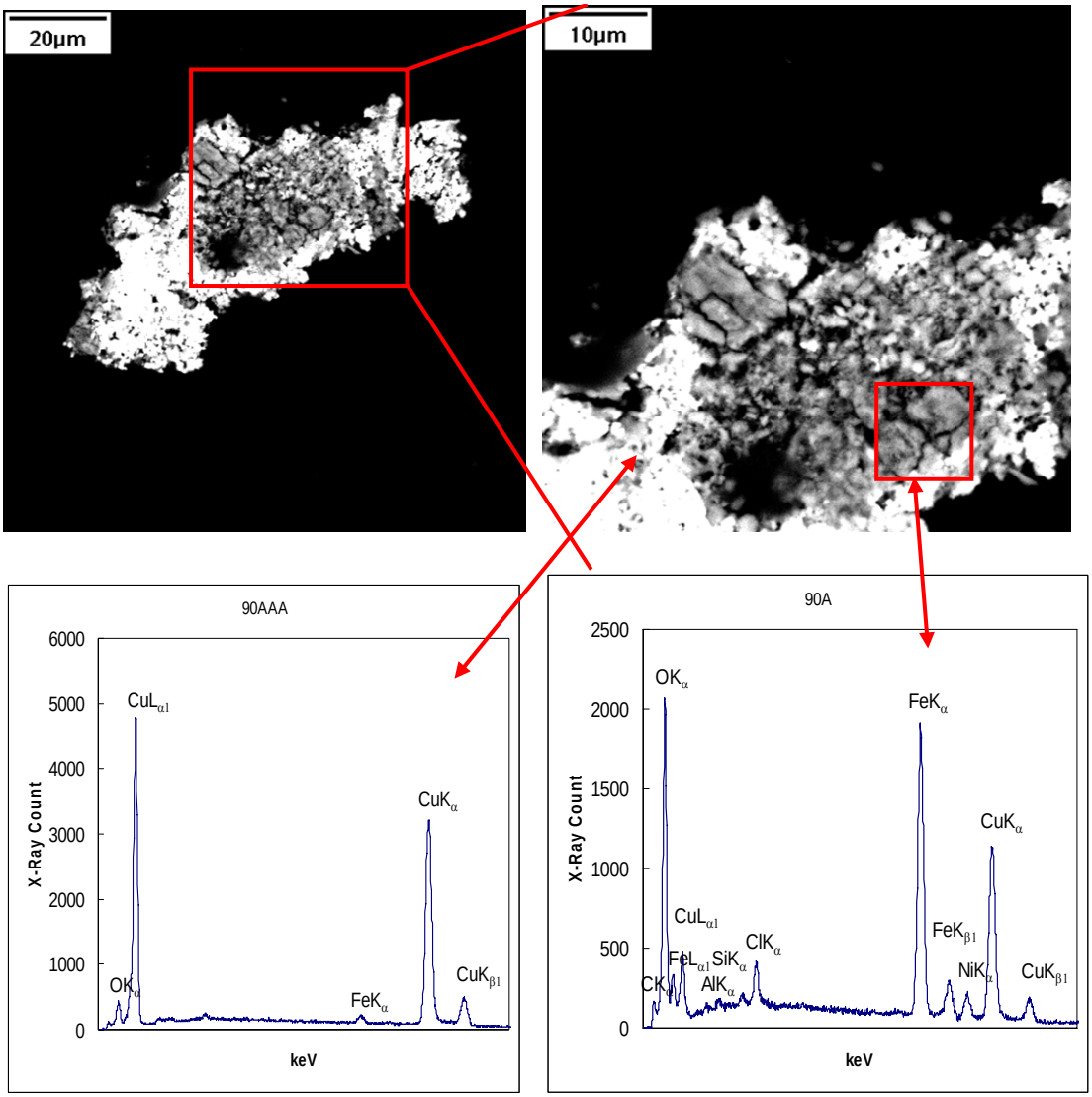

Figure 6-25. SEM/EDX analysis results of particles from the 805TU site sample collected on 9/15/06

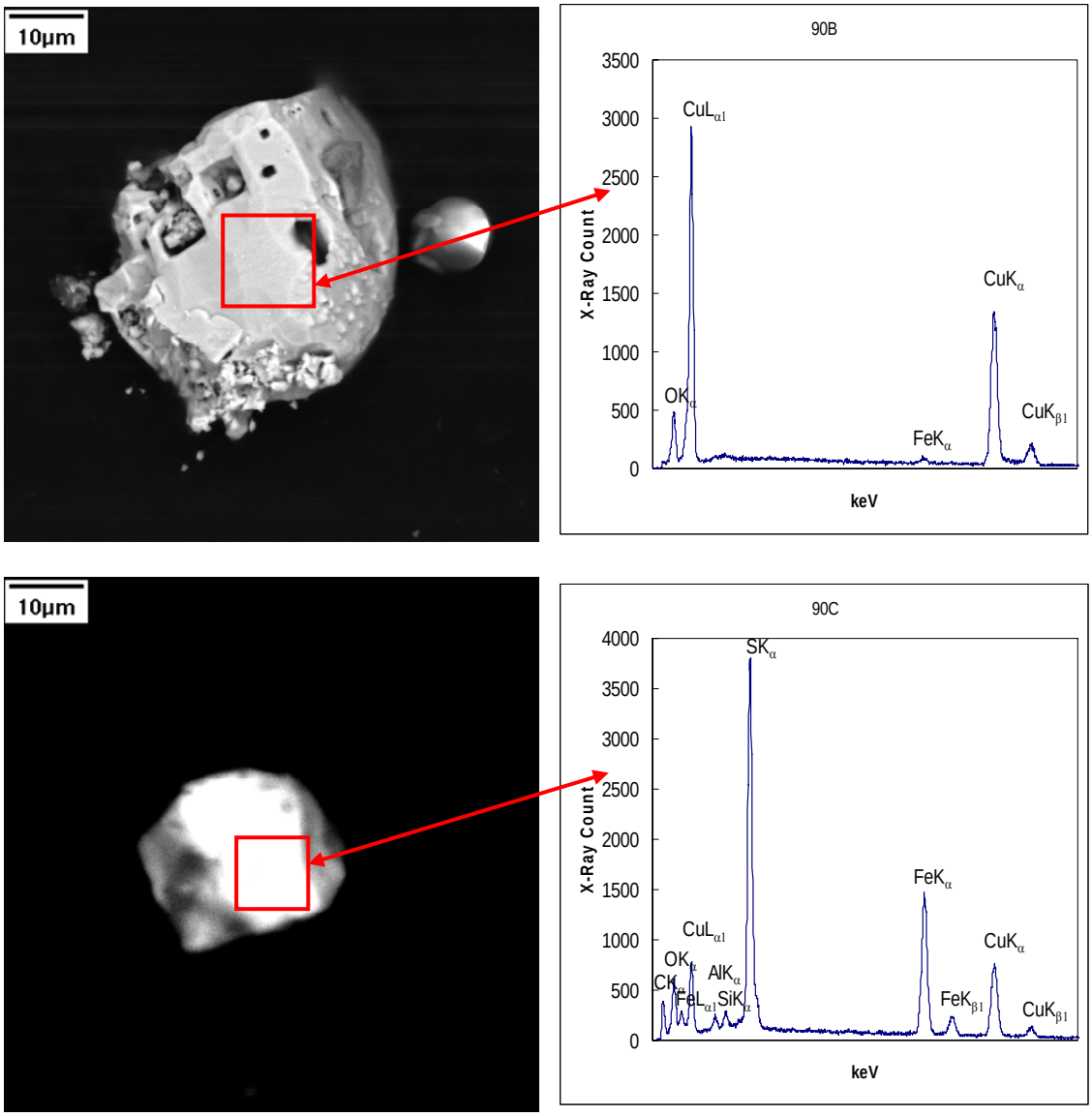

Figure 6-26. SEM/EDX analysis results of particles from the 805TU site sample collected on 9/15/06.

An additional sample from site 805TU (collected 9/22/06) was submitted for SEM/EDX analysis and are presented in Figure 6-27. Copper particles were again found in the 10-20 µm size range associated with iron and sulfur, possibly representing the mineral chalcopyrite ($CuFeS_2$). Copper was also detected associated with titanium and several other elements. Lead and zinc particles were not identified using SEM/EDX in this sample. In comparison, the sample results from the XRF analyses showed a flux rate of 7.8 µg/m^2/day for copper, 11.3 µg/m^2/day for lead, and 29.6 µg/m^2/day for zinc.

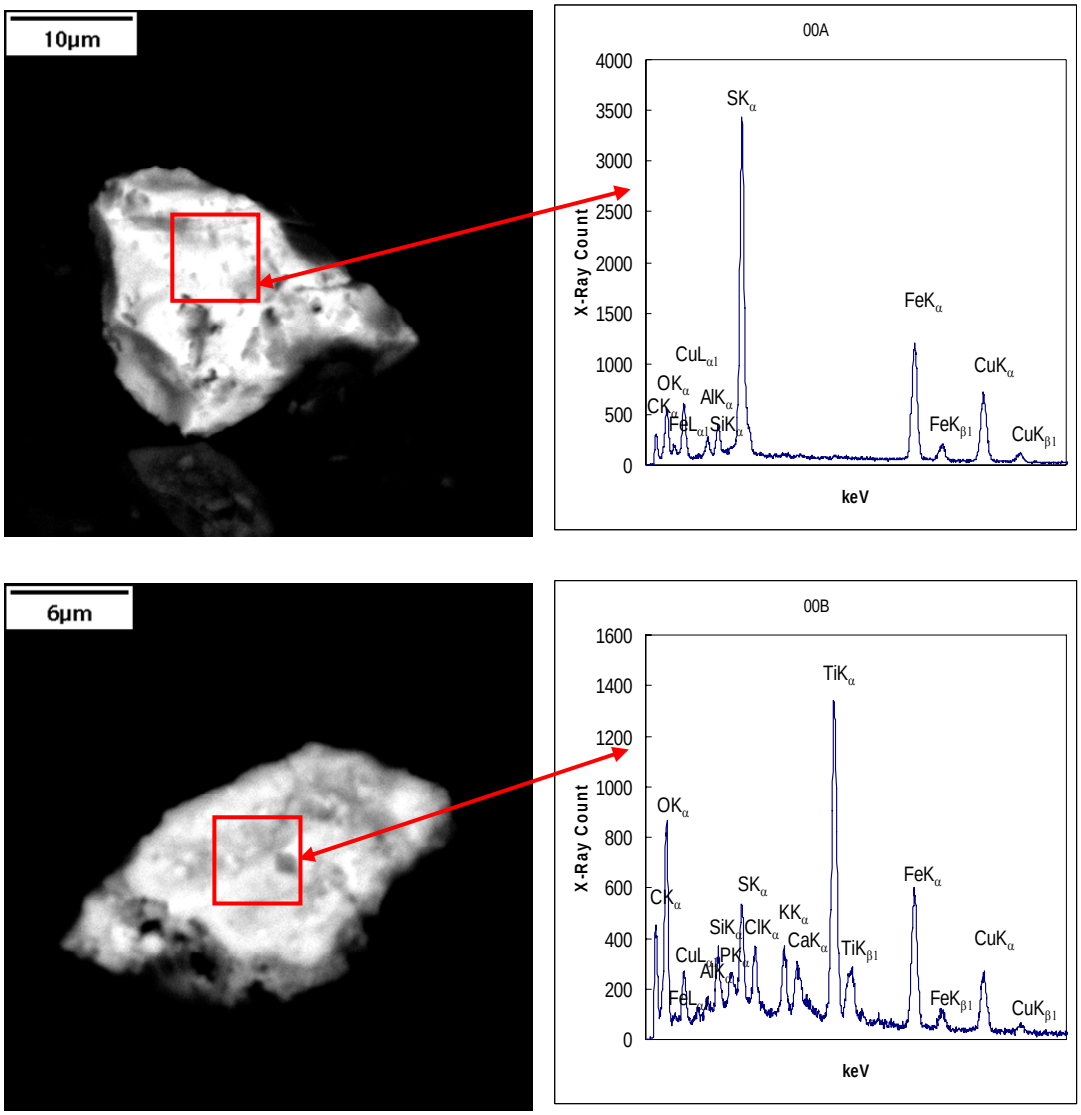

Figure 6-27. SEM/EDX analysis results of particles from the 805TU site sample collected on 9/22/06.

6.2.4.5 Impactor Sampling Results

Air concentrations of 805-Up particulates, characterized by size and by analyte, are shown in Table 6-17. The impactor sample was collected over a 12-hour period on 10/31/06. Across all size classes, iron concentrations were higher than chromium, zinc and lead concentrations by one order of magnitude or greater. Copper and zinc were the second and third most prevalent metals in 805-Up air samples, respectively, across all size classes with the exception of the greater than 7.2 µm size class. Lead was not detected in three of the five particulate size classes. In general, both overall metal concentrations and total particulate concentrations were low in comparison to other sites. The analyzed metals concentrations in 805-Up air samples constituted 1.96 percent of the 39.9 µg/m^3 total particulate concentration.

Table 6-17. Distribution of the concentrations of total particulates and five metals according to particle size in ambient air collected at 805-Up

Particle Size	Total Particulate	Chromium	Iron	Copper	Zinc	Lead
(µm)	(µg/m^3)	(ng/m^3)				
< 0.95	18.4	2.05	111	18.6	8.46	2.53
0.95 - 1.5	1.59	0.939	61.8	10.3	2.61	<0.82
1.5 - 3.0	3.19	1.06	109	9.25	3.04	<0.82
3.0 - 7.2	10.1	1.45	254	8.84	5.92	1.01
> 7.2	6.62	1.12	159	2.95	5.09	<0.82
Total	39.9	6.62	695	49.9	25.1	4.77*

* One half the detection limit was used for values less than the MDL to calculate total lead.

Atmospheric size distributions for 805-Up are presented in Figure 6-28. Overall, the greatest percentage of particle mass for each analyte was contained within the less than 0.95 µm size class. Greater than 70 percent of all lead particulates, and greater than 40 percent of total mass, and greater than 30 percent of all copper, chromium, and zinc particulates were less than 0.95 µm in size. In contrast, the next smallest size class contained the lowest percentages of total mass, iron, chromium, zinc, and lead particulates, but contained the second highest percentage of copper particulates. The 1.5 – 3.0 µm masses for all analytes, with the exception of lead, ranged from 8 to 18.5 percent. No lead was detected in the 1.5 – 3.0 µm particulates. In the coarse particle size classes, the 3.0 – 7.2 µm sized particles contained greater than 20 percent of all zinc, lead, chromium, and total mass particulates, and more than 30 percent of all iron particulates while the greater than 7.2 µm sized particles contained 16.2 percent total mass, 16.9 percent of all chromium, 20.3 percent of all zinc, and 22.9 percent of all iron. No lead, and only 5.9 percent of all copper was greater than 7.2 µm in size.

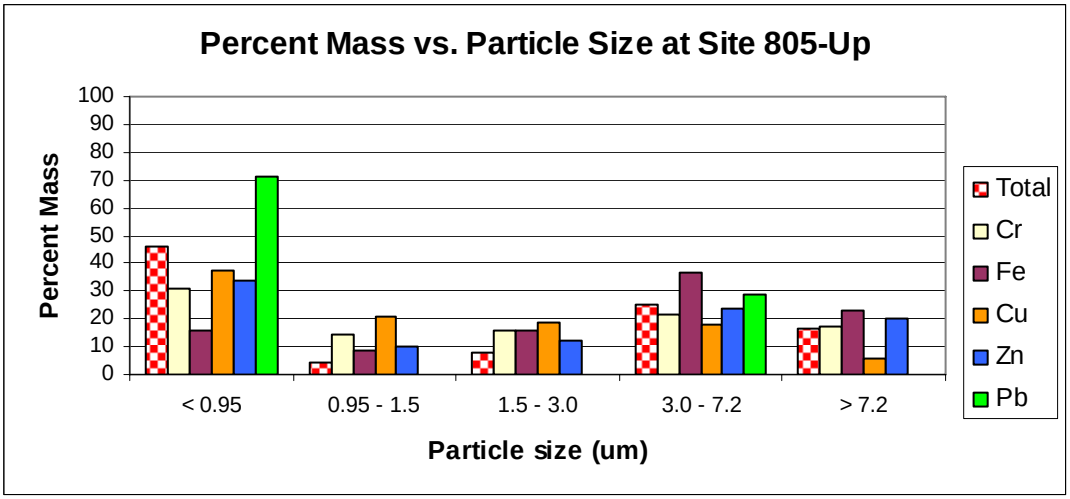

Figure 6-28. Percent mass versus particle size in air samples collected at 805-Up

6.2.5 Site 805T1

Surrogate deposition disks were deployed at 805T1 for a total of eight week-long events. The deposition disks were exposed for a duration of three days during each event. Analytical results from the primary surrogate deposition disks at the 805T1 site are presented in Table 6-18. Replicate disk analyses are provided in Appendix A.

Table 6-18. Copper, Lead, and Zinc Flux at Site 805T1

Date	Net	Copper	Lead	Zinc
	(mg/m^2/day)	(µg/m2/day)		
8/25/06	99.2	8.8	<4.9	148
9/1/06	110	16.0	9.8	174
9/8/06	117	8.3	<4.9	92.4
9/15/06	74.7	8.4	<4.9	154
9/22/06	119	12.1	<4.9	170
9/29/06	83.6	15.4	<4.9	105
10/6/06	89.3	8.3	<4.9	58.8
10/13/06	73.3	8.2	<4.9	82.8

The net depositional flux for total particulate matter ranged from 73.3 to 119 mg/m^2/day and averaged 95.9 mg/m^2/day for the series of deployment events. The lowest net flux occurred during the week of 10/13/06 while the highest net flux occurred during the week of 9/22/06.

The depositional flux for copper ranged from 8.2 to 16.0 µg/m^2/day and averaged 10.7 µg/m^2/day during the deployment event series. The lowest copper depositional flux was observed during the week of 10/13/06 while the highest depositional flux, 16.0 µg/m^2/day, was detected during the week of 9/1/06.

Lead was typically not detected at the 805T1 site except for a single deployment event occurring during the week of 9/1/06 when the depositional flux measured 9.8 µg/m^2/day (Figure 6-29).

The depositional flux for zinc ranged from 58.8 to 174 µg/m^2/day and averaged 123 µg/m^2/day during the deployment event series. The lowest zinc depositional flux occurred during the week of 10/6/06. The highest zinc flux occurred during the week of 9/1/06 (Figure 6-29).

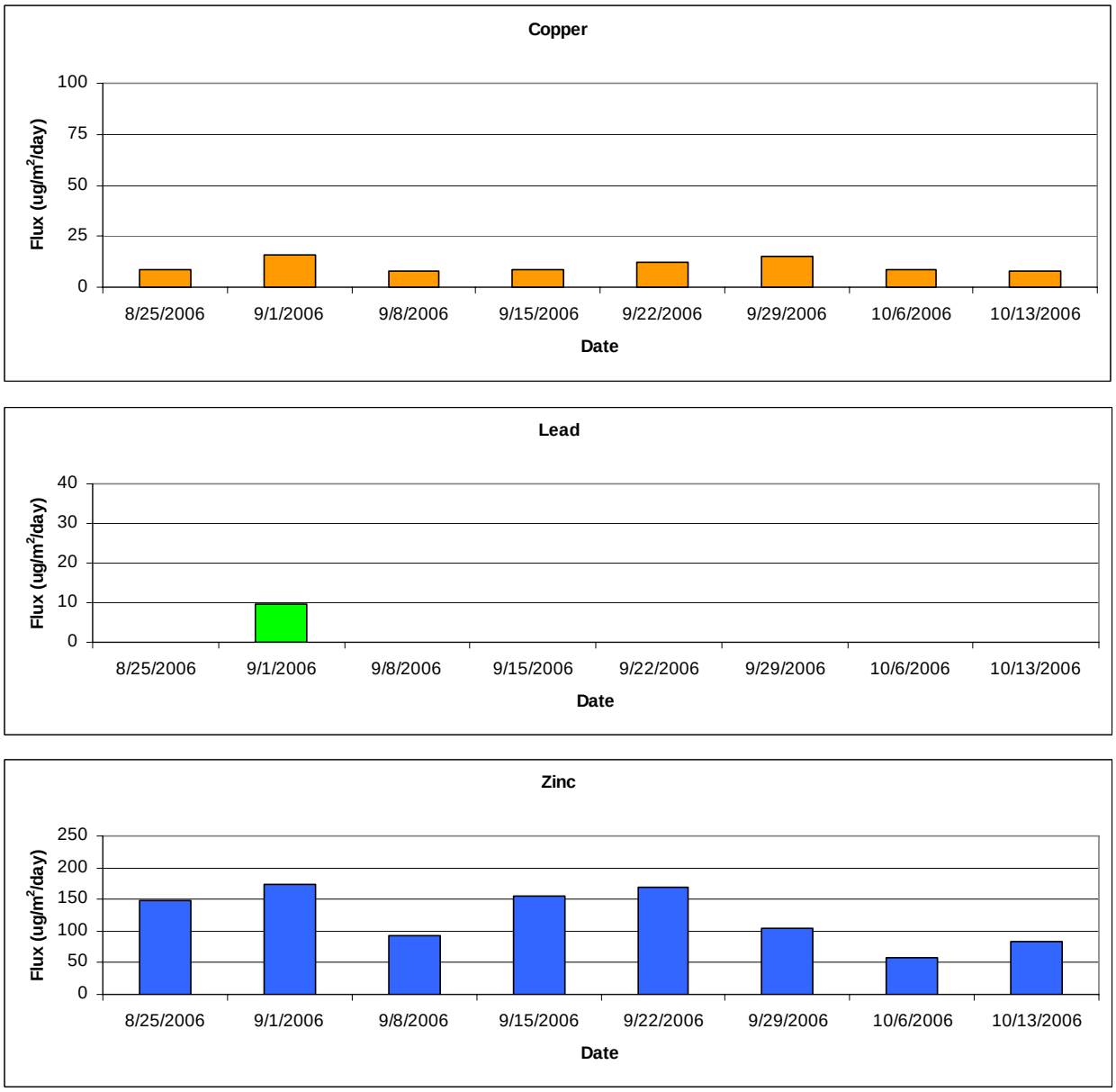

Figure 6-29. Copper, Lead, and Zinc Flux at Site 805T1

6.2.5.1 Photomicroscopy Results

A representative result for the photomicroscopy analysis performed on surrogate disks deployed at site 805T1 is presented in Figure 6-30. The sample date for the surrogate disk represented in Figure 6-30 is 9/22/06.

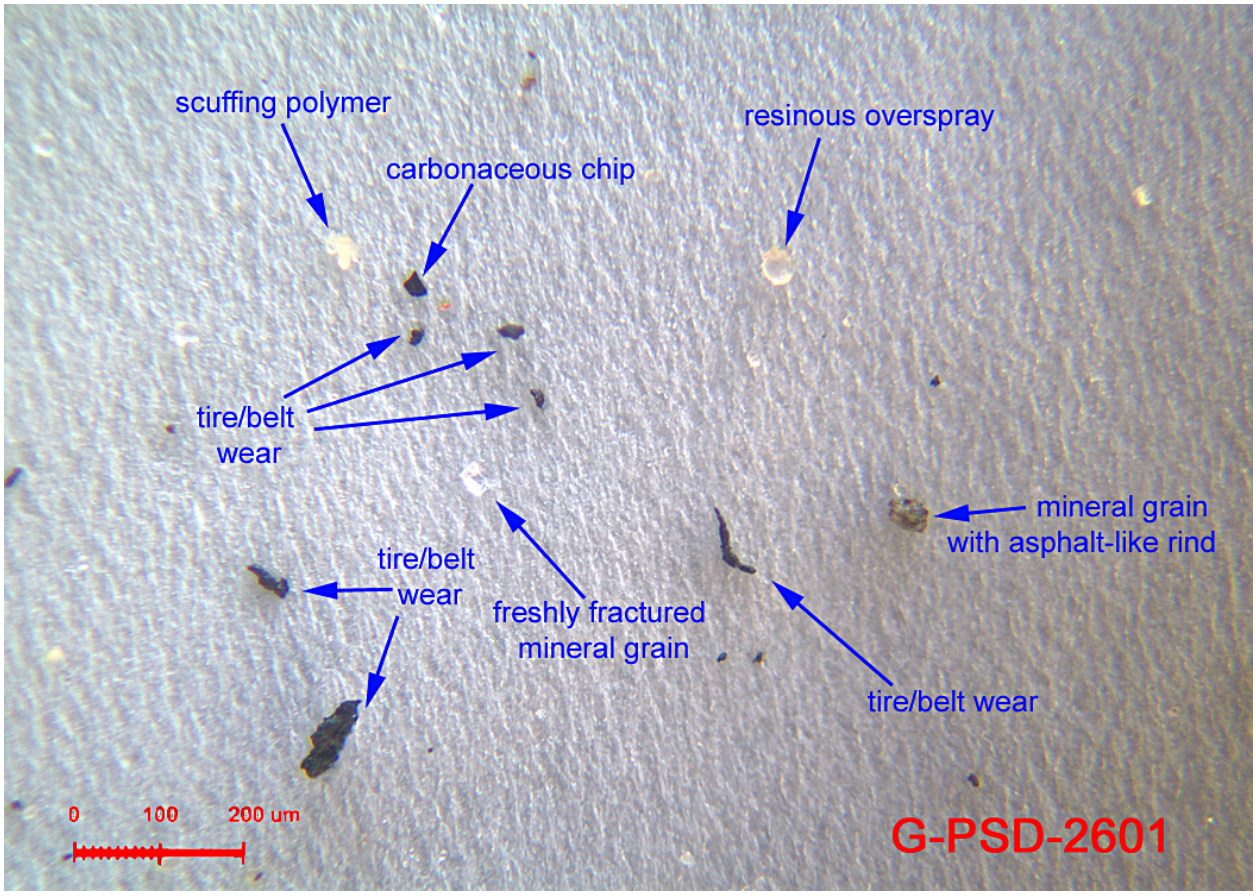

Figure 6-30. Photomicroscopy analysis for site 805T1 on 9/22/06

Particles that were frequently identified in photomicroscopy analysis of the 805T1 disks included resinous overspray, tire/belt wear, and scuffing polymer as well as iron hydroxide/hydrated oxide, woody cellulose, and cleavage fragments. All photomicroscopy results for samples collected at site 805T1 are presented in Appendix B.

6.2.5.2 Particle Size Distribution

Particle size distributions were not analyzed on samples from this site.

6.2.5.3 SEM-EDX Results

SEM/EDX analysis results of particles from the sample collected at Site 805T1 on 9/22/06 are presented in Figure 6-31. Copper particles were detected in the 1 – 5 µm size range as metallic copper and as tarnished bronze. Lead and zinc were not identified in particles using SEM/EDX. In comparison, the sample results from the XRF analyses showed a flux rate of 12.1 µg/m^2/day for copper and 170 µg/m^2/day for zinc. Lead was not detected in this sample using XRF analysis.

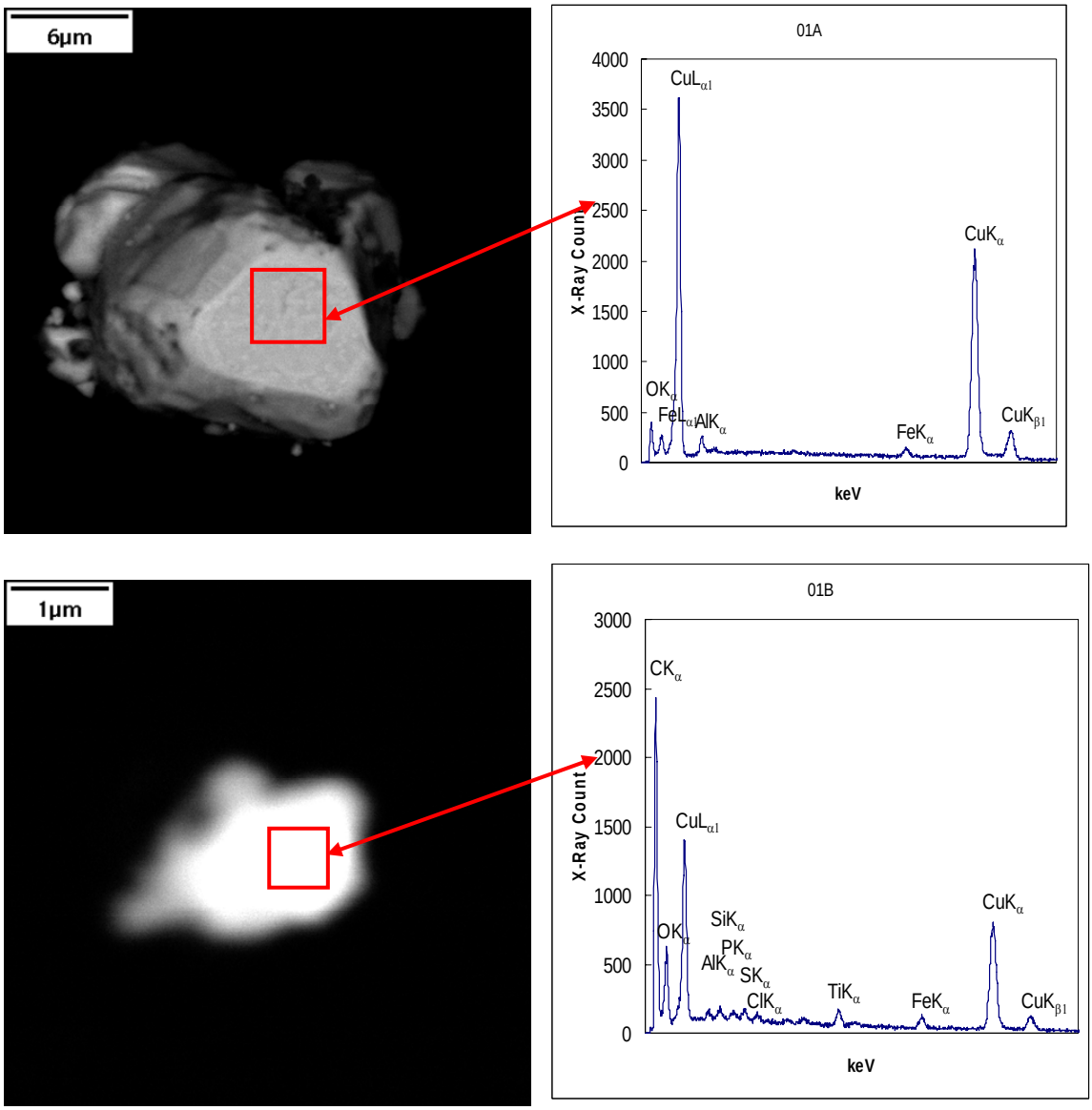

Figure 6-31. SEM/EDX analysis results of particles from the 805T1 site sample collected on 9/22/06

6.2.5.4 Impactor Sampling Results

Air concentrations of 805T1 particulates, characterized by size and by analyte, are shown in Table 6-19. The impactor sample was collected over a 12-hour period on 9/28/06. Across all size classes, iron concentrations were higher than chromium, zinc, copper, and lead concentrations by one order of magnitude or greater. Total zinc (57.8 ng/m^3) and copper (49.4 ng/m^3) were the second and third most prevalent metals in 805T1 air samples, respectively, while chromium and lead had relatively uniform concentrations across the four smallest size classes (less than 0.95 µm to greater than 7.2 µm). The analyzed metals concentrations in 805T1 air samples constituted 2.68 percent of the 58.6 µg/m^3 total particulate concentration across all particle size ranges.

Table 6-19. Distribution of the concentrations of total particulates and five metals according to particle size in ambient air collected at 805T1

Particle Size	Total Particulates	Chromium	Iron	Copper	Zinc	Lead
(µm)	(µg/m^3)	(ng/m^3)				
< 0.95	5.76	1.14	185	2.62	7.83	1.01
0.95 - 1.5	8.46	1.70	418	12.4	11.7	1.86
1.5 - 3.0	6.13	1.30	240	10.2	7.56	1.42
3.0 - 7.2	4.53	1.15	173	9.85	6.78	1.08
> 7.2	33.7	3.02	429	14.3	23.9	5.53
Total	58.6	8.31	1450	49.4	57.8	10.9

Atmospheric size distributions for 805T1 are presented in Figure 6-32. Overall, the greatest percentage of particulate mass for each analyte was found in the less than 0.95 µm size class. Greater than 50 percent of the lead and total mass, and greater than 40 percent of the zinc particulates were less than 0.95 µm in size. Additionally, nearly 30 percent of the copper, iron and chromium mass were bound to particulates in the smallest size class. By comparison, all analyte masses from size classes ranging from 0.95 and 7.2 µm were below 15 percent of their total mass, with the exception of copper in the 0.95 – 1.5 µm and 1.5 – 3.0 µm size classes, and iron and chromium in the 1.5 – 3.0 µm size class. Copper mass was greater than 20 percent in the 0.95 – 1.5, the 1.5 – 3.0, and the 3.0 – 7.2 µm size classes. While the 1.5 – 3.0 µm size class contained the second highest percentage of each analyte, the less than 0.95 µm size class contained the lowest percent masses of copper, lead, and chromium of all five size classes. In general, the vast majority of metal mass and total mass was found in particulates that were either below 0.95 µm in size or between 3.0 and 7.2 µm in size.

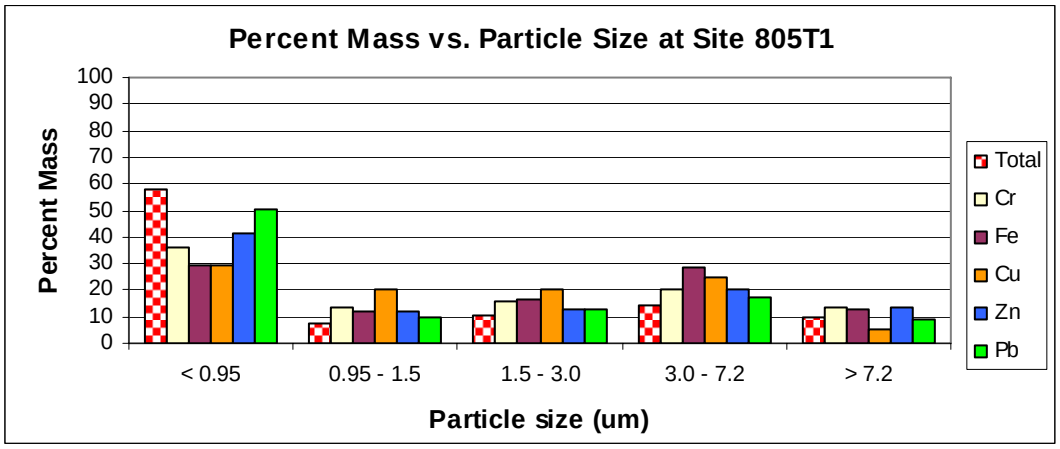

Figure 6-32. Percent mass versus particle size in air samples collected at 805T1

6.2.6 Site Switzer Creek

6.2.6.1 XRF Results

Surrogate deposition disks were deployed at Switzer Creek for a total of eight week-long events. The deposition disks were exposed for a duration of three days during each event. Analytical results from the primary surrogate deposition disks at the Switzer Creek site are presented in Table 6-20. Replicate disk analyses for each sampling date are contained in Appendix A.

Table 6-20. Copper, Lead, and Zinc Flux at Site Switzer Creek

Date	Net	Copper	Lead	Zinc
	($mg/m^2/day$)	(µg/m2/day)		
7/14/06	139	28.4	17.3	142
7/21/06	98.7	7.5	<4.9	34.1
8/11/06	157	14.1	<4.9	97.0
8/18/06	133	11.8	<4.9	199
8/25/06	142	17.4	<4.9	115
9/1/06	144	13.2	<4.9	98.7
9/8/06	111	<1.7	<4.9	42.5
9/15/06	105	7.5	<4.9	37.9

The net depositional flux for total particulate matter averaged 128 $mg/m^2/day$ for the series of deployment events. The lowest net flux (98.7 $mg/m^2/day$) occurred during the week of 7/21/06 while the highest net flux (157 $mg/ m^2/day$) occurred during the week of 8/11/06.

The depositional flux for copper ranged from BDL to 28.4 $\mu g/m^2/day$ and averaged 12.6 $\mu g/m^2/day$ during the deployment event series. The copper depositional flux was BDL during the week of 9/8/06. The highest depositional flux, 28.4 $\mu g/m^2/day$, was detected during the week of 7/14/06.

Lead was typically not detected at the Switzer Creek site except for a single deployment event occurring during the week of 7/14/06 when the depositional flux measured 17.3 $\mu g/m^2/day$ (Figure 6-33).

The depositional flux for zinc ranged from 34.1 to 199 $\mu g/m^2/day$ and averaged 95.9 $\mu g/m^2/day$ during the deployment event series. The lowest zinc depositional flux (34.1 $\mu g/m^2/day$) occurred during the week of 7/21/06 while the highest depositional flux for zinc (199 $\mu g/m^2/day$) occurred during the week of 8/18/06 (Figure 6-33).

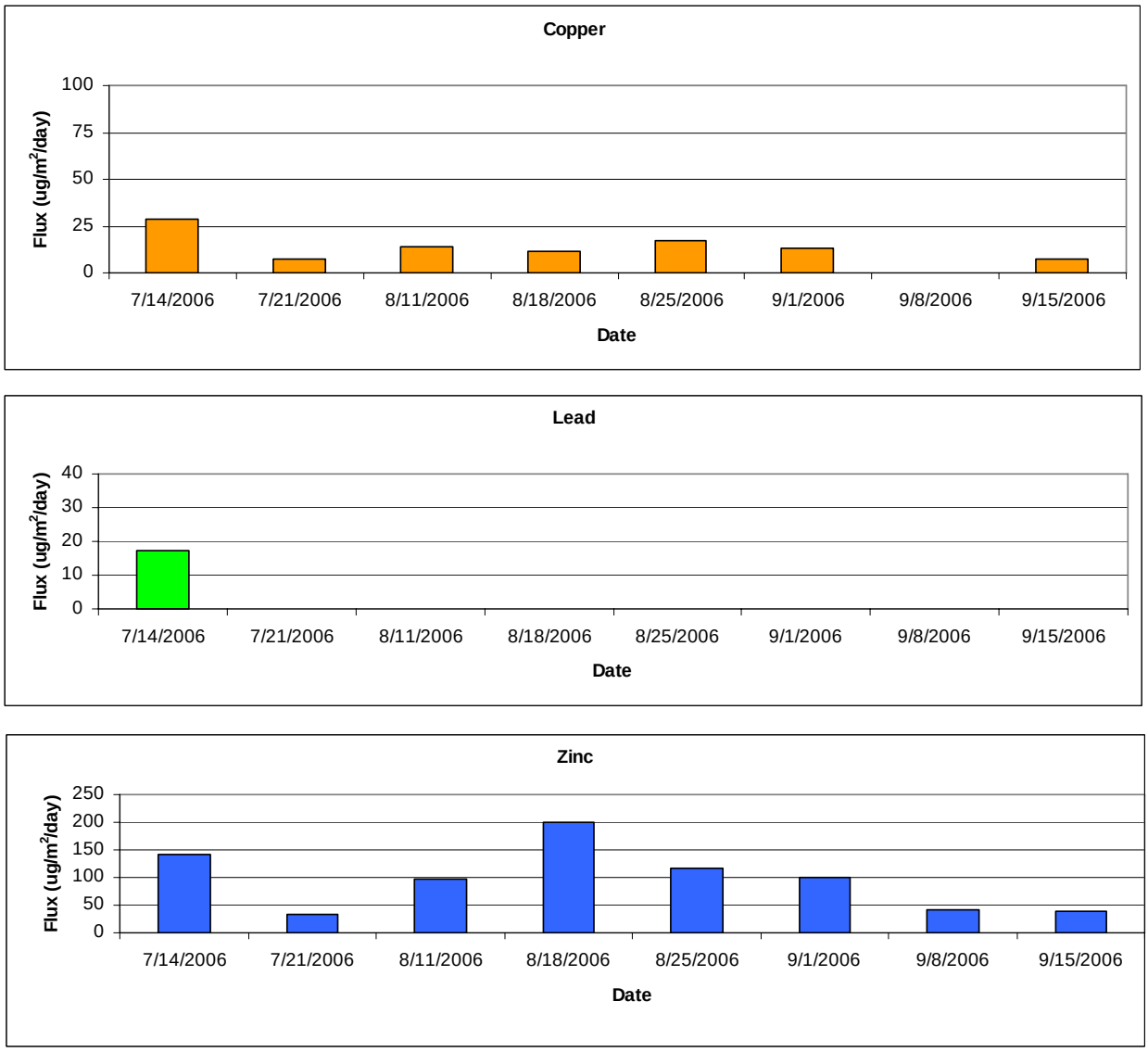

Figure 6-33. Copper, Lead, and Zinc Flux at Site Switzer Creek

6.2.6.2 Photomicroscopy Results

A representative result for the photomicroscopy analysis performed on surrogate disks deployed at site Switzer Creek is presented in Figure 6-34. The sample date for the surrogate disk represented in Figure 6-34 is 8/25/06.

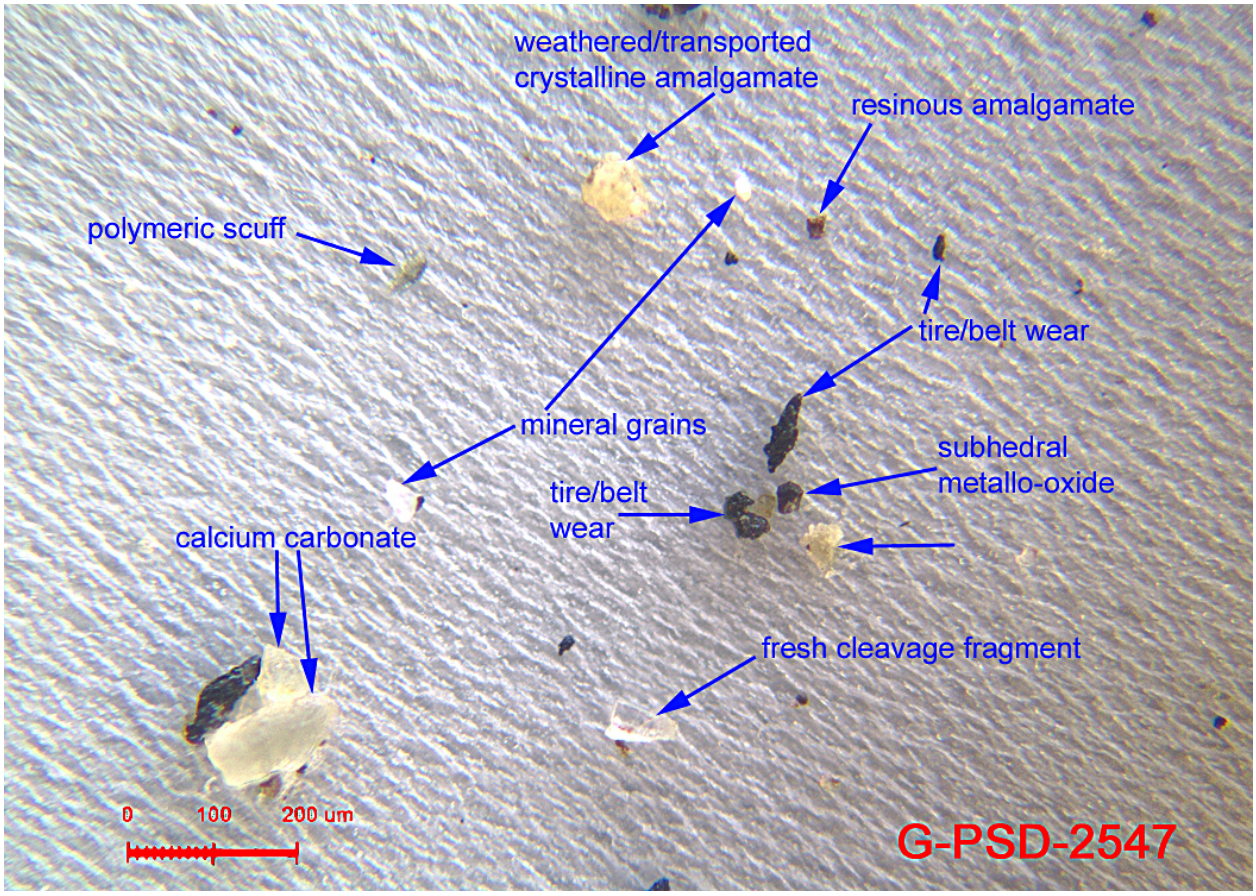

Figure 6-34. Photomicroscopy analysis for site Switzer Creek on 8/25/06.

Frequently identified particles in photomicroscopy analysis at Switzer Creek included polymeric scuff, tire/belt wear, and fresh cleavage as well as weathered mineral grain, carbon cenosphere, and frothy resin. All photomicroscopy results for samples collected at Switzer Creek are presented in Appendix B.

6.2.6.3 Particle Size Distribution

Particle size distributions from surrogate disk samples collected from the Switzer Creek site were determined for three sample dates. Particulate size distributions for these three dates are shown in Table 6-21. The relative percent area was highest in the 25 – 50 µm size range for the 7/14/06 and 7/21/06 sample dates and was highest in the 50-100 µm size range during the 8/11/06 sample event. All three sample dates at site Switzer Creek had a higher percentage of particles in the > 15 µm size range. Aerially deposited particle sizes at Site Switzer Creek would be classified as primarily fine and coarse silt and very fine sand.

Table 6-21. Particle Size Distribution at Switzer Creek.

Size Range (um)	Relative Percent Area		
	7/14/2006	7/21/2006	8/11/2006
0.8-2	0.1	7.1	1.4
2-5	0.5	15.0	2.6
5-15	5.7	26.2	7.4
15-25	21.5	12.4	14.0
25-50	42.4	30.6	33.6
50-100	29.8	8.6	41.1
100-1000	0.0	0.0	0.0
% >15 um	**93.8**	**51.7**	**88.6**
% <15 um	**6.2**	**48.3**	**11.4**

6.2.6.4 SEM-EDX Results

SEM/EDX analysis results of particles from the samples collected at the Switzer Creek site on 8/25/06 are presented in Figure 6-35 and Figure 6-36. Copper was identified as chips associated with iron from mechanical abrasion in the 1 – 2 µm size range (Figure 6-35). Based on this size range, this copper may be associated with brake wear debris. Lead particles were also detected and were associated with tin, likely from solder in the 5 – 15 µm size range (Figure 6-36). Zinc particles were not detected using SEM/EDX. In comparison, the sample results from the XRF analyses showed a flux rate of 17.5 $\mu g/m^2$/day for copper and 115 $\mu g/m^2$/day zinc. Lead was not detected in this sample using XRF analysis.

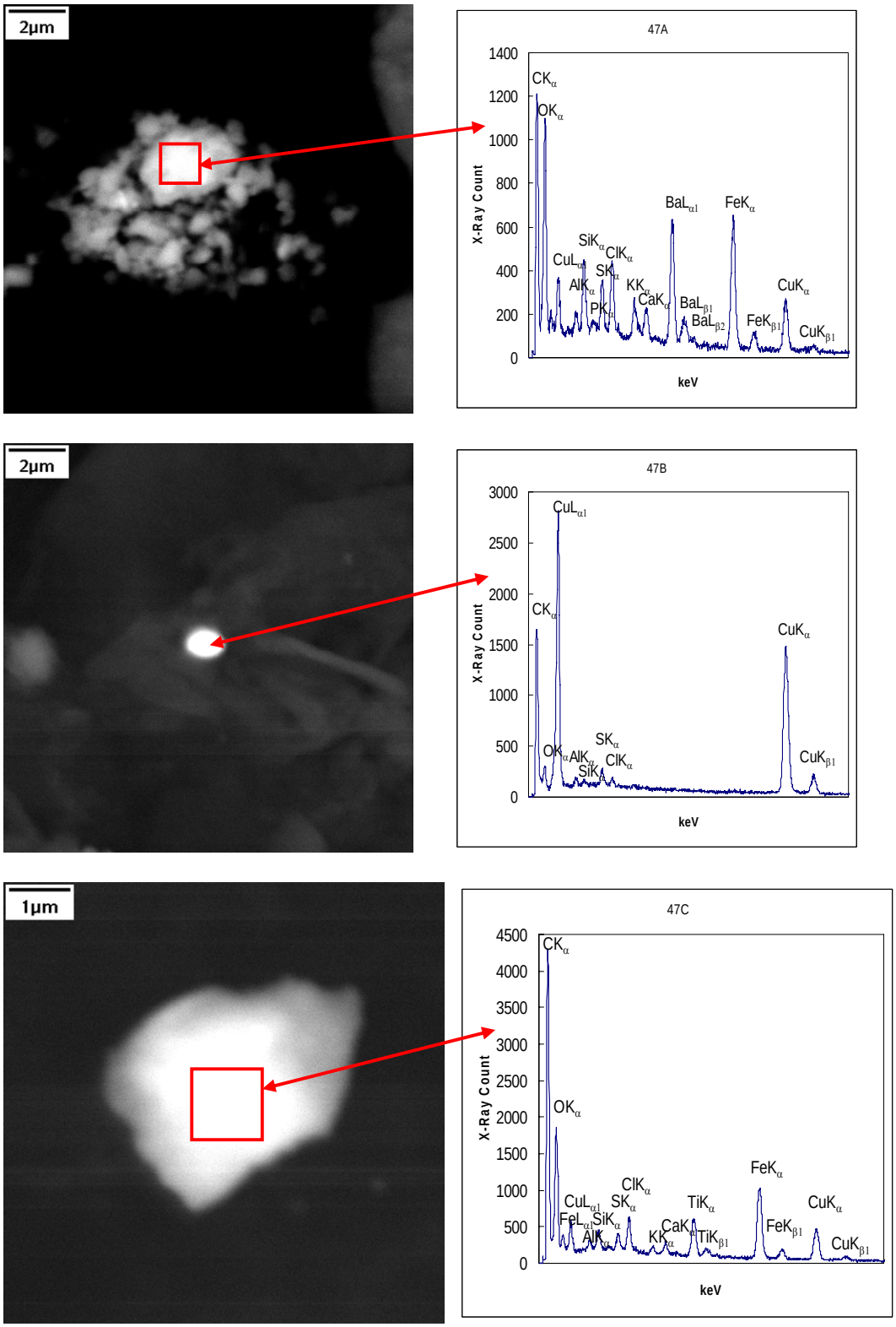

Figure 6-35. SEM/EDX analysis results of particles from the Switzer Creek site sample collected on 8/25/06.

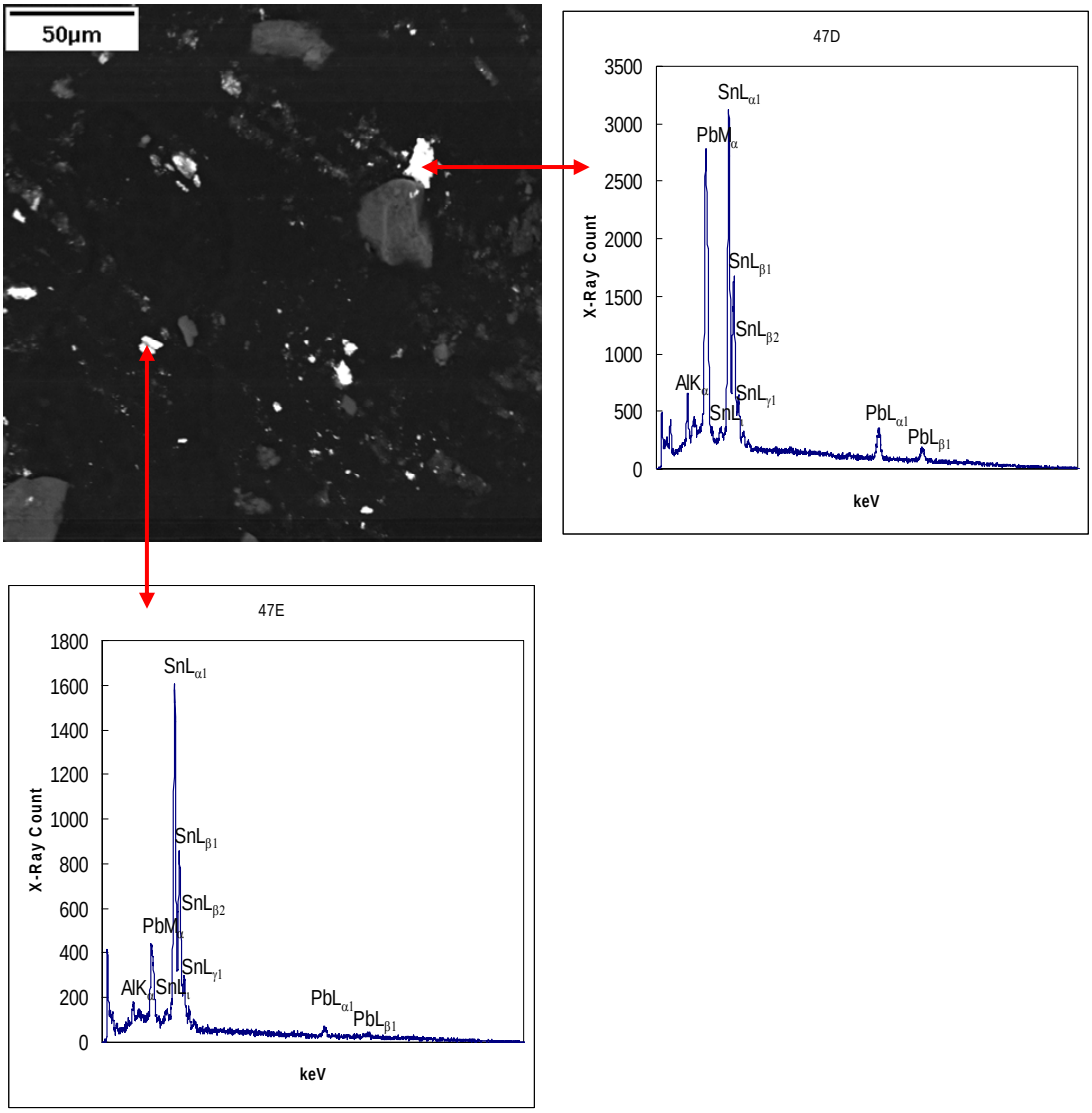

Figure 6-36. SEM/EDX analysis results of particles from the Switzer Creek site sample collected on 8/25/06.

6.2.6.5 Impactor Sampling Results

Air concentrations of Switzer Creek particulates, characterized by size and by analyte, are shown in Table 6-22. The impactor sample was collected over a 12-hour period on 8/30/06. Across all size classes, iron concentrations were higher than copper, chromium, zinc and lead concentrations by one order of magnitude or greater. Zinc and copper were the second and third most prevalent metals in Switzer Creek air samples, respectively, across all size classes. No lead was detected in the 0.95 – 1.5 µm particulate size range. In total, the analyzed metals concentrations constituted 2.16 percent of the 75.0 µg/m^3 total particulate concentration across all size classes.

Table 6-22. Distribution of the concentrations of total particulates and five metals according to particle size in ambient air collected at Switzer Creek

Particle Size	Total Particulates	Chromium	Iron	Copper	Zinc	Lead
(µm)	(µg/m^3)	(ng/m^3)				
< 0.95	33.5	2.84	341	14.3	42.5	3.55
0.95 - 1.5	7.11	0.938	153	10.5	12.6	<0.82
1.5 - 3.0	8.46	1.13	249	9.99	11.0	1.18
3.0 - 7.2	15.6	1.52	468	12.8	15.1	2.07
> 7.2	10.3	1.11	251	4.41	10.2	1.17
Total	75.0	7.54	1460	52.0	91.4	8.38*

* One half the detection limit was used for values less than the MDL to calculate total lead.

Atmospheric size distributions for Switzer Creek are presented in Figure 6-37. Overall, the greatest percentage of particle mass for each analyte, with the exception of iron, was contained within the less than 0.95 µm size class. Greater than 40 percent of all lead, zinc, and total mass particulates and nearly 40 percent of all chromium particulates were less than 0.95 µm in size. The 0.95 – 1.5 µm size class contained relatively low percentages (15 percent or less) of chromium, iron, zinc, lead, and total mass particulates but did contain 20 percent of the total copper particulates. Analysis of the 1.5 – 3.0 µm particulates yielded slight increases in iron, chromium, and total particulate percentages, and a significant increase in the percentage of lead detected. In the coarse particle sizes, the 3.0 – 7.2µm size class contained greater than 20 percent of zinc, copper, chromium and total mass, and more than 30 percent of the total iron while the greater than 7.2 µm size class contained greater than 20 percent of the iron, lead, and zinc particulates, and slightly less than 20 percent of the chromium and total mass particulates. While 24.5 percent of copper particulates were contained in the 3.0 – 7.2 µm size class, only 8.4 percent were contained in the greater than 7.2 µm size class.

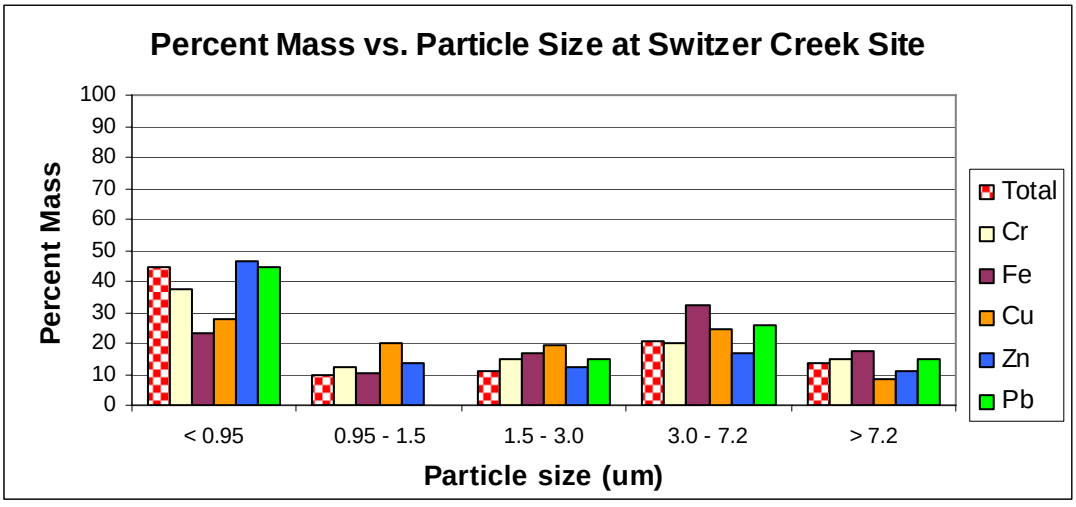

Figure 6-37. Percent mass versus particle size in air samples collected at Switzer Creek

6.2.7 Site 94T

6.2.7.1 XRF Results

Surrogate deposition disks were deployed at the 94T site for one week-long event at locations upwind and 25 m, 100 m, and 250 m downwind from the 94 freeway. The 94T site was originally intended to serve as the location for the Transect study (Section 6.3) but sampling for this purpose was suspended after the first week of sampling due to various logistical difficulties. Results for the single event conducted at this location are included in the Area Wide study in order to provide additional regional aerial deposition data.

The deposition disks were exposed for a duration of three days during the event. Of the four locations deployed for this event, two samples were damaged or contaminated in the field by bird and water disturbance which resulted in the discs being withheld from laboratory analysis. The 94T1 site was located 25 m downwind of the 94 freeway. Analytical results from the primary surrogate deposition disks at the 94T1 and 94T2 sites are presented in Table 6-23. Replicate disk analyses for each sampling date are contained in Appendix A.

Table 6-23. Copper, Lead, and Zinc Flux at Site 94T

Date	Net	Copper	Lead	Zinc
	($mg/m^2/day$)	(µg/m2/day)		
94T1-7/14/06	88.7	19.2	29.0	142
94T2-7/14/06	50.7	12.2	11.0	30.2

The net depositional flux for total particulate matter was 88.7 mg/m^2/day and 50.7 mg/m^2/day for the two disks deployed. The depositional flux was higher for copper, lead, and zinc at site 94T-1 in comparison to site 94T-2. Results are presented graphically in Figure 6-38.

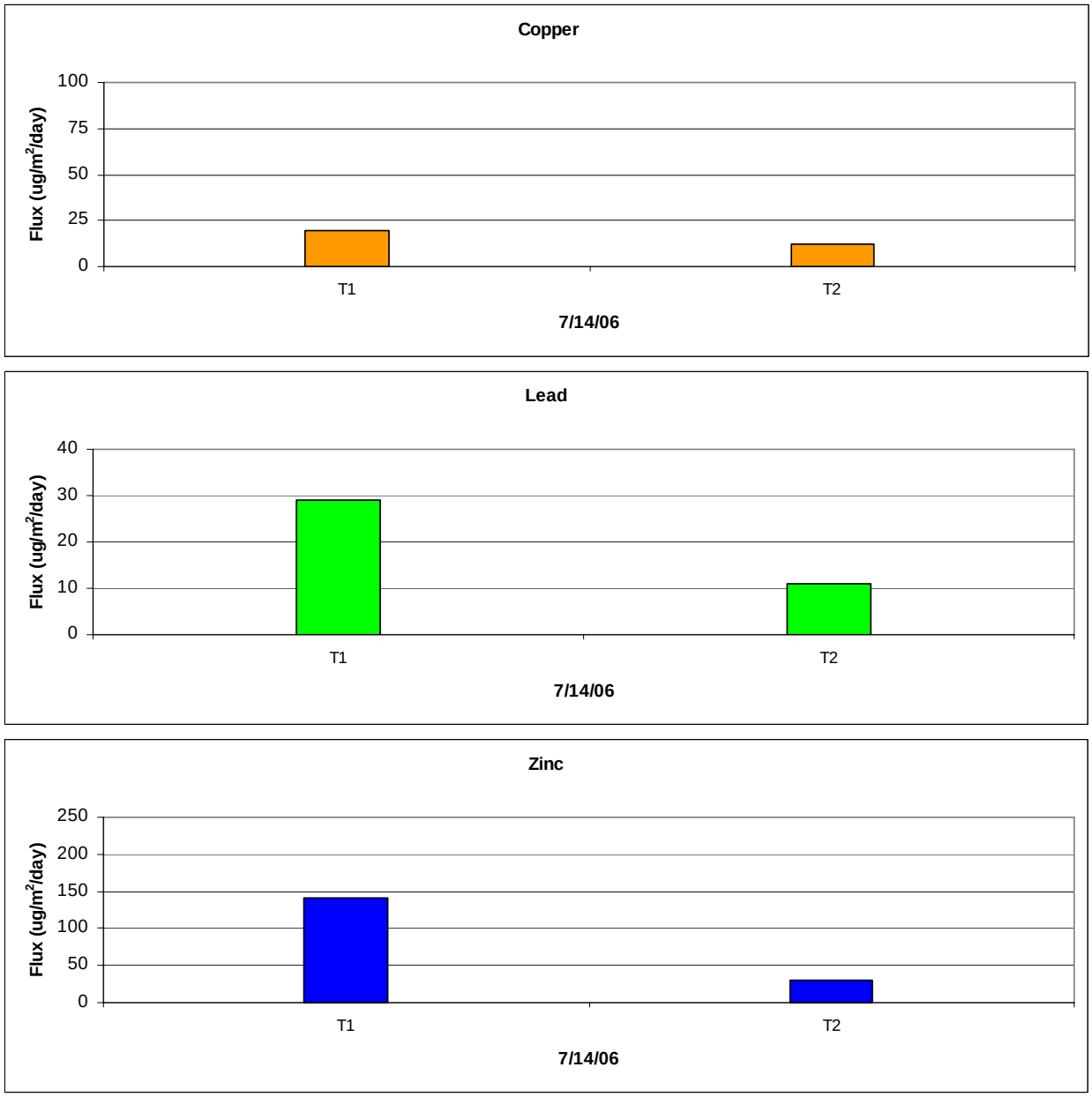

Figure 6-38. Copper, Lead, and Zinc Flux at Site 94T1 and 94T2.

6.2.7.2 Photomicroscopy Results

94T1 and 94T2

A representative result for the photomicroscopy analysis performed on surrogate disks deployed at site 94T1 is presented as Figure 6-39. The sampling date for the surrogate disk represented in Figure 6-39 is 7/14/06. Particles identified in photomicroscopy analysis at 94T1 included scuffed heterogeneous amalgamate, tire/belt wear, mineral grains, scuffed elastomer, and cellulose.

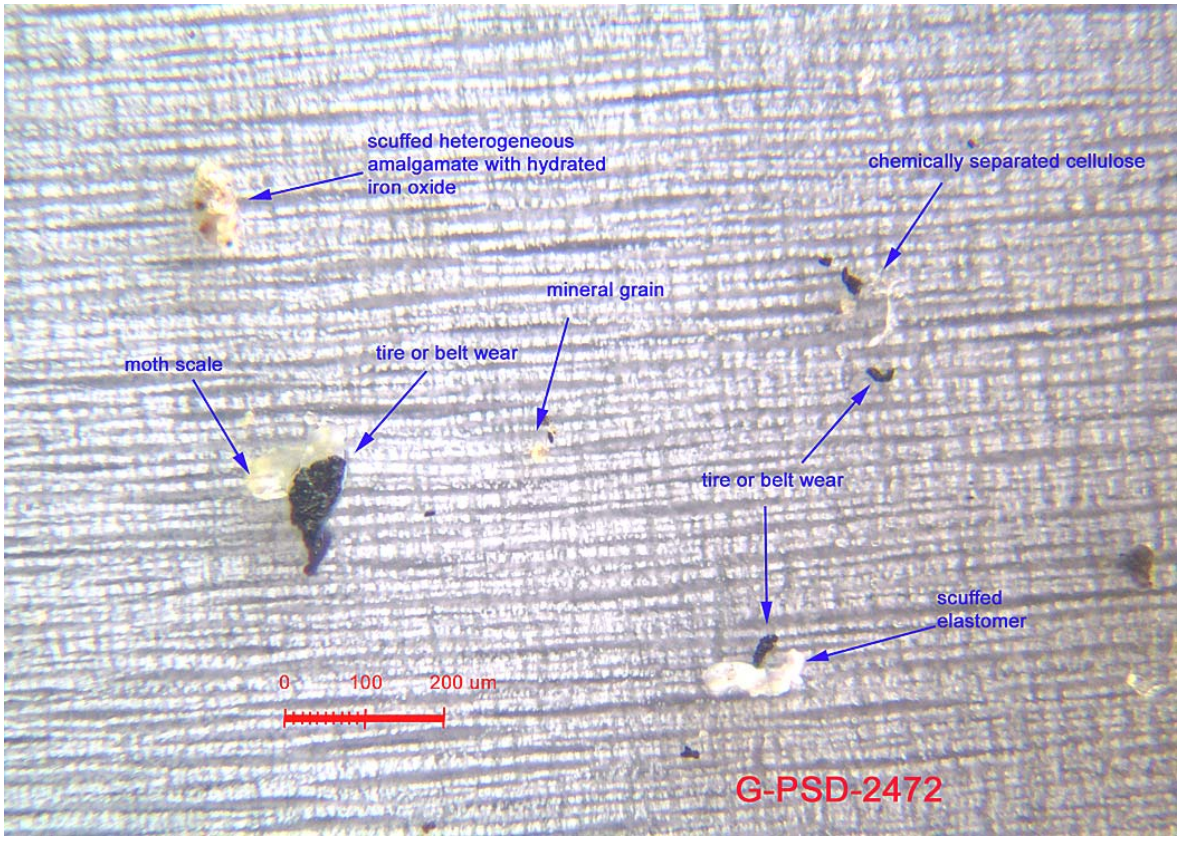

Figure 6-39. Photomicroscopy analysis for site 94 T1 on 7/14/06

A representative result for the photomicroscopy analysis performed on surrogate disks deployed at site 94T2 is presented in Figure 6-40. The sample date for the surrogate disk represented in Figure 6-40 is 7/14/06. Particles identified in photomicroscopy analysis at 94T2 included resinous scuff, tire/belt wear, mineral grains, transported silicate, and woody and chemically separated cellulose.

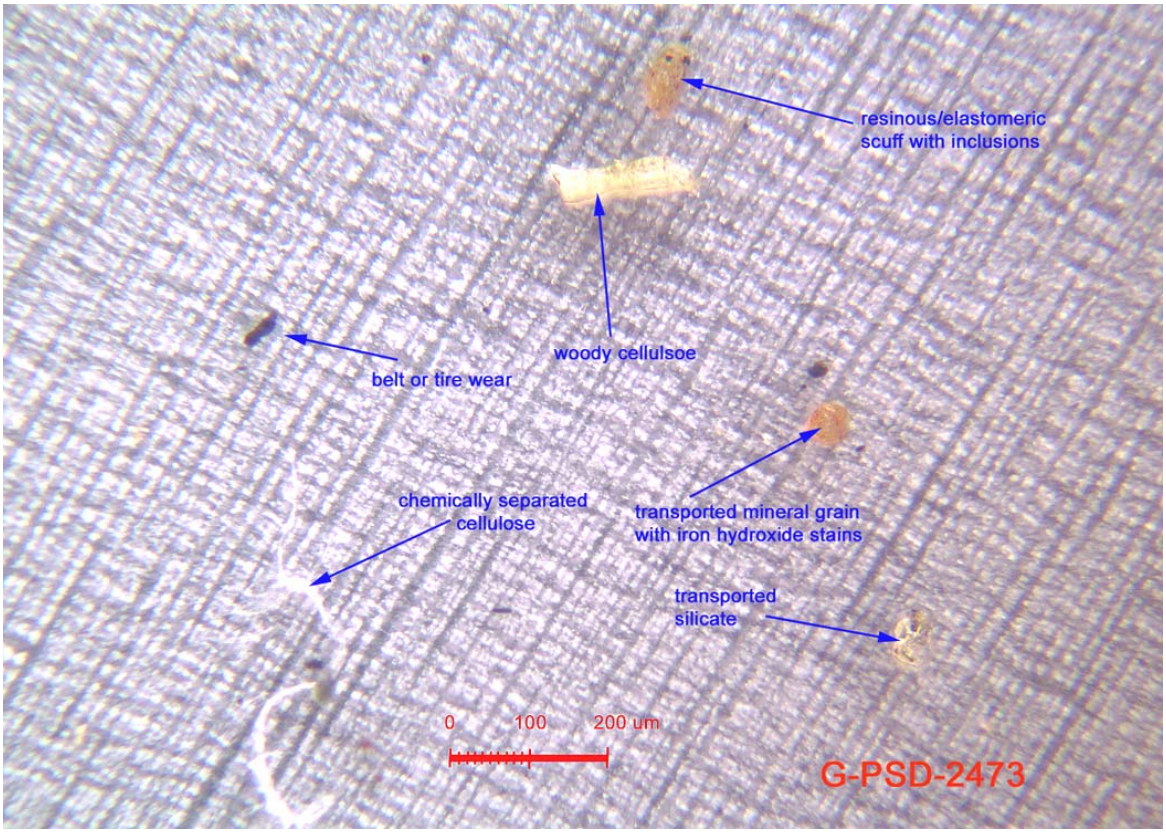

Figure 6-40. Photomicroscopy analysis for site 94 T2 on 7/14/06

6.2.7.3 Particle Size Distribution

Particle size distributions from surrogate disk samples collected from the original transect site off Highway 94 were determined for one sample date (7/14/06) and from only two samples (94T1 and 94T2). As previously mentioned, this site was no longer sampled after the 7/14/06 sample event. Particulate size distributions for these two samples (94T1 and 94T2) are shown in Table 6-24 and Table 6-25 respectively. The relative percent area was highest in the 25-50 µm size range at Site 94T1. The relative percent area was highest in the 50-100 µm size range at Site 94T2. Both sites had relatively few clay size particles. Particle sizes at Site 94T1 would be classified as primarily coarse silt with some very fine sand and fine silt. Aerially deposited particle sizes at Site 94T2 would be classified as primarily coarse silt and very fine sand.

Table 6-24. Particle Size Distribution at Site 94T1

Size Range (µm)	Relative Percent Area 7/14/2006
0.8-2	0.3
2-5	0.9
5-15	11.9
15-25	20.6
25-50	52.9
50-100	13.3
100-1000	0.0
% >15 um	**86.8**
% <15 um	**13.2**

Table 6-25. Particle Size Distribution at Site 94T2

Size Range (µm)	Relative Percent Area 7/14/2006
0.8-2	0.6
2-5	1.7
5-15	6.3
15-25	13.3
25-50	24.6
50-100	53.6
100-1000	0.0
% >15 um	**91.4**
% <15 um	**8.6**

6.2.7.4 SEM/EDX Results

Sample disks from site 94T1 or 94T2 were not submitted SEM-EDX analysis.

6.2.7.5 Impactor Sampling Results

Impactor sampling was not conducted at the Highway 94 Transect Site. This site was not used for the remainder of the study.

6.2.8 Site SD8(1)

6.2.8.1 XRF Results

Surrogate deposition disks were deployed at SD8(1) for a total of nine week-long events. The deposition disks were exposed for a duration of three days during each event. Analytical results from the primary surrogate deposition disks at the SD8(1) site are presented in Table 6-26. Results of replicate disks are provided in Appendix A.

Table 6-26. Copper, Lead, and Zinc Flux at Site SD8(1).

Date	Net	Copper	Lead	Zinc
	($mg/m^2/day$)	($\mu g/m^2/day$)		
6/30/06	138	45.9	<4.9	102
7/6/06	55.4	9.8	<4.9	34.8
7/14/06	162	24.4	17.3	235
7/21/06	70.6	9.9	<4.9	68.3
8/11/06	102	27.4	8.3	116
8/18/06	102	11.1	<4.9	84.3
8/25/06	80.1	19.5	15.5	81.3
9/1/06	82.7	49.2	<4.9	74.2
9/8/06	48.9	7.3	<4.9	57.8

The net depositional flux for total particulate matter ranged from 48.9 to 162 $mg/m^2/day$ and averaged 92.5 $mg/m^2/day$ for the series of deployment events. The lowest net flux occurred during the week of 7/6/06 and the highest net flux occurred during the week of 7/14/06.

The depositional flux for copper ranged from 9.8 to 49.2 $\mu g/m^2/day$ and averaged 22.1 $\mu g/m^2/day$ during the deployment event series. The lowest depositional flux occurred during the week of 7/6/06. The highest depositional flux, 49.2 $\mu g/m^2/day$, was detected during the week of 9/1/06.

Lead was detected during more deployment events at the SD8(1) site than at any other site (three out of the nine deployment events). The depositional flux for lead ranged from BDL to 17.3 $\mu g/m^2/day$ and averaged 5.9 $\mu g/m^2/day$ during the deployment event series. The highest lead fluxes observed were during the 7/14/06 and 8/25/06 events (17.3 and 15.5 $\mu g/m^2/day$, respectively) (Figure 6-41).

The depositional flux for zinc ranged from 34.8 to 235 $\mu g/m^2/day$ and averaged 92.2 $\mu g/m^2/day$ during the deployment event series. Zinc was 34.8 during the week of 7/6/06. The highest zinc depositional flux, 235 $\mu g/m^2/day$ was observed during the week of 7/14/06 (Figure 6-41).

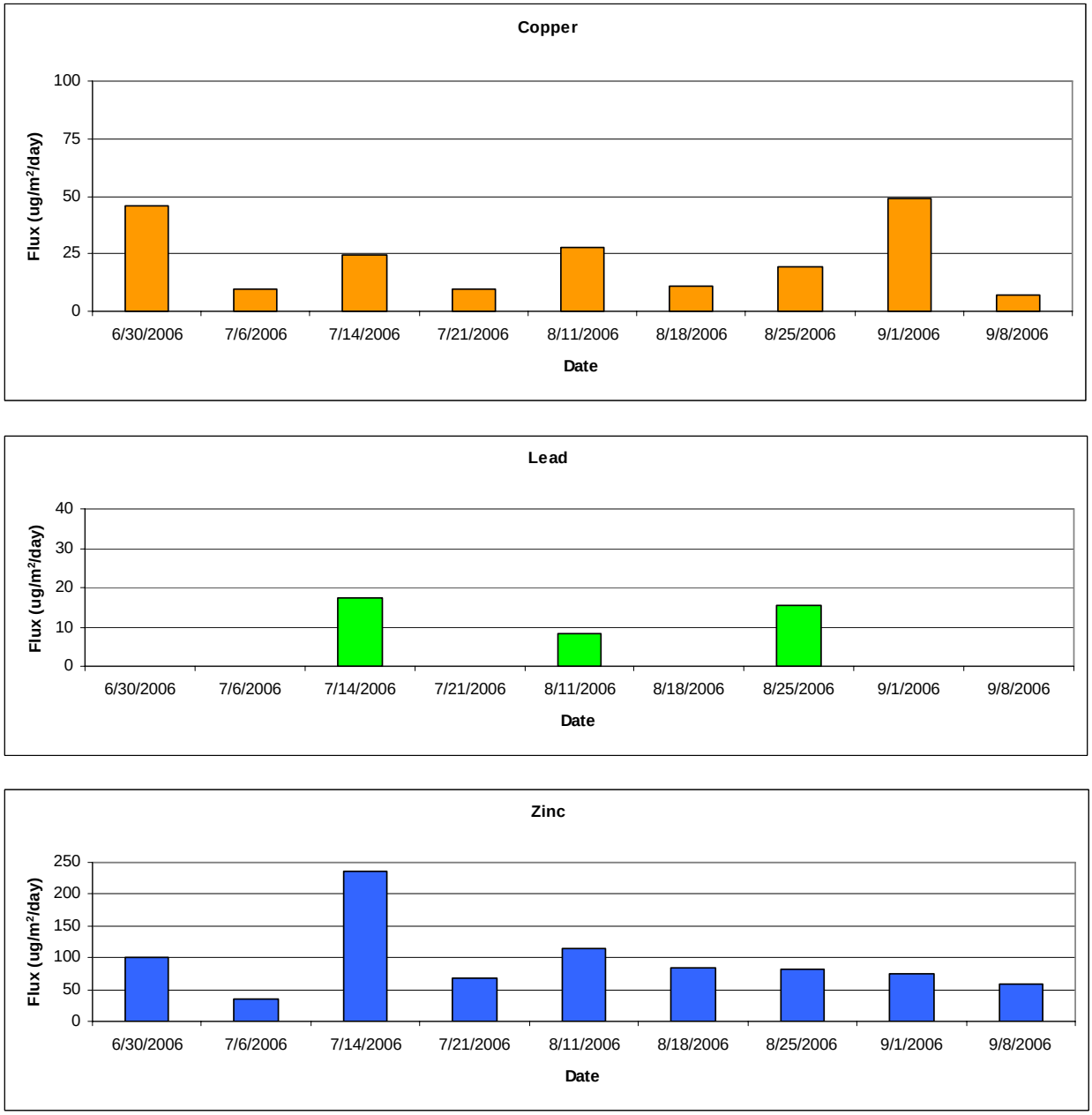

Figure 6-41. Copper, Lead, and Zinc Flux at Site SD8(1).

6.2.8.2 Photomicroscopy Results

A representative result for the photomicroscopy analysis performed on surrogate disks deployed at site SD(8)1 is presented in Figure 6-42. The sample date for the surrogate disk represented in Figure 6-42 is 9/1/06.

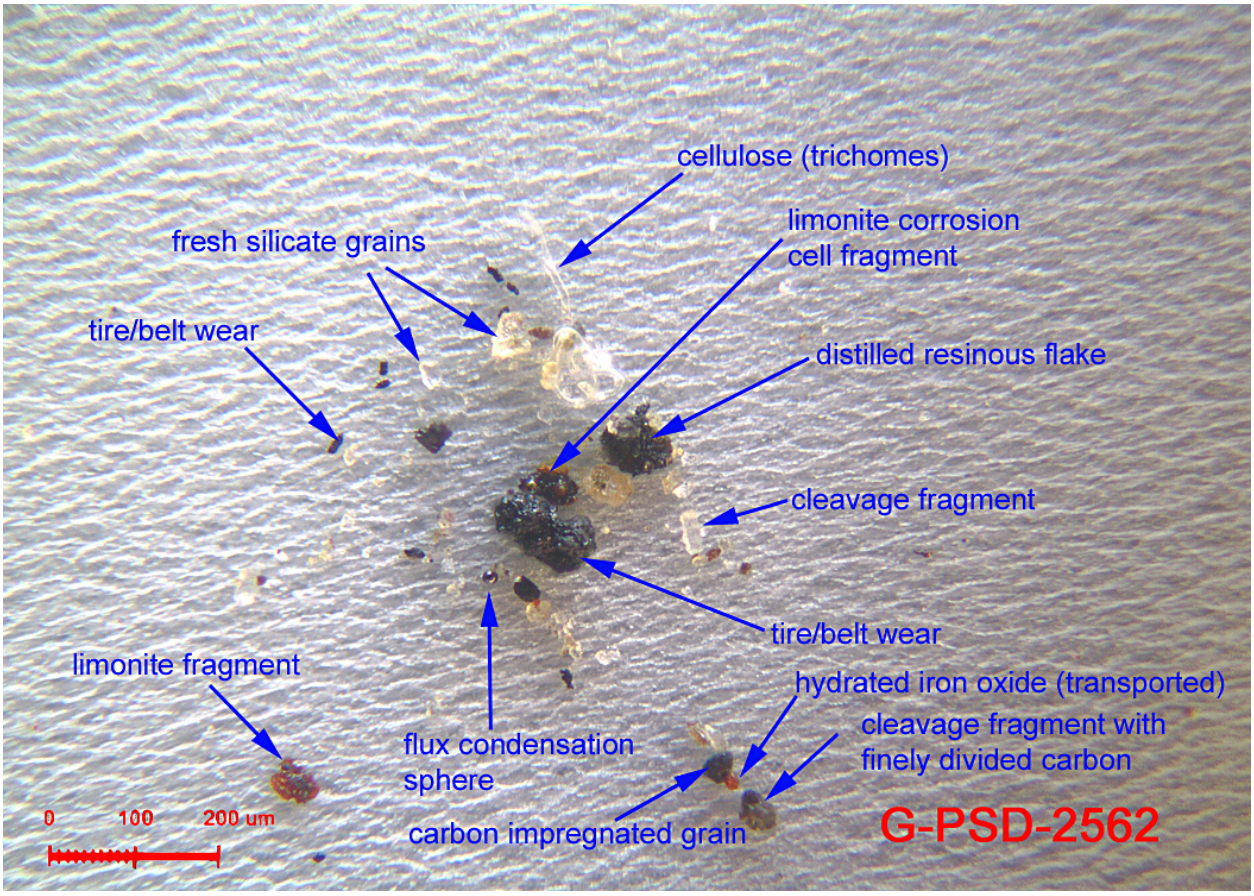

Figure 6-42. Photomicroscopy analysis for site SD(8)1 on 9/1/06.

Most particles identified in photomicroscopy analysis at this site consisted of limonite fragments, tire/belt wear, and hydrated iron oxide as well as thin resinous flake, metallo-oxide flux condensation spheres, and coating overspray. All photomicroscopy results for samples collected at site SD(8)1 are presented in Appendix B.

6.2.8.3 Particle Size Distribution

Particle size distributions from surrogate disk samples collected from Site SD8(1) were determined for four sample dates. Particulate size distributions for these four dates are shown in Table 6-27. The relative percent area was highest in either the 25 – 50 µm size range or the 50 – 100 µm size range during each sample event. All four sample dates at Site SD8(1) had a higher percentage of particles in the >15 µm size range. Aerially deposited particle sizes at Site SD8(1) would be classified as primarily coarse silt and very fine sand.

Table 6-27. Particle Size Distribution at Site SD8(1).

Size Range (um)	Relative Percent Area			
	6/30/2006	7/14/2006	7/21/2006	8/11/2006
0.8-2	0.3	0.3	7.1	4.3
2-5	0.9	1.2	15.0	6.2
5-15	5.4	7.0	26.2	10.4
15-25	12.7	7.9	12.4	10.9
25-50	48.8	34.2	30.6	39.6
50-100	31.9	37.0	8.6	28.5
100-1000	0.0	12.4	0.0	0.0
% >15 um	**93.4**	**91.4**	**51.7**	**79.0**
% <15 um	**6.6**	**8.6**	**48.3**	**21.0**

6.2.8.4 SEM-EDX Results

SEM/EDX analysis results of particles from the sample collected at Site SD8(1) on 9/1/06 are presented in Figure 6-43. Zinc particles were identified in the 5 µm size range as mechanically derived chips and were associated with iron as galvanized steel. Lead particles were also detected as minute particles in the 0.5 µm size range of uncertain origin. Copper was not detected in the particles analyzed using SEM/EDX. In comparison, the sample results from the XRF analyses showed a flux rate of 49.2 µg/m^2/day for copper and 74.2 µg/m^2/day zinc. Lead was not detected in this sample using XRF analysis. Again, with the lead particles shown here (in the 0.5 µm size range), would likely not have sufficient elemental mass to be detected using XRF analysis.

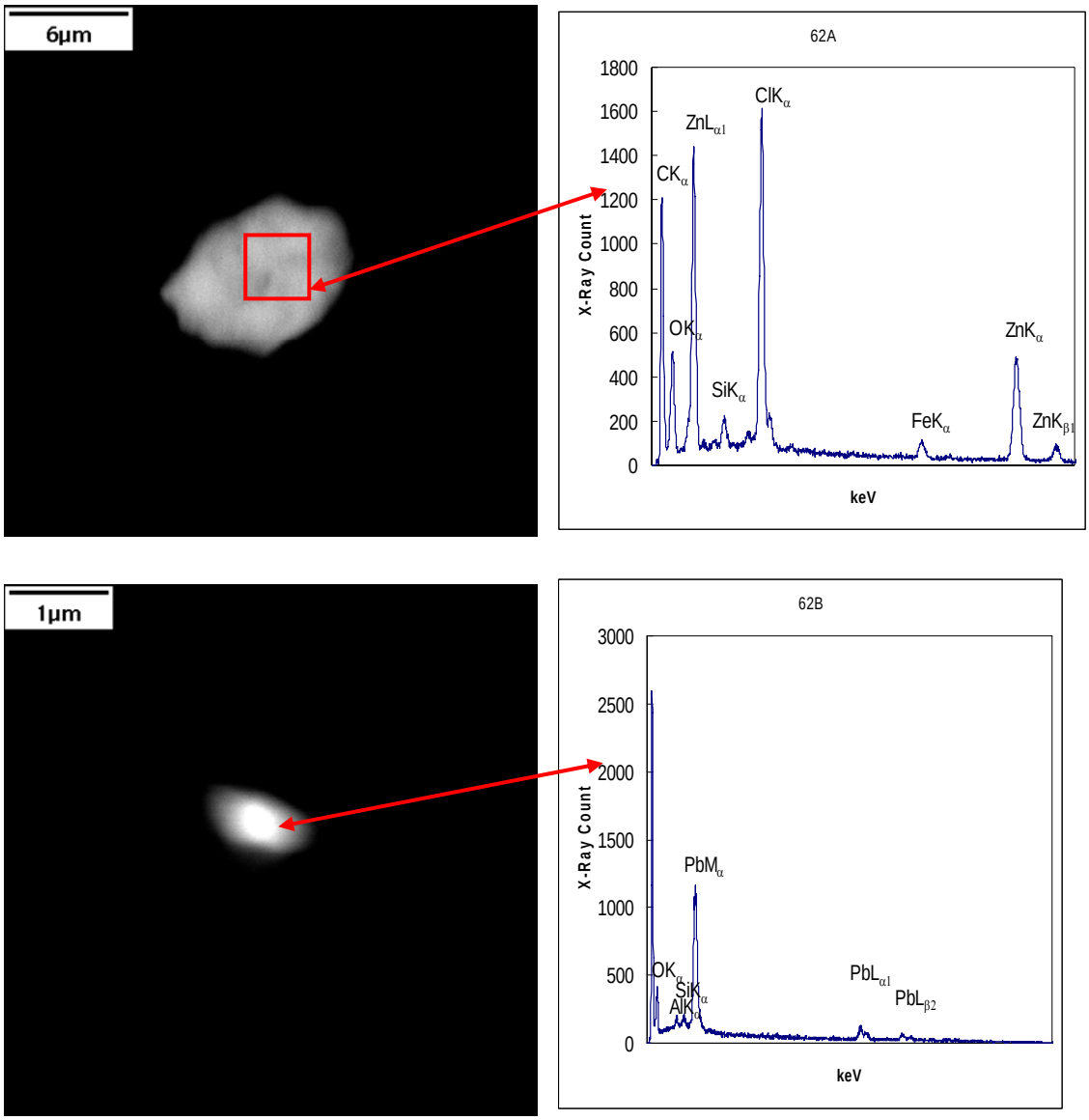

Figure 6-43. SEM/EDX analysis results of particles from the SD8(1) site sample collected on 9/1/06.
Zinc was associated with iron within mechanically derived chips, again appearing to represent galvanized steel. Lead was represented within minute chip-like shapes of uncertain origin.

6.2.8.5 Impactor Sampling Results

Air concentrations of SD8(1) particulates, characterized by size and by analyte, are shown in Table 6-28. The impactor sample was collected over a 12-hour period on 8/24/06. Across all size classes, iron concentrations were higher than copper, chromium, zinc and lead concentrations by approximately one order of magnitude or greater. Zinc and copper were the second and third most prevalent metals captured in SD8(1) air samples, across all size classes. In total, the analyzed metals concentrations constituted 1.98 percent of the 73.5 µg/m^3 total particulate concentration.

Table 6-28. Distribution of the concentrations of total particulates and five metals according to particle size in ambient air collected at SD8(1)

Particle Size	Total Particulate	Chromium	Iron	Copper	Zinc	Lead
(µm)	(µg/m^3)	(ng/m^3)				
< 0.95	32.8	2.77	309	23.7	31.3	5.87
0.95 - 1.5	6.25	0.860	108	14.1	7.12	1.69
1.5 - 3.0	8.33	0.976	205	13.2	10.2	2.08
3.0 - 7.2	16.7	1.40	418	17.2	20.6	3.93
> 7.2	9.44	1.07	232	7.38	15. 6	2.64
Total	73.5	7.08	1270	75.6	69.2	16.2

Atmospheric size distributions for SD8(1) are presented in Figure 6-44. Overall, the greatest percentage of particle mass for each analyte, with the exception of iron, was contained within the less than 0.95 µm size class. Greater than 30 percent of all chromium, copper, zinc, and lead, and greater than 40 percent of the total mass particulates were less than 0.95 µm in size. In contrast, the 0.95 – 1.5 µm size class contained the lowest percentages of iron, zinc, chromium, lead and total particulates of any size class. With the exception of copper, percentages of iron, zinc, chromium, and lead in the 0.95 – 1.5 µm size class were 12 percent or less of their total mass. Within the 1.5 – 3.0 particulate size class, the percent composition of each analyte was nearly uniform, ranging from 11.3 percent for total mass to 17.5 percent for copper mass. The coarse particulate size classes (3.0-7.2 µm and >7.2 µm) had nearly uniform percentages of total mass, chromium, copper, lead and zinc mass. Within the 3.0 – 7.2µm size class, these percentages ranged from 19.8 percent and 24.3 percent, while iron mass was 32.8 percent of the total iron. Particulates greater than 7.2 µm in size contained between 10 and 20 percent of the total iron, zinc, lead, chromium and total mass, and slightly less than 10 percent of the total copper. Similar to other locations, total copper particulates were lowest in total mass in the greater than 7.2 µm size class.

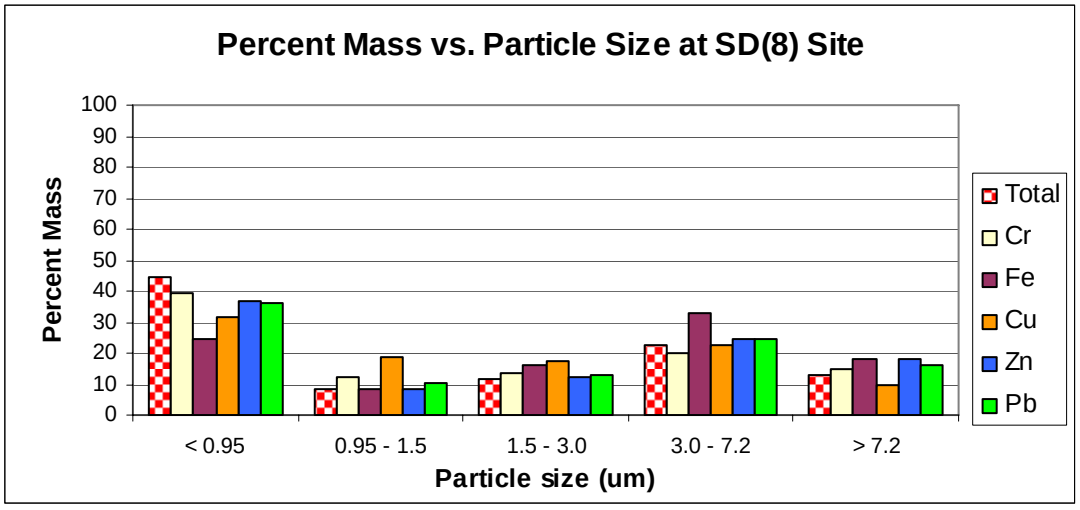

Figure 6-44. Percent mass versus particle size in air samples collected at SD8(1)

6.2.9 Site Prism2

6.2.9.1 XRF Results

Surrogate deposition disks were deployed at site Prism2 for a total of eight week-long events. The deposition disks were exposed for a duration of three days during each event. Analytical results from the primary surrogate deposition disks at the Prism2 site are presented in Table 6-29. Replicate disk analyses are provided in Appendix A.

Table 6-29. Copper, Lead, and Zinc Flux at Site Prism2

Date	Net	Copper	Lead	Zinc
	($mg/m^2/day$)	(µg/m2/day)		
7/14/06	42.6	10.2	<4.9	34.3
7/21/06	32.9	9.9	<4.9	<1.9
8/11/06	27.0	4.2	<4.9	38.1
8/18/06	44.4	5.6	<4.9	47.8
8/25/06	44.7	20.1	<4.9	38.3
9/1/06	38.1	11.9	<4.9	39.3
9/8/06	72.8	<1.7	<4.9	36.0
9/15/06	36.7	9.9	<4.9	<1.9

The net depositional flux for total particulate matter ranged from 27.0 to 72.8 $mg/m^2/day$ and averaged 42.4 $mg/m^2/day$ for the series of deployment events. The lowest net depositional flux occurred during the week of 8/11/06 and the highest net flux occurred during the week of 9/8/06.

The depositional flux for copper ranged from BDL to 20.1 $\mu g/m^2/day$ and averaged 9.1 $\mu g/m^2/day$ during the deployment event series. The copper depositional flux was BDL during the week of 9/8/06. The highest depositional flux, 20.1 $\mu g/m^2/day$, was detected during the week of 8/25/06.

Lead was not detected at the PRISM2 site during any of the deployment events (Figure 6-45).

The depositional flux for zinc ranged from BDL to 47.8 $\mu g/m^2/day$ and averaged 29.4 $\mu g/m^2/day$ during the deployment event series. Zinc was BDL during the weeks of 7/21/06 and 9/15/06. The highest zinc depositional flux, 47.8 $\mu g/m^2/day$ was observed during the week of 8/18/06 (Figure 6-45).

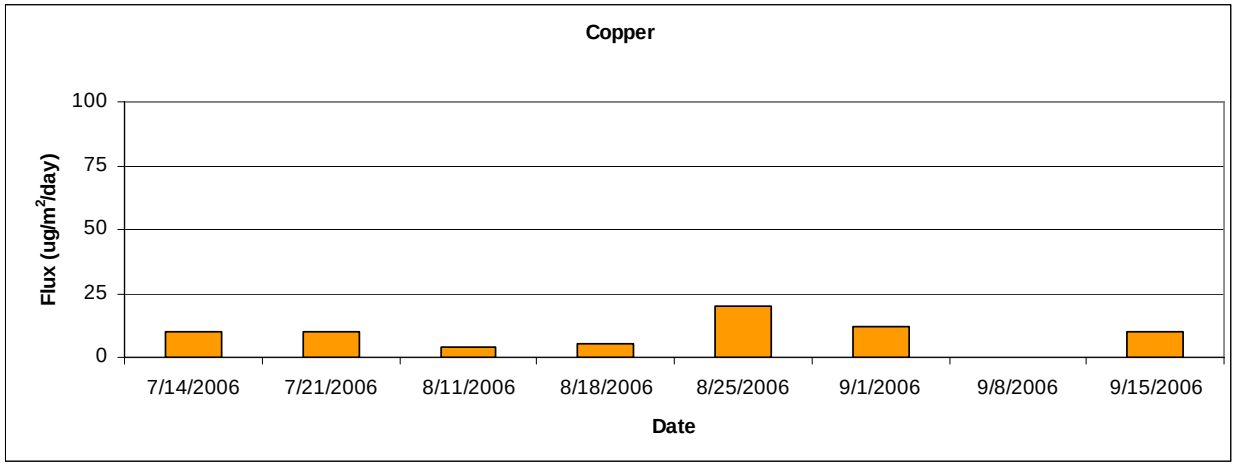

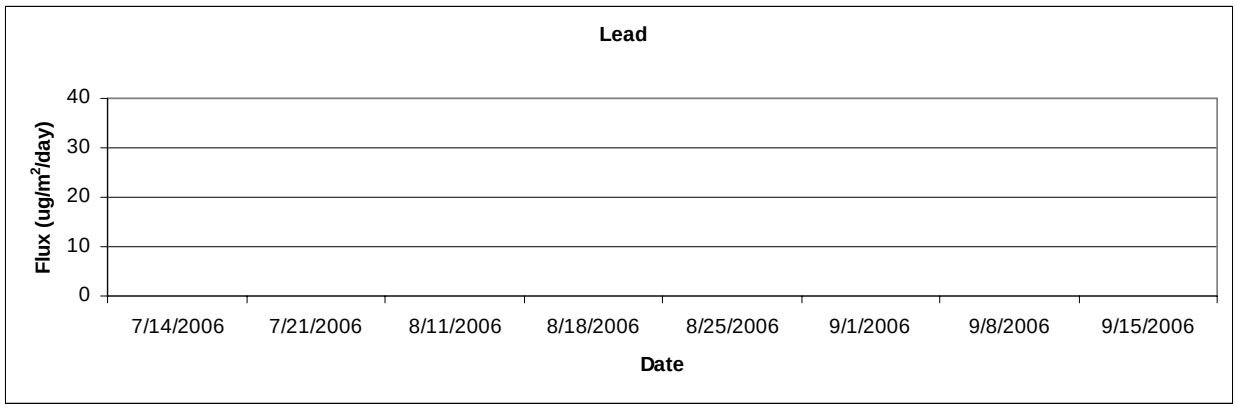

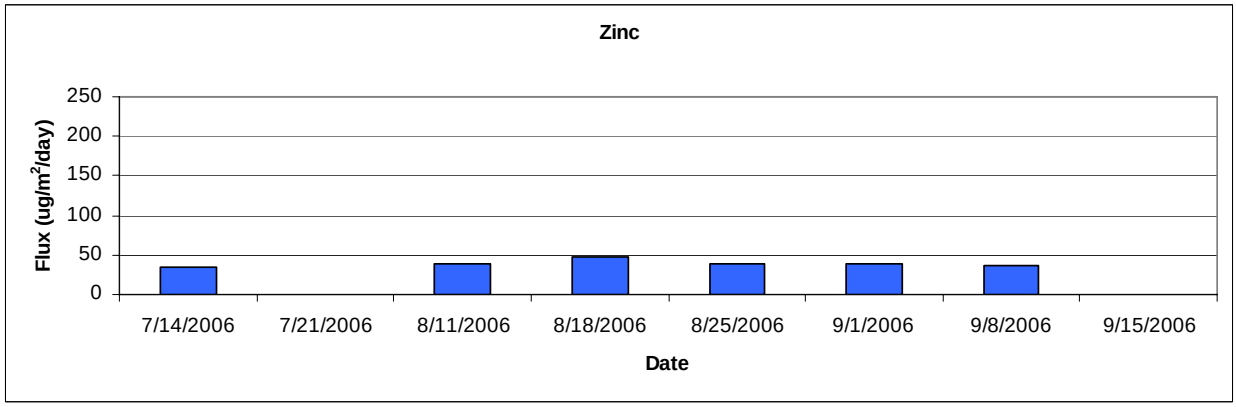

Figure 6-45. Copper, Lead, and Zinc Flux at Site Prism2.

6.2.9.2 Photomicroscopy Results

A representative result for the photomicroscopy analysis performed on surrogate disks deployed at site Prism2 is presented in Figure 6-46. The sample date for the surrogate disk represented in Figure 6-46 is 8/25/06.

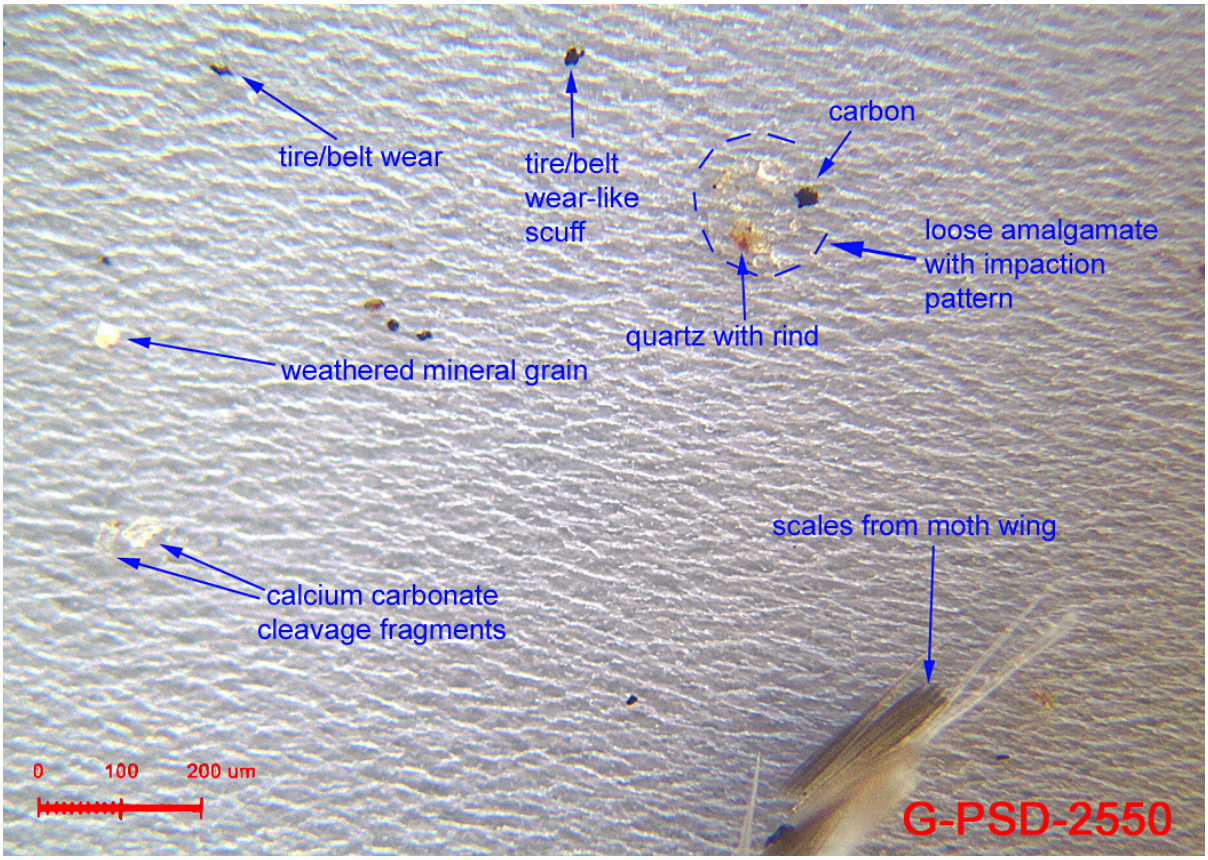

Figure 6-46. Photomicroscopy analysis for site Prism2 on 8/25/06.

Particles often identified in photomicroscopy analysis at this site included weathered mineral grains, tire/belt wear, and calcium carbonate cleavage fragments as well as pigmented polymer, glass fragments, and pollen grains. All photomicroscopy results for samples collected at site Prism2 are presented in Appendix B.

6.2.9.3 Particle Size Distribution

Particle size distributions from surrogate disk samples collected from Site Prism2 were determined for three sample dates. Particulate size distributions for these three dates are shown in Table 6-30. The highest relative percent area varied between each sample date. The highest relative percent area on 7/14/06 was in the 15 – 25 µm size range. The highest relative percent area on 7/21/06 was in the 25 – 50 µm size range. The 8/11/06 sample event had the highest relative percent area in the 5 – 15 µm size range. Particle sizes tended to contain a greater percentage of finer particles with each subsequent sample event. Aerially deposited particle sizes at Site Prism2 would be classified as primarily fine silt and very fine sand with some clay size particles.

Table 6-30. Particle Size Distribution at Site Prism2.

Size Range (µm)	Relative Percent Area		
	7/14/2006	7/21/2006	8/11/2006
0.8-2	0.4	8.6	9.9
2-5	2.3	19.2	22.6
5-15	18.2	17.8	27.2
15-25	28.3	11.7	10.1
25-50	26.5	21.5	20.7
50-100	24.4	21.1	2.7
100-1000	0.0	0.0	6.8
% >15 um	**79.2**	**54.4**	**40.3**
% <15 um	**20.8**	**45.6**	**59.7**

6.2.9.4 SEM-EDX Results

SEM/EDX analysis results of particles from the sample collected at Site Prism2 on 8/25/06 are presented in Figure 6-47. Copper was identified as chips associated with iron from copper plating, or more likely, mechanical abrasion in the 1 – 2 µm size range. Based on this size range, this copper may be associated as brake wear debris. Lead particles were also detected as agglomerated metallic flakes of uncertain origin. The lead was associated with iron and was found in the 5 µm size range. Zinc particles were identified in the 5 µm size range and were associated with iron as galvanized steel. In comparison, the sample results from the XRF analyses showed a flux rate of 20.1 $\mu g/m^2$/day for copper and 38.3 $\mu g/m^2$/day zinc. Lead was not detected in this sample using XRF analysis.

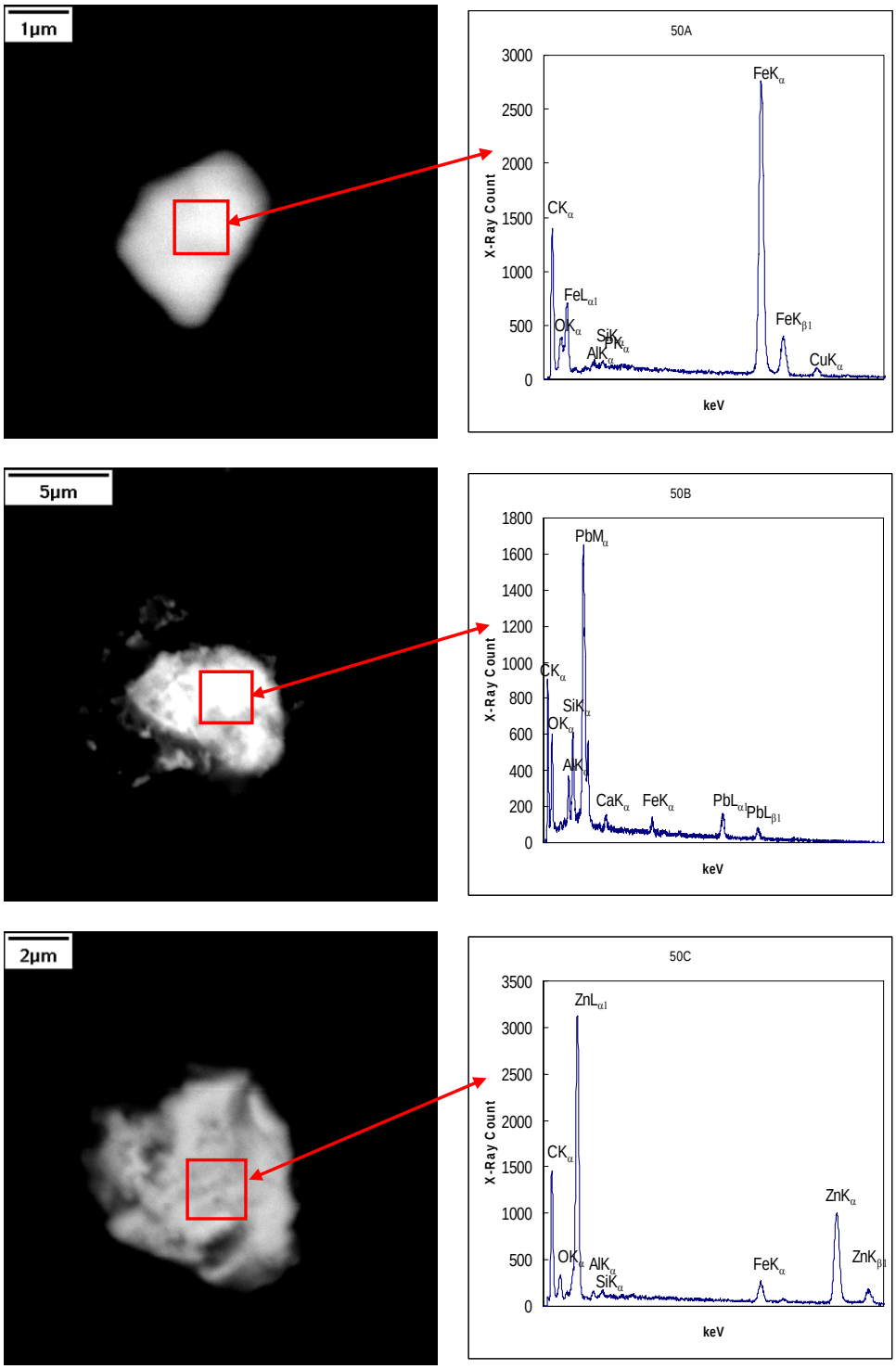

Figure 6-47. SEM/EDX analysis results of particles from the Prism2 site sample collected on 8/25/06

6.2.9.5 Impactor Sampling Results

Air concentrations of Prism2 particulates, characterized by size and by analyte, are shown in Table 6-36. The impactor sample was collected over a 12-hour period on 9/7/06. Across most size classes, iron concentrations were higher than copper, chromium, zinc and lead concentrations by one order of magnitude or greater. Copper and zinc were the second and third most prevalent metal concentrations in Prism2 air samples, respectively, across the four smallest size classes. In the greater than 7.2 µm size class, iron was highest in concentration, followed by zinc and copper, respectively. Lead particulates were not detected in three of the five size classes. In total, the analyzed metals concentrations constituted 1.68 percent of the 45.5 µg/m^3 total particulate concentration across all size classes.

Table 6-31. Distribution of the concentrations of total particulates and five metals according to particle size in ambient air collected at Prism2

Particle Size	Total Particulate Concentration	Chromium	Iron	Copper	Zinc	Lead
(µm)	(µg/m^3)	(ng/m^3)				
< 0.95	15.3	2.490	63.1	19.6	7.66	2.17
0.95 - 1.5	3.31	0.863	45.7	12.5	2.86	<0.82
1.5 - 3.0	5.27	0.892	105	14.8	5.87	<0.82
3.0 - 7.2	11.5	1.11	248	12.5	8.9	0.847
> 7.2	10.1	1.28	195	4.24	7.28	<0.82
Total	45.5	6.64	657	63.6	32.6	4.25*

* One half the detection limit was used for values less than the MDL to calculate total lead.

Atmospheric size distributions for Prism2 are presented in Figure 6-48. Overall, the greatest percentage of particle mass for each analyte, with the exception of iron, was contained within the less than 0.95 µm size class. Greater than 30 percent of all copper, chromium, and total mass particulates and greater than 70 percent of all lead particulates were less than 0.95 µm in size. In contrast, the 0.95 – 1.5 µm size class contained the lowest percentages of iron, zinc, lead, and total particulates (less than 10 percent) of any size class. Nineteen percent of all copper and 13 percent of all chromium detected was contained in particulates ranging from 0.95 to 1.5 µm in size. In 1.5 – 3.0 µm particulates, the percentage of total copper was greater than 20 percent, while zinc, iron, chromium and total mass percentages ranged between 11.6 and 18 percent. Among the coarse particulate sizes, the 3.0 – 7.2 µm size class contained greater than 20 percent of the total zinc, lead, copper, and total mass particulates and more than 30 percent of the total iron particulates, while the greater than 7.2 µm size class contained greater than 20 percent of iron, zinc, and total mass particulates, and slightly less than 20 percent of chromium particulates. Similar to other locations, total copper particulates were lowest in concentration in the largest size class.

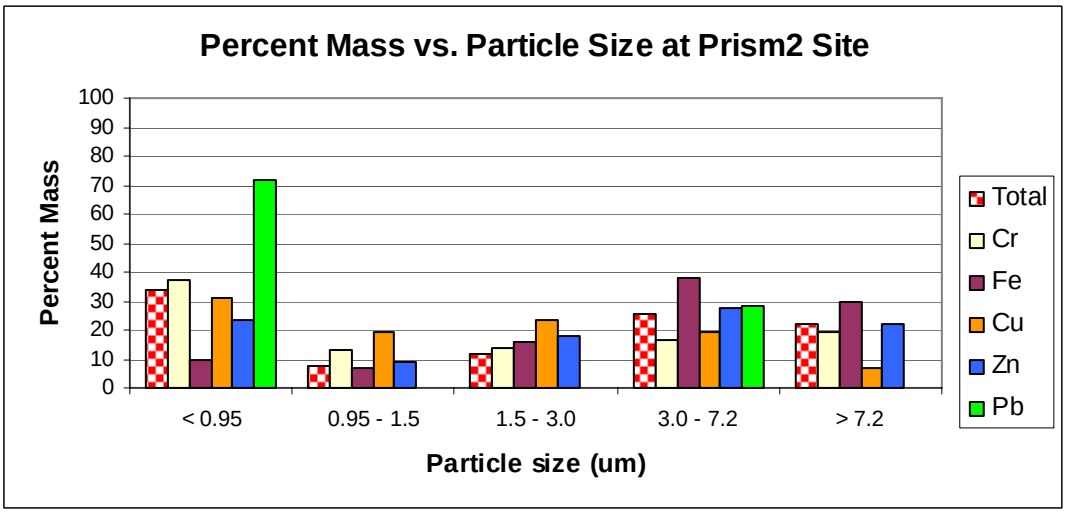

Figure 6-48. Percent mass versus particle size in air samples collected at Prism2

6.2.10 Site DPR(2)

6.2.10.1 XRF Results

Surrogate deposition disks were deployed at site DPR(2) for a total of eight week-long events. The deposition disks were exposed for a duration of three days during each event. Analytical results from the primary surrogate deposition disks at the DPR(2) site are presented in Table 6-32. Replicate disk results are provided in Appendix A.

Table 6-32. Copper, Lead, and Zinc Flux at Site DPR(2)

Date	Net	Copper	Lead	Zinc
	($mg/m^2/day$)	(µg/m2/day)		
7/14/06	63.2	14.1	<4.9	99.9
7/21/06	66.9	11.5	<4.9	32.5
8/11/06	75.6	7.5	<4.9	61.1
8/18/06	42.1	6.7	<4.9	41.6
8/25/06	56.1	12.6	17.3	57.0
9/1/06	59.9	14.4	<4.9	59.4
9/8/06	68.2	<1.7	<4.9	40.5
9/15/06	56.3	11.0	<4.9	32.7

The net depositional flux for total particulate matter ranged from 42.1 to 75.6 $mg/m^2/day$ and averaged 61.0 $mg/m^2/day$ for the series of deployment events. The lowest net flux (42.1 $mg/m^2/day$) occurred during the week of 8/18/06 while the highest net flux (75.6 $mg/m^2/day$) occurred during the week of 8/11/06.

The depositional flux for copper ranged from BDL to 14.4 $\mu g/m^2/day$ and averaged 9.8 $\mu g/m^2/day$ during the deployment event series. The depositional flux was BDL during the week of 9/8/06. The highest depositional flux, 14.4 $\mu g/m^2/day$, was detected during the week of 9/1/06.

Lead was typically not detected at the DPR(2) site except for a single deployment event occurring during the week of 8/25/06 when the depositional flux measured 17.3 $\mu g/m^2/day$ (Figure 6-49).

The depositional flux for zinc ranged from 32.5 to 99.9 $\mu g/m^2/day$ and averaged 53.1 $\mu g/m^2/day$ during the deployment event series. The lowest zinc depositional flux occurred during the week of 7/21/06 while highest zinc flux occurred during the week of 7/14/06 (Figure 6-49).

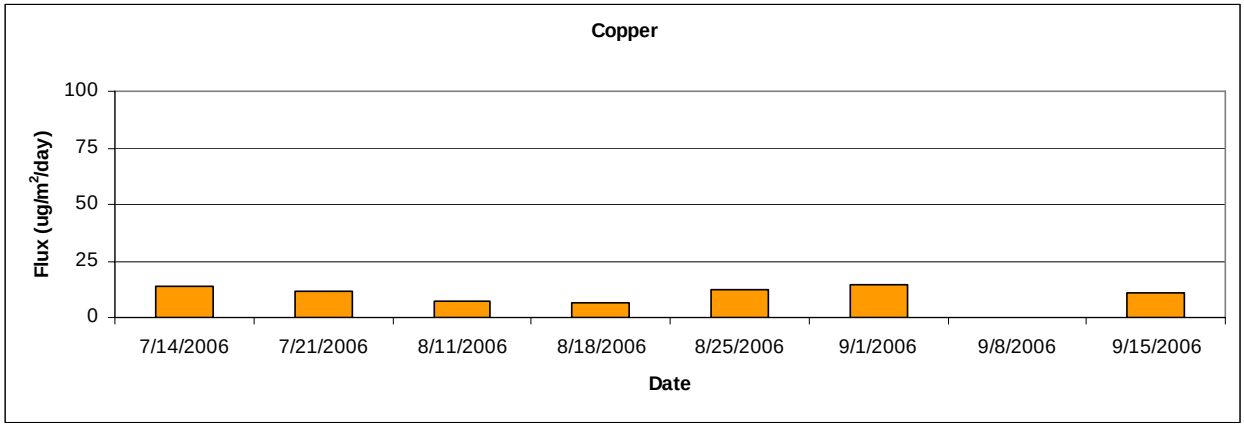

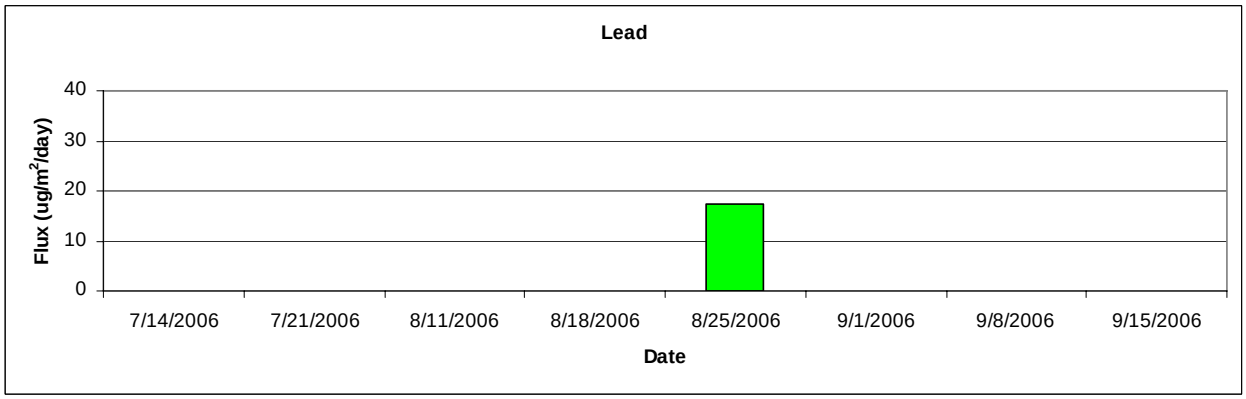

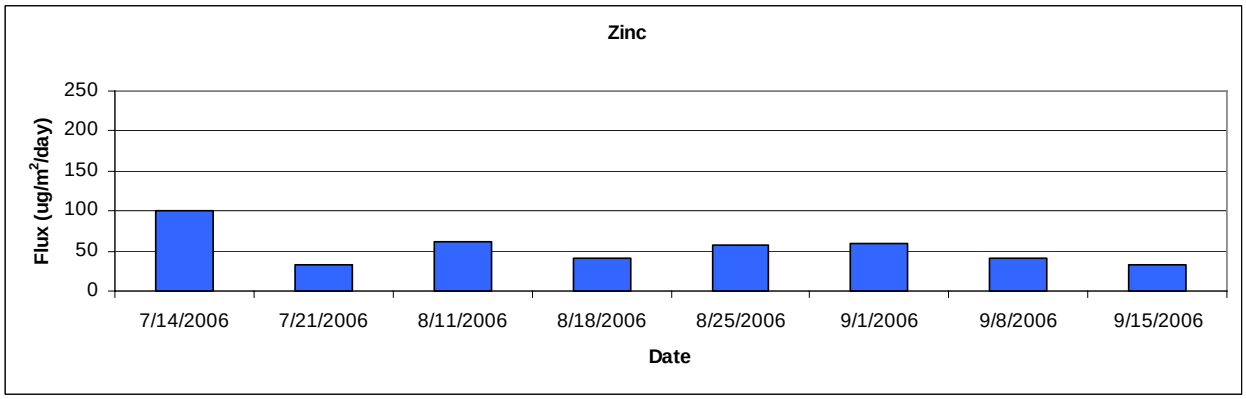

Figure 6-49. Copper, Lead, and Zinc Flux at Site DPR(2).

6.2.10.2 Photomicroscopy Results

A representative result for the photomicroscopy analysis performed on surrogate disks deployed at site DPR(2) is presented in Figure 6-50. The sample date for the surrogate disk represented in Figure 6-50 is 9/1/06.

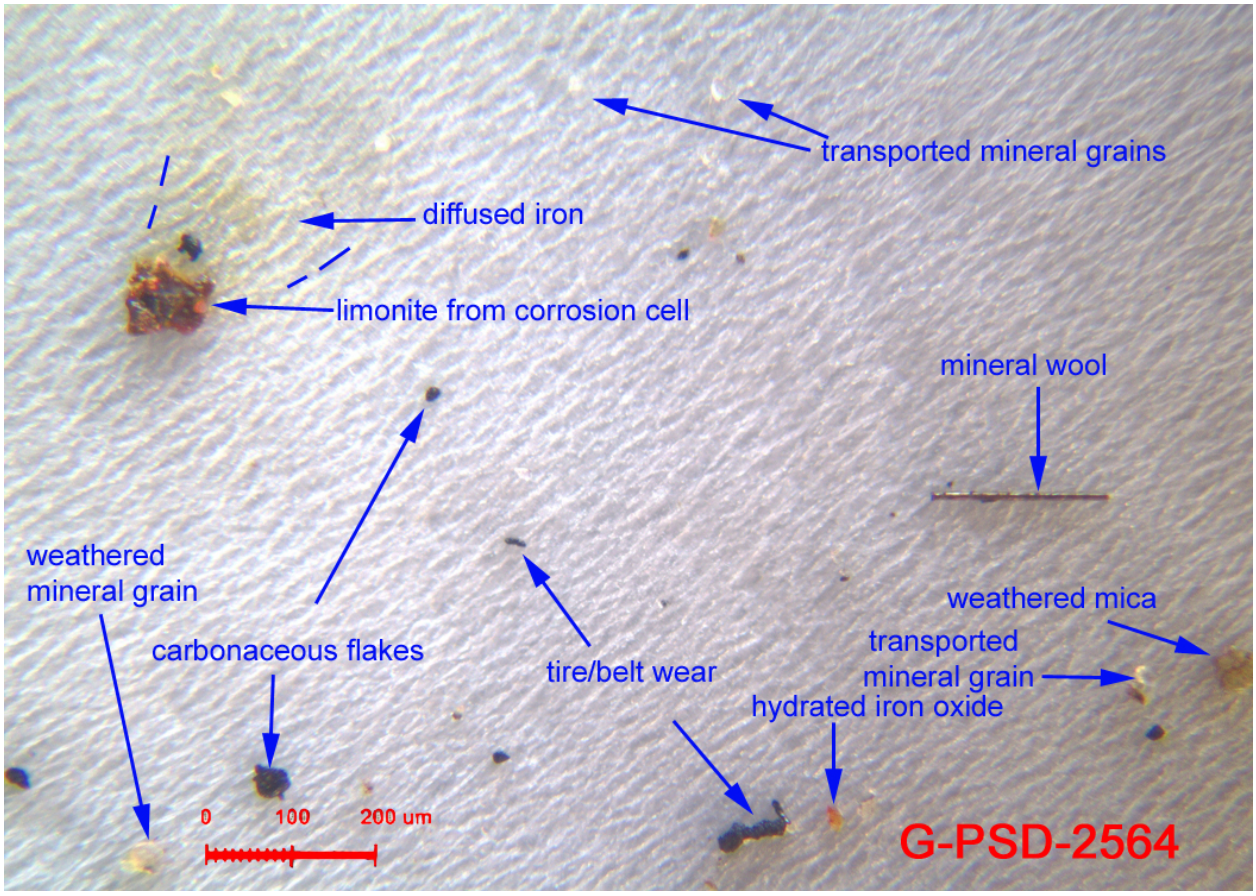

Figure 6-50. Photomicroscopy analysis for site DPR(2) on 9/1/06

Frequently identified particles in photomicroscopy analysis at site DPR(2) included transported mineral grains, tire/belt wear, and limonite from corrosion cell as well as agitation sphere (amalgamate), coating overspray, and cleavage fragments (sulfate). All photomicroscopy results for samples collected at site DPR(2) are presented in Appendix B.

6.2.10.3 Particle Size Distribution

Particle size distributions from surrogate disk samples collected from Site DPR(2) were determined for three sample dates. Particulate size distributions for these three dates are shown in Table 6-33. The highest relative percent area varied between each sample date between the 15-25 µm size range and the 50-100 µm size range during each sample event. All three sample dates at Site DPR2 had a higher percentage of particles in the >15 µm size range. Aerially deposited particle sizes at Site DPR(2) would be classified as primarily coarse silt and very fine sand.

Table 6-33. Particle Size Distribution at Site DPR(2)

Size Range (µm)	Relative Percent Area		
	7/14/2006	7/21/2006	8/11/2006
0.8-2	0.4	3.9	4.8
2-5	1.0	4.8	9.3
5-15	11.9	20.4	10.5
15-25	11.2	27.1	9.7
25-50	31.4	23.9	41.6
50-100	44.0	19.9	24.1
100-1000	0.0	0.0	0.0
% >15 µm	**86.7**	**70.9**	**75.4**
% <15 µm	**13.3**	**29.1**	**24.6**

6.2.10.4 SEM-EDX Results

SEM/EDX analysis results of particles from the sample collected at Site DPR 2 on 9/1/06 are presented in Figure 6-51. Lead particles were detected in the 10-20 µm size range. One particle was of unknown origin and composition while another particle that was identified was associated with tin as abraded solder. Copper and zinc were not detected in the particles analyzed using SEM/EDX. In comparison, the sample results from the XRF analyses showed a flux rate of 14.4 µg/m^2/day for copper and 59.4 µg/m^2/day zinc. Lead was not detected in this sample using XRF analysis.

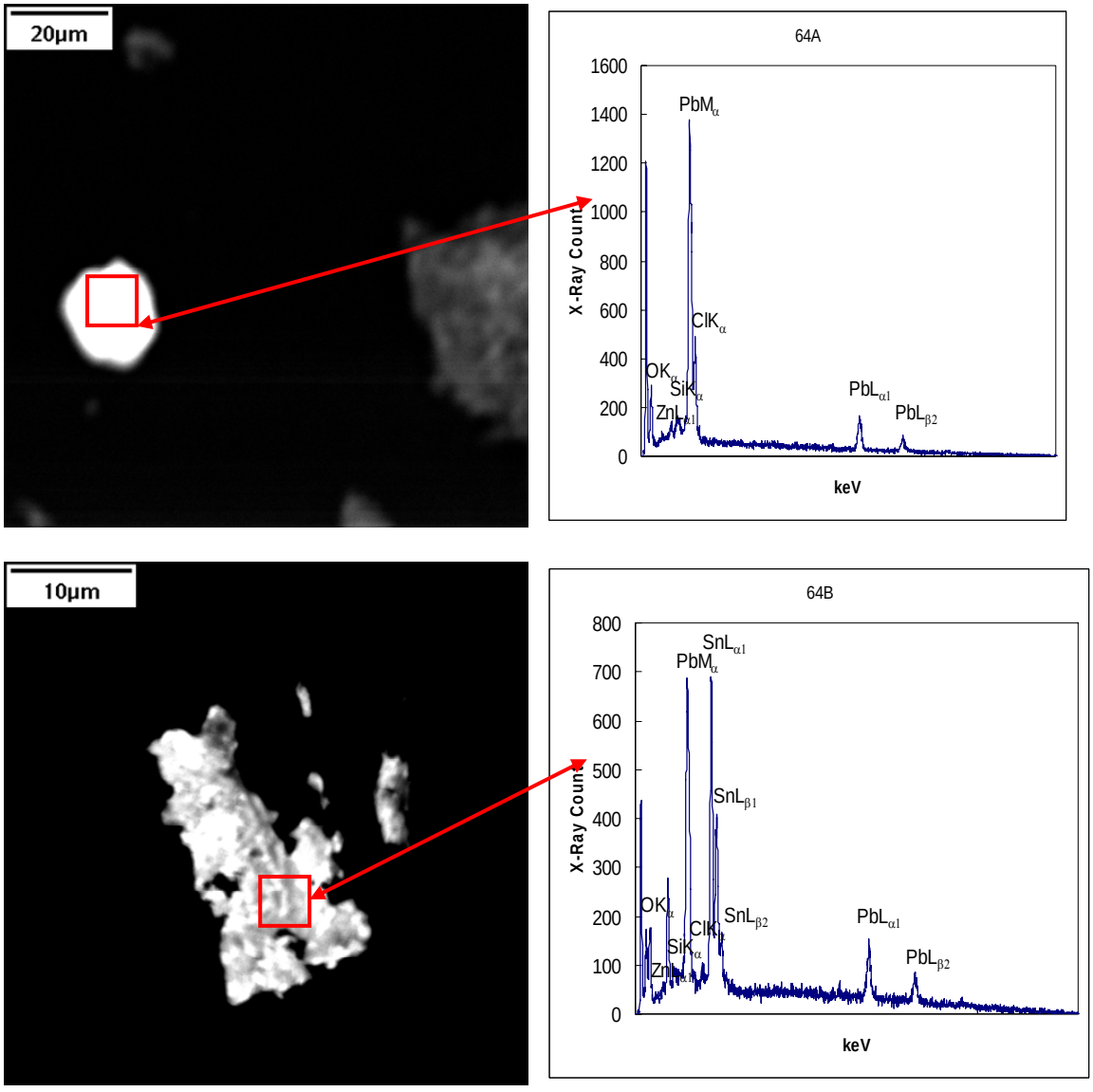

Figure 6-51. SEM/EDX analysis results of particles from the DPR 2 site sample collected on 9/1/06

6.2.10.5 Impactor Results

Air concentrations of DPR(2) particulates, characterized by size and by analyte, are shown in Table 6-34. The impactor sample was collected over a 12-hour period on 9/8/06. Across all size classes, iron concentrations were higher than copper, chromium, zinc and lead concentrations by one order of magnitude or greater. Zinc and copper were the second and third most prevalent metals in DPR(2) air samples, respectively, across all size classes. No lead was detected in particulates ranging in size from 0.95 µm to 1.5 µm. In total, the analyzed metals concentrations constituted 2.19 percent of the 77.1 µg/m^3 total particulate concentration.

Table 6-34. Distribution of the concentrations of total particulates and five metals according to particle size in ambient air collected at DPR(2)

Particle Size	Total Particulate Concentration	Chromium	Iron	Copper	Zinc	Lead
(µm)	(µg/m^3)	(ng/m^3)				
< 0.95	32.4	2.56	333	14.5	30.5	2.66
0.95 - 1.5	5.27	0.942	122	8.52	7.24	<0.82
1.5 - 3.0	8.33	1.04	215	7.51	9.50	1.08
3.0 - 7.2	16.5	1.42	480	11.4	18.6	1.17
> 7.2	14.6	1.39	393	5.01	20.0	1.36
Total	77.1	7.35	1543	46.9	85.8	6.68*

* One half the detection limit was used for values less than the MDL to calculate total lead.

Atmospheric size distributions for DPR(2) are presented in Figure 6-52. Overall, the greatest percentage of particle mass for each analyte, with the exception of iron, was contained within the less than 0.95 µm size class. Greater than 40 percent of all lead and total mass particulates and greater than 30 percent of all chromium, copper and zinc particulates were less than 0.95 µm in size. In contrast, the 0.95 – 1.5 µm size class contained the lowest percentages of iron, zinc, lead, and total mass (less than 10 percent) of any size class. Eighteen percent of copper and 13 percent of chromium was also contained in particulates within 0.95 – 1.5 µm size class. Analysis of 1.5 – 3.0 µm particulates yielded slight increases, with the exception of copper, in all analytes over levels detected in the 0.95 – 1.5 µm particulates. In the coarse particle size classes, the 3.0 – 7.2 µm particles contained greater than 20 percent of zinc, copper, and total mass, and more than 30 percent of the total iron while the greater than 7.2 µm particles contained greater than 20 percent of the iron, lead, and zinc particulates, and slightly less than 20 percent of the chromium and total mass particulates. While 24.3 percent of copper particulates were between 3.0 µm and 7.2 µm in size, only 10.7 percent were greater than 7.2 µm in size.

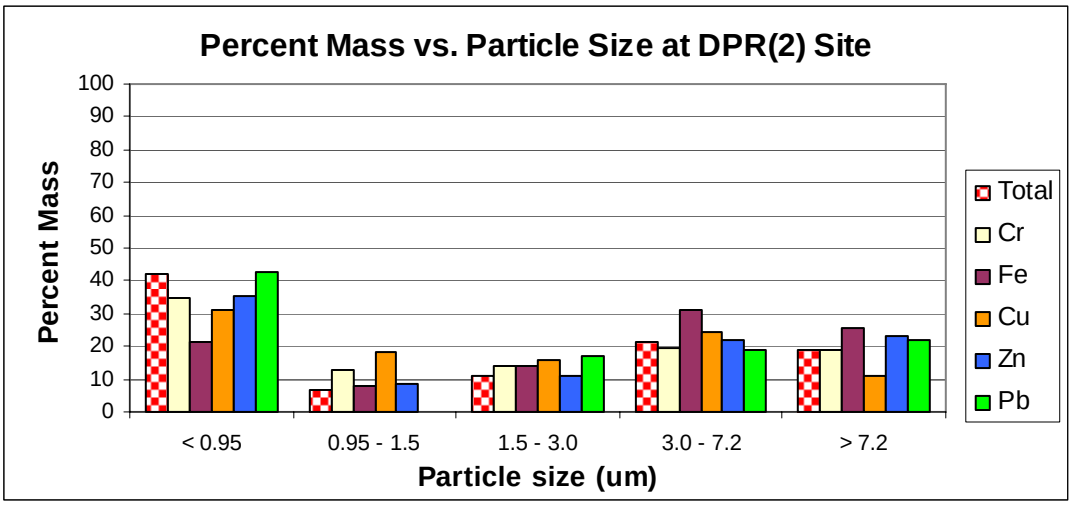

Figure 6-52. Percent mass versus particle size in air samples collected at DPR(2)

6.2.11 Chollas Mouth

6.2.11.1 XRF Results

Surrogate deposition disks were deployed at site Chollas Mouth for a total of ten week-long events. The deposition disks were exposed for a duration of three days during each event. Analytical results from the surrogate deposition disks at the Chollas Mouth site are presented in Table 6-35.

Table 6-35. Copper, Lead, and Zinc Flux at Site Chollas Mouth

Date	Net	Copper	Lead	Zinc
	($mg/m^2/day$)	(µg/m2/day)		
6/29/06	72.8	67.7	12.0	63.3
7/13/06	59.9	18.1	<4.9	94.4
8/18/06	30.8	9.2	<4.9	36.0
8/25/06	44.1	11.1	<4.9	81.6
9/1/06	21.7	16.8	<4.9	21.3
9/8/06	44.9	<1.7	<4.9	15.1
9/15/06	20.7	<1.7	<4.9	16.9
9/22/06	84.1	18.3	<4.9	184
9/29/06	72.8	45.9	<4.9	180
10/6/06	37.1	35.1	<4.9	87.5

The net depositional flux for total particulate matter ranged from 20.7 to 84.1 $mg/m^2/day$ and averaged 48.9 $mg/m^2/day$ for the series of deployment events. The lowest net depositional flux occurred during the week of 9/15/06 and the highest net depositional flux occurred during the week of 9/22/06.

The depositional flux for copper ranged from BDL to 67.7 $\mu g/m^2/day$ and averaged 22.4 $\mu g/m^2/day$ during the deployment event series. Copper was BDL on the weeks of 9/8/06 and 9/15/06 while the highest depositional flux for copper, 67.7 $\mu g/m^2/day$, was detected during the week of 6/29/06.

Lead was typically not detected at the Chollas Mouth site except for a single deployment event occurring during the week of 6/29/06 when the depositional flux measured 12.0 $\mu g/m^2/day$ (Figure 6-53).

The depositional flux for zinc ranged from 15.1 to 184 $\mu g/m^2/day$ and averaged 78.0 $\mu g/m^2/day$ during the deployment event series. The highest zinc depositional fluxes tended to occur during the late part of September with fluxes of 184 and 180 $\mu g/m^2/day$ observed during the weeks of 9/22/09 and 9/29/06, respectively. The lowest depositional flux of 15.1 $\mu g/m^2/day$ occurred during the week of 9/8/06 (Figure 6-53).

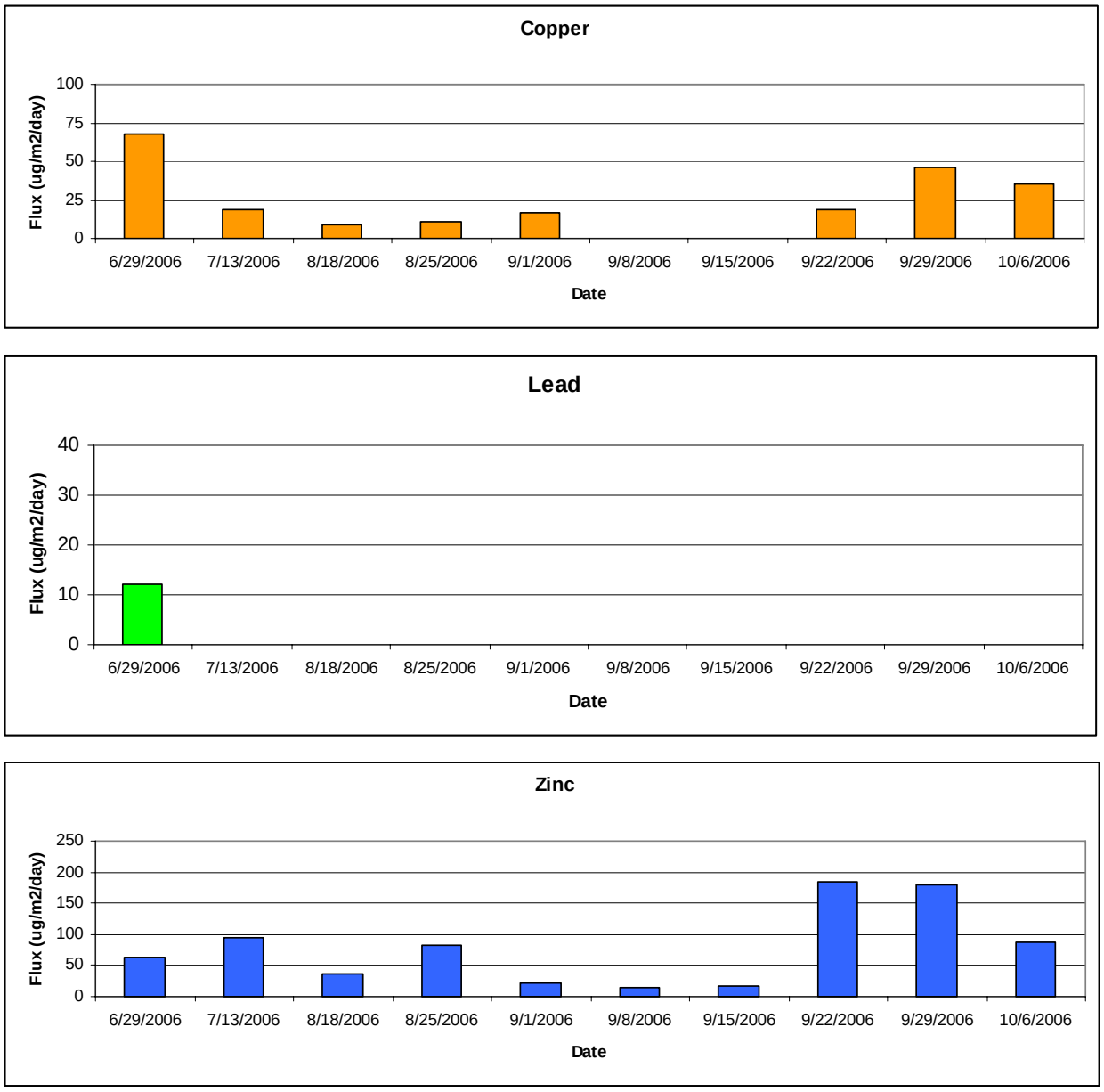

Figure 6-53. Copper, Lead, and Zinc Flux at Site Chollas Mouth

6.2.11.2 Photomicroscopy Results

A representative result for the photomicroscopy analysis performed on surrogate disks deployed at site Chollas Mouth is presented in Figure 6-54. The sample date for the surrogate disk represented in Figure 6-54 is 9/29/06.

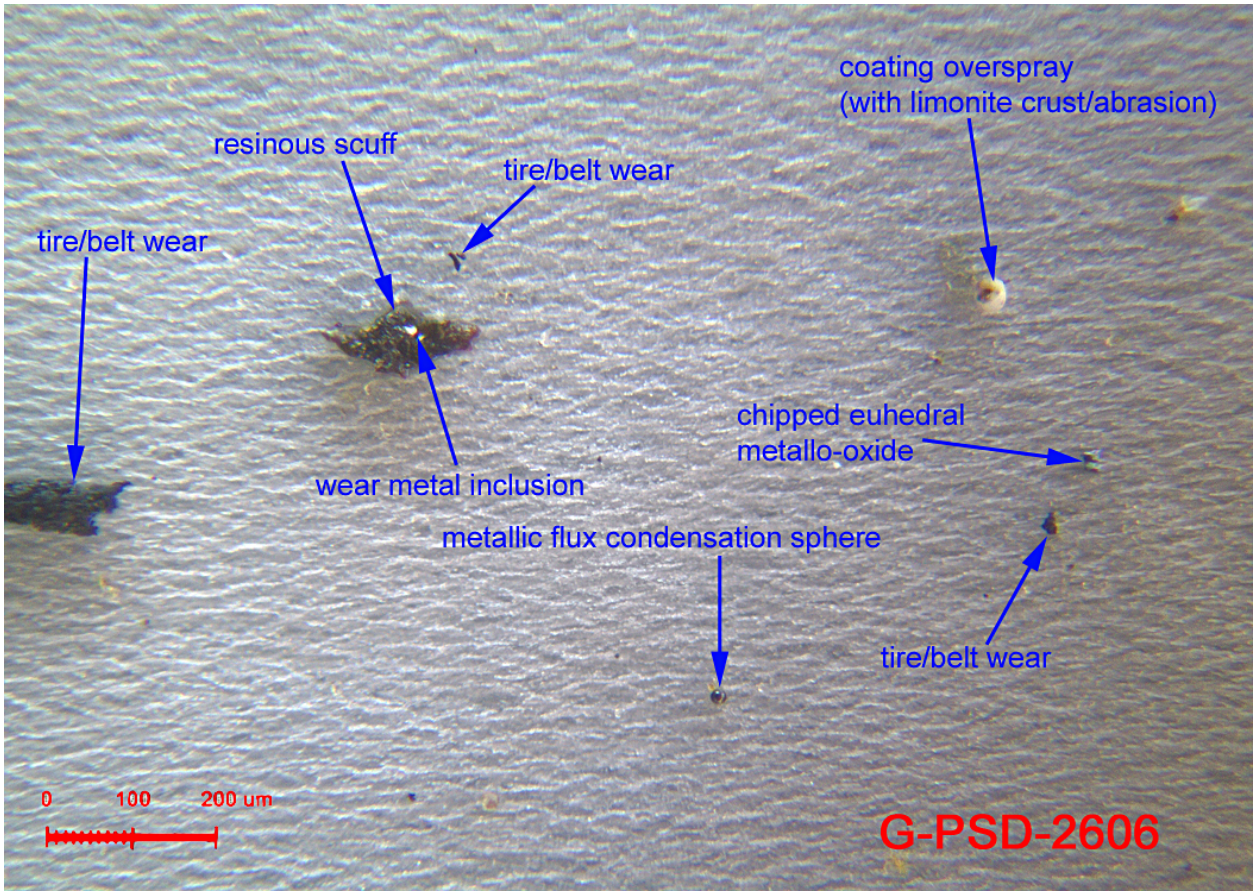

Figure 6-54. Photomicroscopy analysis for site Chollas Mouth on 9/29/06

Frequently identified particles in photomicroscopy analysis at Chollas Mouth included coating overspray, tire/belt wear, and metallic flux condensation sphere as well as spattered metal, iron oxide/hydroxide, and wear metal with limonite blisters. All photomicroscopy results for samples collected at Chollas Mouth are presented in Appendix B.

6.2.11.3 SEM-EDX Results

SEM/EDX analysis results of particles from the sample collected at the Chollas Mouth Site on 9/29/06 are presented in Figure 6-55. Copper particles were detected in the 10-20 µm size range associated with oxygen and iron. Lead and zinc were not identified in particles using SEM/EDX. In comparison, the sample results from the XRF analyses showed flux rates of 36.0 µg/m^2/day for copper and 240 µg/m^2/day for zinc. Lead was not detected in this sample using XRF analysis.

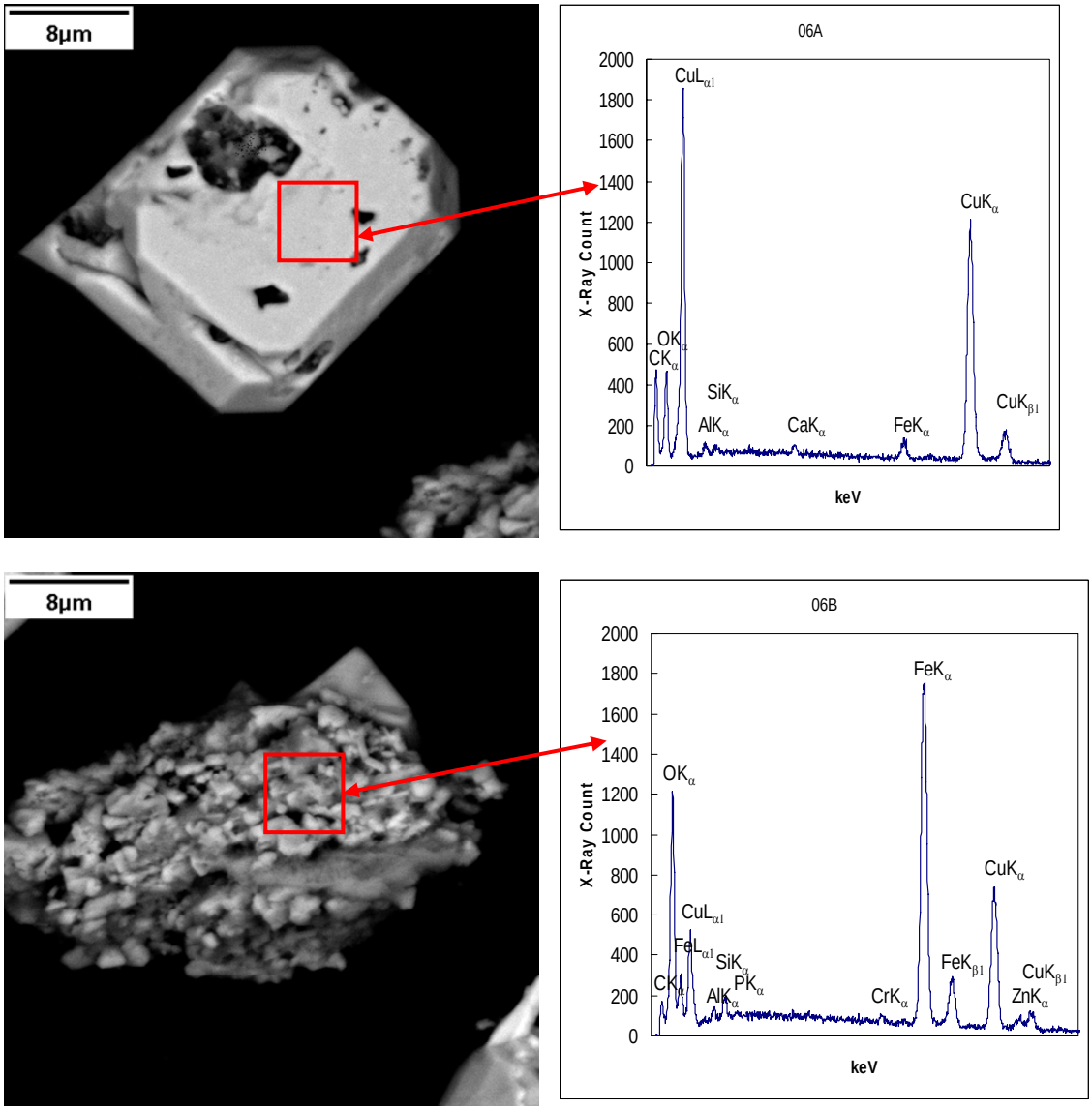

Figure 6-55. SEM/EDX analysis results of particles from the Chollas Mouth site sample collected on 9/29/06

6.2.11.4 Impactor Results

Air concentrations of Chollas Mouth particulates, characterized by size and by analyte, are shown in Table 6-36. The impactor sample was collected over a 12-hour period on 10/30/06. In Chollas Mouth air samples, iron concentrations were higher than copper, chromium, zinc and lead concentrations by more than one order of magnitude. Zinc was second highest in concentration, followed by copper, lead and chromium, respectively. Total particulates across all size classes were measured at 51.0 µg/m^3. Overall, the analyzed metals constituted 2.74 percent of total particulates.

Table 6-36. Distribution of the concentrations of total particulates and five metals according to particle size in ambient air collected at Chollas Mouth

Particle Size	Total Particulates	Chromium	Iron	Copper	Zinc	Lead
(µm)	($\mu g/m^3$)	(ng/m^3)				
< 0.95	17.8	2.46	148	15.1	22.9	10.2
0.95 - 1.5	3.55	1.14	134	10.2	7.61	3.40
1.5 - 3.0	5.27	1.31	238	10.4	8.55	3.69
3.0 - 7.2	15.1	1.63	482	12.5	14.7	6.96
> 7.2	9.31	1.30	239	5.21	12.3	3.20
Total	51.0	7.84	1241	53.4	66.1	27.5

Atmospheric size distributions for Chollas Mouth are presented in Figure 6-56. Overall, the greatest percentage of particle mass for each analyte, with the exception of iron, was contained within the less than 0.95 µm size class. Greater than 30 percent of all lead, zinc, chromium, and total mass particulates and nearly 30 percent of all copper particulates were less than 0.95 µm in size. The 0.95 – 1.5 µm size class contained low percentages of chromium, iron, zinc, lead, and total particulates (less than 15 percent). Copper had the highest percentage of 0.95 – 1.5 µm particulates (19 percent). Analysis of 1.5 – 3.0 µm particulates yielded similar results to those found within the 0.95 – 1.5 µm size class, with the exception of a significant increase in the percent mass of iron. The percentage of iron particulates increased 8.4 percent from the 0.95 – 1.5 µm size range to the 1.5 – 3.0 µm size range, while all other metals and total mass remained nearly the same. In the coarse particle size classes, the 3.0 – 7.2µm size class contained greater than 20 percent of each metal analyte and 30 percent of the total mass while the greater than 7.2 µm size class contained slightly less than 20 percent of iron, zinc, chromium, and total mass, and 9.8 percent copper and 11.6 percent lead.

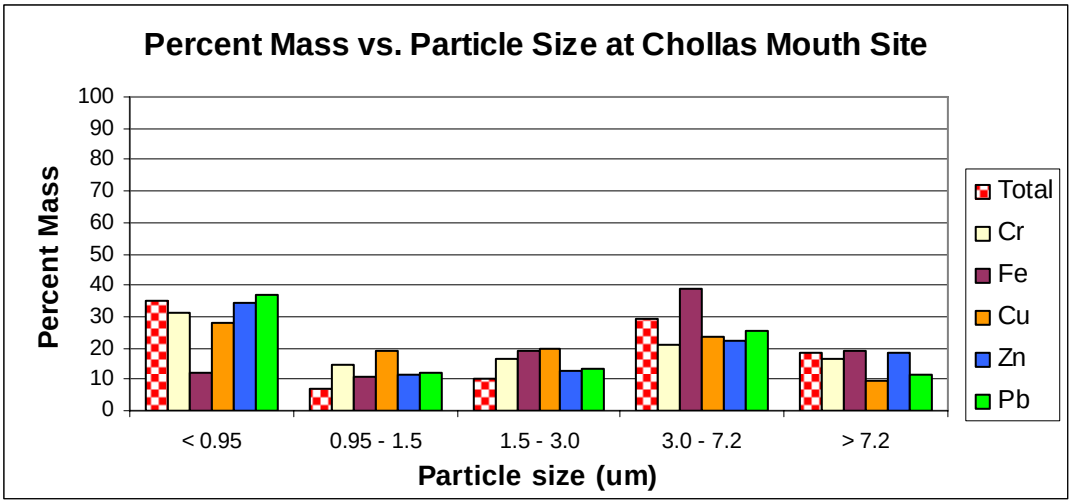

Figure 6-56. Percent mass versus particle size in air samples collected at Chollas Mouth

6.3 Transect Study Results

Results for the 805 Transect study are presented in this section. Results are presented by site, beginning with the Transect reference site (805T-Up) and then arranged in order from site closest to the freeway (805T1) to furthest (805T4). Results are presented for each site by the following analyses:

- XRF Results
- Photomicroscopy results
- Particle size distribution on deposition disks
- SEM-EDX particle analysis on the surrogate deposition disks
- Impactor sampling results (elemental concentrations by particle size in air)

Within each site, discussion of results for the XRF analysis occurs in groups; total net flux for total particulate matter, depositional flux for copper, lead, and zinc. Analytes that were not detected or were detected at concentrations less than three times the detection limit for XRF analysis are presented as Below Detection Limit (BDL) and are shown in tables as a "<" value for the analyte-specific instrument detection limit. Site-specific depositional flux average values are calculated using a value equal to one-half the detection limit for results that were BDL. Surrogate depositional plates were not analyzed at the 805T-Up site on the weeks of 9/29/06 and 10/13/06 and at sites 805T3 and 805T4 on the week of 9/1/06 due to fouling in the field. Results for sites 805T-Up and 805T1 are presented in the Area Wide study (Section 6.2) but are repeated here for reference.

Figure 6-57 presents profiles along the transect by date for the net particulate, copper, lead, and zinc fluxes for the 805 Transect sites.

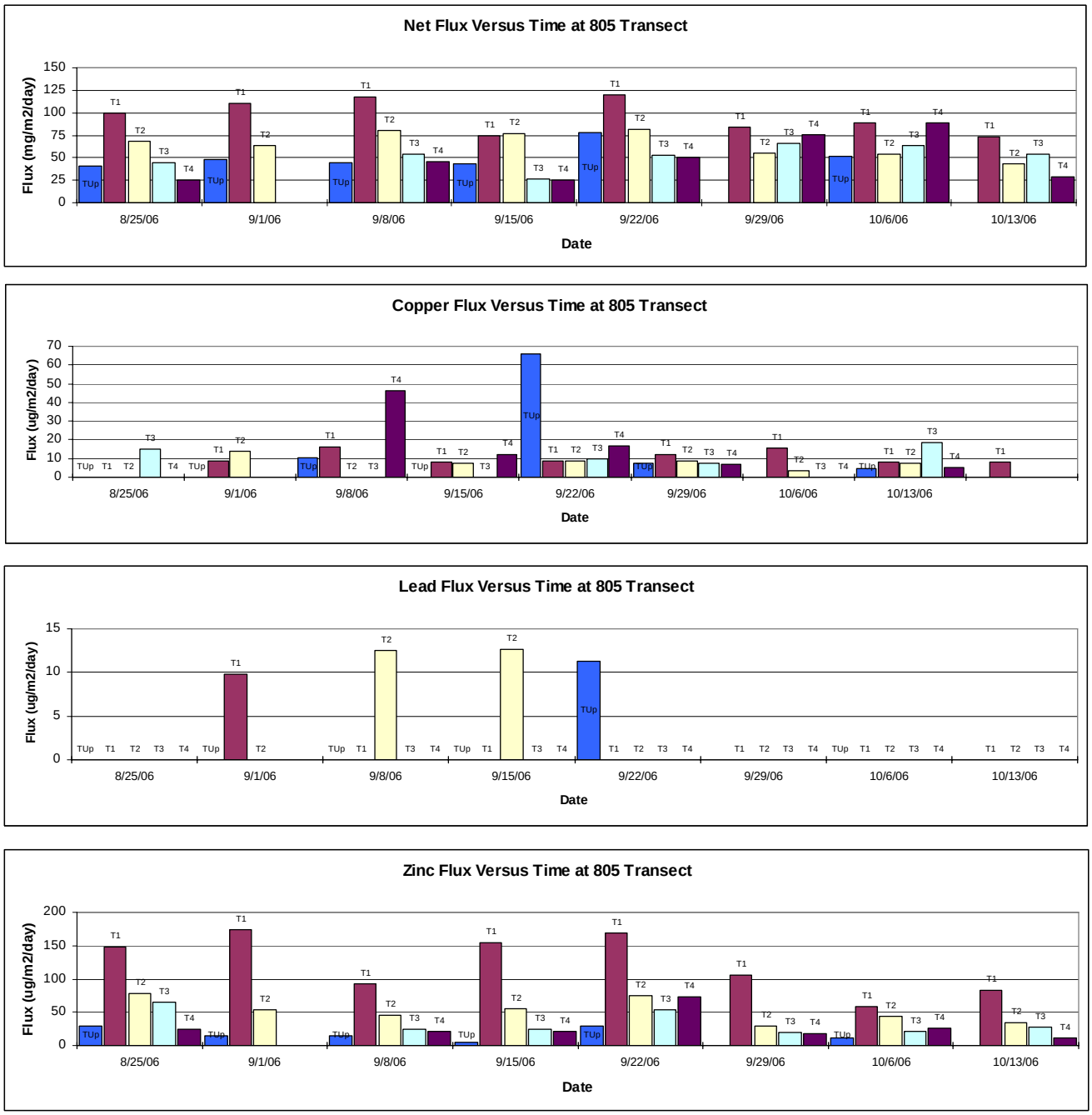

Figure 6-57. Net Particulate, Copper, Lead, and Zinc Flux for the 805 Transect sites

6.3.1 Site 805T-Up

6.3.1.1 XRF Results

Surrogate deposition disks were deployed at 850T-Up for a total of eight week-long events. The deposition disks were exposed for a duration of three days during each event. During two of the deployment events, disks were damaged or contaminated by bird droppings in the field which resulted in those disks being withheld from laboratory analysis. Analytical results from the primary surrogate deposition disks at the 805T-Up site are presented in Table 6-37. Results of replicate disk analyses are presented in Appendix A.

Table 6-37. Copper, Lead, and Zinc Flux at Site 805T-Up.

Date	Net	Copper	Lead	Zinc
	(mg/m^2/day)	(µg/m^2/day)		
8/25/06	40.7	<1.7	<4.9	28.5
9/1/06	48.3	10.2	<4.9	15.2
9/8/06	44.0	<1.7	<4.9	15.3
9/15/06	43.6	66.1	<4.9	5.1
9/22/06	78.5	7.8	11.3	29.6
10/6/06	51.6	4.9	<4.9	12.1

The net depositional flux for total particulate matter ranged from 40.7 to 78.5 mg/m^2/day and averaged 44.1 mg/m^2/day for the series of deployment events. The lowest depositional flux was observed during the week of 8/25/06 while the highest net depositional flux occurred during the week of 9/22/06.

The depositional flux for copper ranged from BDL to 66.1 µg/m^2/day and averaged 15.1 µg/m^2/day during the deployment event series. The depositional flux for copper was BDL during the weeks of 8/25/06 and 9/8/06 while the highest depositional flux, 66.1 µg/m^2/day, was detected during the week of 9/15/06.

Lead was typically not detected at the 805T-Up site except for a single deployment event occurring during the week of 9/22/06 when the depositional flux measured 11.3 µg/m^2/day (Figure 6-57).

The depositional flux for zinc ranged from 5.1 to 29.6 µg/m^2/day and averaged 17.6 µg/m^2/day during the deployment event series. The lowest zinc depositional flux occurred during the week of 9/15/06. The highest zinc flux occurred during the week of 9/22/06 (Figure 6-57).

6.3.1.2 Photomicroscopy Results

A representative result for the photomicroscopy analysis performed on surrogate disks deployed at site 805T-Up is presented in Figure 6-58 and Figure 6-59. The sample date for the surrogate disk represented in Figure 6-58 is 9/15/06 and the surrogate disk represented in Figure 6-59 is 9/22/06.

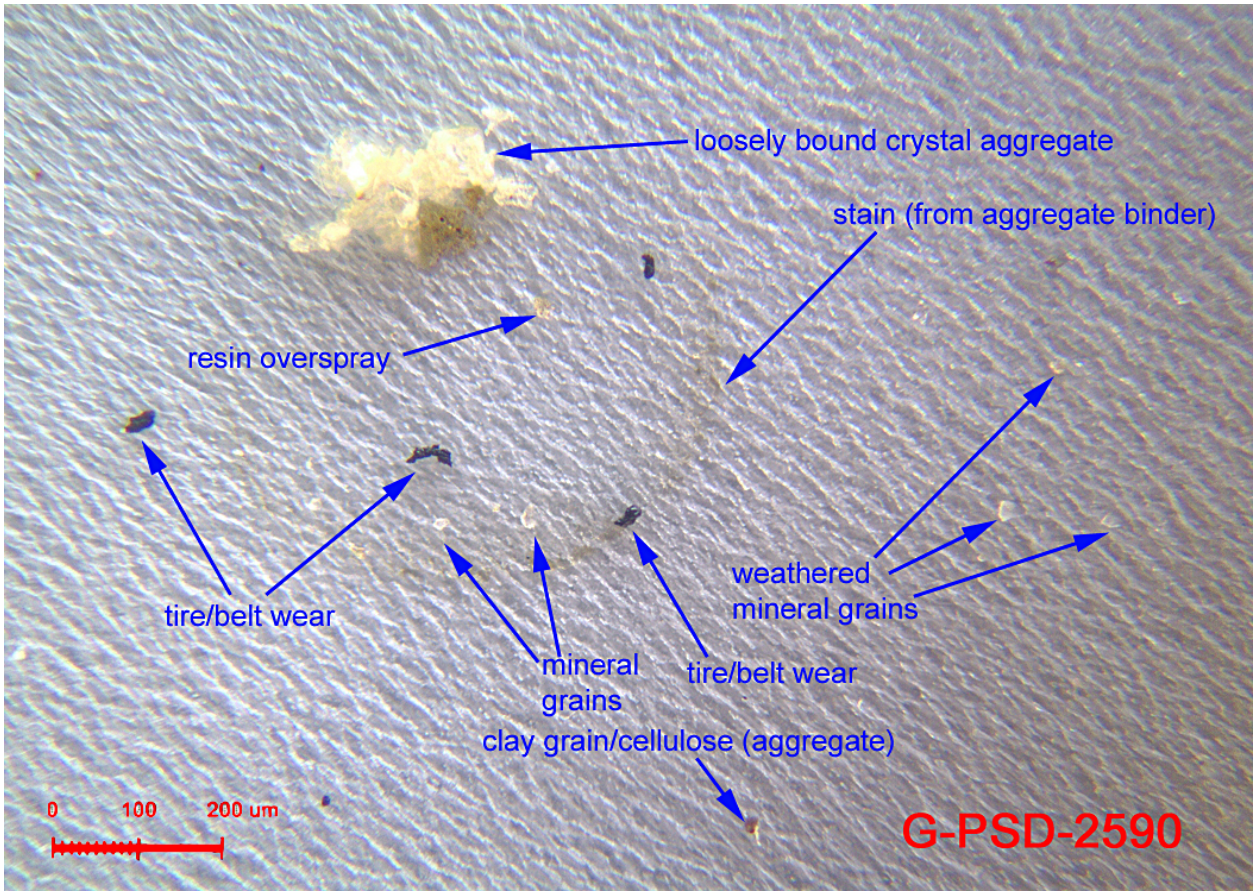

Figure 6-58. Photomicroscopy analysis for site 805T-Up on 9/15/06

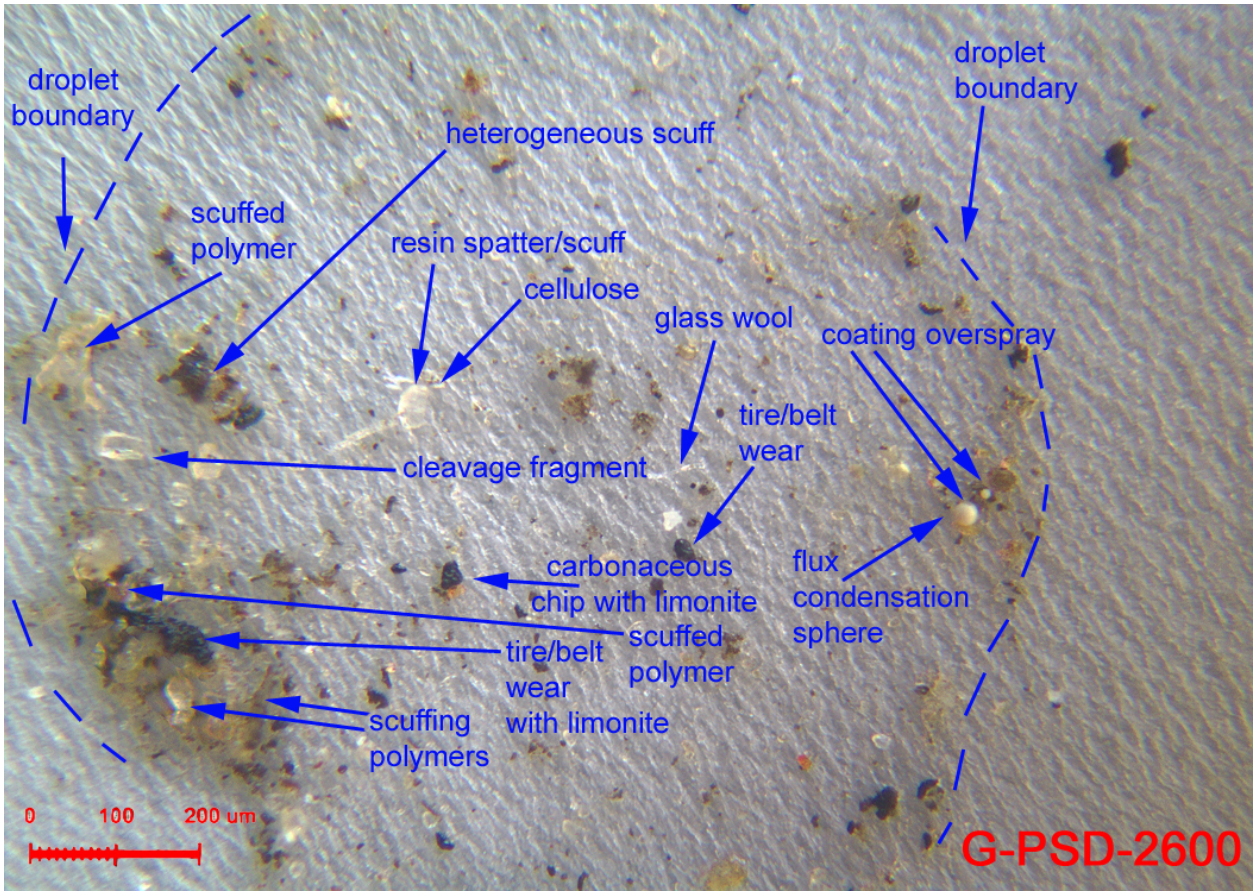

Figure 6-59. Photomicroscopy analysis for site 805T-Up on 9/22/06

Frequently identified particles in photomicroscopy analysis at 805T-Up included mineral grains, tire/belt wear, and clay grain/cellulose (aggregate) as well as flux condensation sphere, scuffed polymer, and pollen. All photomicroscopy results for samples collected at site 805T-Up are presented in Appendix B.

6.3.1.3 SEM-EDX Results

SEM/EDX analysis results of particles from the sample collected at Site 805TU on 9/15/06 are presented in Figure 6-60 and Figure 6-61. Copper particles were detected as steel scuffing fatigue particles in the 10-40 µm size range (Figure 6-60). Particles in Figure 6-61 are observed in the 10 – 20 µm size range as elemental copper associated with iron. These particles also showed chemical wear as opposed to mechanical wear. Lead and zinc particles were not identified using SME/EDX. In comparison, the sample results from the XRF analyses showed a flux rate of 66.1 µg/m^2/day for copper and 5.1 µg/m^2/day for zinc. Lead was not detected in this sample using XRF analysis.

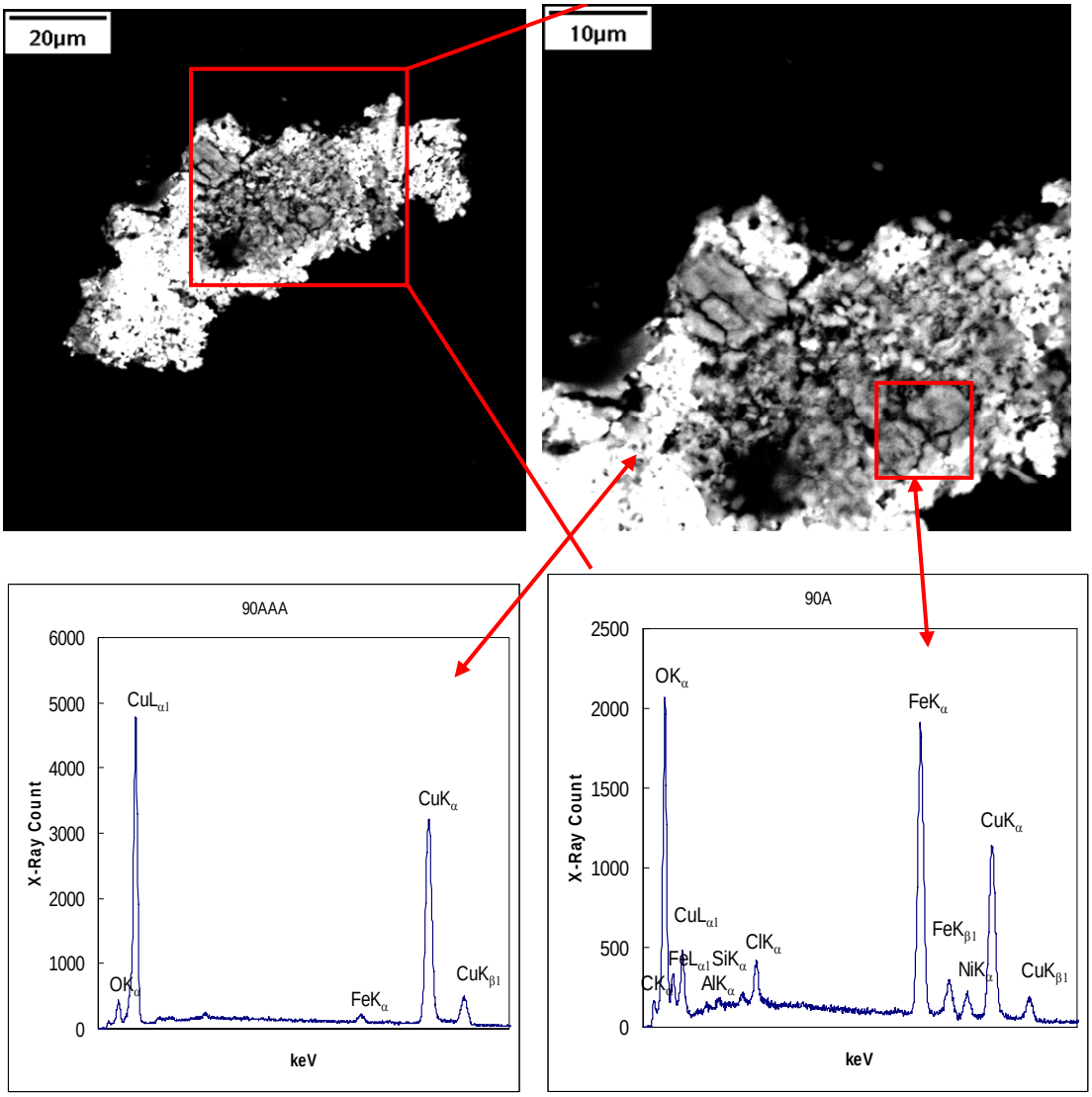

Figure 6-60. SEM/EDX analysis results of particles from the 805TU site sample collected on 9/15/06

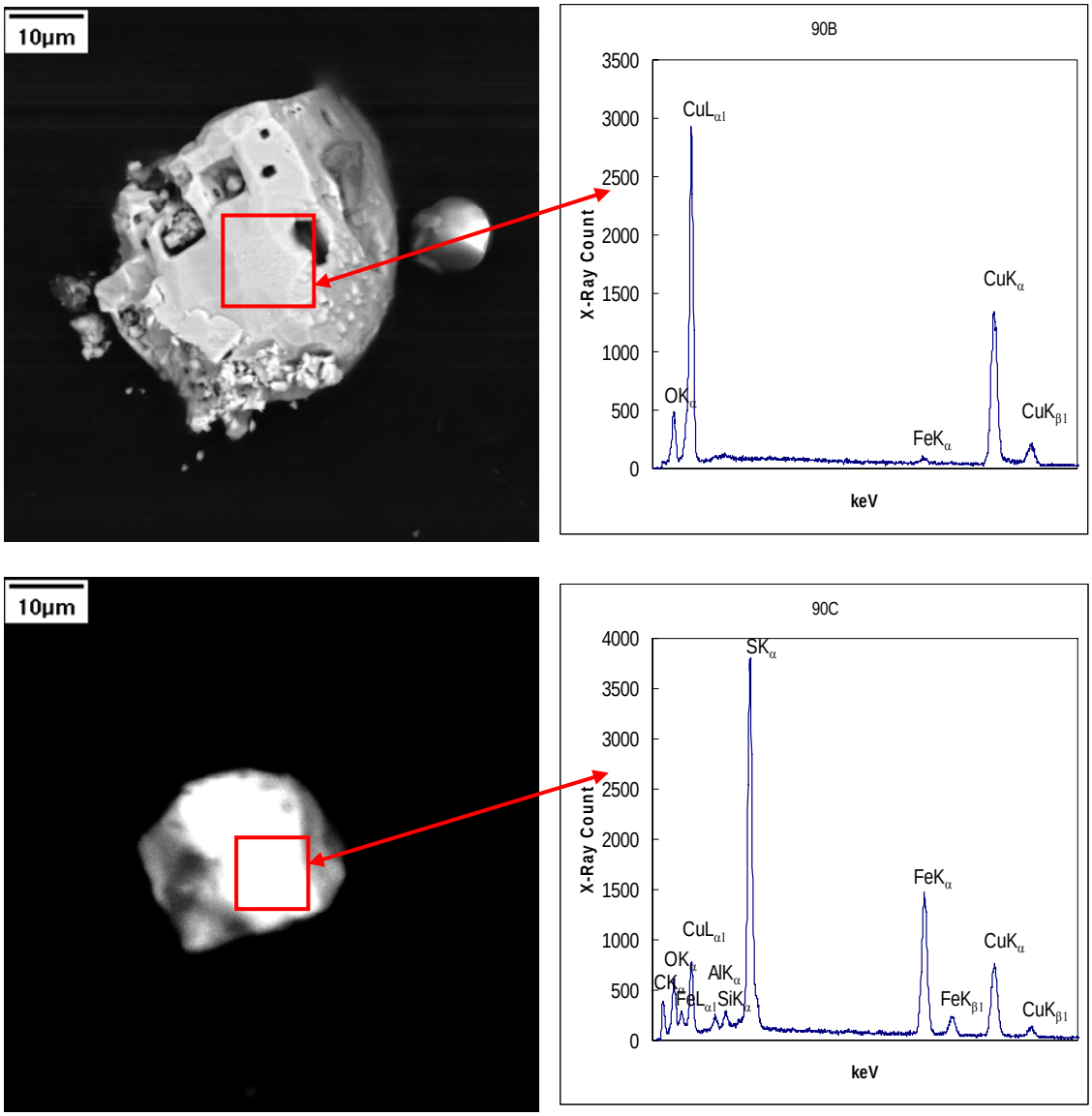

Figure 6-61. SEM/EDX analysis results of particles from the 805TU site sample collected on 9/15/06

An additional sample from site 805TU (collected 9/22/06) was submitted for SEM/EDX analysis and are presented in Figure 6-62. Copper particles were again found in the 10-20 µm size range associated with iron and sulfur, possibly representing the mineral chalcopyrite ($CuFeS_2$). Copper was also detected in association with titanium and several other elements. Lead and zinc particles were not identified using SEM/EDX in this sample. In comparison, the sample results from the XRF analyses showed a flux rate of 7.8 µg/m^2/day for copper, 11.3 µg/m^2/day for lead, and 29.6 µg/m^2/day for zinc.

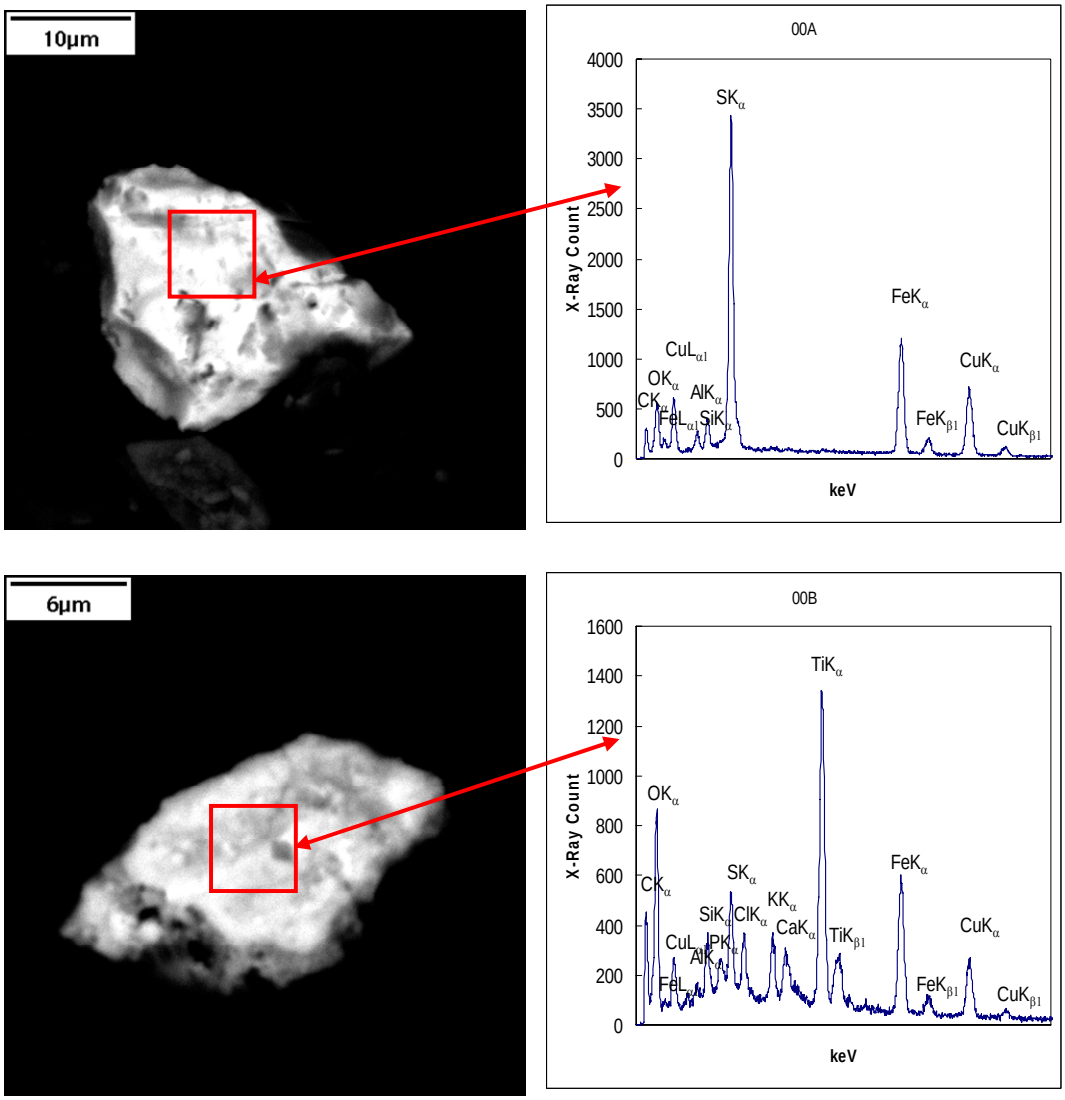

Figure 6-62. SEM/EDX analysis results of particles from the 805TU site sample collected on 9/22/06.

6.3.1.4 Impactor Results

Air concentrations of 805-Up particulates, characterized by size and by analyte, are shown in Table 6-38. The impactor sample was collected over a 12-hour period on 10/31/06. Across all size classes, iron concentrations were higher than chromium, zinc and lead concentrations by one order of magnitude or greater. Copper and zinc were the second and third most prevalent metals in 805-Up air samples, respectively, across all size classes with the exception of the less than 0.95 µm size range. Lead was not detected in three of the five particulate size classes. In general, both overall metal concentrations and total particulate concentrations were low in comparison to other sites. The analyzed metals concentrations in 805-Up air samples constituted 1.96 percent of the 39.9 µg/m^3 total particulate concentration.

Table 6-38. Distribution of the concentrations of total particulates and five metals according to particle size in ambient air collected at 805-Up

Particle Size	Total Particulate	Chromium	Iron	Copper	Zinc	Lead
(µm)	(µg/m^3)	(ng/m^3)				
< 0.95	18.4	2.05	111	18.6	8.46	2.53
0.95 - 1.5	1.59	0.939	61.8	10.3	2.61	<0.82
1.5 - 3.0	3.19	1.06	109	9.25	3.04	<0.82
3.0 - 7.2	10.1	1.45	254	8.84	5.92	1.01
> 7.2	6.62	1.12	159	2.95	5.09	<0.82
Total	39.9	6.62	695	49.9	25.1	3.79*

* One half the detection limit was used for values less than the MDL to calculate total lead.

Atmospheric size distributions for 805-Up are presented in Figure 6-63. Overall, the greatest percentage of particle mass for each analyte was contained within the less than 0.95 µm size class. Greater than 70 percent of all lead particulates, and greater than 40 percent of total mass, and greater than 30 percent of all copper, chromium, and zinc particulates were less than 0.95 µm in size. In contrast, the 0.95 – 1.5 µm size class contained the lowest percentages of total mass, iron, chromium, zinc, and lead particulates but contained the second highest percentage of copper particulates. The 1.5 – 3.0 µm sized particulates ranged from 8 to 18.5 percent in total mass for all analytes, with the exception of lead. No lead was detected in the 1.5 – 3.0 µm particulates. In the coarse particle sizes, the 3.0 – 7.2µm sized particulates contained greater than 20 percent of all zinc, lead, chromium, and total mass, and more than 30 percent of all iron while the greater than 7.2 µm particulates contained 16.2 percent total mass, 16.9 percent of all chromium, 20.3 percent of all zinc, and 22.9 percent of all iron. Only 5.9 percent of all copper and none of the total lead was greater than 7.2 µm in size.

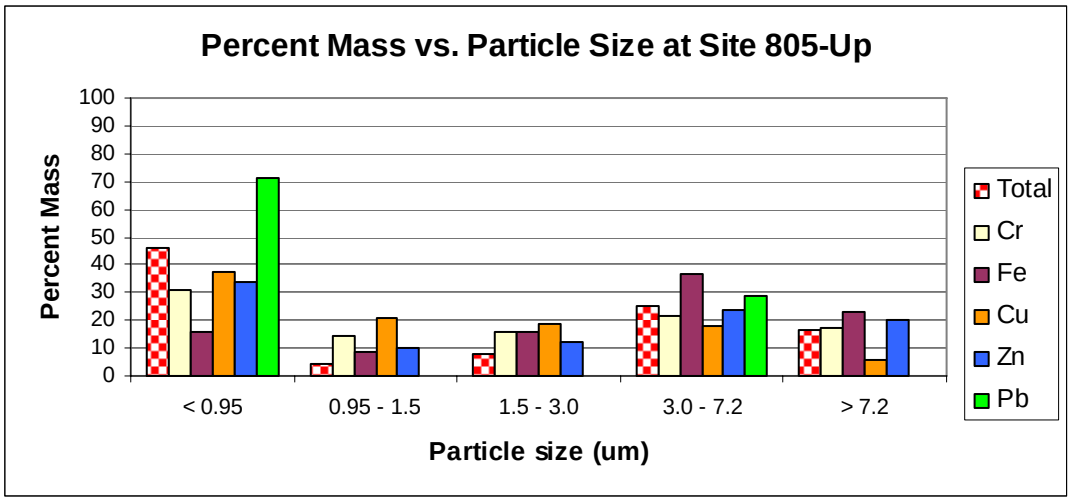

Figure 6-63. Percent mass versus particle size in air samples collected at 805-Up

6.3.2 Site 805T1

6.3.2.1 XRF Analysis

Surrogate deposition disks were deployed at 805T1 for a total of eight week-long events. The deposition disks were exposed for a duration of three days during each event. Analytical results from the surrogate deposition disks at the 805T1 site are presented in Table 6-39.

Table 6-39. Copper, Lead, and Zinc Flux at Site 805T1

Date	Net	Copper	Lead	Zinc
	(mg/m^2/day)	(µg/m2/day)		
8/25/06	99.2	8.8	<4.9	148
9/1/06	110	16.0	9.8	174
9/8/06	117	8.3	<4.9	92.4
9/15/06	74.7	8.4	<4.9	154
9/22/06	119	12.1	<4.9	170
9/29/06	83.6	15.4	<4.9	105
10/6/06	89.3	8.3	<4.9	58.8
10/13/06	73.3	8.2	<4.9	82.8

The net depositional flux for total particulate matter ranged from 73.3 to 119 mg/m^2/day and averaged 95.9 mg/m^2/day for the series of deployment events. The lowest net flux occurred during the week of 10/13/06 while the highest net flux occurred during the week of 9/22/06.

The depositional flux for copper ranged from 8.2 to 16.0 µg/m^2/day and averaged 10.7 µg/m^2/day during the deployment event series. The lowest copper depositional flux was observed during the week of 10/13/06 while the highest depositional flux, 16.0 µg/m^2/day, was detected during the week of 9/1/06.

Lead was typically not detected at the 805T1 site except for a single deployment event occurring during the week of 9/1/06 when the depositional flux measured 9.8 µg/m^2/day.

The depositional flux for zinc ranged from 58.8 to 174 µg/m^2/day and averaged 123 µg/m^2/day during the deployment event series. The lowest zinc depositional flux occurred during the week of 10/6/06. The highest zinc flux occurred during the week of 9/1/06 (Figure 6-57).

6.3.2.2 Photomicroscopy Results

A representative result for the photomicroscopy analysis performed on surrogate disks deployed at site 805T1 is presented in Figure 6-64. The sample date for the surrogate disk represented in Figure 6-64 is 9/22/06.

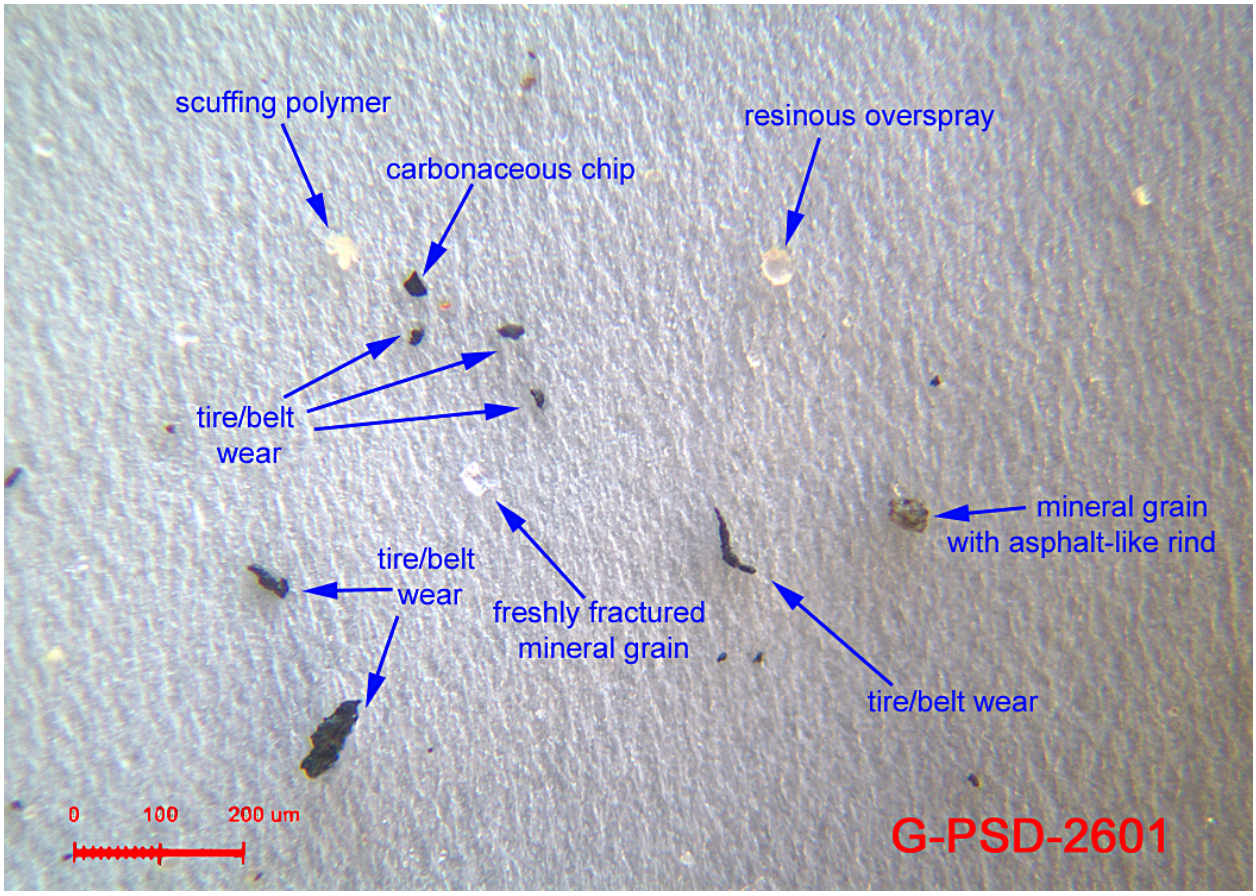

Figure 6-64. Photomicroscopy analysis for site 805T1 on 9/22/06

Frequently identified particles in photomicroscopy analysis at 805T1 included resinous overspray, tire/belt wear, and scuffing polymer as well as iron hydroxide/hydrated oxide, woody cellulose, and cleavage fragments. All photomicroscopy results for samples collected at site 805T1 are presented in Appendix B.

6.3.2.3 SEM-EDX Results

SEM/EDX analysis results of particles from the sample collected at Site 805T1 on 9/22/06 are presented in Figure 6-65. Copper particles were detected in the 1-5 µm size range as metallic copper and as tarnished bronze. Lead and zinc were not identified in particles using SEM/EDX. In comparison, the sample results from the XRF analyses showed a flux rate of 12.1 µg/m^2/day for copper and 170 µg/m^2/day for zinc. Lead was not detected in this sample using XRF analysis.

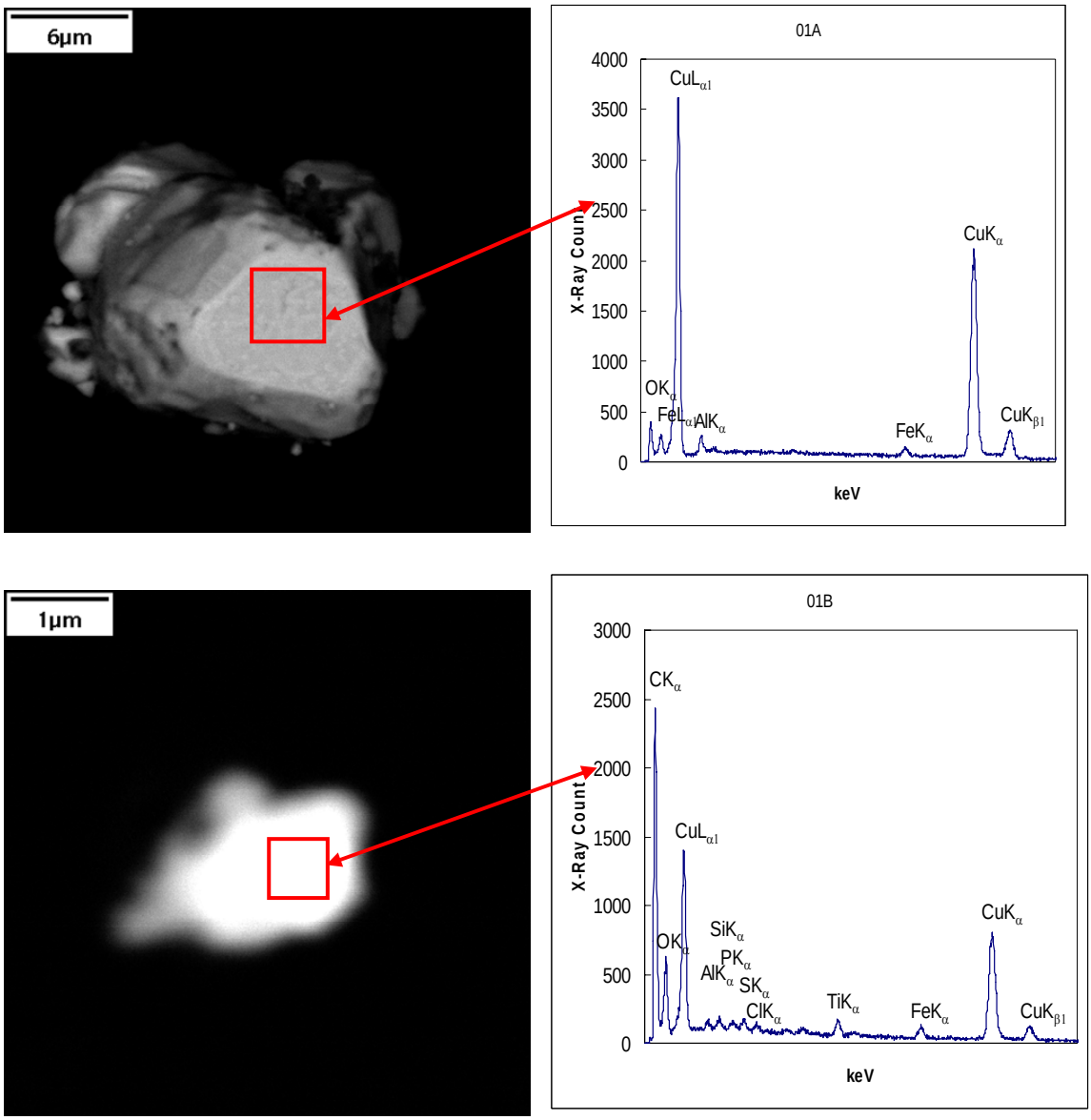

Figure 6-65. SEM/EDX analysis results of particles from the 805T1 site sample collected on 9/22/06.

6.3.2.4 Impactor Results

Air concentrations of 805T1 particulates, characterized by size and by analyte, are shown in Table 6-40. The impactor sample was collected over a 12-hour period on 9/28/06. Across all size classes, iron concentrations were higher than chromium, zinc, copper, and lead concentrations by one order of magnitude or greater. Total zinc (57.8 ng/m^3) and copper (49.4 ng/m^3) were the second and third most prevalent metals in 805T1 air samples, respectively, while chromium and lead had relatively uniform concentrations across the four smallest size ranges (ranging from 1.0 ng/m^3 to 1.9 ng/m^3, respectively). The analyzed metals concentrations in 805T1 air samples constituted 2.68 percent of the 58.6 µg/m^3 total particulate concentration across all size classes.

Table 6-40. Distribution of the concentrations of total particulates and five metals according to particle size in ambient air collected at 805T1

Particle Size	Total Particulates	Chromium	Iron	Copper	Zinc	Lead
(µm)	(µg/m^3)	(ng/m^3)				
< 0.95	33.7	3.02	429	14.3	23.9	5.53
0.95 - 1.5	4.53	1.15	173	9.85	6.78	1.08
1.5 - 3.0	6.13	1.3	240	10.2	7.56	1.42
3.0 - 7.2	8.46	1.7	418	12.4	11.7	1.86
> 7.2	5.76	1.14	185	2.62	7.83	1.01
Total	58.6	8.31	1450	49.4	57.8	10.9

Atmospheric size distributions for 805T1 are presented in Figure 6-66. Overall, the greatest percentage of particulate concentration for each analyte was found in the less than 0.95 µm size class. Greater than 50 percent of the lead and total mass, and greater than 40 percent of the zinc particulates were less than 0.95 µm in size. Additionally, nearly 30 percent of the copper, iron and chromium mass were bound to particulates that were less than 0.95 µm in size. By comparison, all analyte masses in the 0.95 – 1.5 µm, 1.5 – 3.0 µm, and the greater than 7.2 µm size classes were below 15 percent of their total mass with the exception of copper in the 0.95 – 1.5 µm and 1.5 – 3.0 µm size classes, and iron and chromium in the 1.5 - 3.0 µm size class. Copper mass was greater than 20 percent in the 0.95 – 1.5 µm, 1.5 – 3.0 µm, and the 3.0 – 7.2 µm size classes. While the 3.0 – 7.2 µm size class contained the second highest percentage of each analyte, the percent masses of copper, lead, and chromium in the greater than 7.2 µm size class were the lowest across all size classes. In general, the vast majority of metal mass and total mass was found in particulates that were either below 0.95 µm in size or between 3.0 and 7.2 µm in size.

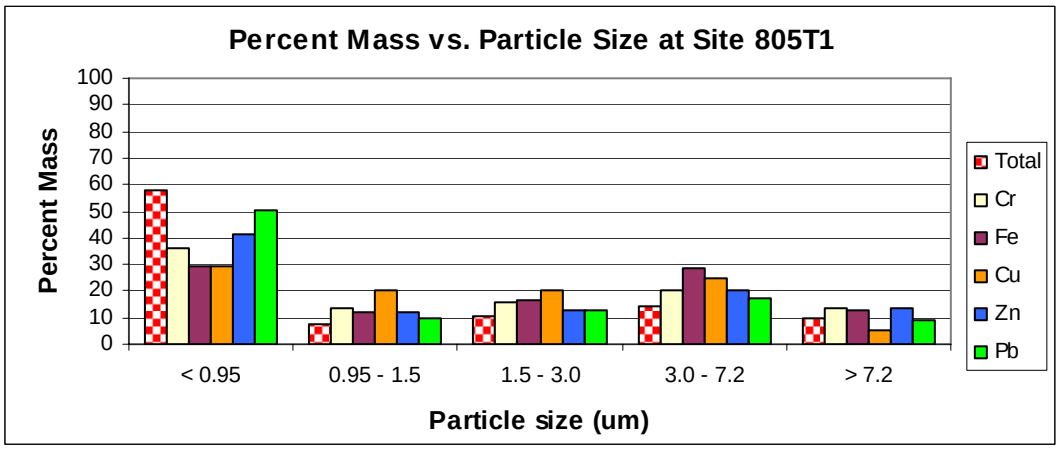

Figure 6-66. Percent mass versus particle size in air samples collected at 805T1

6.3.3 Site 805T2

6.3.3.1 XRF Analysis

Surrogate deposition disks were deployed at 805T2 for a total of eight week-long events. The deposition disks were exposed for a duration of three days during each event. Analytical results from the primary surrogate deposition disks at the 805T2 site are presented in Table 6-41. Results from analyses of replicate disks are provided in Appendix A.

Table 6-41. Depositional flux results at site 805T2.

Date	Net	Copper	Lead	Zinc
	(mg/m^2/day)	(µg/m^2/day)		
8/25/2006	67.8	<1.7	<4.9	78.6
9/1/2006	63.8	13.9	<4.9	53.2
9/8/2006	80.7	<1.7	12.5	46.2
9/15/2006	77.3	7.5	12.6	55.4
9/22/2006	81.1	8.6	<4.9	74.8
9/29/2006	55.3	8.9	<4.9	28.8
10/6/2006	53.6	3.6	<4.9	43.4
10/13/2006	43.5	7.4	<4.9	34.3

The net depositional flux for total particulate matter ranged from 43.5 to 81.1 mg/m^2/day and averaged 65.4 mg/m^2/day for the series of deployment events. The lowest net flux occurred during the week of 10/13/06. The highest net flux occurred during the week of 9/22/06.

The depositional flux for copper ranged from BDL to 13.9 µg/m^2/day and averaged 6.5 µg/m^2/day during the deployment event series. The copper depositional flux was BDL during the week of 8/25/06 and 9/8/06 while the highest depositional flux (13.9 µg/m^2/day) was detected during the week of 9/1/06.

Lead was typically not detected at the 805T2 site except for the deployment events occurring during the week of 9/8/06 when the depositional flux measured 12.5 µg/m^2/day and 9/15/06 when the depositional flux measured 12.6 µg/m^2/day. The average lead depositional flux result for all deployments was 5.0 µg/m^2/day.

The depositional flux for zinc ranged from 28.8 to 78.6 µg/m^2/day and averaged 51.9 µg/m^2/day during the deployment event series. The lowest zinc depositional flux occurred during the week of 9/29/06 while the highest zinc flux occurred during the week of 8/25/06.

6.3.3.2 Photomicroscopy Results

A representative result for the photomicroscopy analysis performed on surrogate disks deployed at site 805T2 is presented in Figure 6-67. The sample date for the surrogate disk represented in Figure 6-67 is 9/15/06.

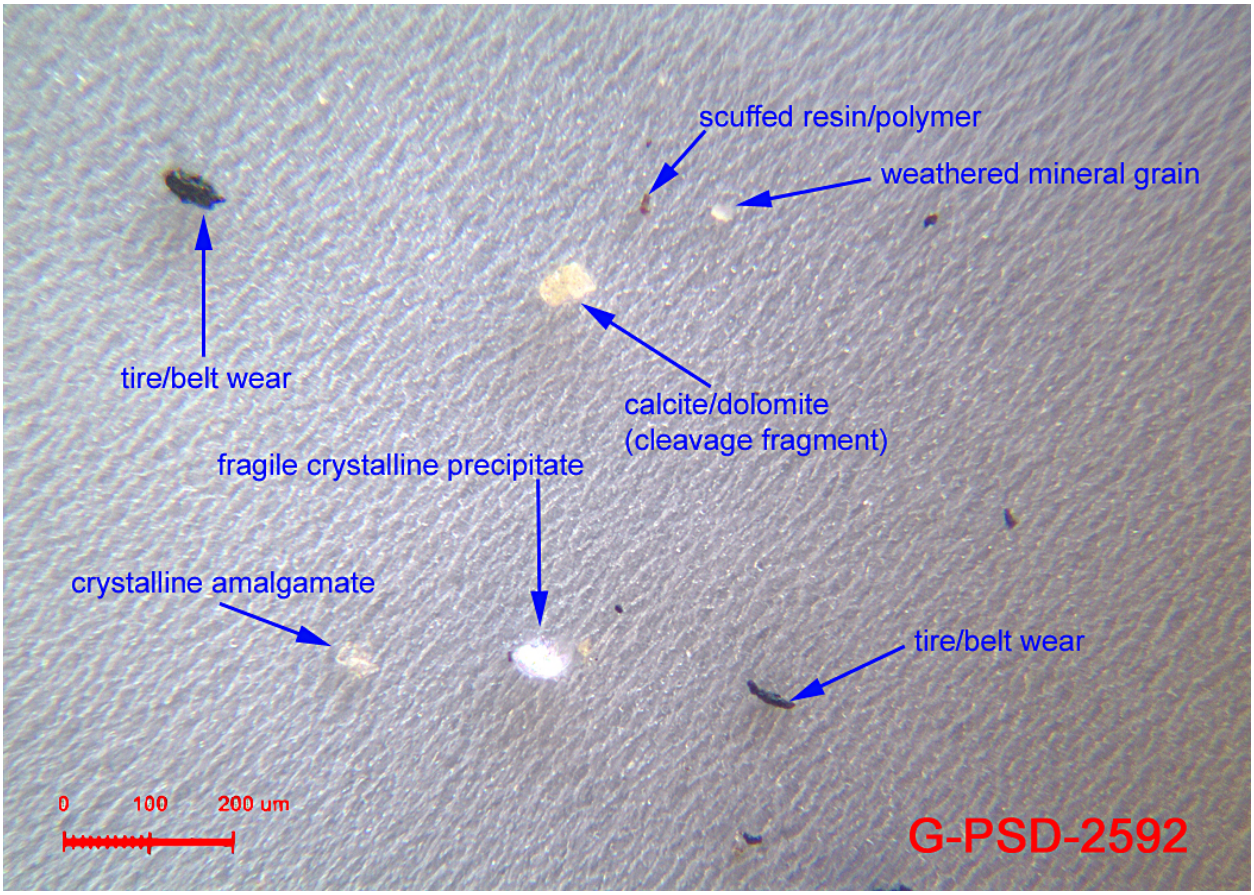

Figure 6-67. Photomicroscopy analysis for site 805T2 on 9/15/06.

Frequently identified particles in photomicroscopy analysis at 805T2 included scuffed resin/polymer, tire/belt wear, and calcite/dolomite as well as metal chips, iron oxide/hydroxide, and clay-like aggregate. All photomicroscopy results for samples collected at site 805T2 are presented in Appendix B.

6.3.3.3 SEM-EDX Results

SEM/EDX analysis results of particles from the sample collected at Site 805T2 on 9/15/06 are presented in Figure 6-68. Lead particles were detected in the 1-5 µm size range associated with iron, chrome and nickel steel formulation interpreted here, based on the proportion of the metals, as stainless steel. Copper was also detected associated with zinc as brass but was not illustrated. In comparison, the sample results from the XRF analyses showed flux rates of 7.5 µg/m^2/day for copper, 12.6 µg/m^2/day for lead, and 55.4 µg/m^2/day for zinc.

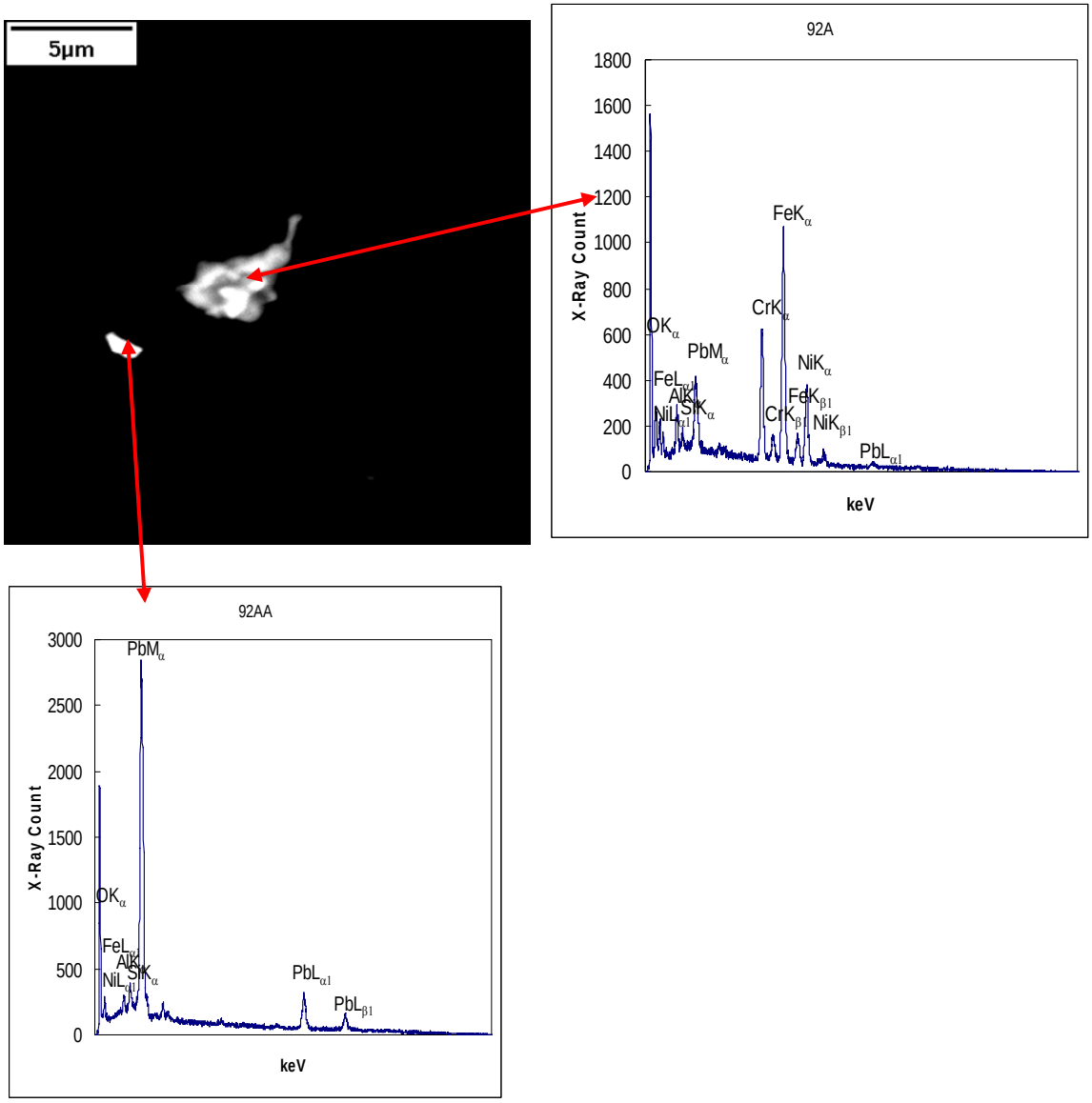

Figure 6-68. SEM/EDX analysis results of particles from the 805T2 site sample collected on 9/15/06

6.3.3.4 Impactor Results

Air concentrations of 805T2 particulates, characterized by size and by analyte, are shown in Table 6-42. Across all size classes, iron concentrations were higher than chromium, zinc, copper, and lead concentrations by one order of magnitude or greater. Total copper (56.3 µg/m^3) and zinc (49.0 µg/m^3) were the second and third most prevalent metals in 805T2 air samples, respectively, while chromium and lead had relatively uniform concentrations across the four largest size classes and higher concentrations of particulates that were less than 0.95 µm in size. The analyzed metals concentrations in 805T2 air samples constituted 2.35 percent of the 52.699 µg/m^3 total particulate concentration across all size classes.

Table 6-42. Distribution of the concentrations of total particulates and five metals according to particle size in ambient air collected at 805T2

Particle Size	Total Particulates	Chromium	Iron	Copper	Zinc	Lead
(µm)	(µg/m^3)	(ng/m^3)				
< 0.95	25.7	2.79	243	16.9	17.8	3.91
0.95 - 1.5	4.78	1.18	148	12.4	5.75	1.04
1.5 - 3.0	6.01	1.19	206	10.9	6.97	1.29
3.0 - 7.2	10.7	1.48	364	13.4	11.3	1.70
> 7.2	5.52	1.08	154	2.71	7.17	1.00
Total	52.7	7.72	1120	56.3	49.0	8.94

Atmospheric size distributions for 805T2 are presented in Figure 6-69. Overall, the greatest percentage of mass for each analyte was contained within the less than 0.95 µm size class. Greater than 40 percent of the lead mass and total mass, and greater than 30 percent of the zinc, chromium, and copper mass was less than 0.95 µm in size. Analyte masses of particulates in the 0.95 µm to 1.5 µm size range were 22 percent for copper and were below 15 percent for zinc, iron, lead, chromium, and total mass. Between 10 and 20 percent of all analyte masses were between 1.5 and 3.0 µm in size. In the 0.95 – 1.5 µm particulate size class, the percent mass for each analyte was higher than in all other size classes, with the exception of the less than 0.95 µm size class. In general, the majority of the metals' mass and the total mass were found in particulates that were either below 0.95 µm in size or between 3.0 and 7.2 µm in size. Only 4.8 percent of all copper was bound to particulates that were greater than 7.2 µm in size, while between 10 and 15 percent of all chromium, zinc, lead, and iron were bound to large particulates.

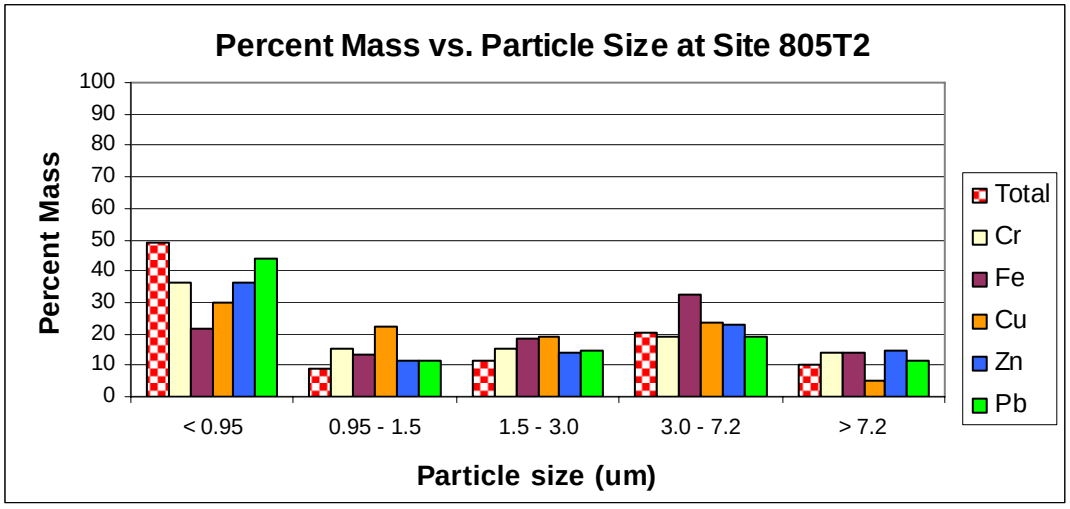

Figure 6-69. Percent mass versus particle size in air samples collected at 805T2

6.3.4 Site 805T3

6.3.4.1 XRF Analysis

Surrogate deposition disks were deployed at 805T3 for a total of eight week-long events. The deposition disks were exposed for a duration of three days during each event. During one of the deployment events occurring on 9/1/06, disks were damaged in the field which resulted in those disks being withheld from laboratory analysis. Analytical results from the primary surrogate deposition disks at the 805T3 site are presented in Table 6-43. Replicate disk analyses are presented in Appendix A.

Table 6-43. Depositional flux results at site 805T3

Date	Net	Copper	Lead	Zinc
	($mg/m^2/day$)	($\mu g/m^2/day$)		
8/25/06	44.9	14.8	<4.9	65.1
9/8/06	54.5	<1.7	<4.9	23.9
9/15/06	26.4	<1.7	<4.9	25.2
9/22/06	52.5	9.8	<4.9	54.2
9/29/06	65.7	7.7	<4.9	20.3
10/6/06	63.6	<1.7	<4.9	20.8
10/13/06	53.4	18.7	<4.9	26.9

The net depositional flux for total particulate matter ranged from 26.4 to 65.7 $mg/m^2/day$ and averaged 51.6 $mg/m^2/day$ for the series of deployment events. The lowest net flux occurred during the week of 9/15/06. The highest net flux occurred during the week of 9/29/06.

The depositional flux for copper ranged from BDL to 18.7 $\mu g/m^2/day$ and averaged 7.7 $\mu g/m^2/day$ during the deployment event series. The copper depositional flux was BDL during the week of 9/8/06, 9/15/06 and 10/6/06. The highest depositional flux, 18.7 $\mu g/m^2/day$, was detected during the week of 10/13/06.

Lead was not detected at the 805T3 site during any of the deployment events.

The depositional flux for zinc ranged from 20.3 to 65.1 $\mu g/m^2/day$ and averaged 33.8 $\mu g/m^2/day$ during the deployment event series. The lowest zinc depositional flux occurred during the week of 9/29/06 while the highest zinc flux occurred during the week of 8/25/06.

6.3.4.2 Photomicroscopy Results

A representative result for the photomicroscopy analysis performed on surrogate disks deployed at site 805T3 is presented in Figure 6-70. The sample date for the surrogate disk represented in Figure 6-70 is 9/22/06.

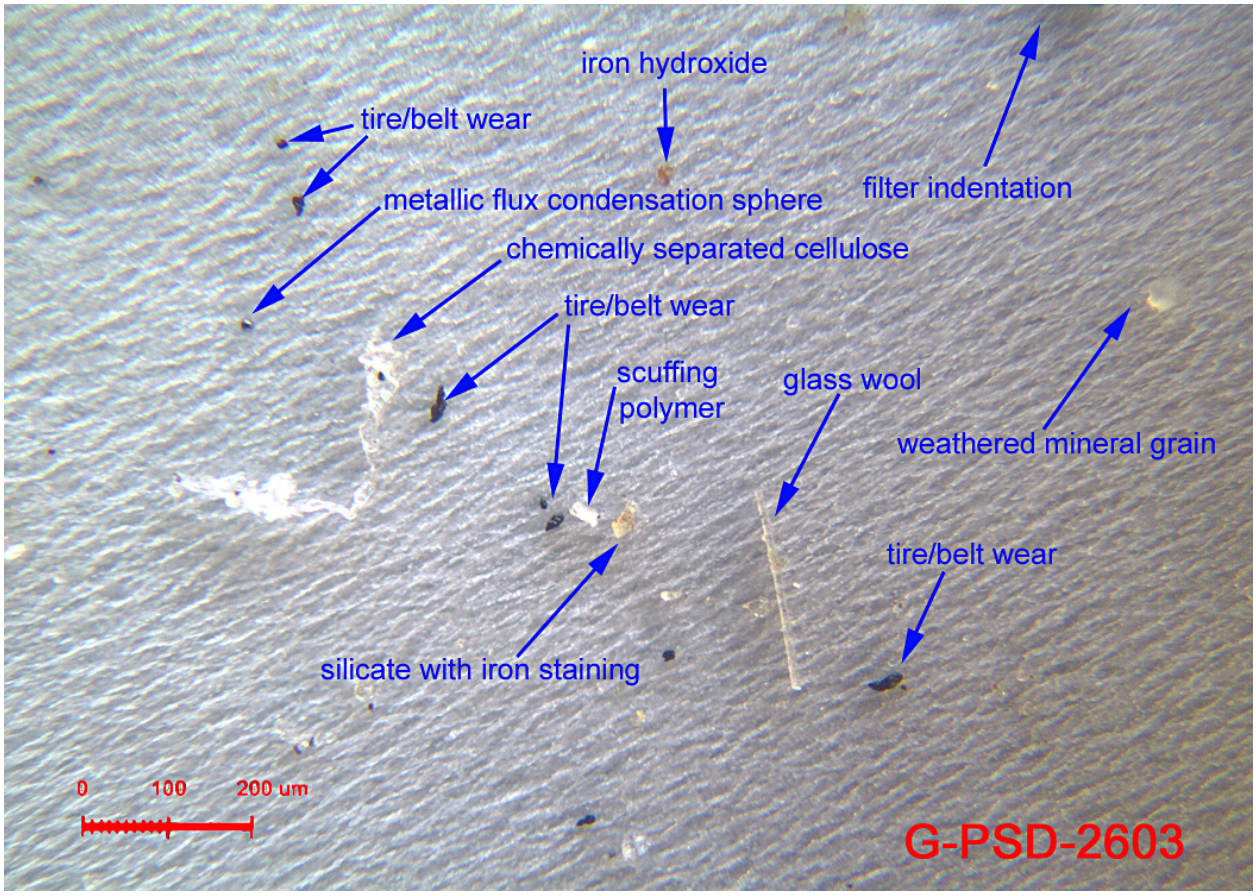

Figure 6-70. Photomicroscopy analysis for site 805T3 on 9/22/06

Frequently identified particles in photomicroscopy analysis at 805T3 included glass wool, tire/belt wear, and silicate with iron staining as well as cleavage fragment, coating scuff, and fungal hypha. All photomicroscopy results for samples collected at site 805T3 are presented in Appendix B.

6.3.4.3 SEM-EDX Results

SEM/EDX analysis performed on the sample collected from Site 805T3 on 9/22/06 did not identify any particles containing copper, lead or zinc despite a survey of several hundred particles. In comparison, the sample results from the XRF analyses showed a flux rate of 9.8 $\mu g/m^2$/day for copper and 54 $\mu g/m^2$/day for zinc. Lead was not detected in this sample using XRF analysis.

6.3.4.4 Impactor Results

Air concentrations of 805T3 particulates, characterized by size and by analyte, are shown in Table 6-44. Total iron concentrations were more than 20 times greater than total copper and zinc concentrations, and more than 100 times greater than total chromium and lead concentrations. Within each particulate size class, iron was highest in concentration, followed by either copper or zinc. The analyzed metals concentrations in 805T3 air samples constituted 2.07 percent of the 38.0 $\mu g/m^3$ total particulate concentration across all size classes.

Table 6-44. Distribution of the concentrations of total particulates and five metals according to particle size in ambient air collected at 805T3

Particle Size	Total Particulates	Chromium	Iron	Copper	Zinc	Lead
(µm)	(µg/m^3)	(ng/m^3)				
< 0.95	15.2	2.24	114	8.80	8.00	1.80
0.95 - 1.5	2.21	0.880	71.8	6.80	3.05	<0.82
1.5 - 3.0	4.17	1.09	121	6.99	4.34	0.94
3.0 - 7.2	10.1	1.16	246	7.65	8.32	1.36
> 7.2	6.37	1.20	158	2.61	7.41	1.30
Total	38.0	6.57	711	32.9	31.1	5.81

* One half the detection limit was used for values less than the MDL to calculate total lead.

Atmospheric size distributions for 805T3 are presented in Figure 6-71. Overall, the highest percentage of mass for lead, chromium, total mass, and copper was contained within the less than 0.95 µm size class. Greater than 40 percent of the total mass, 30 percent of the lead and chromium mass, and 25 percent of the copper and zinc mass were less than 0.95 µm in size. Percent masses of analytes, with the exception of copper, were lower in the 0.95 µm to 1.5 µm size class than in all other size classes. While 20 percent of all copper was bound to 0.95 – 1.5 µm particulates, 0 percent of all lead, and less than 11 percent of all zinc, total mass, and iron mass were in this size class. In the 1.5 – 3.0 µm size class, percentages of analyte masses ranged from 11.0 for total mass to 21.3 for copper. A greater percentage of iron and zinc were in the 3.0 – 7.2 µm size class than in any other size class. More than 20 percent of copper, zinc, lead, and total mass, and more than 30 percent of iron was bound to particulates that were between 3.0 µm and 7.2 µm in size. In general, the majority of metals and total mass were found in particulates that were either below 0.95 µm in size or between 3.0 and 7.2 µm in size. Between 18.2 percent and 24.4 percent of all chromium, zinc, lead, and iron were bound to particulates larger than 7.2 µm in size while only 7.9 percent of all copper was detected in this size class.

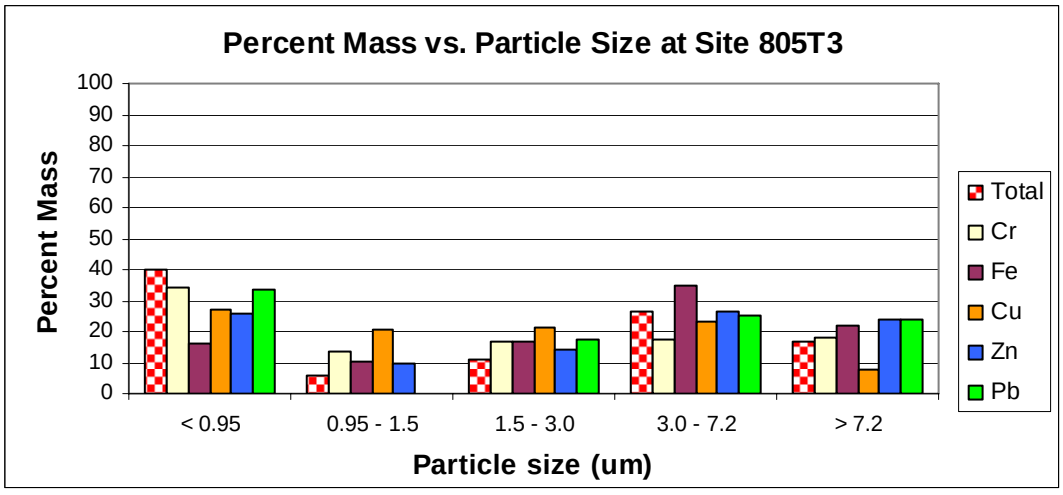

Figure 6-71. Percent mass versus particle size in air samples collected at 805T3

6.3.5 Site 805T4

6.3.5.1 XRF Analysis

Surrogate deposition disks were deployed at 805T4 for a total of eight week-long events. The deposition disks were exposed for a duration of three days during each event. During one of the deployment events occurring on 9/1/06, disks were damaged in the field which resulted in those disks being withheld from laboratory analysis. Analytical results from the primary surrogate deposition disks at the 805T4 site are presented in Table 6-45. Results of replicate disk analyses are presented in Appendix A.

Table 6-45. Depositional flux results at site 805T4

Date	Net	Copper	Lead	Zinc
	($mg/m^2/day$)	($\mu g/m^2/day$)		
8/25/2006	24.9	<1.7	<4.9	23.7
9/8/2006	45.2	46.3	<4.9	20.4
9/15/2006	25.0	12.2	<4.9	21.8
9/22/2006	50.5	16.9	<4.9	72.4
9/29/2006	76.1	6.9	<4.9	18.2
10/6/2006	89.2	<1.7	<4.9	26.8
10/13/2006	28.2	5.4	<4.9	11.3

The net depositional flux for total particulate matter ranged from 24.9 to 89.2 $mg/m^2/day$ and averaged 48.4 $mg/m^2/day$ for the series of deployment events. The lowest net flux occurred during the week of 8/25/06. The highest net flux occurred during the week of 10/6/06.

The depositional flux for copper ranged from BDL to 46.3 $\mu g/m^2/day$ and averaged 12.8 $\mu g/m^2/day$ during the deployment event series. The copper depositional flux was BDL during the week of 8/25/06 and 10/6/06. The highest depositional flux, 46.3 $\mu g/m^2/day$, was detected during the week of 9/8/06.

Lead was not detected at the 805T4 site during any of the deployment events.

The depositional flux for zinc ranged from 11.3 to 72.4 $\mu g/m^2/day$ and averaged 27.8 $\mu g/m^2/day$ during the deployment event series. The lowest zinc depositional flux occurred during the week of 10/13/06. The highest zinc flux occurred during the week of 9/22/06.

6.3.5.2 Photomicroscopy Results

A representative result for the photomicroscopy analysis performed on surrogate disks deployed at site 805T4 is presented in Figure 6-72. The sample date for the surrogate disk represented in Figure 6-72 is 9/8/06.

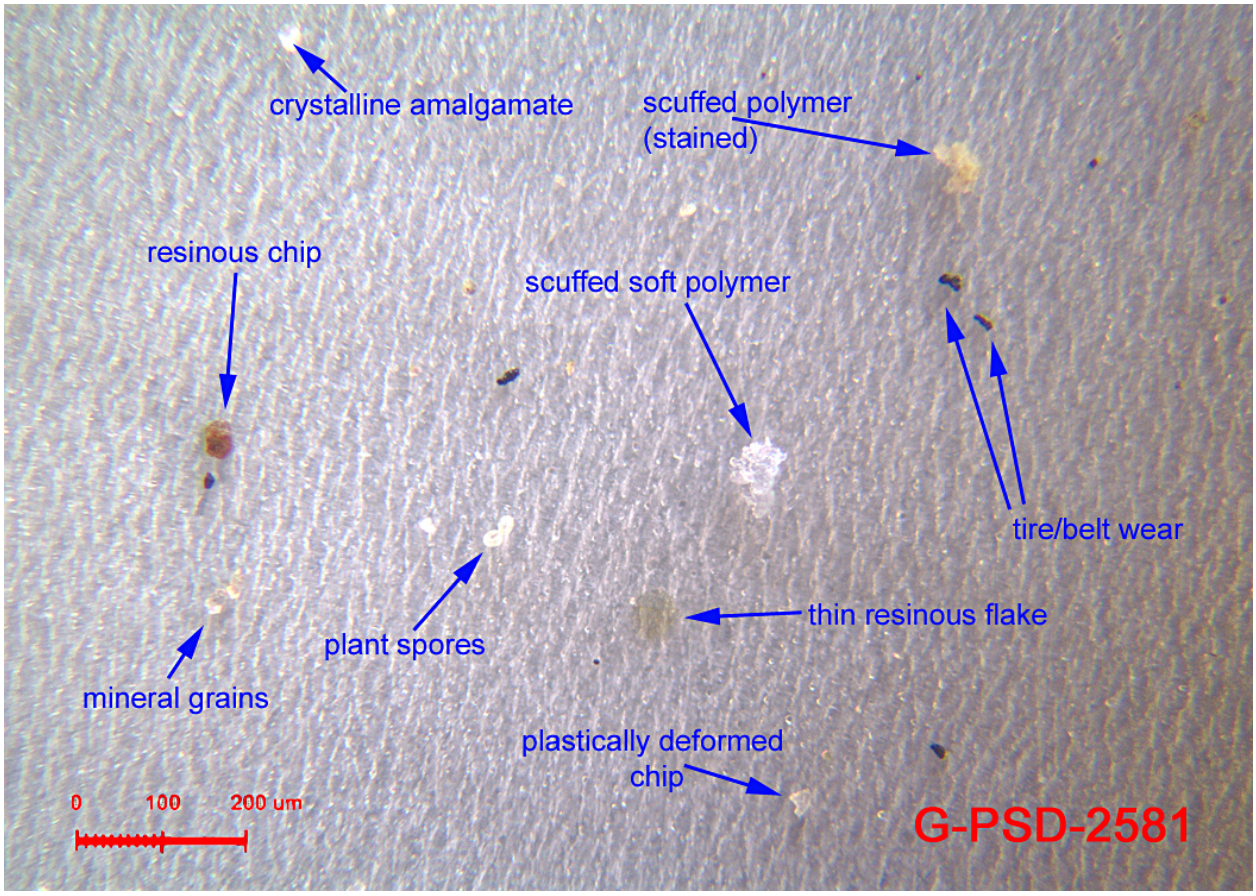

Figure 6-72. Photomicroscopy analysis for site 805T4 on 9/8/06

Frequently identified particles in the photomicroscopy analysis of the 805T4 disk included crystalline amalgamate, tire/belt wear, and mineral grains as well as limonite spheres, c carbonaceous sphere, and moss/fern spores. All photomicroscopy results for samples collected at site 805T4 are presented in Appendix B.

6.3.5.3 SEM-EDX Results

SEM/EDX analysis performed on the sample collected from Site 805T4 on 9/8/06 did not identify any particles containing copper, lead or zinc despite a survey of several hundred particles. In comparison, the sample results from the XRF analyses showed flux rates of 46.3 µg/m^2/day for copper and 20.4 µg/m^2/day for zinc. Lead was not detected in this sample using XRF analysis.

6.3.5.4 Impactor Results

Air concentrations of 805T4 particulates, characterized by size and by analyte, are shown in Table 6-46. Across all size classes, iron concentrations were higher than chromium, zinc, copper, and lead concentrations by one order of magnitude or greater. Total iron was measured at 1600 ng/m^3, while copper and zinc concentrations were measured at 83.6 ng/m^3 and 104 ng/m^3. The analyzed metals concentrations in 805T4 air samples constituted 3.70 percent of the 49.0 µg/m^3 total particulate concentration.

Table 6-46. Distribution of the concentrations of total particulates and five metals according to particle size in ambient air collected at 805T4

Particle Size	Total Particulate	Chromium	Iron	Copper	Zinc	Lead
(µm)	(µg/m^3)	(ng/m^3)				
< 0.95	32.4	4.41	737	37.5	57.2	8.86
0.95 - 1.5	1.84	1.03	169	14.2	10.2	2.19
1.5 - 3.0	3.43	1.16	186	11.4	9.18	1.34
3.0 - 7.2	6.99	1.42	330	14.3	15.0	1.86
> 7.2	4.29	1.15	180	6.14	11.9	1.46
Total	49.0	9.17	1600	83.5	103	15.7

Atmospheric size distributions for 805T4 are presented in Figure 6-73. Overall, the highest percent mass for each analyte was contained within the less than 0.95 µm size class. Greater than 60 percent of the total mass, greater than 50 percent of the lead and zinc mass, and greater than 40 percent of the chromium, iron, and copper mass was less than 0.95 µm in size. With the exception of iron in the 0.95 – 1.5 µm size class, all other size classes contained less than 20 percent of any given analyte. In general, the majority of metals and total mass was found in particulates that were either below 0.95 µm in size or between 3.0 µm and 7.2 µm in size. The 0.95 – 1.5 µm size class contained the lowest percentage of total mass (3.8 percent) and approximately 10 percent of all chromium, iron, and zinc mass. Similarly, the 1.5 – 3.0 µm size class contained approximately 10 percent of each metallic analyte and seven percent of the total mass. The 3.0 µm to 7.2 µm coarse particulate size class contained the second largest percentage of total mass, chromium, iron, copper, and zinc, while the greater than 7.2 µm size class contained 7.3 percent copper, 8.8 percent total mass, 12.6 percent chromium, 11.3 percent iron, 11.5 percent zinc, and 9.3 percent lead.

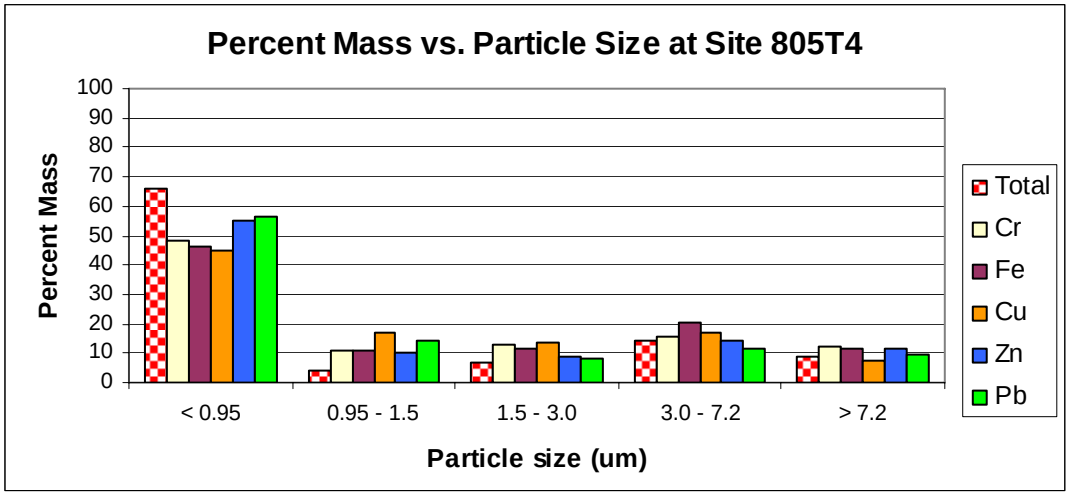

Figure 6-73. Percent mass versus particle size in air samples collected at 805T4

6.4 Extended Deployment Study Results

Results for the Extended Deployment study are presented in this section. The purpose of this study was to determine if particulates accumulated at a linear rate and reach a maximum accumulation point. Three groups of triplicate surrogate deposition discs were deployed at the SD(8) site between 9/15/06 and 10/2/06. A single group of triplicate disks was recovered from the site after periods of 7, 14 and 17 days. Results for each replicate disk are presented in Figure 6-74. A 'best fit' trend line has been added to indicate the overall trend of the data.

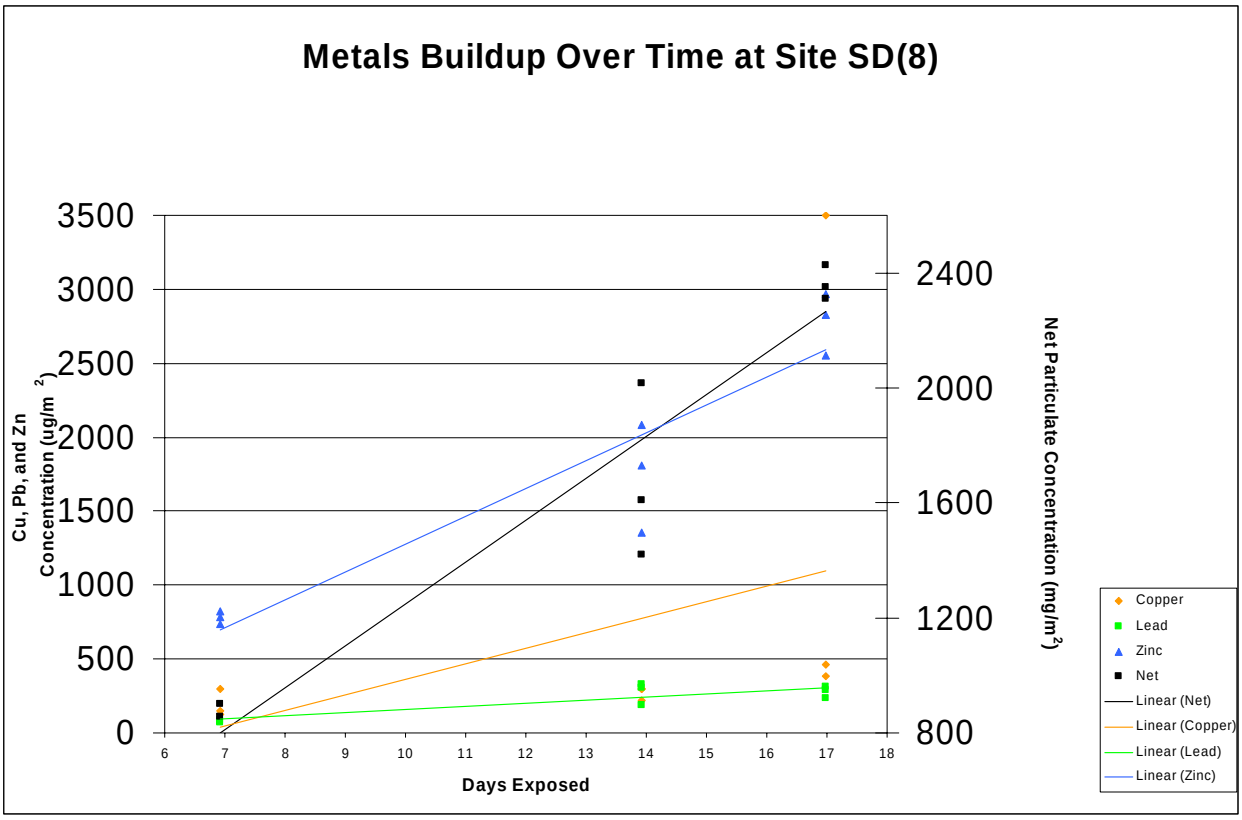

Figure 6-74. Metals buildup over time at Site SD(8)

The net concentration for total particulate matter increased from an average of 842 mg/m^2 after seven days of deployment to an average of 2360 mg/m^2 after 17 days of deployment. There was little variation among replicate samples for each deployment interval. The coefficients of variation for the 7-, 14-, and 17-day deployments were 8%, 18%, and 3%, respectively.

The concentration of copper increased from an average of 189 µg/m^2 after seven days of deployment to an average of 1450 µg/m^2 after 17 days of deployment. There was significant variation among replicate samples for two of the three deployment intervals. The coefficients of variation for the 7-, 14-, and 17-day deployments were 49%, 16%, and 123%, respectively.

The concentration of lead increased from an average of 79.0 µg/m^2 after seven days of deployment to an average of 278 µg/m^2 after 17 days of deployment. There was little variation among the replicates for each deployment interval. The coefficients of variation for the 7-, 14-, and 17-day deployments were 11%, 27%, and 14%, respectively.

The concentration of zinc increased from an average of 780 µg/m^2 after seven days of deployment to an average of 2780 µg/m^2 after 17 days of deployment. There was little variation among the replicates for each deployment interval. The coefficients of variation for the 7-, 14-, and 17-day deployments were 6%, 21%, and 8%, respectively.

Based on these results, it was concluded that linear buildup occurred for the 17-day exposure period. Longer exposure periods would be required to determine the maximum accumulation rate.

5.0 WIND DATA PROCESSING

Atmospheric conditions are an important component in evaluating ambient air measurements, including deposition. Wind direction is a major determinant of ambient air impacts, especially at measurement sites near sources of emissions (e.g., freeways, roadways, and industrial and commercial areas). Combining geographical data on sources and records of wind direction during sampling can provide insights into measured air concentrations or deposition.

Wind data recorded at two stations operated in the study area by the San Diego County Air Pollution Control District (APCD) were used to aid in the analysis of the deposition data collected during the study. The wind data were used to generate three types of information to support the data analysis:

1) wind roses to visualize the frequencies of hourly wind speeds and directions;
2) direction distribution variables for each sampling period for statistical analyses; and
3) mean downwind and crosswind component variables for statistical analyses at two locations near emissions sources of interest.

The following subsections describe the data available from APCD, and the processing of the data for use in the study.

APCD Wind Data

APCD operates a network of continuous ambient air monitors for criteria pollutants (SO_2, NO_x, O_3, CO) that includes meteorological stations at several locations. The locations of these meteorological stations relative to the deposition sampling sites are shown in Figure 5-1.

Based on their proximity to the deposition sites, two of these stations were used to develop the wind data sets for analysis: the San Diego Beardsley (Downtown) and Del Mar Winston School (Del Mar) stations. The Downtown station was used to represent all deposition sites except for the Mira Mesa site. The Mira Mesa site is located significantly farther north than the other deposition sites. Therefore, the Del Mar station was used to represent the Mira Mesa site.

The wind data collected at these stations included three parameters that were used for analysis: hourly vector mean wind direction, hourly scalar mean wind speed, and standard deviation of horizontal wind direction (also referred to as sigma theta, sigma, or σ_θ). The hourly vector mean wind direction was the only available wind direction parameter. Although scalar mean wind directions are more appropriate for use in conjunction with σ_θ, vector mean wind directions are generally within a few degrees of the scalar average wind direction. The data used were taken from the raw daily report files posted to the Internet by the APCD (http://www.jtimmer.cts.com/).

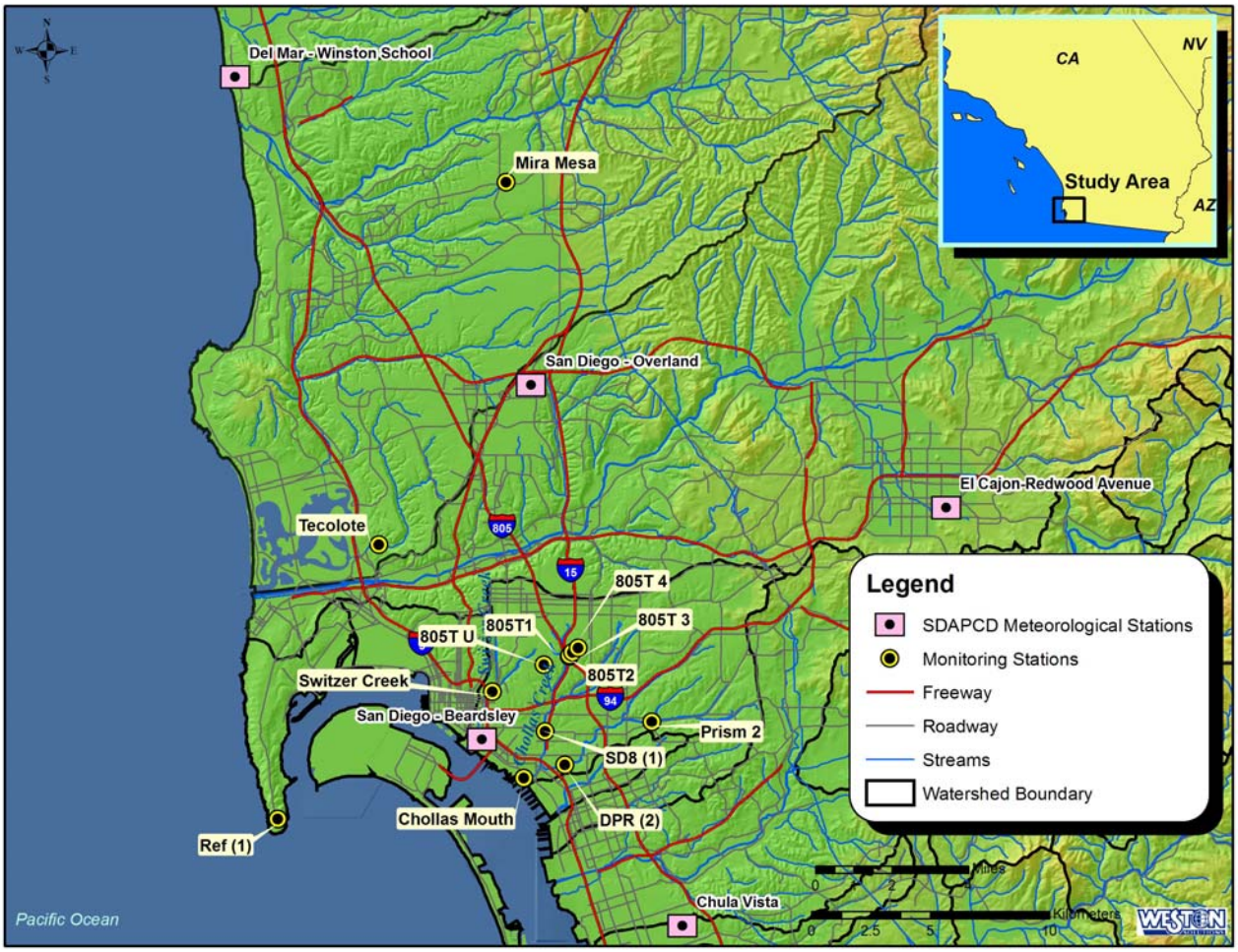

Figure 5-1. Map Depicting Meteorological Stations in the San Diego Area

Wind Roses

Wind roses are graphical tools used to visualize the joint variations in wind speed and wind direction over time at a site. They are most often used with long-term climatological data, but are equally useful for ambient air sampling applications. Wind roses are based on two-way frequency counts, using categories of wind direction and wind speed.

Wind direction is typically divided into 16 sectors centered on points of the compass (N, ENE, NE, NNE, etc.), each 22.5 degrees wide. However, other numbers of sectors (e.g., 8 or 36) can be used for specific applications. The sector range endpoints fall halfway between adjacent directions. Wind speed is typically divided into 6 categories, with lower limits chosen to suit the application. Calm winds are tabulated separately. Each observation of wind is counted in an appropriate speed and direction 'bin' (96 of them for a typical rose). The resulting total counts in the speed and direction bins are then converted to percentages of the total observations for plotting.

An example of a typical wind rose is shown in Figure 5-2. The rose is based on hourly data from the San Diego Lindbergh Field Airport National Weather Service (NWS) station for the period 1985 through 1995. The plot includes a table showing the percentages (as decimal fractions) within each of the 96 bins. These percentages are proportional to the lengths of the segments in each "petal" of the rose. The prevalent wind directions are from the west-northwest (17.89% of hours). The table indicates that the longest segment of the WNW petal is for the 6-10 knot speed category, with 8.28% of the hours.

Wind roses were generated for each deployment period for the deposition disks and impactor sampling. For consistency with the statistical wind analysis, the roses were generated with 8 direction sectors, 45 degrees wide (N, NE, E, SE, S, SW, W, NW). Each rose was based on the hourly data available for each period from the SDAPCD stations. The roses are included in Appendix C.

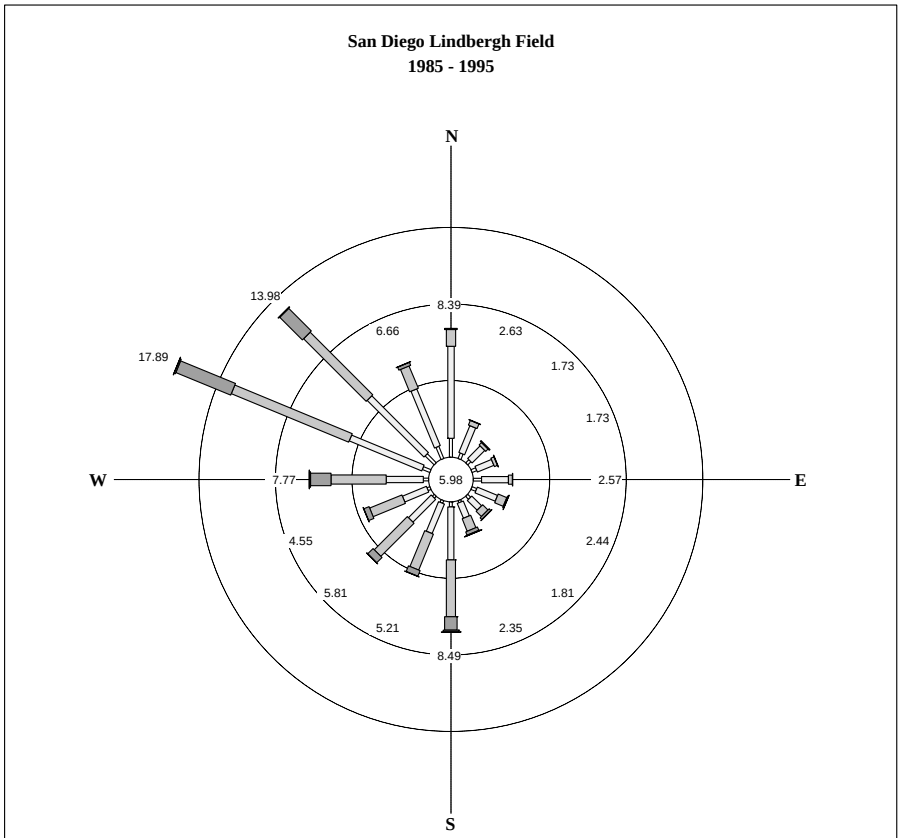

PERCENT OCCURRENCE: Wind Speed (Knots)
LOWER BOUND OF CATEGORY

DIR	0	3	6	10	16	21
N	1.23	6.00	1.10	0.07	0.00	0.00
NNE	0.39	1.88	0.32	0.03	0.00	0.00
NE	0.29	1.16	0.21	0.06	0.01	0.00
ENE	0.33	1.16	0.21	0.03	0.00	0.00
E	0.53	1.75	0.26	0.02	0.00	0.00
ESE	0.33	1.43	0.61	0.07	0.01	0.00
SE	0.26	0.90	0.48	0.15	0.01	0.00
SSE	0.15	1.05	0.87	0.23	0.04	0.01

TOTAL OBS = 96397 MISSING OBS = 0

PERCENT OCCURRENCE: Wind Speed (Knots)
LOWER BOUND OF CATEGORY

DIR	0	3	6	10	16	21
S	0.33	3.44	3.70	0.87	0.12	0.02
SSW	0.18	2.09	2.54	0.39	0.02	0.00
SW	0.17	2.09	3.06	0.49	0.01	0.00
WSW	0.19	1.70	2.28	0.36	0.02	0.00
W	0.34	2.43	3.60	1.33	0.07	0.01
WNW	0.53	5.12	8.28	3.87	0.08	0.01
NW	0.84	5.23	5.77	2.09	0.04	0.00
NNW	0.85	4.01	1.57	0.21	0.01	0.00

CALM OBS = 5765 PERCENT CALM = 5.98

Figure 5-2. Example of Wind Rose from San Diego Lindbergh Field

Direction Distributions

Wind direction is a constantly fluctuating parameter due to turbulence in the atmosphere. Average wind direction captures information on the main transport direction during a period, but loses information on variability of the wind direction. The standard deviation of wind direction (σ_θ) parameter can be used to compensate for some of this lost information. For statistical analyses, the hourly σ_θ data was used to calculate frequency distributions "compensated" for fluctuations in wind direction during each hour of a deployment period. These compensated distributions provide more representative variables for correlation with observed deposition fluxes, compared to using strictly a wind rose frequency bin tabulation.

More representative frequencies can be calculated using sigma theta data to reduce bias introduced by discrete binning of mean wind directions. The bias enters when the mean is near a sector boundary. Compensated distributions are calculated by considering the σ_θ values to be analogous to the standard deviation of a normal distribution, and spreading the frequency during the hour according to the resulting bell curve. This is illustrated in Figure 5-3.

Figure 5-3 shows an example compensated frequency distribution for a mean wind direction of 189 degrees, with σ_θ = 20 degrees. The shape of the normal curve is shown, along with the sector endpoints of a typical 16-sector rose. The sectors are labeled with their direction and the total integrated frequency in the sector for the hour. The frequency for the hour is spread over six sectors. The central S and SSW sectors share the majority of the frequency, with approximately 39% and 35% respectively. The next two sectors from the center (SSE and SW) split 24% of the frequency. The remaining 2% falls into the SE and WSW sectors.

The compensation process effectively smoothes out the more discrete frequency distribution generated by a simple wind rose histogram. The continuous distributions are more suitable for statistical correlations, as they preserve the major patterns while limiting the potential bias that can exist in discretely calculated distributions.

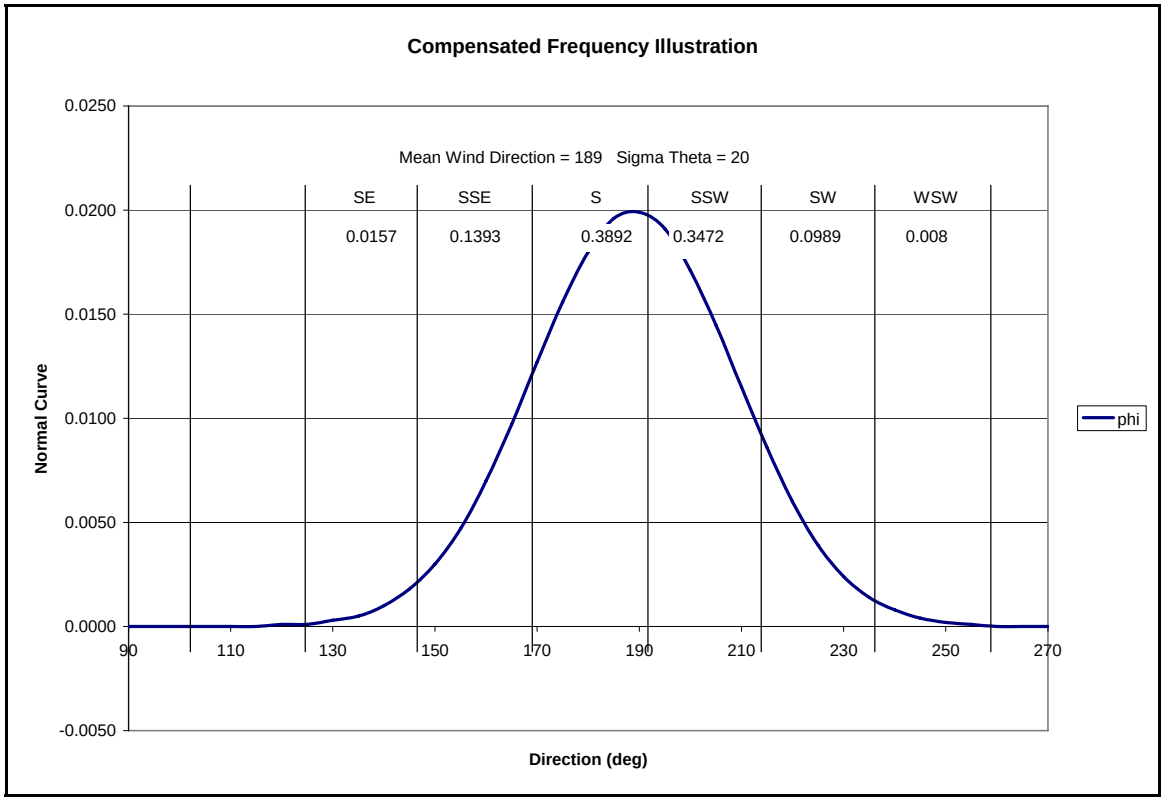

Figure 5-3. Example of a Compensated Frequency Distribution

For this study, 8-sector compensated distributions were calculated for each disk deployment period. The hourly wind direction and σ_θ data were used to calculate fractional frequencies in all 8 sectors for each hour. These were summed in each sector over all hours, and divided by the total number of hours. The compensated frequencies were used as variables in the statistical analysis presented in Section 7.

4.0 SAMPLING METHODS

The following sections describe the methodology used for the data collection for this project. Three methods are used in this process including a surrogate sample disk method, a surrogate plate method using Apiezon grease, and a high volume impactor sampler.

4.1 Dry Deposition Flux Measurements

4.1.1 Surrogate Sample Disk Method

Dry deposition flux measurements were obtained using a pre-tared 47 mm oil coated Teflon® disk mounted in a Teflon® passive sampler. The exposed surface area of the disk mounted in its holder was 39.5 mm in diameter. The oil coating is a metal-free mineral oil that provides adequate adhesion to prevent particle bounce and subsequent analyte loss. The Teflon® oil coated disks are mounted in a cassette sample holder (Figure 4-1) and were then deployed on a surrogate surface plate with leading knife edge (<10°) to prevent turbulent flow (Figure 4-2 and Figure 4-3). One to three sample disks were mounted on the plate using the three marked recessed positions so that replicate or triplicate samples could be collected.

Figure 4-1. Surrogate sample disk cartridge

Figure 4-2. Cross sectional view of the aerodynamic deposition plate. Leading edge is at an angle of 10 degrees.

Figure 4-3. View from above the aerodynamic deposition plate showing three positions available for the sample cartridges.

The 47 mm deposition disks were not touched at any time during the transfer of the disks to the sample cassettes or back to the shipping cartridge. Disks were transferred using pre-cleaned plastic or stainless steel forceps. The disks are received pre-tared from the laboratory in a disk shipping cartridge (Figure 4-4).

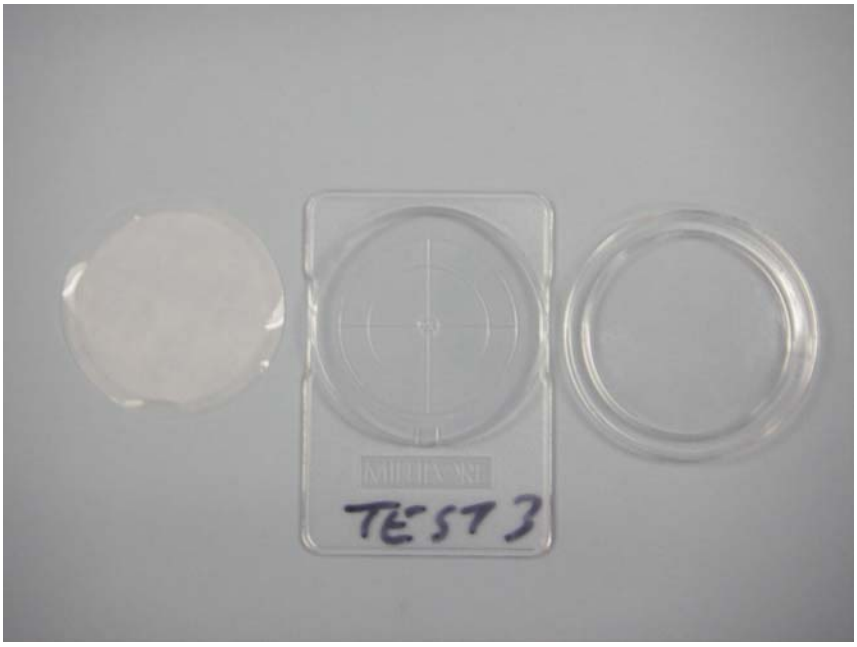

Figure 4-4. Teflon sample disk (left), shipping cartridge (middle), and cover (right).

Sample disks were removed from the shipping cartridge and were then assembled in the sample cassette (Figure 4-5). The sample cassettes were carefully separated using a pre-cleaned flat blade screwdriver. Care was taken not to damage the backing screen. The deeper inset portion of the cassette was on top.

Figure 4-5. Teflon sample disk (left), and passive sampler cassette parts, backing screen (second from left), base (second from right), and top (right)

Care was taken when assembling the disk into the passive sampler cassette so that the disk was not touched, stretched, or broken. Samplers were only assembled one day prior to the day of deployment and were labeled on the bottom with a fine point sharpie. Samplers were then enclosed in a new 5 ½ oz. plastic soufflé cup until the samples were deployed. Samples were not exposed until the moment before they are placed in the aerodynamic plate holder at the site and were removed and transferred to the laboratory under chain-of-custody in the same manner.

A field sample log was completed during each plate deployment and plate recovery. Field sample logs are provided in Appendix A.

4.1.2 Apiezon Grease Method

Aerial deposition studies have used a number of different sampling and laboratory analytical methodologies. However, there are no EPA-approved or standardized methods for deposition measurements. One commonly used method is to apply Apiezon grease to a Mylar film in a controlled environment. The grease provides adequate adhesion to prevent particle bounce and subsequent analyte loss of deposited particles. This method then requires a solvent to remove the grease from the Mylar film, the solvent evaporated, and the resulting particles digested in an acidic solution. Analysis is then performed by inductively coupled plasma mass spectroscopy (ICP-MS).

The Southern California Coastal Water Research Project (SCCWRP) was concurrently performing an aerial deposition study using this method at the mouth of Chollas Creek concurrently with the beginning of this study. The SCCWRP study was being performed to provide data inputs for the development of the TMDL model for the mouth of Chollas Creek. The surrogate surface method used by SCCWRP uses Apiezon grease that is spread over a Mylar film which is then placed on an aerodynamic PVC plate holder as shown below (Figure 4-6 and Figure 4-7).

This method is similar to the surrogate disk method described and used in this study, except for the differences in deposition substrate and the analysis by ICP-MS. The first round of sampling conducted by Weston Solutions using the oil coated Teflon® disks were collocated and coordinated with SCCWRP personnel in order to compare results of the two methodologies. The results of this pilot study are presented in Section 6.1. Upon evaluation of the two methodologies and determination of the usability of the surrogate disk method, sampling continued for the remainder of the monitoring events.

Source: Stolzenbach, 2006

Figure 4-6. 28 cm Mylar deposition plate with Apiezon grease coating and leading knife edge.

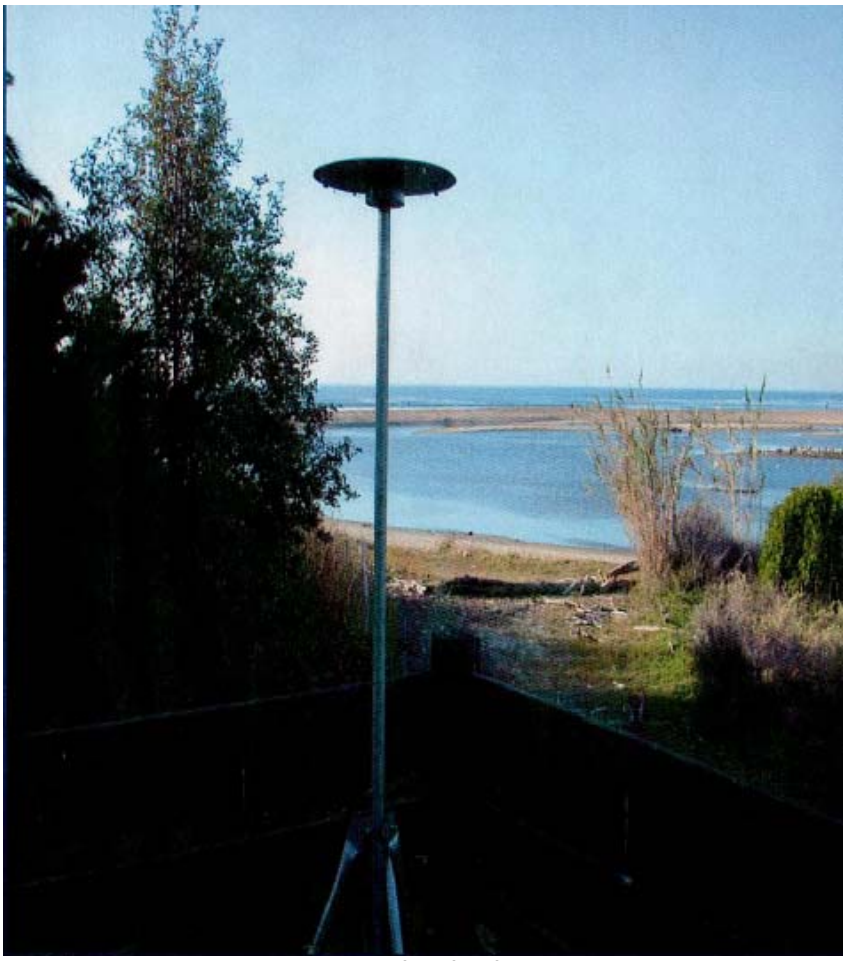

Source: Stolzenbach, 2006

Figure 4-7. 2-meter height deposition plate

4.1.3 Sample Duration

Sample disks for the area wide study and transect study were deployed for a minimum of 48 hours but no longer than 96 hours to ensure adequate loading of particulate matter to the disk surface area. Idealized sample durations for this study occurred over 72 hours (three days) from Tuesday through Friday of each week. Access to sample locations resulted in slight variations of the sample duration depending on the site.

Samples were removed in the reverse order to which they were deployed. Care was taken to ensure that samples were kept level. Samples were then placed back in the soufflé containers at the point of removal from the aerodynamic plate and then transferred back to a clean environment for sample processing.

4.1.4 Sample Deployment and Deposition Plate Location

The National Atmospheric Deposition Program Instruction Manual on Site Selection and Installation (NADP Manual 2001-01) provides guidelines on selecting stations for measuring concentrations in the air. These guidelines recommend placing collectors no less than 100 meters from transportation related sources, maintenance yards, or parking lots for local studies. The guidelines also recommend placing collectors no less than 10 km (upwind from) or 20 km (downwind from) from industrial or manufacturing sources in regional studies. These guidelines are designed to ensure representative measurements of background atmospheric conditions, rather than studying source-related impacts.

It should be made clear that the purpose of this investigation was to determine if differences in concentrations exist within the City of San Diego and to relate the locations with areas where water quality problems related to metals exist. Also, it would be nearly impossible to meet the NADP locating criteria in the highly developed and urban setting of San Diego. While the NADP guidelines are useful, they are intended to be used for regional assessments on an airshed scale rather than a watershed scale.

Fully assembled surrogate sample disks were deployed on an aerodynamic plate mounted on a pole at a minimum height of 2 meters and a maximum of 10 meters (or a single story roof top). Aerodynamic plates were also placed on existing rain gauge mounting poles where available (Figure 4-8). Sample locations were ideally located approximately two times the distance away from the tallest objects in the nearby vicinity as depicted in Figure 4-9. Samplers are also located such that there are few or no obstacles within 30 meters of the collector in a 30-degree wide corridor centered on the prevailing wind direction (as illustrated in Figure 4-10).

Figure 4-8. Aerodynamic deposition plate mounted on the rain gauge pole at site DPR(2)

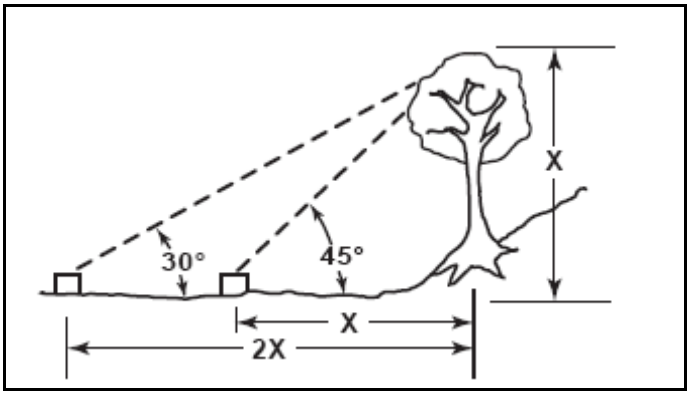

Source: NADP Manual 2001-01

Figure 4-9. Idealized distance to be located away from objects of taller height. If samplers can not be placed farther from the object, sampler height should be increased to minimize the effects of the surrounding object.

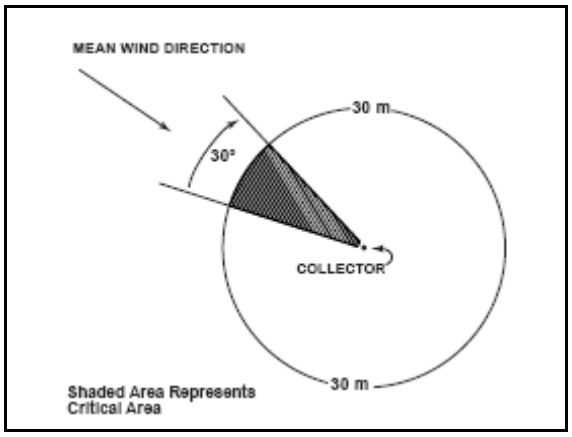

Source: NADP Manual 2001-01

Figure 4-10. Samplers should be placed in an area with respect to the critical area of effects in relation to the mean wind direction.

Each sampling event was recorded on a sample field log. Site conditions, weather, confounding factors, and other general observations were recorded for each sample deployment and sample retrieval. The dates and times of sample deployment and retrieval were recorded for each sample event immediately after each action.

Weekly area observations, weather conditions, and news events were also documented when available. This included local fires, wind and weather conditions such as fog, rain, Santa Ana winds, fireworks events, and other news that may indicate unusual site conditions that would otherwise go un-noticed during field deployments.

4.1.5 Laboratory Analyses

Samples were analyzed by Chester LabNet in Tigard Oregon for individual metals by x-ray fluorescence (XRF) following EPA Compendium Method IO-3.3 (EPA/625/R-96/010a). The samples were also analyzed for total accumulated mass by gravimetry. These analyses are non-destructive and enable further analyses to be conducted.

Upon completion of the mass and elemental analyses, a select set of samples were also sent to Chemoptix Microanalysis to be analyzed for particle size distribution and photomicrography. A qualitative analysis of the particles identified was also made and are presented as annotated photomicrographs in Appendix B. Based on the findings of the photomicrography and if significant differences were observed amongst sites, additional analyses were made on individual particles by scanning electron microscopy (SEM) and energy dispersive x-ray diffraction (EDX) to identify particles of interest.

4.2 Tisch Environmental High Volume Cascade Impactor

A Tisch Environmental High Volume Cascade Impactor Model TE-234 was used to measure the size distribution of airborne particles during the air monitoring events. The Model TE-234 sizes particles according to their aerodynamic size rather than geometric size. Aerodynamic size determines the trajectory of a particle in a gas stream because it accounts for the size, shape and, mass density of the particle. Aerodynamic diameter is important in particle collection efficiency and the transport and diffusion of particles in ambient air. Particle size cut points are determined based on the flow rate of the sampler. The particle cut-off size for each impaction jet is given in Table 4-1.

Table 4-1. Particle size fractions of impactor stages for operation at 40 scfm.

Stage #	Particle Size Range Dp, 50 * (in microns)
1	> 7.2
2	3.0 to 7.2
3	1.5 to 3.0
4	0.95 to 1.5
Hi-vol Filter	< 0.95
* (Dp,50) The cut-points are experimental values obtained from the calibration with mono-disperse aerosols	

The Model TE-234 was operated at a nominal flow rate of 40 scfm (standard cubic feet/minute @760mm Hg and 25°C). Type A slotted 5.625 x 5.375 inch pre-tared quartz filter media were used for the collection substrate on the four impactor stages. The substrates are thin flat sheets with 10 perforated slots. During operation, the vacuum motor pulls air through the stacked impactor stages. Airborne particulate matter passes through the slotted jets in the impactor stages. Particles impact on the collection substrates and are thereby deposited or collected based on their momentum (aerodynamic size). At each stage, particles larger than the stage's cut point

are unable to negotiate the curved path to pass to the next stage, and impact on that stage's substrate. Smaller particles continue through to subsequent stages until they either impact another substrate or are collected on the final hi-vol filter (a filter with no slots).

The impactor was deployed for 12-hour continuous sampling events. One impactor sampling event was performed for each site location. Sampling events were scheduled to occur concurrently during the deployment of the oil-coated Teflon® deposition disks to allow comparisons between the snapshot airborne particle size distributions and the particles that were deposited on the disks.

Impactor samples were sent to Chester LabNet and were analyzed for copper, chromium, lead, zinc, and iron by inductively coupled plasma optical emission spectroscopy (ICP-OES). Samples were also analyzed gravimetrically for the total mass collected per sample and per size fraction. Each impactor sample therefore consisted of five individually analyzed samples: the four slotted substrates and the hi-vol filter.

4.3 Analytical Methods

Several laboratory analytical techniques were used to analyze sample media collected during this study. Energy dispersive x-ray fluorescence (XRF) was used to analyze the surrogate deposition disks while digestion and analysis using inductively coupled argon plasma-optical emission spectroscopy (ICP-OES) was used to analyze the high volume impactor samples. Samples analyzed by SCCWRP during the pilot study used digestion and analysis by inductively coupled argon plasma-mass spectroscopy (ICP-MS). Photomicroscopy and particle size distribution were performed on selected surrogate deposition disk samples. Samples of interest were further analyzed by scanning electron microscopy/energy dispersive x-ray fluorescence (SEM-EDX) to identify representative particles from the surrogate deposition disk samples. The following subsections further describe each method.

4.3.1 Energy Dispersive X-Ray Fluorescence

Surrogate deposition disks collected from the area wide and transect studies were analyzed by EPA Compendium Method IO-3.3 (EPA/625/R-96/010a) using energy dispersive x-ray fluorescence (XRF). Analysis was performed by Chester LabNet in Tigard, Oregon. Total mass deposited on the pre-tared deposition disks was measured by gravimetry prior to XRF analysis. Chester LabNet uses a Kevex EDX-770 energy dispersive x-ray spectrometer which utilizes secondary excitation from selectable targets or fluorescers and is calibrated with thin metal foils and salts for 44 chemical elements. Spectra are acquired by menu-driven procedures and stored for off-line processing. Spectral deconvolution is accomplished by a least squares algorithm which fits stored pure element library spectra and background to the sample spectrum under analysis. X-ray attenuation corrections are tailored to the fine particle layer and the discrete coarse particle fraction. Spectral interferences are corrected by a subtractive coefficient determined during calibration. The detection limits are determined by propagation of errors in which the magnitude of error from all measured quantities is calculated or estimated as appropriate. Data are reported in µg/filter for all samples including the analytical uncertainty for each element. Comprehensive quality control measures are taken to provide data on a broad

range of parameters, excitation conditions and elements. Elements analyzed for this project are presented in Table 4-2. Protocol 6 was used for the elements sodium through cobalt and palladium through lanthanum. All other elements listed (including copper, lead, and zinc) were analyzed using Protocol 9 which provides roughly an order of magnitude lower detection capability.

Comprehensive quality control measures are taken to provide data on a broad range of parameters, excitation conditions and elements. Each analytical batch of samples includes the analysis of precision and accuracy data. Precision is measured using a Micromatter Multi-elemental Quality Control Standard. Accuracy is measured using a National Institute of Standards and Technology Standard Reference Material (NIST SRM 1832 and 1833).

Table 4-2. Analyte List and Detection Limits for Surrogate Deposition Disks

Interference-Free Detection Limits (µg/filter) For 47mm Teflon Filters		
Element	XRF Protocol Number	
	6	9
Sodium (Na)	1.695	-
Magnesium (Mg)	0.203	-
Aluminum (Al)	0.090	-
Silicon (Si)	0.063	-
Phosphorus (P)	0.054	-
Sulfur (S)	0.045	-
Chlorine (Cl)	0.054	-
Potassium (K)	0.034	-
Calcium (Ca)	0.022	-
Titanium (Ti)	0.016	-
Vanadium (V)	0.011	-
Chromium (Cr)	0.011	-
Manganese (Mn)	0.018	-
Iron (Fe)	0.014	-
Cobalt (Co)	0.010	-
Nickel (Ni)	-	0.005
Copper (Cu)	-	0.005
Zinc (Zn)	-	0.005
Gallium (Ga)	-	0.010
Germanium (Ge)	-	0.009
Arsenic (As)	-	0.008
Selenium (Se)	-	0.007
Bromine (Br)	-	0.006
Rubidium (Rb)	-	0.007
Strontium (Sr)	-	0.008
Yttrium (Y)	-	0.010
Zirconium (Zr)	-	0.012
Molybdenum (Mo)	-	0.017
Palladium (Pd)	0.081	-
Silver (Ag)	0.086	-
Cadmium (Cd)	0.088	-
Tin (Sn)	0.154	-
Antimony (Sb)	0.123	-
Indium (In)	0.224	-
Barium (Ba)	0.949	-
Lanthanum (La)	0.580	-
Mercury (Hg)	-	0.017
Lead (Pb)	-	0.019
"-" not applicable Deposit Area (cm^2)		11.3

4.3.2 ICP – OES

Quartz media from high volume impactor samples were analyzed following EPA Method 200.7 using inductively coupled argon plasma-optical emission spectroscopy (ICP-OES). Analysis was performed by Chester LabNet in Tigard, Oregon. Each sample filter stage was pre-tared prior to use and was weighed by the laboratory after 24 hours of equilibration. The quartz media filters were then digested in a strong acid solution and analyzed by ICP-OES. Elements analyzed and detection limits are presented in Table 4-3.

Table 4-3. Analyte List and Detection Limits for Quartz Media Filters

Element	Detection Limit (µg/filter)
Chromium (Cr)	0.05
Iron (Fe)	0.49
Copper (Cu)	0.49
Zinc (Zn)	0.12
Lead (Pb)	1.22
Extraction Area (cm^2) = 66.4	

Each analytical batch of samples includes the analysis of preparation blanks, method blanks, laboratory control samples, matrix spike samples and duplicate samples.

4.3.3 ICP – MS

Samples collected from the mouth of Chollas Creek for the pilot study were collected simultaneously as the samples for XRF for comparison of the two collection and analytical methods. Samples were collected by SCCWRP personnel and submitted to CRG Marine Laboratories, Inc in Carson, CA for analysis. Mylar film samples coated with Apiezon grease were solvent extracted, digested in a strong acid, and analyzed by inductively coupled argon plasma mass spectrometry (ICP-MS) detection using EPA Method 200.8. Elements analyzed and detection limits are presented in Table 4-4.

Each analytical batch of samples included the analysis of method blanks, laboratory control samples, and duplicate samples.

Table 4-4. Analyte List and Detection Limits for Mylar Coated Apiezon Grease Samples

Analyte	Reporting Limit (µg/filter)
Aluminum (Al)	0.01
Antimony (Sb)	0.0005
Arsenic (As)	0.0005
Barium (Ba)	0.0005
Beryllium (Be)	0.0005
Cadmium (Cd)	0.0004
Chromium (Cr)	0.0005
Cobalt (Co)	0.0005
Copper (Cu)	0.0008
Iron (Fe)	0.01
Lead (Pb)	0.0001
Manganese (Mn)	0.0005
Molybdenum (Mo)	0.0005
Nickel (Ni)	0.0005
Selenium (Se)	0.0005
Silver (Ag)	0.001
Strontium (Sr)	0.0005
Thallium (Tl)	0.0005
Tin (Sn)	0.0005
Titanium (Ti)	0.0005
Vanadium (V)	0.0005
Zinc (Zn)	0.0005

4.3.4 Photomicroscopy and Particle Size Distribution

Surrogate deposition disks collected from the area wide and transect studies were submitted to Chemoptix Microanalysis, Inc. in West Linn, Oregon following XRF analysis. Sample disks from the area wide and the initial transect study were submitted for photomicroscopy and particle size distribution (PSD)

analyses. Sample disks from the I-805 transect study were submitted for photomicroscopy only due to a change in the disk manufacturer during the course of the study. The change in disk types did not allow for PSD analysis due to the reflective nature of the disk material. Samples for microscopy were selected based on the sample results and interest in particle size distribution for selected samples. The sample disks were photographed using a SPOT RT digital camera with image analysis by Image Pro Plus at 100x magnification. Qualitative identification of particles was made for each sample disk submitted. The qualitative or annotated photomicrographs provide a visual understanding of the type, amount, and depositional characteristics of the particles from each site. Annotated photomicrographs were prepared based on laboratory experience and are provided in Appendix B.

Particle size distribution by ASTM Method F312-97 was completed using a Zeiss Universal research microscope equipped with NIST traceable optics. Particle size distribution performed on sample disks submitted for XRF provides the benefit of determining the relative particle size distribution of the samples to which deposition is occurring. This method is different than the atmospheric size distribution measured using the impactor sampler which only measures the particle size distribution in the air. However, the PSD analysis performed here does not provide a breakdown of the concentration by size fraction. The number of particles per square centimeter and the relative area are provided for each particle size range. Particle size ranges in microns are 0.8-2, 2-5, 5-15, 15-25, 25-50, 50-100, and 100-1000 respectively.

4.3.5 Scanning Electron Microscopy/Energy Dispersive X-Ray Diffraction

Particles on the original disk membrane surface were removed both by dissection of specific particles, and by blotting with a sticky carbon substrate during examination under a stereo microscope. Samples were then put in a vacuum chamber and analyzed via scanning electron microscopy/energy dispersive x-ray diffraction (SEM/EDX) and backscattering. SEM/EDX provides a qualitative analytical identification of the particles elemental composition. An estimated 300 particles were examined for each sample; particles showing high electron density were analyzed via EDX and a light element detector. Some low-density particles were similarly analyzed. When possible, scanned particles were reexamined optically with brightfield and darkfield episcopic illumination.

3.0 LAND USE ANALYSIS

The City of San Diego is highly urbanized. Aerial deposition is often a function of the sources and activities that occur in specific regions. Several studies reviewed prior to initiating this project suggest that the majority of particles greater than 2.5 um will generally settle out (or deposit) within 1000 meters of the emission source. To better understand the observed results from the sample stations selected, land use analysis was employed to characterize the sample sites within 1000 meters. Land use information combined with directional wind data may also indicate the likely sources of pollution.

3.1 Site Descriptions and Spatial Assessment

This section provides descriptions of the sample locations and spatial analysis for sites used in the Area-Wide and Transect studies. A total of ten study sites were located throughout the San Diego area (Figure 3-1).

A Geographical Information System (GIS) was utilized to create "buffer zones of influence" and "wind direction sectors" in order to characterize the landscape of each site. To accomplish this, a series of five different "buffer zones" or concentric circles were generated, each originating at the sample location and extending out at radii of 25 m, 100 m, 250 m, 500 m, and 1,000 m in order to characterize land use patterns within the immediate area defined by the concentric circles near each site. Each circle was subdivided into eight wind direction sectors, centered on the eight compass points (north, northeast, east, etc.). At each sampling site, the total amount of land area that lies within each land use class was calculated within each buffer and prominent wind direction sector. The results of this spatial analysis provide information to help examine relationships between observed aerial deposition, land use, and proximity to nearby roadways. The results are illustrated for each site, respectively, and discussed further in Section 7.

A GIS database of current regional land use developed by the San Diego Association of Governments (SANDAG, 2006) was used to develop the land use summaries. The land use classifications in the SANDAG database include approximately 100 specific land use codes. For this spatial analysis, the land use codes found within the 1000 m site buffer regions were grouped into eight general categories:

- Low Density Residential
- High Density Residential
- Industrial
- Freeways
- Transportation [including surface street right of ways (ROWs)]
- Commercial
- Open Space and Parks
- Water

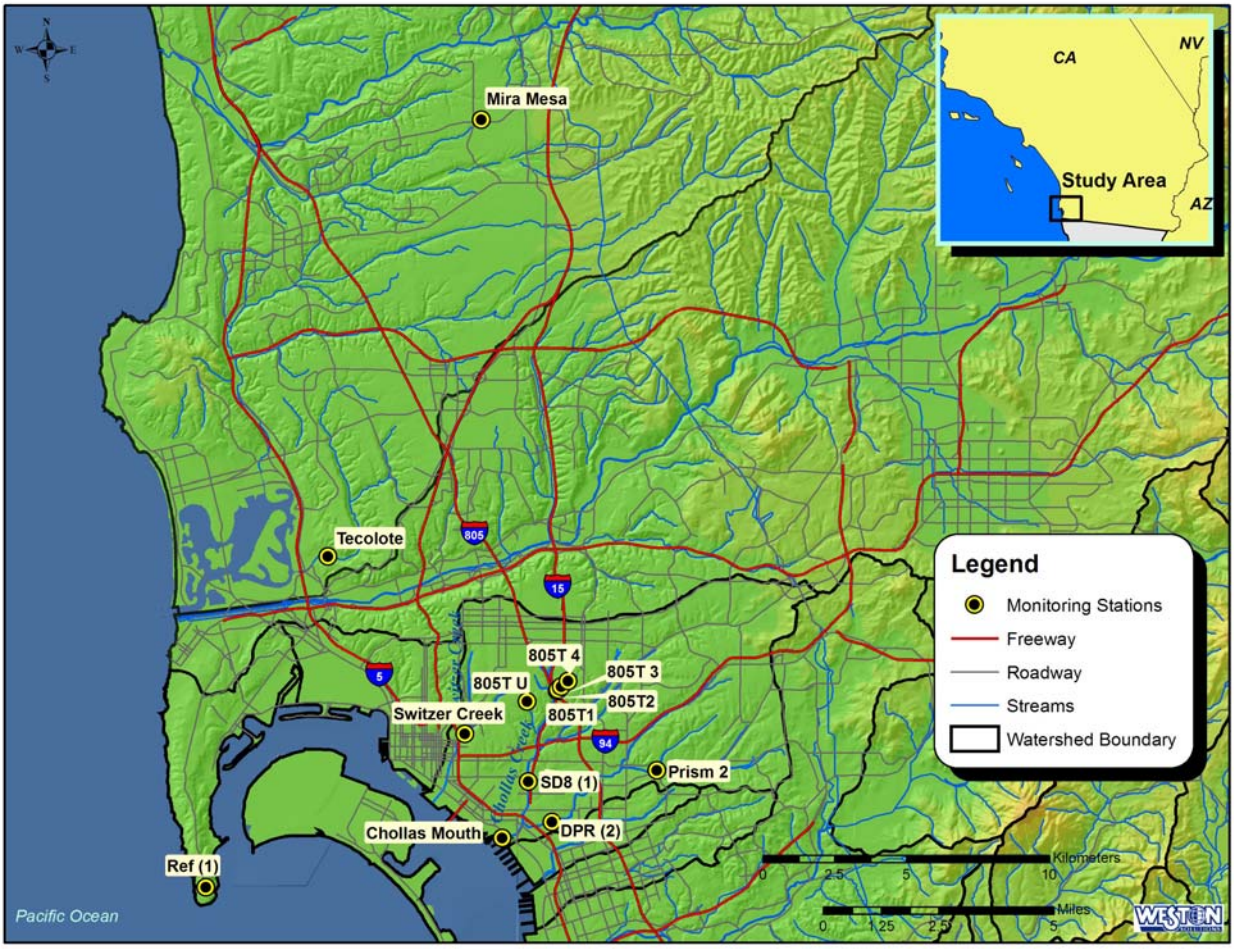

Figure 3-1. Sample site locations.

3.1.1 Area-Wide Study Sites

Sites are described regionally from north to south in this section, with the exception of the study reference site which is described first. Sites 805T-UP and 805T1 were included in the Area-Wide study analysis but are described as part of the Transect Study sites in Section 3.1.2.

3.1.1.1 Reference Site- Ref(1)

Site Ref(1) (32.735278ºN 117.360278ºW, elevation – 409 feet) was located within Cabrillo National Monument near the southern end of Point Loma. The site was bounded by the Pacific Ocean to the west and south and by San Diego Bay to the east. This site was chosen as a reference location due to its location within a federally protected park with limited traffic and little development. The deposition surrogate sample plate was mounted on the northwest corner of the fence that surrounds Navy Bunker T-17, south of the old lighthouse, at 2.3 m above the ground. The Point Loma Wastewater Treatment Plant was located approximately 1 km northwest of the sample site. There are also several unidentified U.S. Navy facilities located approximately one mile to the north of the site on the western edge of Point Loma. Low flying aircraft bound for North Island Naval Air Station on Coronado Island may also fly over the site.

The predominant land use within the 1000 m concentric circle of the site was water (60.6%), followed by open space/parks and recreation (27.2%) and commercial (8.6%) (SANDAG, 2006). The total percentage of impervious surface within the 1000 m circle was approximately 17.7% (Figure 3-2).

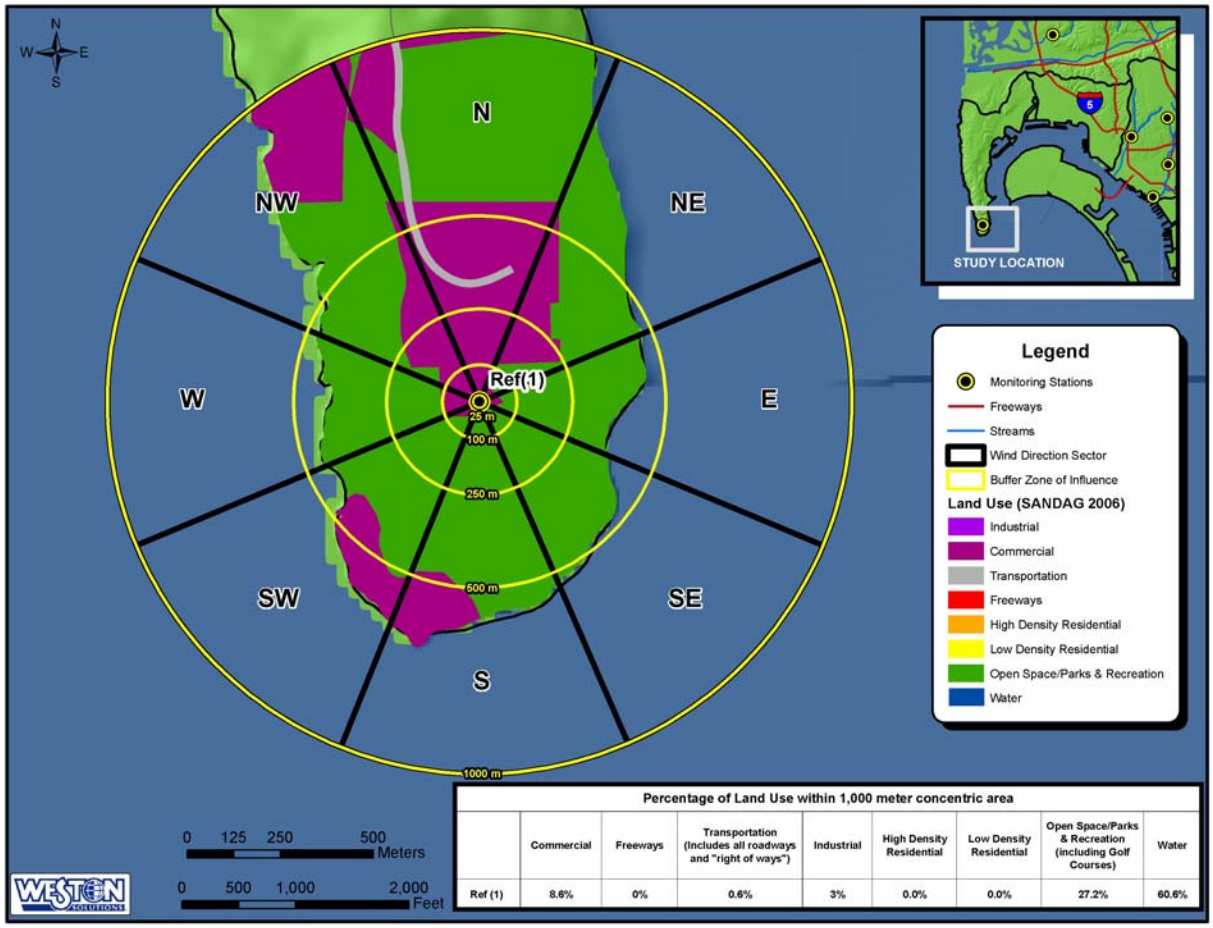

Percentage of Land Use within 1,000 meter concentric area

	Commercial	Freeways	Transportation (Includes all roadways and "right of ways")	Industrial	High Density Residential	Low Density Residential	Open Space/Parks & Recreation (including Golf Courses)	Water
Ref (1)	8.6%	0%	0.6%	3%	0.0%	0.0%	27.2%	60.6%

Figure 3-2. Land use of area surrounding Point Loma reference location.

3.1.1.2 Mira Mesa

Site Mira Mesa (32.91345°N 117.14089°W, elevation – 435 feet) was located close to the northern boundary of the San Diego city limits in Mira Mesa Park. The site was bounded by a large commercial area located to the west and the intersection of Mira Mesa Boulevard and Camino Ruiz located to the southwest. The Mira Mesa site was chosen to represent a high volume surface street area, as Mira Mesa Blvd. is a major thoroughfare between the I-15 and I-805 freeways. The deposition surrogate sample plate was fixed atop a traffic sign near the middle of the parking lot at an elevation of 2.7 m in order to locate the plate as far as possible from any vertical obstruction as well as to minimize the visual exposure of the plate.

The predominant land uses within the 1000 m concentric circle of the site were low density residential (35.5%), transportation (21.6%), Commercial (20.5%), and High Density Residential (17.8%) (SANDAG, 2006). The total percentage of impervious surface within the 1000 m circle was approximately 63.7% (Figure 3-3).

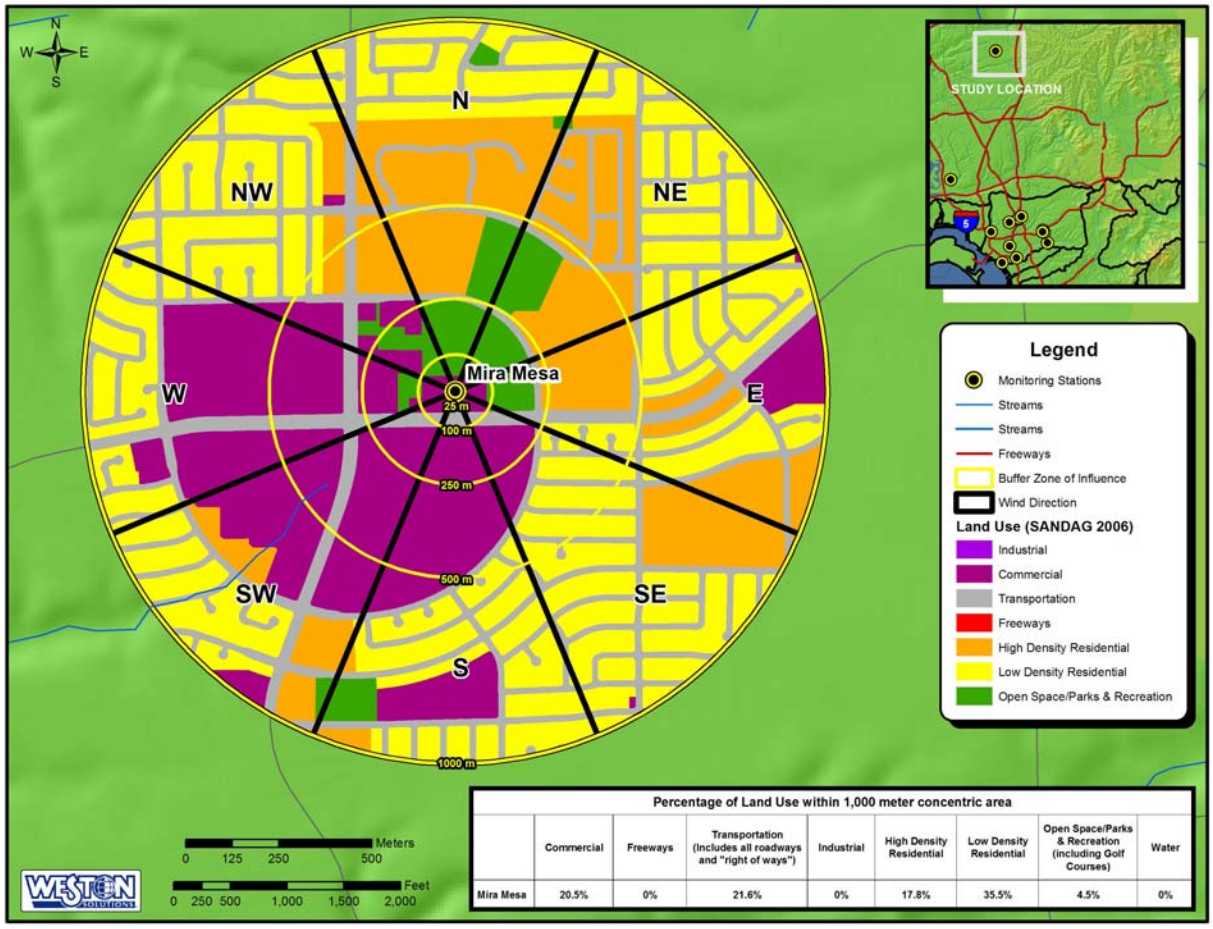

Percentage of Land Use within 1,000 meter concentric area

	Commercial	Freeways	Transportation (Includes all roadways and "right of ways")	Industrial	High Density Residential	Low Density Residential	Open Space/Parks & Recreation (including Golf Courses)	Water
Mira Mesa	20.5%	0%	21.6%	0%	17.8%	35.5%	4.5%	0%

Figure 3-3. Land use of area surrounding Mira Mesa sampling location.

3.1.1.3 Tecolote

Site Tecolote (32.77541°N 117.19671°W, elevation – 45 feet) was located within the Tecolote Canyon Natural Park near the eastern border of Mission Bay. The site was bounded by residential neighborhoods to the north and south and by an undeveloped canyon to the east. The site was chosen to represent a low urban traffic volume setting; as the nearest publicly-accessible roadway was approximately 150 m west of the sample site and provided limited traffic flow in and out of the park at a posted speed limit of 15 miles per hour (mph). However, the site was also approximately 1 km east of the I-5 freeway. The deposition surrogate sample plate was mounted atop a portable concrete pier base at an elevation of approximately 2 m above the ground inside a secure fence within the park.

The predominant land uses within the 1000 m concentric circle of the site were low density residential (36.1%), transportation (20.7%), Open Space/Parks & Recreation (19.9%) and Commercial (16.5%) (SANDAG, 2006). The total percentage of impervious surface within the 1000 m circle was approximately 57.6% (Figure 3-4).

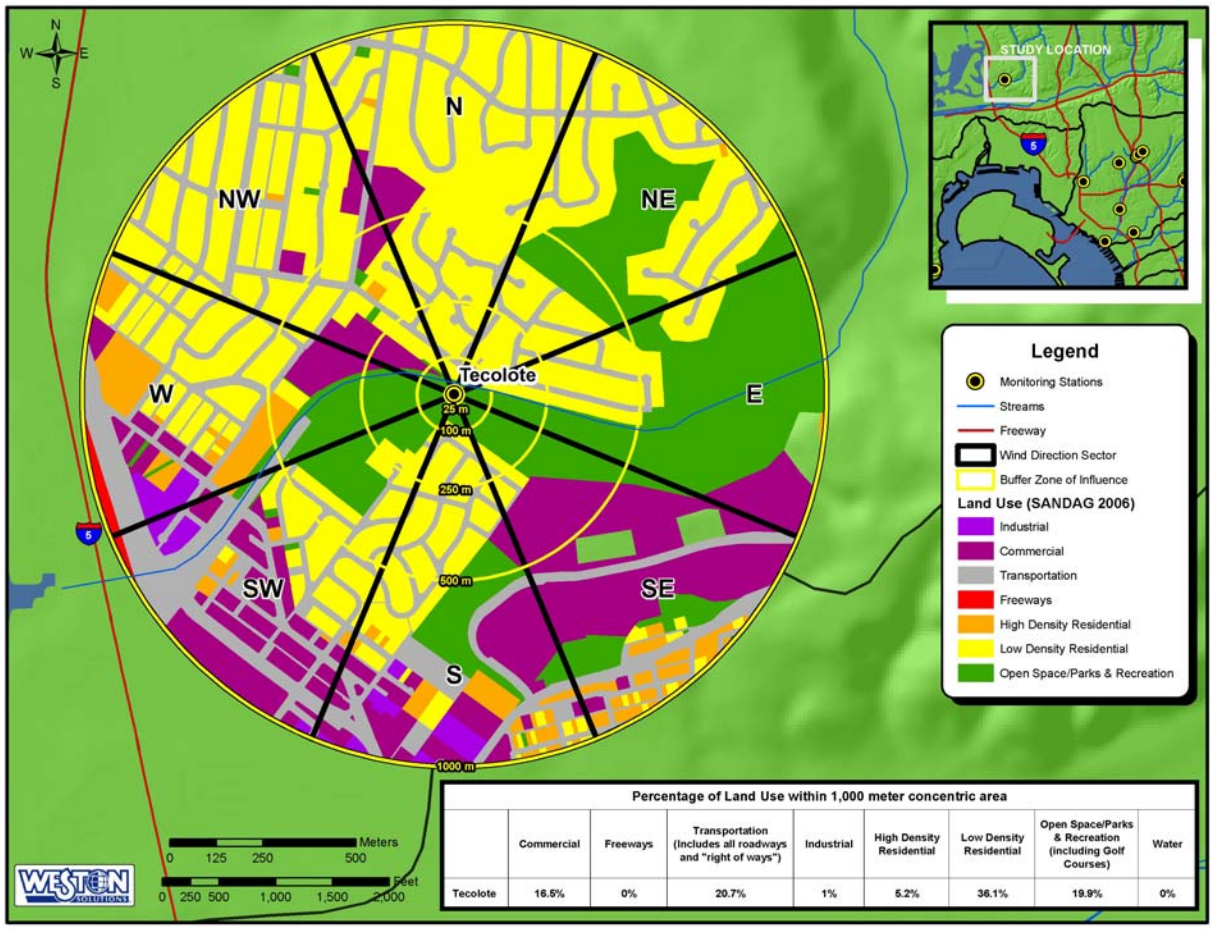

Percentage of Land Use within 1,000 meter concentric area

	Commercial	Freeways	Transportation (Includes all roadways and "right of ways")	Industrial	High Density Residential	Low Density Residential	Open Space/Parks & Recreation (including Golf Courses)	Water
Tecolote	16.5%	0%	20.7%	1%	5.2%	36.1%	19.9%	0%

Figure 3-4. Land use of area surrounding Tecolote sampling location.

3.1.1.4 Switzer Creek

Site Switzer Creek (32.71990°N 117.14512°W, elevation – 81 feet.) was located at 1970 B Street near the southern edge of Balboa Park. The site was bounded by park and residential areas to the east and south and was adjacent to Pershing Drive. The site was chosen to be representative of the downtown San Diego area, with high urban surface street traffic volume. The site was adjacent to the drainage basin of Powerhouse Canyon and approximately 300 m to the east of Interstate 5. The freeway at this location is elevated approximately 30 feet above the surface and is generally upwind of the sample location based on the prevailing westerly winds. The deposition surrogate sample plate was mounted to a fence on the northwest side of the facility 2.7 m above the ground.

The predominant land uses within the 1000 m concentric circle of the site were commercial (26.5%), transportation (25.0%), and Open Space/Parks & Recreation (SANDAG, 2006). The total percentage of impervious surface within the 1000 m circle was approximately 57.6% (Figure 3-5).

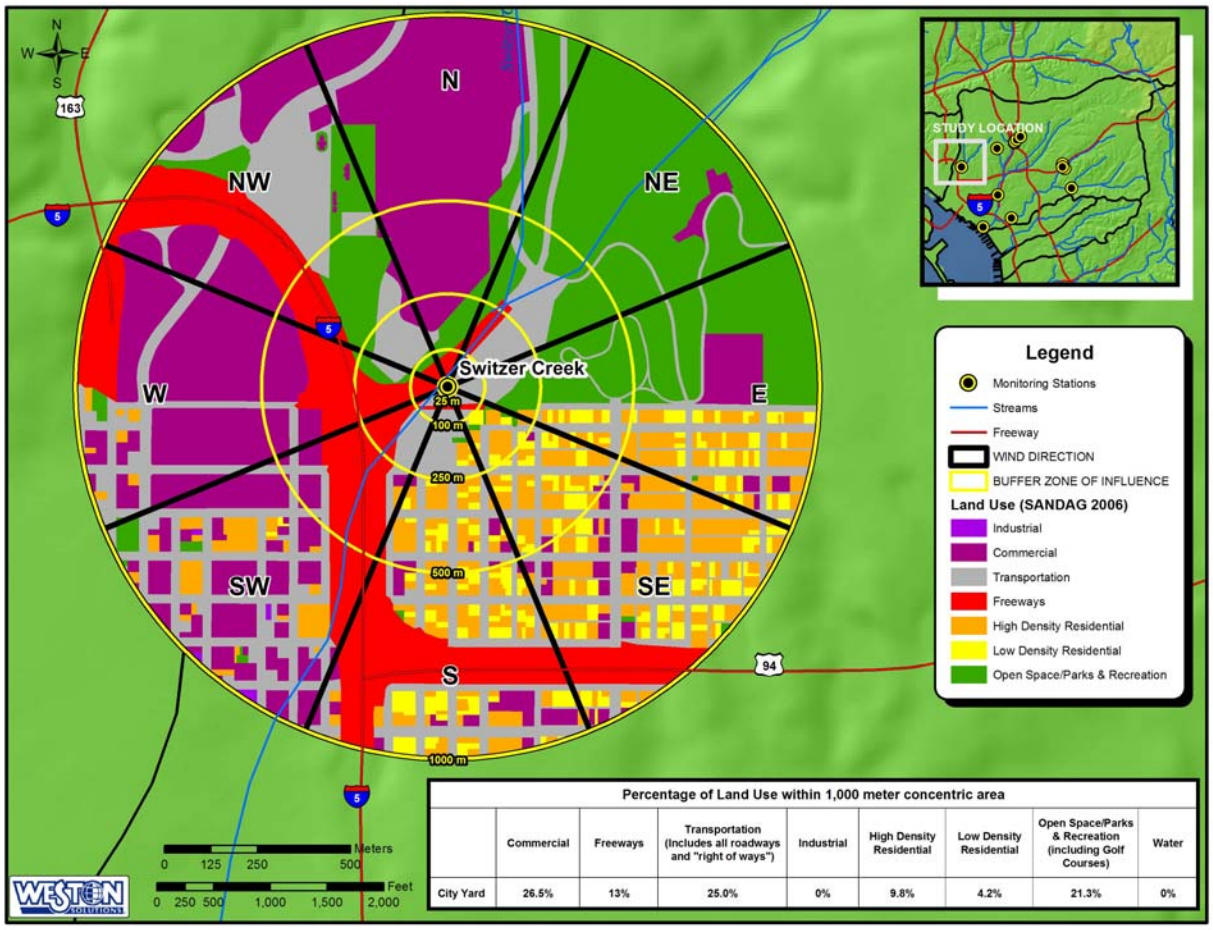

Percentage of Land Use within 1,000 meter concentric area

	Commercial	Freeways	Transportation (Includes all roadways and "right of ways")	Industrial	High Density Residential	Low Density Residential	Open Space/Parks & Recreation (including Golf Courses)	Water
City Yard	26.5%	13%	25.0%	0%	9.8%	4.2%	21.3%	0%

Figure 3-5. Land use of area surrounding Switzer Creek sampling location.

3.1.1.5 SD8(1)

Site SD8(1) (32.78222ºN 117.19417ºW, elevation – 38 feet) was located in a primarily residential neighborhood near the South Fork of Chollas Creek. The site was bounded by residential neighborhoods to the north and south and was located near a low urban surface street traffic volume setting. The nearest publicly-accessible roadway was a cul-de-sac with a posted speed limit of 25 mph. The I-15 freeway was located approximately 45 m to the east, or downwind, based on the prevailing west wind. The adjacent freeway was considered to have a particulate mixing zone that included the site. The site was approximately 400 m east of Commercial Street, which has numerous potential point sources such as auto wrecking yards, and sandblasting and painting facilities. The deposition surrogate sample plate was mounted atop the rain gauge mounting pole of the San Diego County Municipal Storm Water Program mass loading station at an elevation of 3.4 m above the ground.

The predominant land uses within the 1000 m concentric circle of the site were low density residential (29.8%) and transportation (25.7%) (SANDAG, 2006). The total percentage of impervious surface within the 1000 m circle was approximately 62.6% (Figure 3-6).

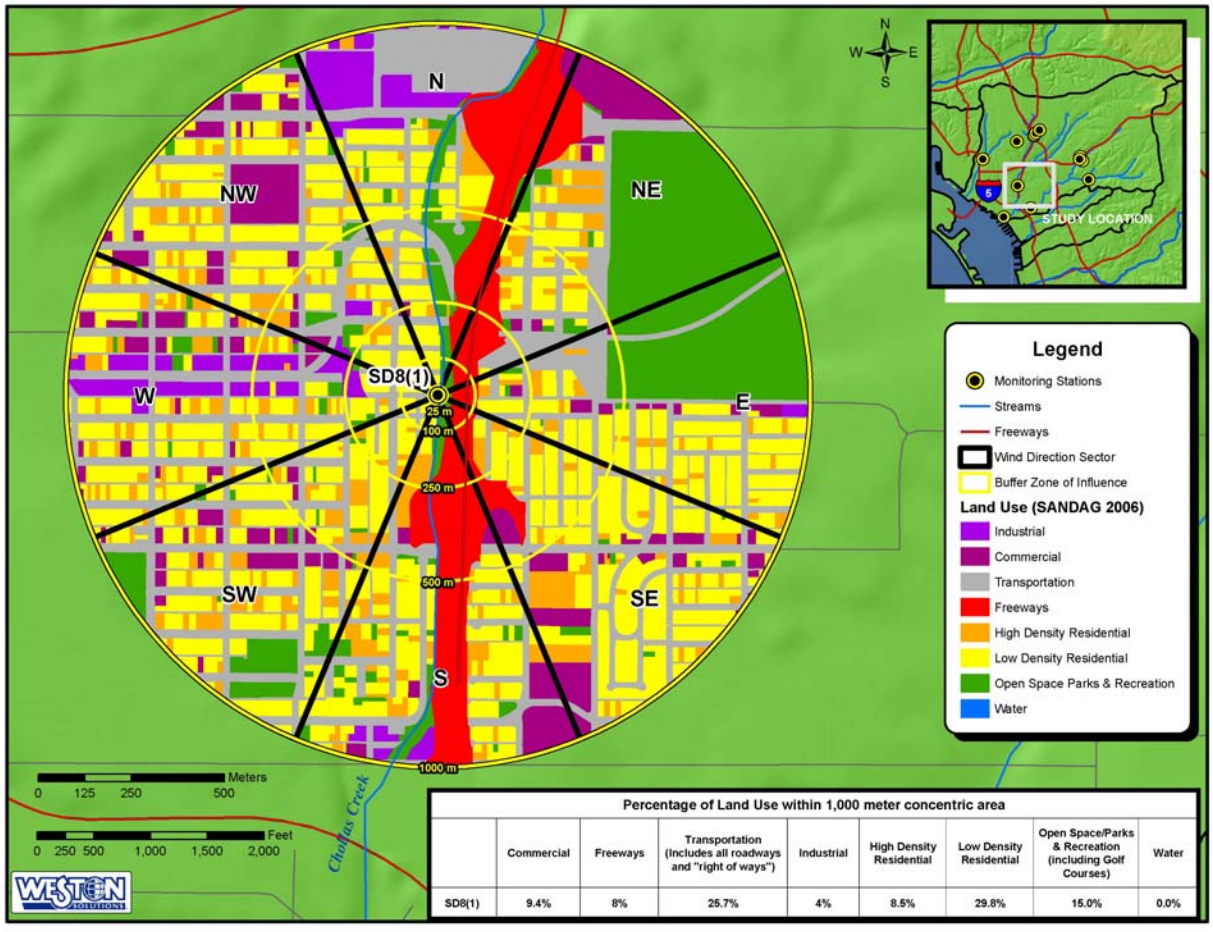

Percentage of Land Use within 1,000 meter concentric area

	Commercial	Freeways	Transportation (Includes all roadways and "right of ways")	Industrial	High Density Residential	Low Density Residential	Open Space/Parks & Recreation (including Golf Courses)	Water
SD8(1)	9.4%	8%	25.7%	4%	8.5%	29.8%	15.0%	0.0%

Figure 3-6. Land use of area surrounding SD8(1) sampling location.

3.1.1.6 DPR(2)

Site DPR(2) (32.69227ºN 117.11232°W, elevation – 16 feet) was located in a primarily residential neighborhood adjacent to 38th Street near the intersection of 38th Street and Alpha and located next to the south fork of Chollas Creek. The site was chosen to represent a low traffic volume, urban surface street traffic setting. The site was bounded by residential neighborhoods to the north and south and was approximately 700 m east of the I-5 freeway. The deposition surrogate sample plate was mounted atop the rain gauge mounting pole of a City of San Diego Municipal Storm Water Program mass loading station at an elevation of 3.4 m above the ground.

The predominant land uses within the 1000 m concentric circle of the site were low density residential (32.0%) and transportation (23.3%) (SANDAG, 2006). The total percentage of impervious surface within the 1000 m circle was approximately 64.3% (Figure 3-7).

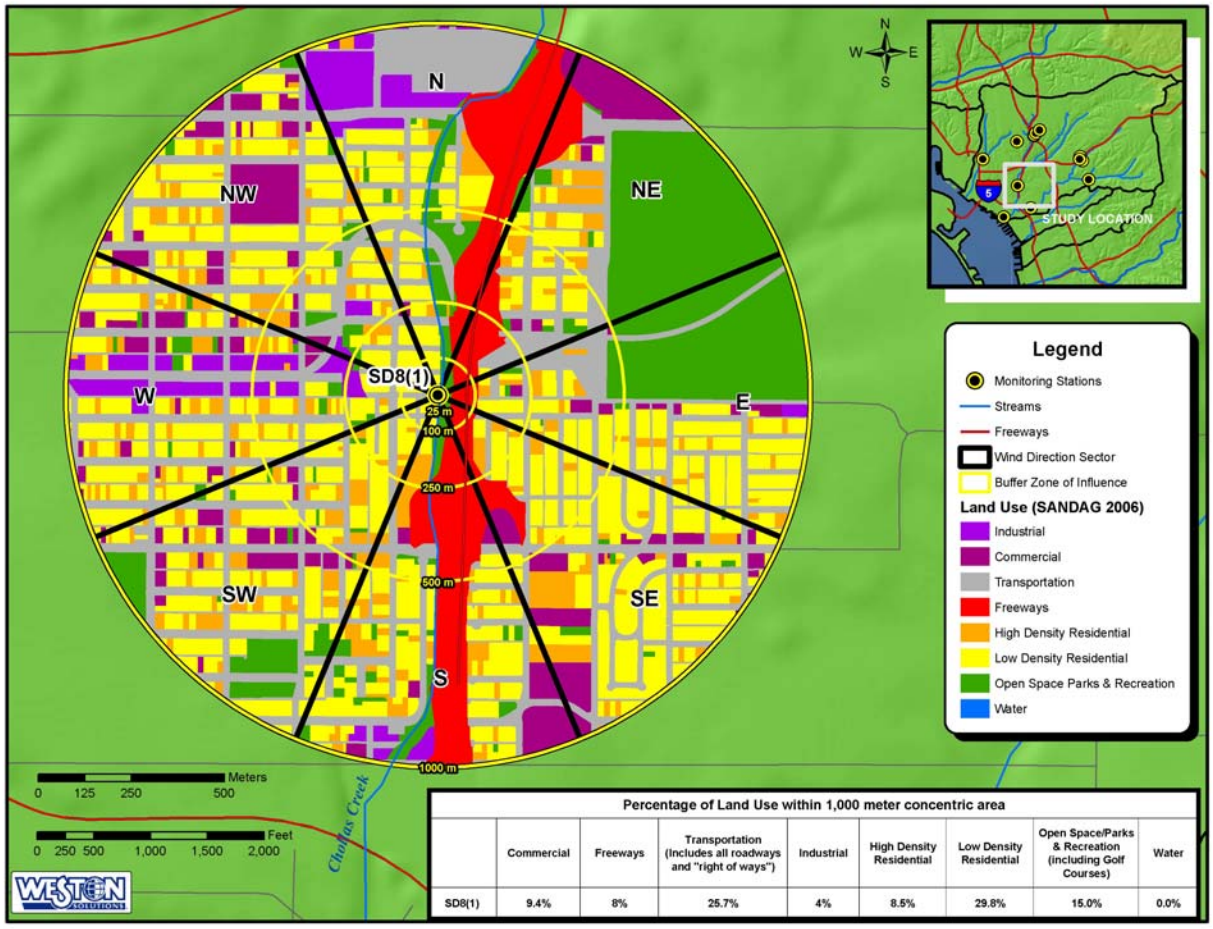

Percentage of Land Use within 1,000 meter concentric area

	Commercial	Freeways	Transportation (Includes all roadways and "right of ways")	Industrial	High Density Residential	Low Density Residential	Open Space/Parks & Recreation (including Golf Courses)	Water
SD8(1)	9.4%	8%	25.7%	4%	8.5%	29.8%	15.0%	0.0%

Figure 3-7. Land use of area surrounding DPR(2) sampling location.

3.1.1.7 PRISM 2

Site PRISM 2 (32.70886ºN 117.07350ºW, elevation – 14 feet) was located in a mixed commercial, residential, and open space area near the south fork of Chollas Creek. The site was bounded by residential neighborhoods and open space to the north, east, and south and by a mix of residential and commercial uses to the west. The site was chosen to be representative of a medium traffic volume, urban surface street setting and was near the intersection of Stevens Way and Imperial Avenue. The San Diego Trolley System Orange Line and Market Street were both located north of the site by approximately 75 m and 150 m, respectively. The deposition surrogate sample plate was mounted atop the rain gauge mounting pole of the City of San Diego Storm Water Program mass loading station at an elevation 3.4 m above the ground. Imperial Avenue, the Orange Line and Market Street all run parallel to the prevailing wind direction with this site.

The predominant land uses within the 1000 m concentric circle of the site were low density residential (49.4%) and transportation (20.4%) (SANDAG, 2006). The total percentage of impervious surface within the 1000 m circle was approximately 55.5% (Figure 3-8).

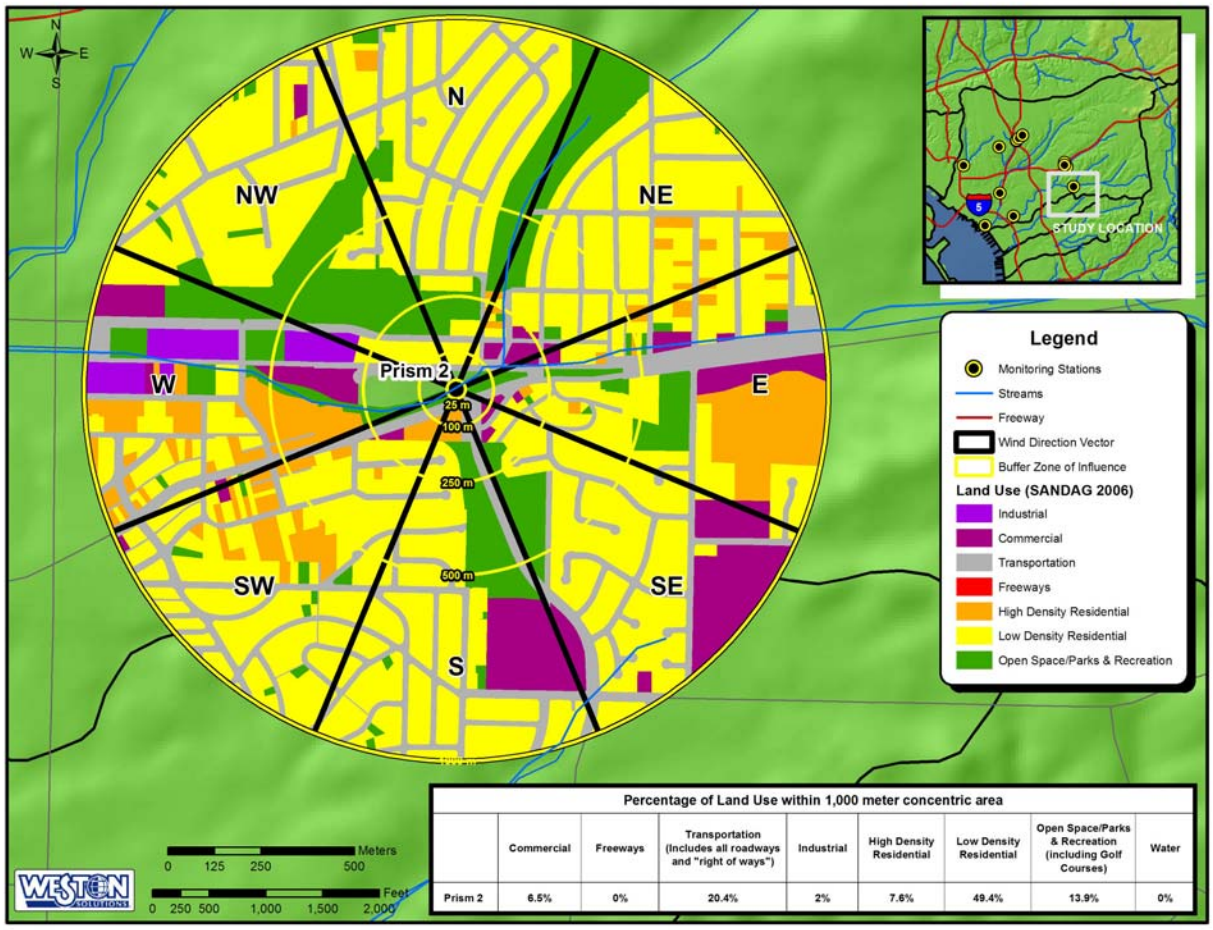

Percentage of Land Use within 1,000 meter concentric area

	Commercial	Freeways	Transportation (Includes all roadways and "right of ways")	Industrial	High Density Residential	Low Density Residential	Open Space/Parks & Recreation (including Golf Courses)	Water
Prism 2	6.5%	0%	20.4%	2%	7.6%	49.4%	13.9%	0%

Figure 3-8. Land use of area surrounding PRISM2 sampling location.

3.1.1.8 Chollas Mouth

Site Chollas Mouth (32.68770°N 117.13077°W, elevation – 9 feet) was located within the Naval Station San Diego near the intersection of 32nd Street and East Harbor Drive. The sample site was located directly adjacent and on the south side of the Mouth of Chollas Creek. The Chollas Mouth site was also approximately 400 m to the east from the General Dynamics NASSCO Shipyard. During the deployment event series, several large ships were docked nearby undergoing repairs or were under construction. The oil tanker Alaskan Legend was in port prior to the first deployment on June 26, 2006 and departed the General Dynamics NASCCO facility during the week of August 22, 2006. Another unidentified vessel was docked beginning August 23, 2006. The deposition surrogate sample plate was mounted on a portable concrete pier base on top of the Port Operations Building #150 at an elevation of 2 m above the building roof and 6.2 m above the ground.

The Chollas Mouth site was also chosen in order to co-locate and sample concurrently with, the Southern California Coastal Water Research Project (SCCWRP) program for method and sample comparisons. The SCCWRP program is being performed to support the TMDL model being developed for the mouth of Chollas Creek and utilizes the Apiezon grease method to measure aerial deposition.

The predominant land uses within the 1000 m concentric circle of the site were water (36.2%) and industrial (29.4%) (SANDAG, 2006). The total percentage of impervious surface within the 1000 m circle was approximately 64.3% (Figure 3-9).

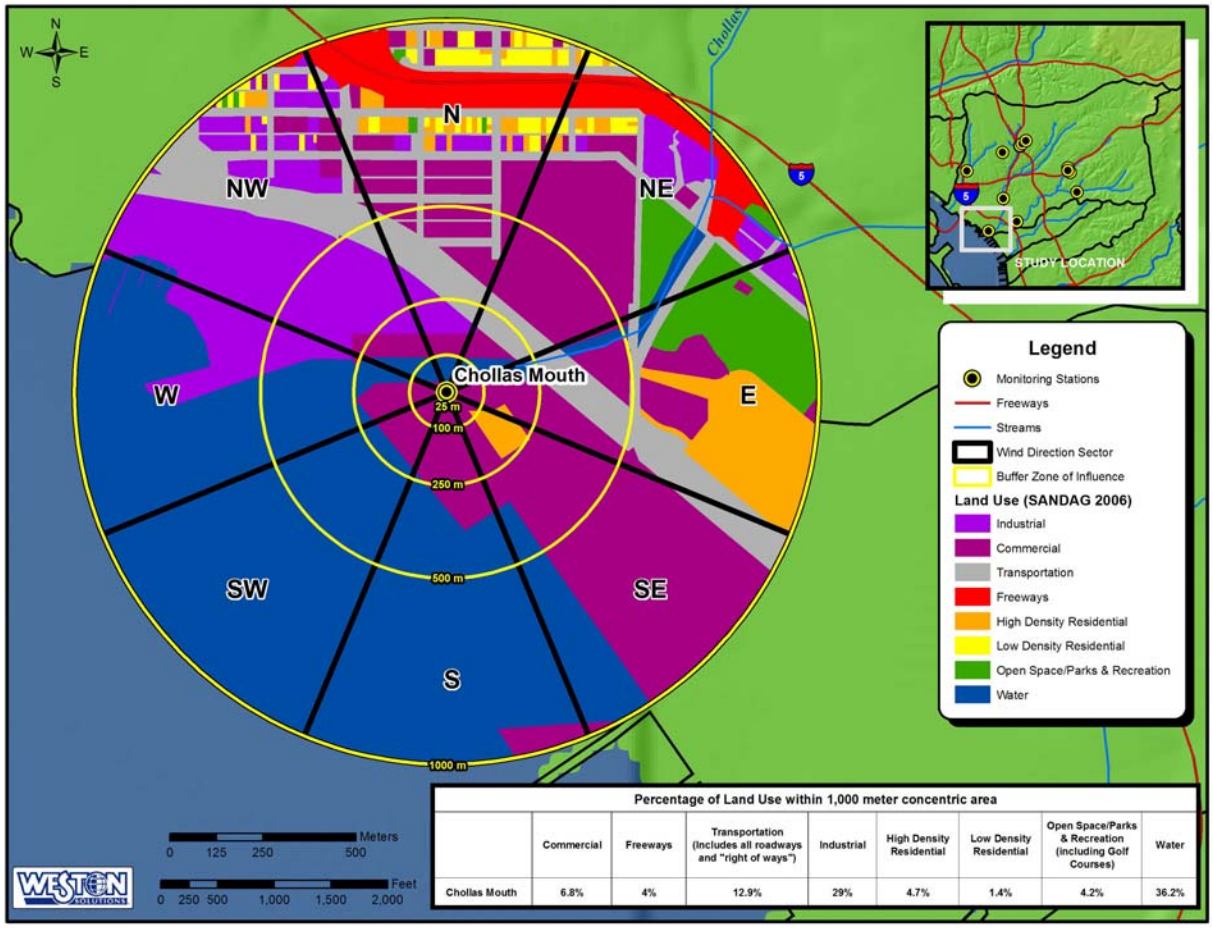

Percentage of Land Use within 1,000 meter concentric area

	Commercial	Freeways	Transportation (Includes all roadways and "right of ways")	Industrial	High Density Residential	Low Density Residential	Open Space/Parks & Recreation (including Golf Courses)	Water
Chollas Mouth	6.8%	4%	12.9%	29%	4.7%	1.4%	4.2%	36.2%

Figure 3-9. Land use of Area Surrounding Chollas Mouth Sampling Location

3.1.2 Transect Study

A transect analysis was designed to sample perpendicular and downwind of a freeway in the Chollas Creek watershed in order to evaluate the depositional flux and particle size characteristics based on distance from a freeway source. The Transect study was begun near Highway 94 at the Chollas Radio Site open space. The initial round of sampling, conducted July 11, 2006 through July 14, 2006, revealed that the prevailing wind traveled up the Highway 94 corridor (valley) from west to east parallel, rather than perpendicular, to the highway. Additional site reconnaissance also revealed that the only possible upwind location was not feasible due to an inadequate buffer zone from a nearby surface street with heavy traffic volume, a large commercial facility located directly upwind, and sloping terrain surrounding the site. Sampling at the 94 Transect site was thus discontinued after one week of sampling.

An alternate Transect study location was identified near the interchange of I-805 and I-15. This location provided an adequate upwind location free from the effects of a major surface street or other industrial or commercial source as well as an open space canyon orientated perpendicular to the prevailing wind pattern, downwind of the freeway.

Sites are described from west to east. Site 805T-UP was located east of the I-805/I-15 freeway interchange area. Sites 805T1-4 were located west of the freeway interchange (Figure 3-10).

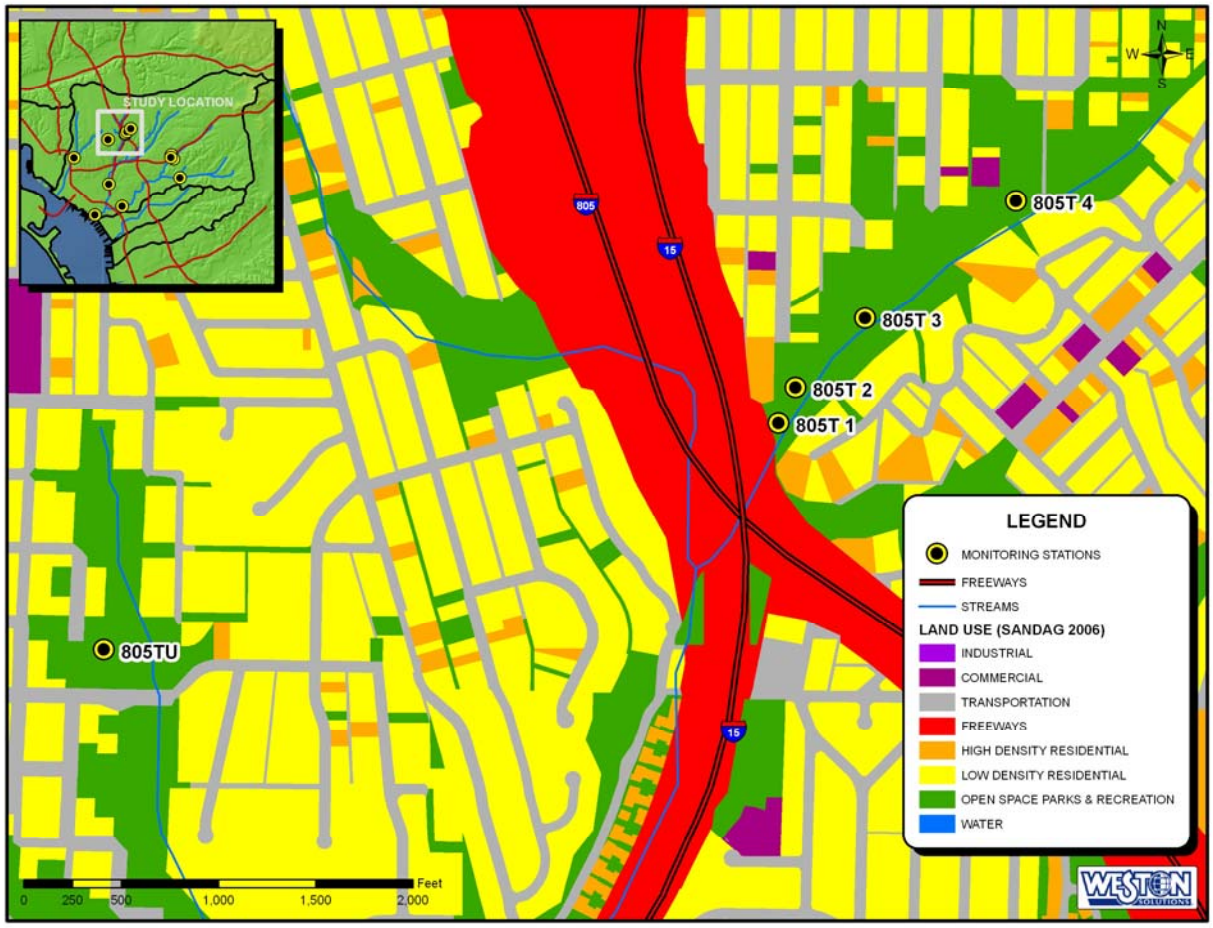

Figure 3-10. Land use of area surrounding Transect study sampling locations.

3.1.2.1 805T-UP

Site 805T-UP (32.73028ºN 117.12209°W, elevation – 237 feet) was located in a primarily residential neighborhood adjacent to 33rd Street and Juniper Street. The site was chosen to represent an area directly upwind of the I-805/I-15 freeway interchange with little influence from major roadways. The site was located within a small open space owned by the City of San Diego and bounded by residential neighborhoods. The site was located approximately 500 m southwest of the freeway interchange. The deposition surrogate sample plate was mounted atop a portable concrete pier base at an elevation 2.8 m above the ground.

The predominant land uses within the 1000 m concentric circle of the site were low density residential (43.6%) and transportation (21.6%) (SANDAG, 2006). The total percentage of impervious surface within the 1000 m circle was approximately 56.4% (Figure 3-11).

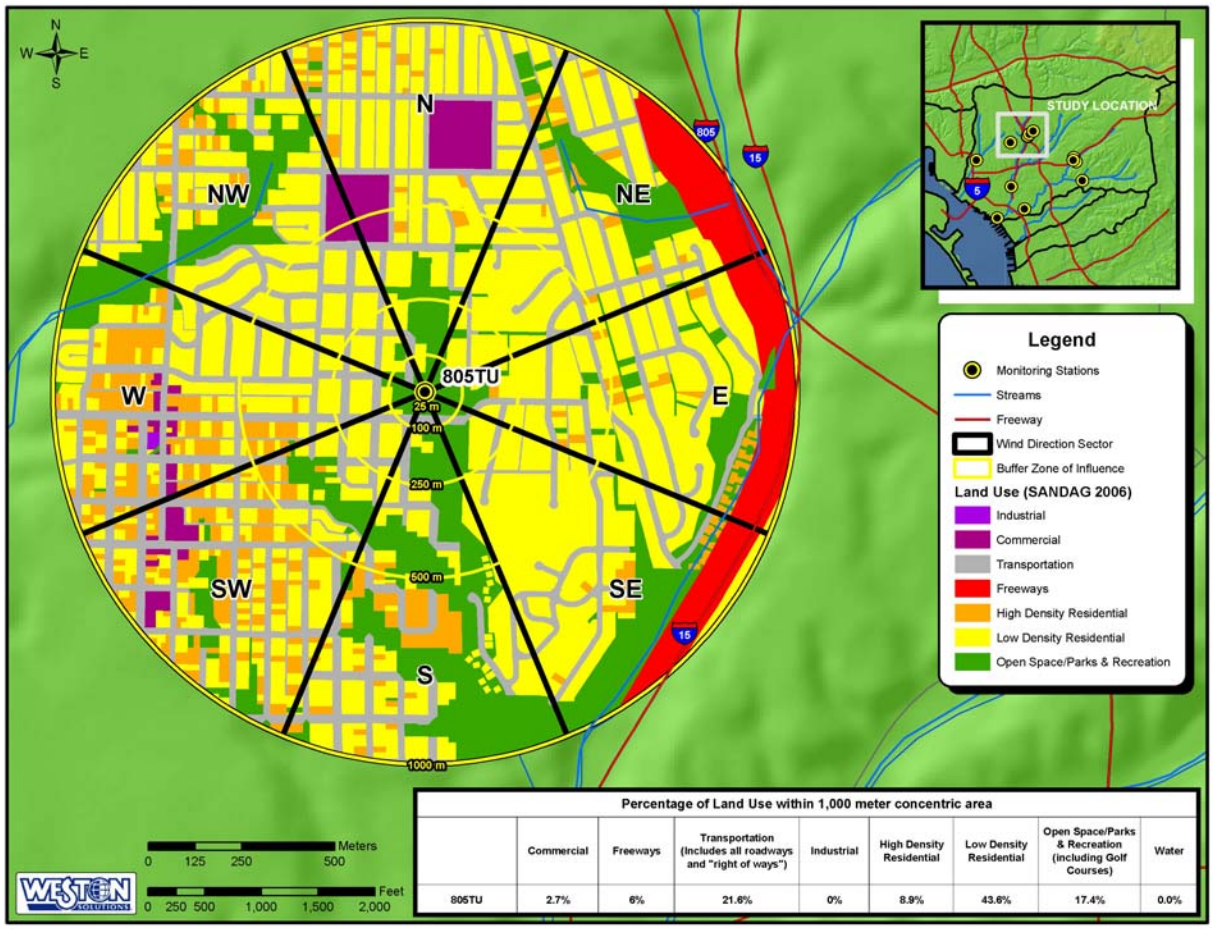

Percentage of Land Use within 1,000 meter concentric area

	Commercial	Freeways	Transportation (Includes all roadways and "right of ways")	Industrial	High Density Residential	Low Density Residential	Open Space/Parks & Recreation (including Golf Courses)	Water
805TU	2.7%	6%	21.6%	0%	8.9%	43.6%	17.4%	0.0%

Figure 3-11. Land use of area surrounding 805TU sampling location.

3.1.2.2 805T1

Site 805T1 (32.73357ºN 117.11084°W, elevation – 195 feet) was located in the City of San Diego-owned open space adjacent to 39th Street and Quince Street. The site was chosen to represent an area influenced by a major roadway and was located 25 m downwind of the I-805/I-15 freeway interchange. The site was bounded by residential neighborhoods to the north and south and the open space to the east. The deposition surrogate sample plate was mounted atop a portable concrete pier base at an elevation 2.7 m above the ground.

The predominant land uses within the 1000 m concentric circle of the site were low density residential (42.9%) and transportation (18.2%) (SANDAG, 2006). The total percentage of impervious surface within the 1000 m circle was approximately 60.0% (Figure 3-12).

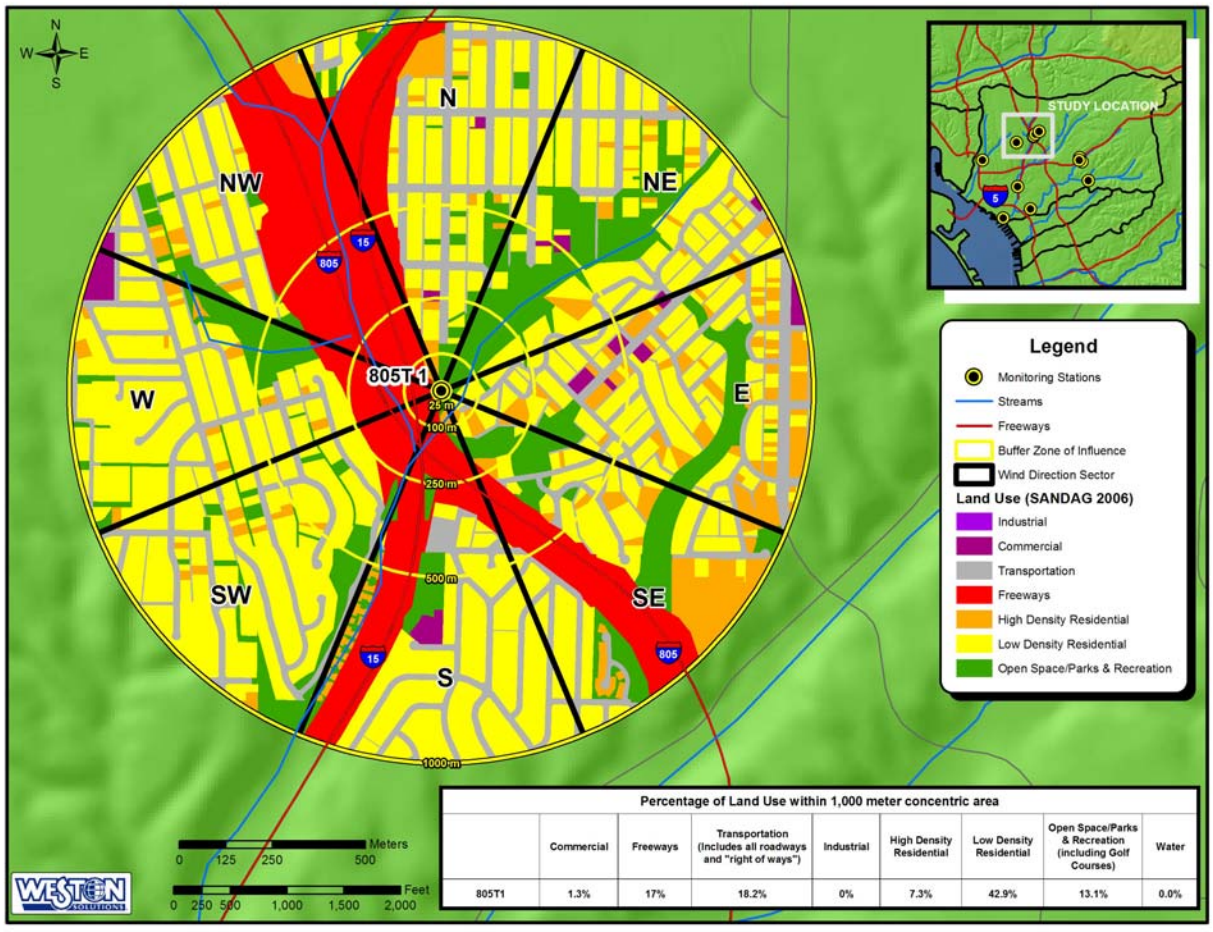

Percentage of Land Use within 1,000 meter concentric area

	Commercial	Freeways	Transportation (Includes all roadways and "right of ways")	Industrial	High Density Residential	Low Density Residential	Open Space/Parks & Recreation (including Golf Courses)	Water
805T1	1.3%	17%	18.2%	0%	7.3%	42.9%	13.1%	0.0%

Figure 3-12. Land use surrounding 805T1 sampling location.

3.1.2.3 805T2

Site 805T2 (32.73408ºN 117.11056°W, elevation – 186 feet) was located in the City of San Diego-owned open space adjacent to 39th Street and Quince Street. The site was chosen to represent an area influenced by a major roadway and was located 100 m downwind of the I-805/I-15 freeway interchange. The site was bounded by residential neighborhoods to the north and south and the open space to the east. The deposition surrogate sample plate was mounted atop a portable concrete pier base at an elevation 2.9 m above the ground.

The predominant land uses within the 1000 m concentric circle of the site were low density residential (42.1%) and transportation (18.6%) (SANDAG, 2006). The total percentage of impervious surface within the 1000 m circle was approximately 60.3% (Figure 3-13).

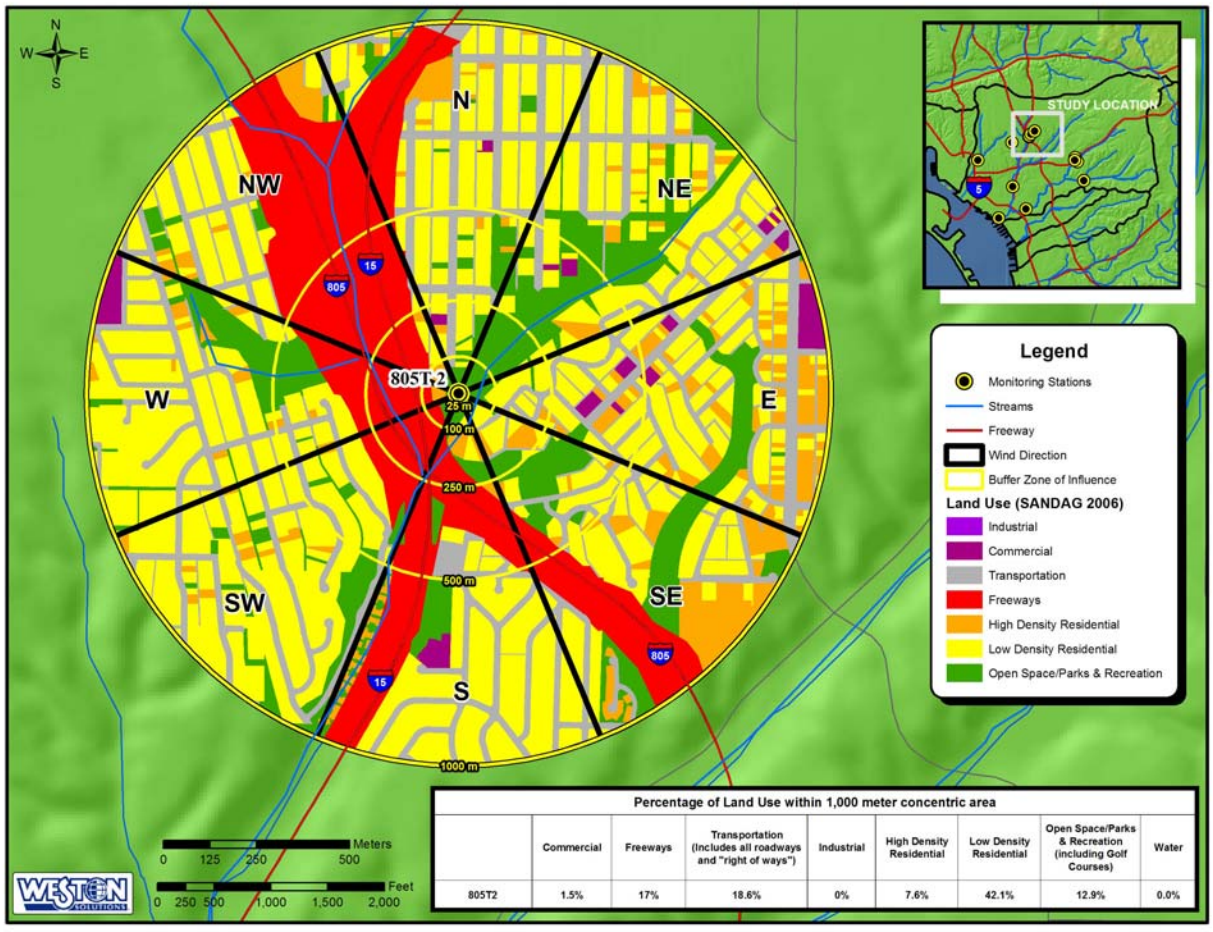

Percentage of Land Use within 1,000 meter concentric area

	Commercial	Freeways	Transportation (Includes all roadways and "right of ways")	Industrial	High Density Residential	Low Density Residential	Open Space/Parks & Recreation (including Golf Courses)	Water
805T2	1.5%	17%	18.6%	0%	7.6%	42.1%	12.9%	0.0%

Figure 3-13. Land use surrounding 805T2 sampling location.

3.1.2.4 805T3

Site 805T3 (32.73507ºN 117.10941°W, elevation – 199 feet) was located in the City of San Diego-owned open space adjacent to Redwood Street and Central Street. The site was chosen to represent an area influenced by a major roadway and was located 250 m downwind of the I-805/I-15 freeway interchange. The site was bounded by residential neighborhoods to the north and south and the open space to the east. The deposition surrogate sample plate was mounted atop a portable concrete pier base at an elevation 2.7 m above the ground.

The predominant land uses within the 1000 m concentric circle of the site were low density residential (38.8%) and transportation (19.7%) (SANDAG, 2006). The total percentage of impervious surface within the 1000 m circle was approximately 64.3% (Figure 3-14).

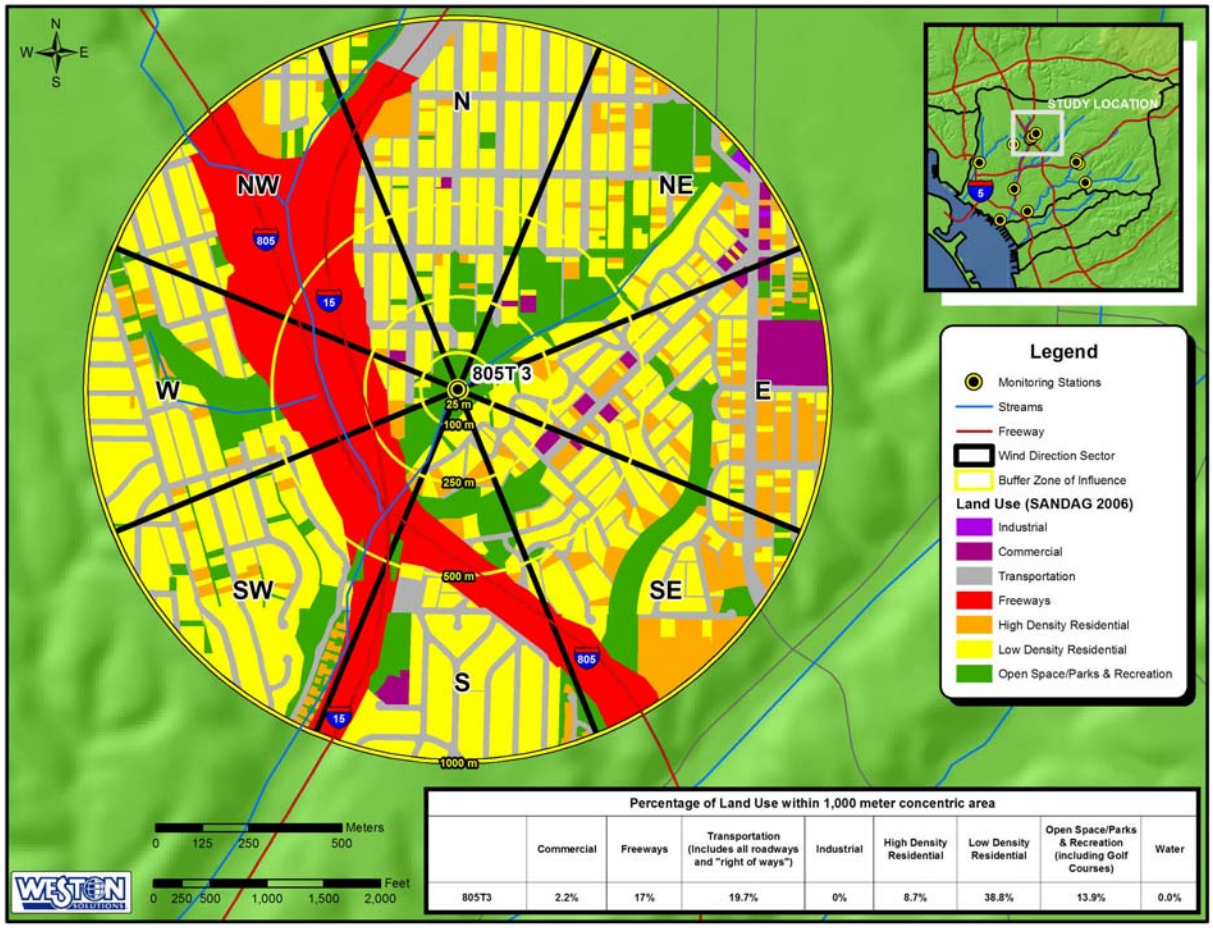

Percentage of Land Use within 1,000 meter concentric area

	Commercial	Freeways	Transportation (Includes all roadways and "right of ways")	Industrial	High Density Residential	Low Density Residential	Open Space/Parks & Recreation (including Golf Courses)	Water
805T3	2.2%	17%	19.7%	0%	8.7%	38.8%	13.9%	0.0%

Figure 3-14. Land use surrounding 805T3 sampling location.

3.1.2.5 805T4

Site 805T4 (32.73675ºN 117.1069°W, elevation – 220 feet) was located in the City of San Diego-owned open space adjacent to Redwood Street and Central Street. The site was chosen to represent an area influenced by a major roadway and was located 500 m downwind of the I-805/I-15 freeway interchange. The site was bounded by residential neighborhoods to the north and south and by the open space to the east. The deposition surrogate sample plate was mounted atop a portable concrete pier base at an elevation 2 m above the ground.

The predominant land uses within the 1000 m concentric circle of the site were low density residential (33.3%) and transportation (21.4%) (SANDAG, 2006). The total percentage of impervious surface within the 1000 m circle was approximately 58.5% (Figure 3-15).

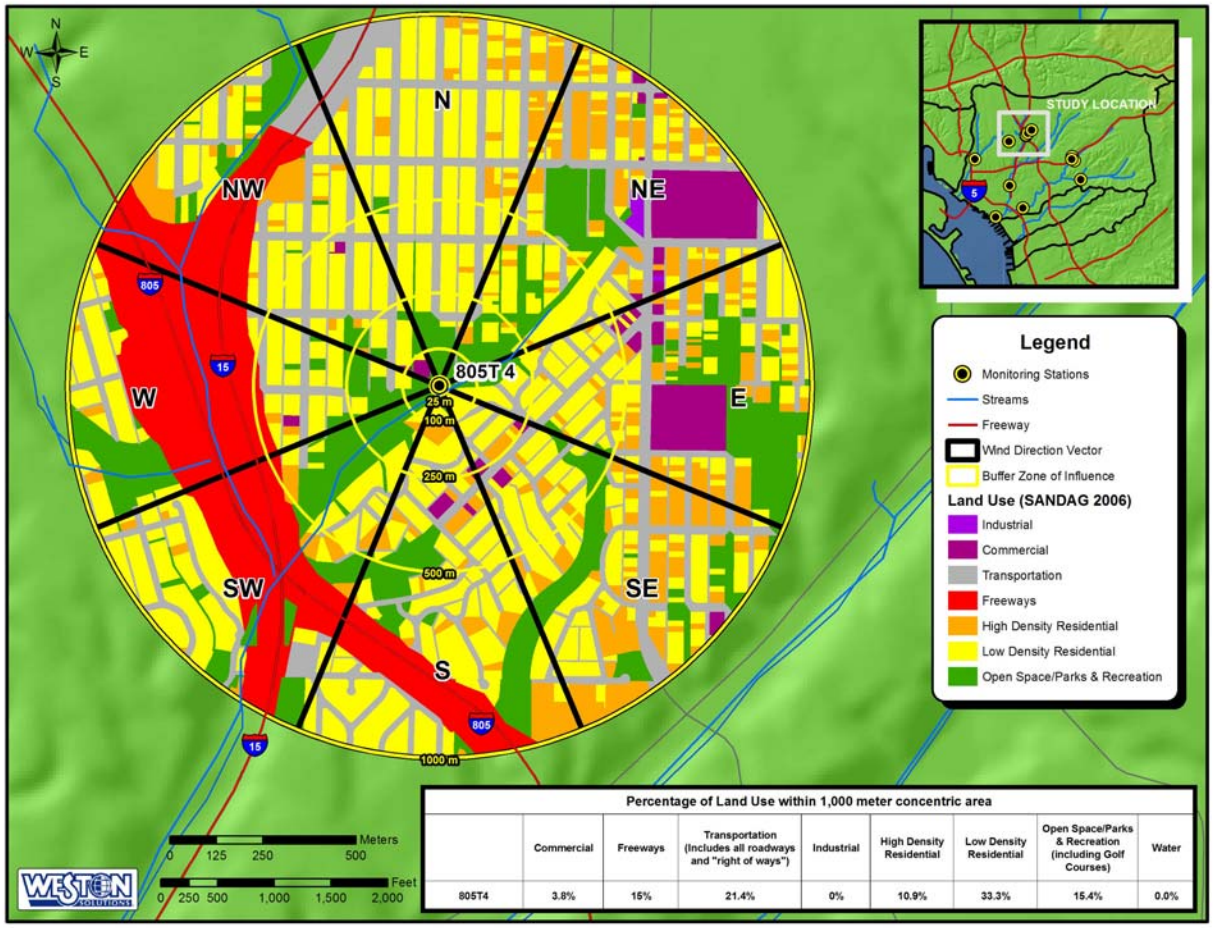

Percentage of Land Use within 1,000 meter concentric area

	Commercial	Freeways	Transportation (Includes all roadways and "right of ways")	Industrial	High Density Residential	Low Density Residential	Open Space/Parks & Recreation (including Golf Courses)	Water
805T4	3.8%	15%	21.4%	0%	10.9%	33.3%	15.4%	0.0%

Figure 3-15. Land use surrounding 805T4 sampling location.

3.2 Transportation Land Use Patterns

A variety of studies have demonstrated that the majority of the deposition of airborne particulate matter re-suspended from major roadways and freeways is highest near the roadway source and decreases with distance from the roadway (Moncrieff, 2004). An analysis was conducted to characterize the relationship of roadway proximity and traffic volumes (generated from CalTrans 2003) to the stream channels in this study using GIS. A 250 m buffer around major streams within the Chollas Creek and Tecolote Creek sub-watersheds was created, and the percentage of major roadways within this buffer zone was calculated. This analysis provides information that can be used to facilitate estimating the direct deposition of particulate mass to the tributary itself. Though direct deposition analysis was not performed for this study, it may be an important factor in determining wash off concentrations within the creeks during dry weather or low flow conditions.

Two watersheds were selected for this analysis; the Chollas Creek watershed and the Tecolote Creek watershed. Of the two, the Chollas Creek watershed is more urbanized, having 43.3% of its area comprised of freeway, transportation, commercial or industrial land use. Approximately 46% of its total area is residential; 10.9% high density residential, and 34.7% low density residential. In contrast, the Tecolote Creek watershed is more rural with 33.2% of its total area as residential; 27.3% existing as low density residential and 5.7% existing as high density residential. Only 36.8% of its total area is freeway, transportation, commercial or industrial land use. About 21.4% of the Tecolote Creek watershed is comprised of open space land use area, compared to only 10.7% open space land use area in the Chollas Creek watershed. Refer to Figure 3-16 for a land-use comparison between the two watersheds.

According to the GIS analysis, 10.6% (643 of 6043 total meters) of the total length of freeway in the Tecolote Creek Watershed fell within 250 m of the stream network. The Chollas Creek watershed showed a higher percentage of freeways within the stream buffer; 41.4% (13854 of 33495 total meters) of the total length of freeway in the Chollas Creek watershed fell within 250 m of the stream network. The Tecolote Creek and Chollas Creek watersheds were similar when comparing the major roads that fell within the stream buffer; 20.2% (7743 of 38419 total meters) of the total length of non-freeways in the Tecolote watershed fell within 250 m of the stream network and 22.5% (33488 of 148759 total meters) of the total length of non-freeways in the Chollas Creek watershed fell within 250 m of the stream network. Figure 3-17 and Figure 3-18 show the freeways within the 250 m stream buffer for the Tecolote Creek and Chollas Creek watersheds respectively. These figures show the proportion of these freeways by their traffic volumes.

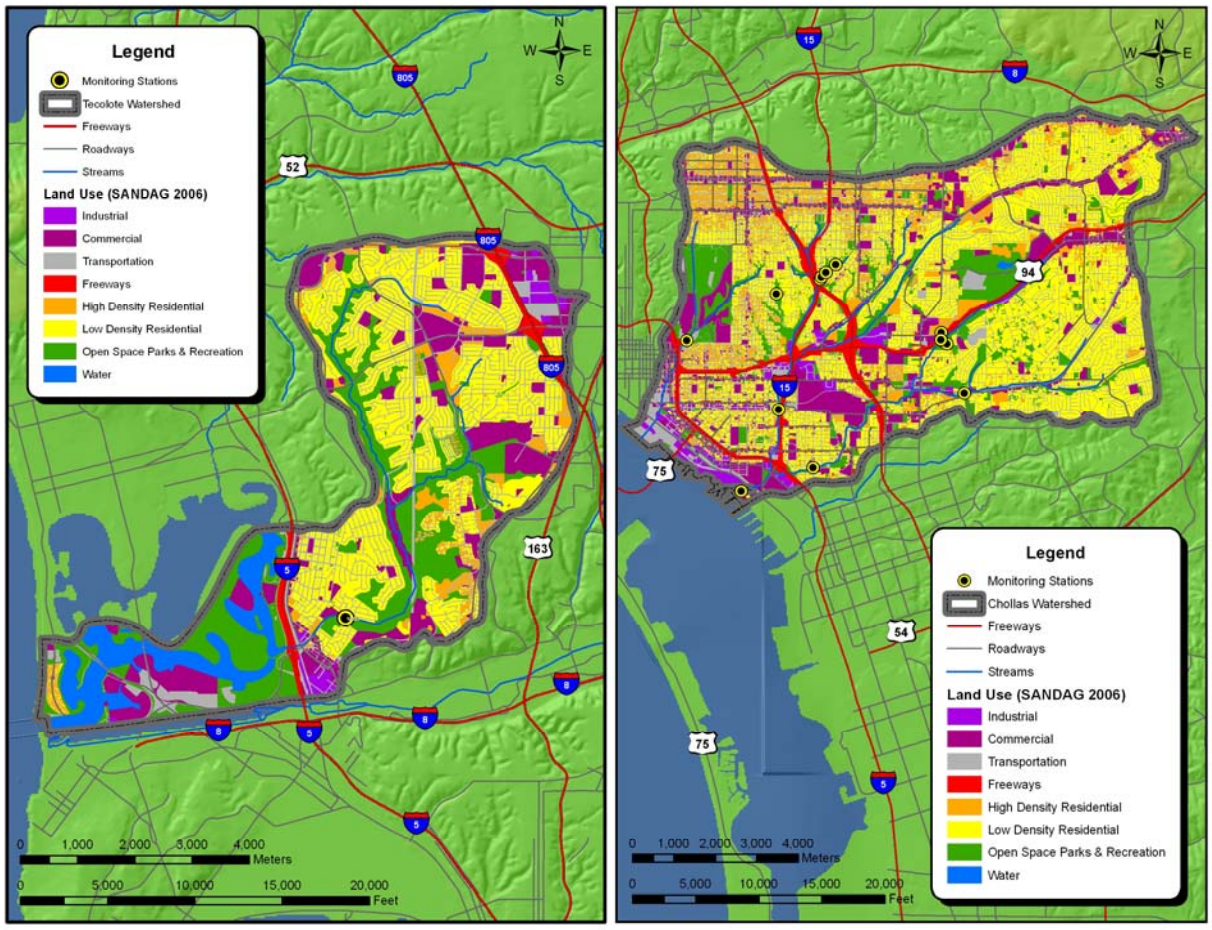

Figure 3-16. Tecolote and Chollas Watersheds land use comparison.

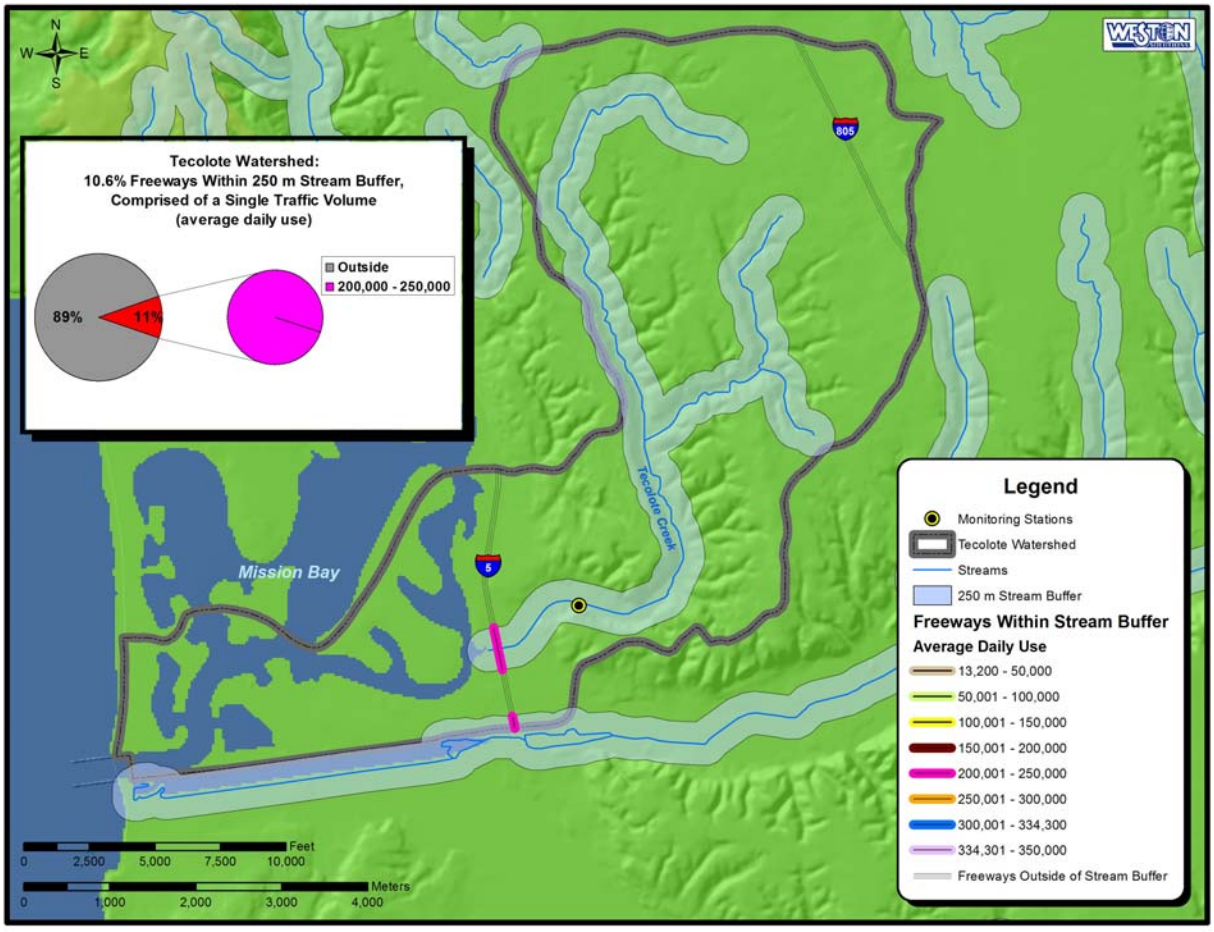

Figure 3-17. Freeways within the 250 m buffer for the Tecolote Creek watershed.

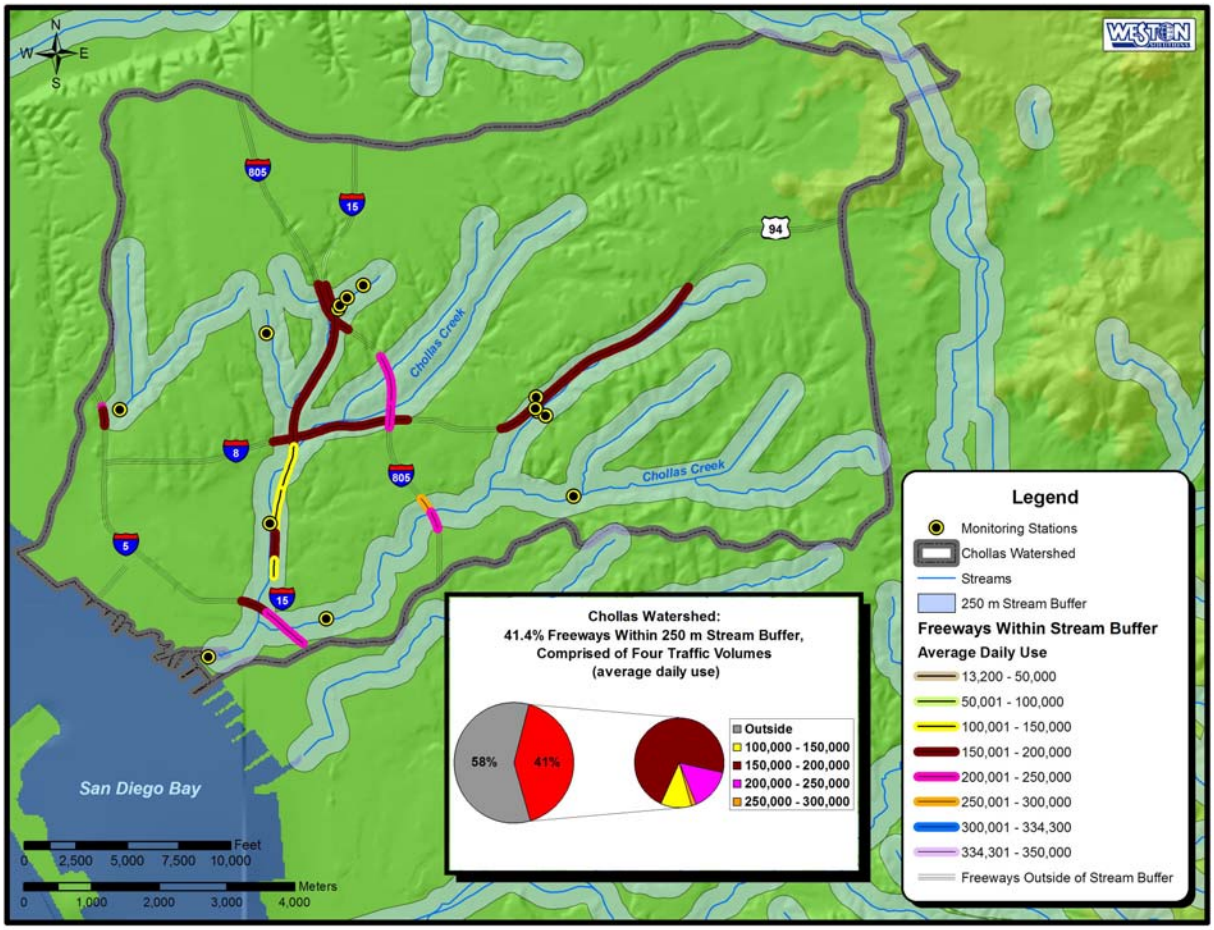

Figure 3-18. Freeways within the 250 m stream buffer for the Chollas Creek watershed.

Figure 3-19 and Figure 3-20 show the major roads within the 250 m stream buffer for the Tecolote Creek and Chollas Creek watersheds respectively. Again, these figures also show the proportion of these major roads according to their respective traffic volumes.

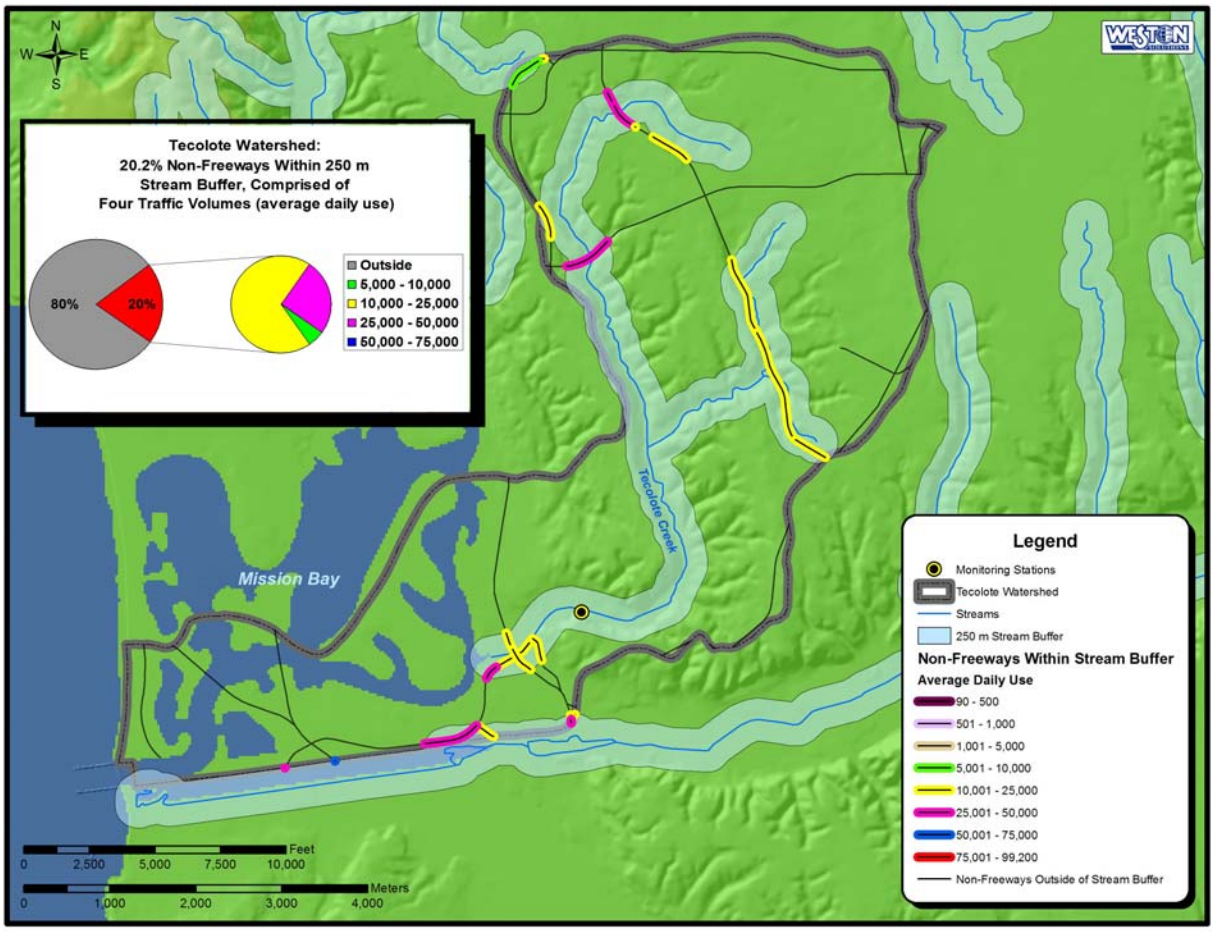

Figure 3-19. Non-freeways within the 250 m buffer for the Tecolote Creek watershed.

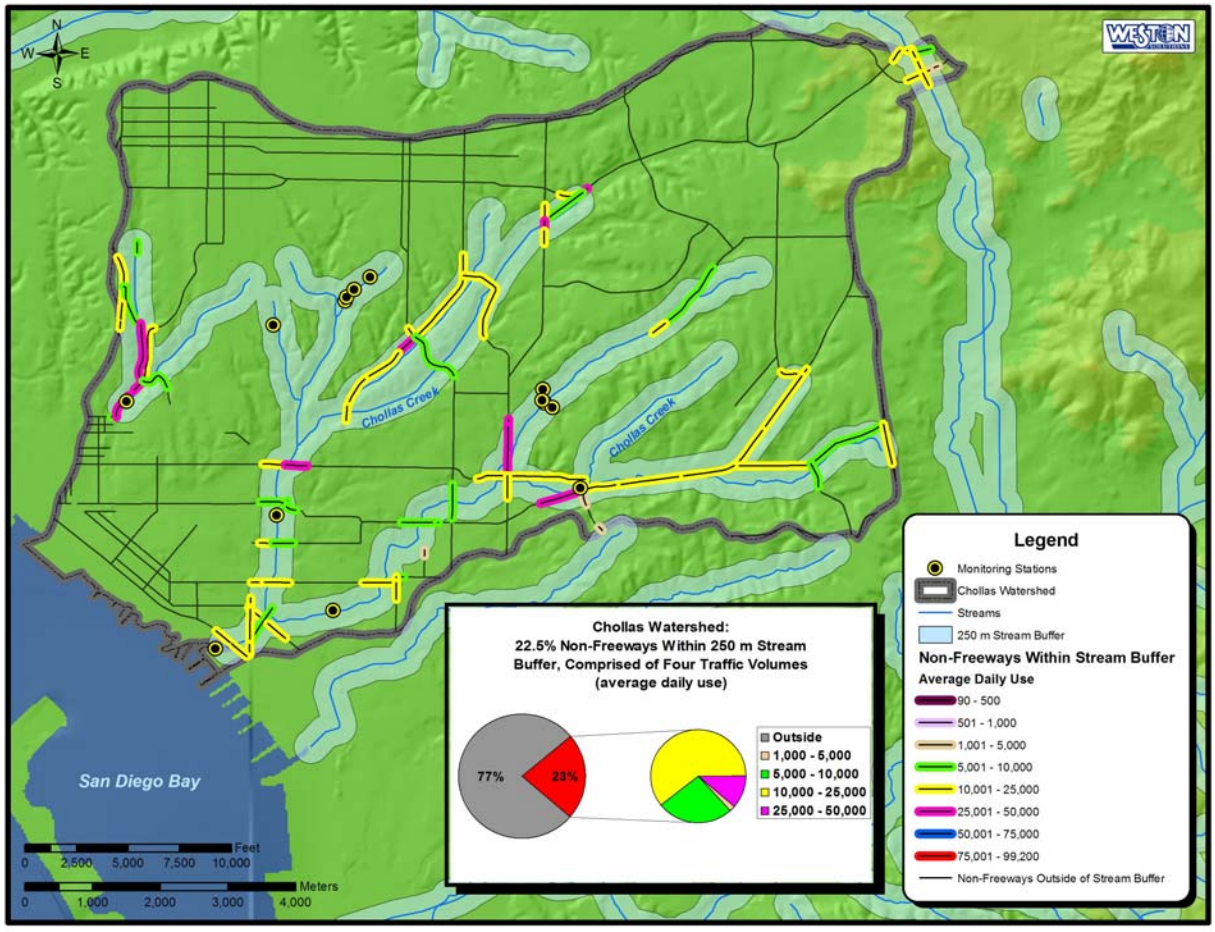

Figure 3-20. Non-freeways within the 250 m stream buffer for the Chollas Creek watershed.

2.0 STUDY DESIGN

Three integral studies were performed for this project to answer the questions related to how much, where, and which metals are depositing as a result of aerial deposition within the City of San Diego. This included a pilot study, an area wide study, and a freeway transect study (Figure 2-1). All three studies were performed within the City of San Diego. The following section describes the reasoning and methodology of the three studies.

2.1 Pilot Study

A pilot study was performed to ensure that the methods proposed for this study were within an acceptable range of variability and were comparable to other commonly used aerial deposition measurement methods. The study also sought to compare results with a separate study being performed at the mouth of Chollas Creek by the Southern California Coastal Water Research Project (SCCWRP).

The SCCWRP study was performed over a 10 week period beginning on June 23, 2006. The study location is within the U.S. Naval Base San Diego at the mouth of Chollas Creek. The study utilized sample plates 33 cm in diameter coated with Apiezon grease, a method similar to previous aerial deposition studies (Paode et al., 1998; Lin et al., 1993), mounted on a 2-meter tripod on top of a one story roof. The samples for the SCCWRP study were analyzed using inductively coupled argon plasma mass spectrometry (ICP-MS) detection using EPA Method 200.8.

The deposition plates employed as part of the pilot study for this report used a plate method based on similar principles to the SCWWRP study but are smaller (47 mm sample disks), utilize a mineral oil-coated deposition surface, and are analyzed by X-Ray Fluorescence Spectroscopy (XRF) using EPA Compendium Method IO-3.3 (EPA/625/R-96/010a).

In order to compare these two methods, the pilot study collocated and deployed samples during the same time periods as the SCCWRP study. Comparisons of the results obtained by the two different sampling and analytical methods were conducted to evaluate the sample variability and comparability of these two methods. Based on this comparison, the method using the smaller oil-coated disks combined with XRF analysis was chosen for this study since it is a non-destructive analysis technique that would allow for additional characterization of individual particulates found in the samples. Additionally, gross particulate mass could be measured and a greater list of individual elemental analytes was also able to be quantified.

A second facet of the pilot study included a sampling regime to determine the optimal number of days required for adequate loading on the surrogate surface sample disks to occur. Adequate loading is required so that non-detect values are minimized and results can be compared amongst sites. The initial sampling duration study was performed at a site near the intersection of 33rd and Durant Street at the County of San Diego Storm Water Monitoring Station SD8(1) on Chollas Creek (Figure 2-1) and at the Chollas Mouth site during the week of June 26, 2006. Sample results from the SD8(1) site and the Chollas Mouth site were compared to a third location that was deployed as a reference site, at Point Loma within the Cabrillo National Monument. This reference site was predicted to have the lowest depositional loading of the majority of the urban settings in San Diego since the primary wind direction is from the west-northwest and it is located on a peninsula far from major roadways and industries.

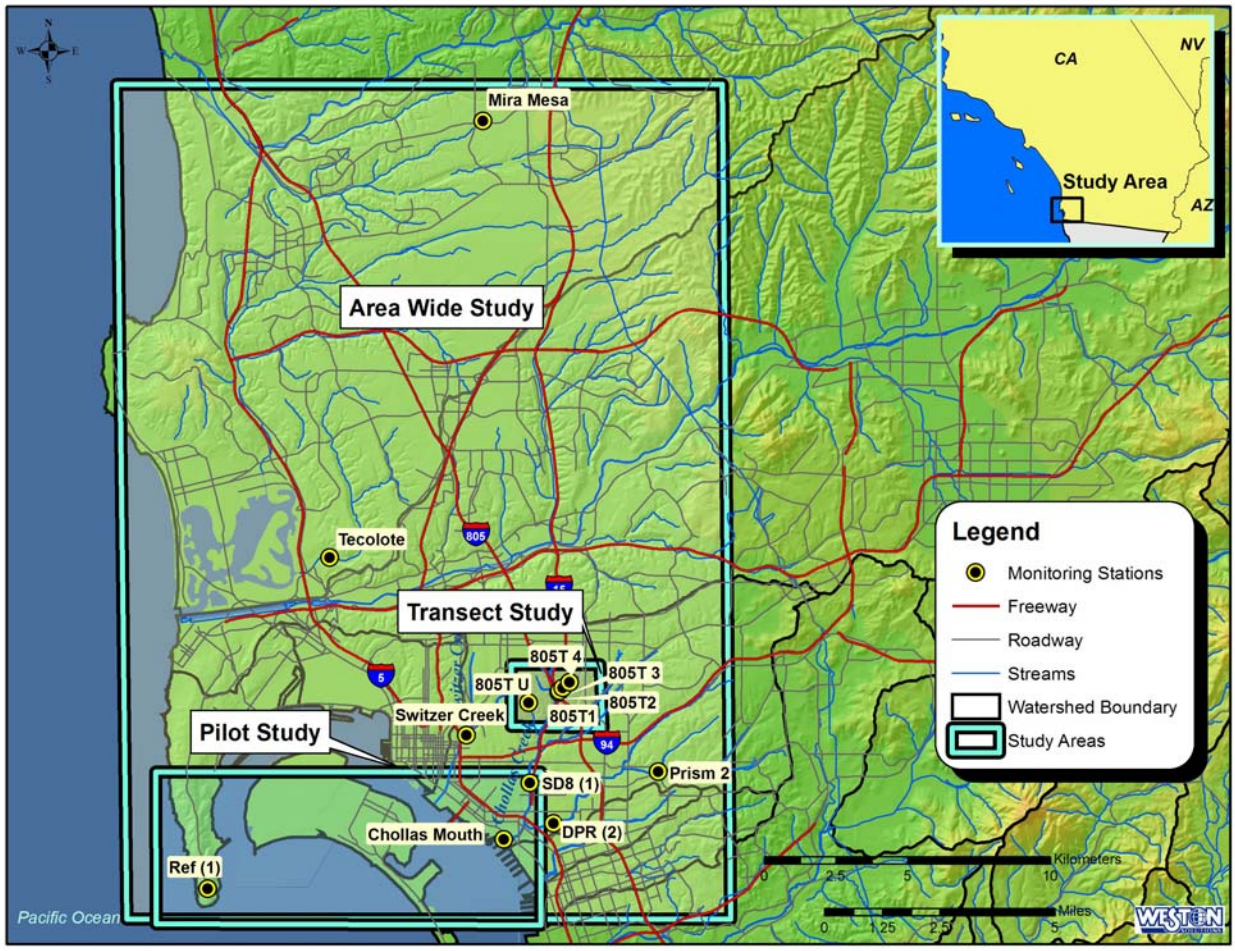

Figure 2-1. Study area.

A second round of sampling also occurred during the week of July 3, 2006 at the SD8(1) location. A total of 3 sample cassettes were deployed for 2, 3, and 4 days to determine the variation in deposition over these deployment durations.

Results from these studies indicated that three days of exposure were sufficient to provide adequate loading to the deposition disks so that results would be comparable among sites and non-detect values would be minimized. Sampling proceeded for the Area Wide and Transect studies based on acceptable results determined by the Pilot Study.

2.2 Area-Wide Study

The Area-Wide study was designed to assess the regional differences in average daily depositional flux within the City of San Diego. Sites were chosen based on the following criteria:

- geographic location
- surrounding land use characteristics
- proximity to freeways and roadways with varying amounts of average daily traffic volume

- areas that have been identified through storm water and dry weather field screening programs to have elevated metals concentrations

The study was designed to deploy disks at each of the nine sites for at least eight events in order to capture both the spatial and temporal variation in aerial deposition at the chosen sites. Also, the particle size of pollutants present in the air at each site was measured using a cascade impactor sampler designed to quantify the concentration of pollutants based on particle size.

The Area Wide study was conducted from July, 2006 to November, 2006 throughout the City of San Diego. Deposition disks were typically deployed on Tuesday and recovered on Friday, resulting in three-day exposure durations. At least eight deployment events occurred at each site, although some sites were sampled more frequently. Cascade impactor sampling occurred once at each site during a single 12-hour event that typically occurred between the hours of 6:00 am and 6:00 pm.

2.3 Transect Study

The Transect study was designed to assess the local differences in average daily depositional flux and particle size distribution at sites arrayed at varying distances from a major roadway or freeway. The initial Transect study was begun near Highway 94 at the Chollas Radio open space near the intersection of Highway 94 and Kelton Road. An array of four measurement sites was set up east, or downwind of the prevailing west wind pattern, of Highway 94. A single measurement site was established west of Highway 94 to serve as a control site. An initial deployment event was conducted between July 11-14, 2006 at this site. This event revealed that due to the unique geographical features of the site, the prevailing wind traveled from southwest to northwest, which is parallel, rather than perpendicular, to Highway 94. Additional site reconnaissance also revealed that the only possible upwind location was not feasible due to an inadequate buffer zone from a nearby surface street with heavy traffic volume, a large commercial facility located directly upwind, and sloping terrain surrounding the site. Sampling at the 94 Transect site was thus discontinued after one week of sampling.

An alternate Transect study location was identified near the intersection of the I-805 and I-15 freeway (Figure 2-1). This location provided both an adequate upwind and downwind location from of the freeway. The upwind location was free from the effects of a major surface street or other industrial or commercial source. The downwind site was an open space canyon orientated perpendicular to the prevailing wind pattern. An array of sampling sites were positioned in the downwind open space at distances as near as practical to 25 m, 100 m, 250 m, and 500 m away from the freeway. A single upwind site was positioned at the available upwind open space location that was approximately 500 m from the freeway, situated in a mainly residential neighborhood with low volume urban traffic.

The I-805 Transect study was conducted from August 2006 to October 2006 at the selected freeway location. Deposition disks were typically deployed on Tuesday and recovered on Friday resulting in three day exposure durations. At least eight deployment events occurred at each transect site, although some sites were subject to suspected animal interference in the field and were not analyzed. Cascade impactor sampling occurred once at each Transect site during separate 12-hour events that typically occurred between the hours of 6:00 am and 6:00 pm.

1.0 INTRODUCTION

The City of San Diego encompasses a land area of approximately 342 square miles. Much of the land use area within the city limits is highly urbanized and developed. Several areas within the City of San Diego experience detections of specific metals (copper, lead, and zinc) above dry weather action levels during dry weather flows or above the San Diego Basin Plan water quality objectives during wet weather flows. Often times, dry weather illicit connection and illicit discharge (IC/ID) investigations for metals exceedances are inconclusive with no specific point sources being identified. A watershed monitoring study in Chollas Creek during 1999-2001 concluded that concentrations of copper, lead, and zinc were ubiquitous in the watershed and that no specific point sources could be identified (MEC, 2002).

Aerially deposited contaminants that accumulate and subsequently wash off from dry weather or wet weather flows are one suspected source of contamination that has routinely been recognized but has not been studied within the City of San Diego to date. An atmospheric deposition study conducted in Santa Monica Bay (Stoltzenbach et al., 2001) concluded that the major source of contaminants to the air is re-suspended dust, primarily from roads, and that atmospheric loadings are primarily the result of dry deposition of large diameter particles (>10 um) on the watershed. A conceptual diagram of the processes affecting aerial deposition is shown in Figure 1-1.

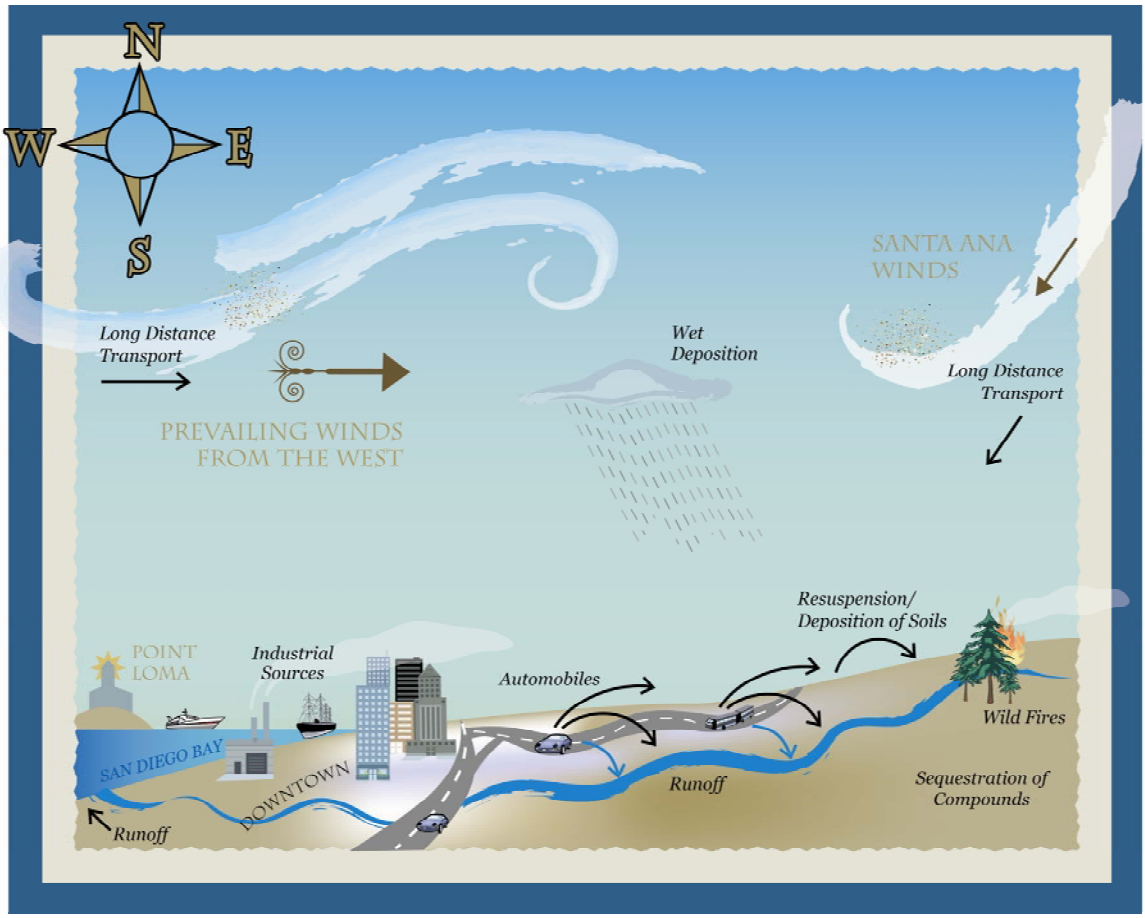

Figure 1-1. Conceptual diagram of processes affecting aerial deposition.

The City of San Diego has a high density of urban roadways and freeways within close proximity to many creeks and drainages leading to the receiving waters. Land use in the surrounding area of the watershed also contains a high density of industrial and commercial facilities. Many of the water quality exceedances of copper, lead, and zinc noted during a two year PRISM Grant Study in Chollas Creek (2004-2006) showed that these three metals had strong statistical correlations to total suspended solids. This implies that samples with higher concentrations of TSS have higher concentrations of the metals copper, lead, and zinc. The PRISM Grant study showed a weaker correlation to dissolved metals which suggests that metal solubility and particle size may play a role in the concentration of dissolved metals found in the creek.

To better understand the overall contribution of aerially deposited copper, lead, and zinc, The City of San Diego's Storm Water Pollution Prevention Division determined the need for a City wide aerial deposition study. This is important with the implementation of city wide best management practices (BMPs) for metals such as those associated with the total maximum daily load (TMDL) for Chollas Creek. The BMPs needed to comply with the Chollas Creek Metals TMDL have been estimated to cost in excess of 500 million dollars (Weston, 2006). If treatment BMPs are installed throughout the watershed, particles deposited downstream of the treatment system as a result of aerial deposition loading may result in non-compliance with the TMDL if deposition loading rates are significant.

This report presents the results and data analysis from dry deposition and air concentration samples collected from June 27, 2006 through November 7, 2006. Dry deposition is considered to be a major source of aerially deposited particulates due to the primarily dry semi-arid climate of the San Diego Region. Wet deposition is not considered in this report due to the infrequent rainfall events in the San Diego Region. Wet deposition is suspected of contributing less than 10 % of the total deposition load based on a similar study conducted in Los Angeles, CA (Sabin et al., 2005) which has a climate similar to San Diego.

This report is organized by the following sections:

Section 1 – Introduction
Section 2 – Study Design
Section 3 – Land Use Analysis
Section 4 – Methods
Section 5 – Wind Data Processing
Section 6 – Results
Section 7 – Data Analysis Results
Section 8 – Quality Control
Section 9 – Air Quality Modeling
Section 10 – Industrial Emissions Inventories
Section 11 – Buildup/Wash Off Modeling
Section 12 – Conclusions and Recommendations
Section 13 – References

1.1 Problem Statement

The primary focus of this study is directed to answer specific questions relating to total maximum daily loads (TMDLs) and 303(d) listings (specifically related to metals) in the City of San Diego. Currently, Chollas creek has a concentration based TMDL for dissolved copper, lead, and zinc with no known point sources with the exception of the MS4s. TMDLs are also being developed for San Diego Bay at the mouth of Chollas Creek, Switzer Creek, and Paleta Creek. Tecolote Creek is 303(d) listed for cadmium, copper, lead, and zinc, and Mission Bay is 303(d) listed for lead. Indirect and direct aerial deposition of pollutants is thought to be a contributor (but to an unknown degree) to the pollutant load in this highly urbanized setting. A recent atmospheric deposition study conducted in Los Angeles concluded that aerially deposited trace metals accounted for 57 – 100% of the total trace metal load in storm water run off (Sabin et al., 2005).

Many studies relating to TMDLs and violations of water quality are based on methods that have been developed over time since the inception of the Federal Clean Water Act. These methods have been specifically used to measure the concentrations of pollutants in water. The methods have been standardized and are typically performed by laboratories certified to perform the tests as required by federal and state regulations. Well over a thousand analytical tests of water quality have been performed in the San Diego region over the past decade. This data has shown that some water bodies contain significantly higher concentrations of pollutants that pose threats to the beneficial uses listed in the San Diego Basin Plan. These data are also used to list impaired waters and develop the TMDLs. Once pollutants are identified to exceed water quality objectives, municipalities will often perform investigations to determine the source of the pollutants. Examples of these investigations are bacterial source tracking, illicit discharge/illicit connection studies, and other general water quality tracking studies. In many of these cases, the root cause of the pollution source can be identified since the flow of water is often continual and can be traced out using deductive reasoning.

This is not the case with atmospheric deposition. Atmospheric deposition has only recently been studied in depth to determine its contribution to water quality issues. Atmospheric deposition is highly variable depending on wind speed, direction, and the available sources that may contribute particulate matter to a basin. Airsheds are considerably larger than watersheds and may span multiple regions. Wind patterns and mixing may likely mask the true sources of the pollutants that are available to be dispersed. It should be noted that while air quality methods have also been developed over time, primarily by the U.S Environmental Protection Agency (EPA) and since the inception of the Clean Air Act, they have not been developed to address water quality pollution. Many air quality standards and regulations primarily address the particles that are considered inhalable, which are discussed later in this section. Due to the complex nature of atmospheric deposition, there are no EPA standardized methods to measure the transfer rates of pollutants to a land surface or directly to a water body. Though many measurement approaches have been developed to research aerial deposition for a variety of contaminants, they all have inherent variability that presents challenges to determining the sources of aerially deposited particulates.

This study is intended to provide the City of San Diego with a baseline understanding of the contribution of atmospheric deposition of copper, lead, zinc, and other particles to land surfaces and its subsequent relationship to water quality.

The key questions we are seeking to provide information for are as follows:

1. *What are the aerial contributions of metals (copper, lead, and zinc)?*
2. *Are these metals associated with different sources or land uses?*
3. *What is the particle size distribution of metals in air particulates verses what particle size distribution is deposited?*
4. *Where is pollutant loading from aerial deposition occurring within the City of San Diego?*
5. *What is the contribution of aerial deposition to water quality concentrations observed in Chollas Creek?*

To better understand aerial deposition, two key factors must be understood.

1. Aerially deposited pollutants originate from land use sources. Metals sources can be attributable to brake pads and tires from automobiles, galvanized fencing and gutters, roof tiles, fertilizers and fungicides, welding operations, painting, sanding and sand-blasting, auto-dismantling, and various other industrial practices.
2. Wind is the driving factor that mobilizes these pollutants. Wind from nature, and wind from automobiles on freeways and roadways are the two primary forces in aerial deposition particle transport. While natural wind typically is the source that carries pollutants and dominates the direction which the pollutants travel, automobiles can also be a key factor that resuspends the particles into the air from turbulence. Particle size and density also play a role in the distance the particles will travel.

By evaluating the questions above and understanding the aerial deposition contribution within the City, the City of San Diego will be able to understand what potential BMP solutions are available, applicable, and feasible for implementing. This study bridges one of the data gaps listed in the Chollas Creek TMDL Source Loading, Best Management Practices, and Monitoring Strategy Assessment (Weston, 2006).

1.2 Air Quality and Water Quality Concepts and Overview

The terminology used throughout this document bridges two fundamental sciences: 1) the study of air quality and 2) the study of water quality.

- **Emission** – An emission is the release of gases or particulates into atmosphere. Emission rates are a measure of the pollutant mass released from a point source over time (e.g., grams of copper per day).
- **Dispersion** – Dispersion is the spreading of gasses or particulates from a small volume of air near the emission source into the surrounding atmosphere.
- **Deposition** – Deposition is the process of particulates being transferred from the atmosphere to the underlying surface.

- **Flux** – For the purposes of this report, flux, or mass flux, is the rate of a specific metal depositing from the atmosphere to a surface. The units are typically presented as micrograms (µg) of metal per square meter (m^2) per day (expressed as $\mu g/m^2/day$).
- **Net Flux** – Similar to the example above, the net flux is the rate of the total mass that deposits on a surface and includes both inorganic and organic particulates (expressed as $\mu g/m^2/day$ or $mg/m^2/day$).
- **Buildup** – Buildup is a term used in water quality studies to explain the process of particulate accumulation. Similar to a surface (e.g. as a roadway, sidewalk, or automobile) that accumulates dust and dirt that may be available to contribute pollutants to storm water runoff.
- **Wash Off** – Wash Off is the process of removing the particulates from the surface. This is primarily associated with rainfall, but may occur with irrigation, car washing, power washing, and other processes.
- **TMDL** – Total maximum daily load (TMDL) is a regulatory water quality term used to define the total amount of a pollutant that can be discharged to a water body. The load can be assigned as pounds per year of a given pollutant or also on a concentration basis in terms of milligrams per liter or micrograms per liter (µg/L).

The Air Resources Control Board is the lead air agency in the state. The ARB is responsible for enforcing the Federal Clean Air Act. Industrial and commercial emissions are controlled by 35 local districts which include the San Diego Air Pollution Control District (SDAPCD). Air quality regulations are primarily based on threats to human health and do not consider impacts to aquatic ecological health. Many of the toxic air compounds monitored by the SDAPCD (e.g. ozone, nitrogen dioxide, carbon monoxide, and sulfur dioxide) are not considered to impact the water quality of the San Diego Region. However, particulate matter is monitored by the SDAPCD. Elevated concentrations of particulate matter can cause both health and water quality impairments. Particulates are classified as fine, coarse, and large particles. Particles that are less than 10 µm in aerodynamic diameter are called PM_{10} (inhalable particles). Particles less than 2.5 µm in aerodynamic diameter are called $PM_{2.5}$ (respirable particles). Particles will settle out based on several factors related to particle size, density and wind speed and are summarized below.

Fine Particles (<2.5 µm)

- greatest health relevance (increased disease and premature death greatest health relevance)
- low deposition rates and mass contribution
- long transport distances

Coarse Particles (2.5-10 µm)

- health relevant (increased disease and premature death)
- moderate deposition rates and mass contribution
- shorter transport distances

Large Particles (>10 µm)

- not health relevant (not inhalable; relatively sparse recent data)

- high deposition rates and mass contribution
- short transport distances, decreasing with increased particle size

Particulates are comprised of nitrates, sulfates, organic chemicals, metals, soil, dust, and other material. Some particulates are directly emitted to the air from a variety of sources as follows:

- cars, trucks, buses, and heavy equipment

Smog – Source: JimmyAkin.org

- industrial sources, construction sites, stone crushing and finishing, sandblasting, welding, and painting.

Concrete Cutting Photo Source: Health & Safety Executive (CIS# 54)

Sandblasting Photo. Source: Weston, 2006.

- resuspended dust from paved and unpaved areas

Leaf Blower- Source: Goldenspirit.com

- wood burning and forest fires

Smoke plume from 2003 San Diego forest fires - Source: NASA.gov

Particles may also be formed in the air via condensation, nucleation, and coagulation from the vapor phase. However, the majority of these particles are typically less than 1 µm in size. Particles greater than 1 µm in size are generally derived from mechanically generated processes. As previously stated particles less than 2.5 µm in size tend to have low deposition rates and lower mass contributions. In addition, these particles are dispersed over much larger areas. The SDAPCD reports that San Diego meets the Federal $PM_{2.5}$ standard, but has not attained the state $PM_{2.5,}$ or the Federal and state PM_{10} air quality standard (SDAPCD, 2006). Particulate matter greater than 10 µm is not regulated by the ARB since it is not considered to be an inhalable fraction.

The SWRCB is the lead water quality agency in the state. The SWRCB is responsible for enforcing the Clean Water Act and California's Porter Cologne Water Quality Act. Water quality discharges are regulated by the nine regional boards including the San Diego Regional Water Quality Control Board (RWQCB) which regulates both human health and aquatic life impacts. Aquatic life criteria for copper and zinc are roughly 100 times lower than the human health standard for consumption. However, both copper and zinc are not listed as regulated hazardous air pollutants (HAP) under the Clean Air Act (CAA). The CAA establishes a National Ambient Air Quality Standard (NAAQS) for lead, and lists lead compounds as a category of HAPs.

On February 9, 2006, a joint Air Resources Control Board and State Water Resources Control Board (SWRCB) meeting occurred in Sacramento. Several topics were discussed between the two agencies to gain a more comprehensive understanding between air quality and water quality regulations and concepts.

The following is a summary of the principles of storm water regulations and why air regulations do not address water quality concerns.

Storm water permits

- Urban runoff is regulated under general storm water permits
- Permits use a best management practices (BMP) approach to regulate pollutants
- The owner or operator of a storm drain system is generally responsible for pollutants discharging from the storm drain, e.g., pesticides in runoff from lawn watering that ends up in the storm drain becomes the system owner's responsibility. The same is true for pollutants in storm water due to aerial deposition.
- Storm water inspectors will often visit industrial/commercial sites to ensure what is running off as point source pollution will not impair water. Though BMPs may be in place to control pollutant runoff (e.g. controlling parking lot runoff), the daily emissions from activities from these sites may spread over several kilometers and not appear as a visual concern. However, as buildup occurs over time, the non-visual pollutant that was emitted, may be significant. As previously mentioned, there is no regulatory framework to control aerial emissions of copper and zinc.

TMDL program

- Aerial deposition can be a significant source of pollutants to an impaired water body and can be a critical element in some TMDL calculations.
- If aerial deposition occurs directly onto a water body, the deposition can be assigned a load allocation as a nonpoint source. If aerial deposition indirectly affects water quality through storm water runoff, the owner or operator of the storm drain can be assigned a waste load allocation. However, this waste load allocation comes in the form of the discharge of water in the storm drain system. This is the case for the Chollas Creek Watershed.

Permits

- There are no cases in which ***aerial sources***, e.g., industrial facilities have been considered point sources, subject to an NPDES permit solely on the basis of their air emissions (i.e., some facilities with air emissions may also have NPDES permits due to other discharge issues).
- EPA considers aerial deposition to be a nonpoint source.

One observation from the joint ARB-SWRCB meeting was that it was a one sided issue. It was apparent that air pollutants can cause significant water quality degradation whereas poor water quality rarely causes poor air quality. Human health criteria are different from aquatic health criteria, and as a result, the air quality regulations do not address water quality issues related to aerial deposition. Air quality studies are often performed on an airshed basis whereas water quality studies are performed on a watershed basis. Airsheds are considerably larger and often cover multiple watersheds and regions. If aerial deposition from transportation sources is the primary contributor to water quality issues in the Chollas Creek area, then it is logical to assume it occurs at similar rates in other similar watersheds. If the aerial deposition is higher in the Chollas Creek area in comparison to similar transportation-dense areas, it stands to reason that other emission sources may be influencing the water quality concentrations. It is on the basis of this concept that localized emission sources may play a significant role on a watershed scale.

1.3 Pollutants of Concern

The primary pollutants of concern for this study were copper, lead, and zinc. Other elemental data were also collected and are discussed in the methods section of this report. This section describes the background information and sources of each pollutant of concern.

1.3.1 Copper

Copper (Cu) has an estimated crustal abundance of approximately 55 mg/kg (Kennedy, 2003). Copper commonly substitutes in minerals such as plagioclase and apatite and ranges from 10 mg/kg in granite to 100 mg/kg in basalt (Kennedy, 2003). Copper has a specific gravity of 8.96. Copper is an essential element for all higher living organisms. However, dissolved copper is considered to be toxic to aquatic organisms such as algae, salmon, and other marine species in even minute concentrations. The Chollas Creek metals TMDL water quality objective (WQO) for dissolved copper is based on the California Toxic Rule (CTR) and varies depending on the hardness concentration from the sample collected. At a hardness concentration of 100 mg $CaCO_3$/l, the dissolved copper CTR acute WQO is 13.4 µg/L. The saltwater numeric criteria for dissolved copper for the Shelter Island Yacht Basin Dissolved Copper TMDL is set at 4.8 µg/L for the acute criteria. In comparison, the Federal Safe Drinking Water Act maximum contaminant level goal for total or dissolved copper is set at 1,300 µg/L.

Copper is a commonly used consumer product used in building construction (e.g. plumbing, architectural copper roofs, mailboxes and railings), electrical and electronic products (e.g. wiring and cables), metal plating and alloys, antifouling paints, and sandblasting material. Copper is also used as an algaecide and fungicide for swimming pool treatments and as a wood preservative. As of the writing of this document, the EPA announced it is taking legal action to ban the use of acid copper chromate (ACC) in wood preservatives for residential use. Copper has also been shown to erode from overhead trolley wires from electric trains (Kennedy, 2003).

Copper is also used in brake pads as an additive to prevent brake disk screeching. Copper in brake pads has been extensively studied in recent years by the Brake Pad Partnership (BPP). The BPP is an organization of government regulators, brake pad manufacturers, storm water management agencies, and environmentalists. The brake pad manufacturers have agreed to change their product formulations "if brake pad wear debris is found to impair water quality" (BPP Website, 2006, http://www.suscon.org/brakepad/). The BPP has a technical library of over 197 studies related to the fate and transport of copper associated with brake wear debris.

Copper slag is used for sandblasting as an economical choice of abrasive grain for shipyards and contractors. Shipyard related industries are concentrated in the areas around downtown San Diego. Many of the facilities in the vicinity of Chollas Creek have also reported their annual emissions of copper to be in the range of several hundred to several thousand pounds per year. This information is readily available for the San Diego Region on the California Air Resources Board (ARB) Community Health Air Pollution Information System (CHAPIS) website (http://www.arb.ca.gov/ch/chapis1/chapis1.htm). These facilities may include the use of copper slag and copper based paints in their processes. Industrial emissions are further discussed in Section 10 of this report.

1.3.2 Zinc

Zinc (Zn) is the 23rd most abundant element in the earth's crust (USGS, 2006). It is the fourth most common metal used behind iron, aluminum, and copper. In the United States, about two-thirds of zinc is produced from ores (primary zinc) and the remaining one-third from scrap and residues (secondary zinc). Zinc uses range from metal products, to rubber, and medicines. About three-fourths of zinc used is consumed as metal, mainly as a coating to protect iron and steel from corrosion (galvanized metal), as alloying metal to make bronze and brass, as zinc-based die casting alloy, and as rolled zinc. The remaining one-fourth is consumed as zinc compounds mainly by the rubber, chemical, paint, and agricultural industries. Zinc is also a necessary element for proper growth and development of humans, animals, and plants; it is the second most common trace metal, after iron, naturally found in the human body. Though, in its dissolved form it has been shown to cause toxic responses to aquatic organisms in elevated concentrations (Councell et al., 2004). The EPA has set the maximum water quality goal for zinc at 120 µg/L. The Chollas Creek metals TMDL water quality objective (WQO) for zinc is based on the California Toxic Rule (CTR) and varies depending on the hardness concentration from the sample collected. At a hardness of 100 mg CaCO3/L, the dissolved zinc CTR acute WQO is 117 µg/L. In comparison, the Federal Safe Drinking Water Act does not regulate the concentration of zinc in drinking water. California sets the secondary (aesthetic) maximum contaminant level, which is not enforceable, at 5,000 µg/L.

Sources of zinc to air and water include fertilizer, cement production, and transportation activities (e.g., combustion exhaust, galvanized parts, fuel and oil, brake wear, and tire wear). Zinc chromate primer is commonly used in the marine and aircraft industries. Zinc oxide is used in the vulcanization process of tires and rubber (estimated at 1% by weight). In urban environments, several studies reviewed by Councell (2004) reported positive correlations of zinc to traffic volume, primarily as tire-wear. Researchers concluded that 60% of the total zinc load in South San Francisco Bay was attributable to tire-wear debris. There is less information related to zinc contamination from fan belt wear from automobiles. It stands to reason that the density of cars, trucks, and other industrial motors, including ventilation fans, air compressors, and other machinery using rubber belts, may also be a significant source of zinc containing particulates. However, further investigation is needed to determine the contribution of fan belt wear to atmospheric deposition.

Galvanized metal is also used in numerous products that have the potential to release zinc containing particulates to the atmosphere. These include fences, sign posts, guardrails, and galvanized metal roofs which are frequently observed in the San Diego region industrial areas. Galvanized roofs have been shown to release elevated concentrations of zinc in storm water runoff captured directly from these sources. Other sources of galvanized products include scrap metal recycling and auto dismantling operations. Several automotive dismantling facilities have been observed in the area of Commercial Street and directly west of the North Fork of Chollas Creek.

1.3.3 Lead

Lead (Pb) has the highest atomic number (82) of all stable elements. The main lead mineral is called Galena (lead sulfide) which contains ~86% lead. It is estimated that 50% of the lead used today comes from recycling. Lead is not an essential element to living organisms and is known historically to be toxic to both humans and aquatic organisms. Lead has been shown to damage the nervous system and cause brain and blood disorders. It is detrimental to the development of young children. While lead awareness has significantly increased and exposure to public health has significantly decreased, lead is still commonly found in the environment. The EPA suggests the primary sources of lead exposure in the urban environment are:

- deteriorating lead-based paint
- lead contaminated dust and
- lead contaminated residential soil

The EPA's Lead Awareness Program continues to work to protect human health and the environment against the dangers of lead. Information about lead can be found at http://www.epa.gov/lead/. The Federal Safe Drinking Water Act sets the drinking water action level for lead at 15 µg/L and the maximum contaminant level goal is 0 µg/L. The Chollas Creek metals TMDL water quality objective (WQO) for dissolved lead is based on the California Toxic Rule (CTR) and varies depending on the hardness concentration from the sample collected. At a hardness of 100 mg CaCO3/L, the dissolved lead CTR acute WQO is 64 µg/L and the chronic WQO is considerably lower at 2.5 µg/L.

Lead has been widely used in the transportation industry, primarily for lead acid batteries, solder, bearings, and wheel balancing weights. Lead is a soft malleable metal also used as lead shot, fishing weights, sailboat keels for ballast, leaded glass, and television glass. Lead has been used historically in paint and is commonly found in homes built prior to 1978. Many older homes will often have larger concentrations of lead in soil in the areas directly adjacent to the home where paint chips will degrade and eventually slough off. Homeowners and remodelers have often used mechanical sanders to remove this older paint, in some cases, unaware of the hazards involved in releasing this material to the atmosphere as inhalable articulates. Lead was also used in gasoline to prevent "engine knock". The use of leaded gasoline peaked during the 1970s but was eventually phased out during the 1980s. Many researchers have shown that lead in soil is primarily a residual effect of the historic use of leaded gasoline and that storm water containing lead is likely a result of the erosion of soils near roadways. The concentration of lead in soil is steadily decreasing over time. Total lead in Chollas Creek has also shown a significant decreasing trend over time (Weston, 2006).

CITY OF SAN DIEGO
Dry Weather Aerial Deposition Study
Final Report

Prepared For:

The City of San Diego
1970 B Street, MS 27 A
San Diego, CA 92102

Prepared By:

Weston Solutions, Inc.
2433 Impala Drive
Carlsbad, California 92010

September 4, 2007

TABLE OF CONTENTS

LIST OF FIGURES

LIST OF TABLES

LIST OF CONTRIBUTORS

Project Manager	David Renfrew
Assistant Project Manager	Bryn Evans

Field Sampling Team

Task Leader	Bryn Evans
Field Monitoring Team	Niki Woodward, Bryn Evans, David Renfrew, Elizabeth Batliner, Esther Goldstein, Damon Owen, Andrew Lovell, Chris Clark, Dan McCoy, Jessica Hansen, Laurence Campagna, Alex Butkus, Yat-Long Poon, Anthony Trinh, Tyheshia Smith-Kruck, Andrea Crumpacker

Report Team

Report Authors	Andrea Crumpacker, Bryn Evans, Bruce Ferguson, Samantha Leskie, Steve Mauch, Dan McCoy, Dave Renfrew
Data Management and Statistics	Andrea Crumpacker
Air Quality Modeling	Steve Mauch, Marianne Aydil
Water Quality Modeling	Bruce Ferguson
Graphics	Bruce Ferguson, Samantha Leskie, Carla Cummings
Report Production	Michelle Patzius
Editors	Steve Mauch, Lisa Marie Kay, David Pohl

Acknowledgements
We also thank Andrea Crompton of the Cabrillo National Monument, National Park Service for allowing access to the park for the reference location. Additionally, we also thank Lisa Sabin and Ken Schiff of the Southern California Coastal Water Research Project for their input and coordination with the Pilot Study.